STRATEGIES FOR *IN SITU* RECOVERY OF UTAH'S HEAVY OIL AND BITUMEN RESOURCES

by Steven Schamel

OPEN-FILE REPORT 551
UTAH GEOLOGICAL SURVEY
a division of
UTAH DEPARTMENT OF NATURAL RESOURCES
2009

STRATEGIES FOR *IN SITU* RECOVERY OF UTAH'S HEAVY OIL AND BITUMEN RESOURCES

by Steven Schamel
GeoX Consulting Inc

Cover photo: *Amoco A-67 core at the Sunnyside heavy and extra-heavy oil (tar sand) deposit in Carbon County, Utah.*

OPEN-FILE REPORT 551
UTAH GEOLOGICAL SURVEY
a division of
UTAH DEPARTMENT OF NATURAL RESOURCES
2009

STATE OF UTAH
Jon Huntsman, Jr., Governor

DEPARTMENT OF NATURAL RESOURCES
Michael Styler, Executive Director

UTAH GEOLOGICAL SURVEY
Richard G. Allis, Director

PUBLICATIONS
contact
Natural Resources Map & Bookstore
1594 W. North Temple
Salt Lake City, UT 84116
telephone: 801-537-3320
toll-free: 1-888-UTAH MAP
Web site: mapstore.utah.gov
email: geostore@utah.gov

UTAH GEOLOGICAL SURVEY
contact
1594 W. North Temple, Suite 3110
Salt Lake City, UT 84116
telephone: 801-537-3300
Web site: geology.utah.gov

STRATEGIES FOR *IN SITU* RECOVERY OF UTAH'S HEAVY OIL AND BITUMEN RESOURCES

by

Steven Schamel
GeoX Consulting Inc

Table of Contents

List of Figures

List of Tables

STRATEGIES FOR *IN SITU* RECOVERY OF UTAH'S HEAVY OIL AND BITUMEN RESOURCES

by

Steven Schamel
GeoX Consulting Inc

ABSTRACT

The Uinta Basin contains a very large volume of stranded, shallow, immobile oil. These oil accumulations are immobile due to (1) high viscosity related to composition of the oil or (2) pour points in excess of the ambient reservoir temperature. Oils in the first category are heavy oils and bitumens, which have API gravities of 10º to 20º and less than 10º, respectively. They form the "tar sand" deposits that rim the Uinta Basin and are known in shallower parts of many conventional oil fields in the basin interior. Oils in the second category are found in shallow pools overlying several of the conventional oil fields. Both types of oils are currently stranded and will require application of *in situ* thermal recovery methods to produce them commercially.

Distinct differences exist between the three geologic settings for shallow, immobile oil accumulations in the Uinta Basin. Along the south flank of the basin, lenticular distributary channel and marginal lacustrine sandstones intercalated within the lower members of the Green River Formation are the principal reservoir across more than 600 square miles of the West and East Tavaputs Plateaus. Although the sandstones are relatively porous and permeable, averaging 24.8% and 912 md, respectively, they tend to have both low oil saturations (43.7%) and oil-impregnated net thickness (34.6 ft). Consequently, the volume of original oil-in-place per unit area in these deposits is very small, averaging just 26.9 MBO/acre in the P.R. Spring-Hill Creek deposit. With the exception of the several-square-mile Dry Creek Canyon-Bruin Point-Range Creek area, the Sunnyside deposit beneath the West Tavaputs Plateau is similar to the P.R. Spring-Hill Creek deposit east of the Green River. In this small area, stacked fluvial channels in the Douglas Creek Member, many over 100 ft thick with cumulative net thickness of many hundreds of feet, locally hold oil resources that are more than an order of magnitude greater than the other parts of the south flank deposits. Throughout, the reservoired oils are extra-heavy (bitumen) to heavy, averaging less than 10º API. These oils are asphaltine-rich, saturate-poor, and very viscous. Biomarkers indicate that these are immature Green River oils that have been heavily biodegraded.

Along the north margin of the Uinta Basin, heavy oil is reservoired (1) in Mesozoic sandstones on the up-turned hanging-wall of the Uinta Basin Boundary Fault and (2) in fluvial and marginal lacustrine sandstones of the late Eocene strata that unconformably onlap the thrust fault. The only known deposits of consequence are Asphalt Ridge and Whiterocks, although exploratory drilling within buried portions of the thrust sheet could reveal others. The main reservoir at Asphalt Ridge is stacked fluvial channels of the Mesaverde Group, which contains original oil-in-place in the range 120 to 190 MBO/acre. At Whiterocks, the Nugget Sandstone (Triassic-Jurassic) is the only reservoir. This eolian sandstone is porous (16 to 32%), moderately permeable (50 to 250 md), and relatively homogeneous. As the reservoir is

subvertical, the height of the oil column, not the 90 ft thickness of the reservoir, determines the original oil-in-place, which is in the range 450 to 485 MBO/acre. The heavy oil in both deposits has API gravity in the 10º to 14º range; it has the composition of a moderately biodegraded normal Uinta Basin oil. It is relatively high in saturates, low in asphaltines, and thereby easily upgraded to marketable products. Viscosities are considerably lower than those of the south flank oils.

In shallow, central parts of the Uinta Basin, lenticular, fluvial channel sandstones in the upper Eocene Uinta Formation reservoir contain both moderately biodegraded heavy oil and normal oil having a pour point that is greater than the ambient reservoir temperature. If the Wonsits Valley shallow oil pools are representative of the many other similar accumulations scattered across the basin, the oils change in character down section from degraded to normal, but immobile, to mobile oils at current production depths below about 4000 ft. Many of these deposits produce small volumes of biogenic gas, indicating active biodegradation of the shallow, reservoired immobile oil.

INTRODUCTION

Sandstone reservoirs in Utah contain a very large volume of stranded, shallow, immobile oil (Ritzma, 1979; Kuuskraa and others, 1987; Meyer and Schenk, 1988). These oil accumulations are immobile due to high viscosity related to composition of the oil or due to pour points in excess of the ambient reservoir temperature. Oils in the first category are heavy and bitumens, which have API gravities of 10º to 20º and less than 10º, respectively. They form the "tar sand" deposits that rim the Uinta Basin , are known in shallower parts of many conventional oil fields in the Uinta Basin interior, and are scattered across the western margin of the Paradox basin. Oils in the interior of the Uinta Basin are found in shallow pools overlying several of the conventional oil fields. Both categories of oils are currently stranded and will require application of *in situ* thermal recovery methods to produce them commercially. Both have remained remarkably resistant to commercial exploitation either by surface mining and retorting or by *in situ* recovery.

In Utah, as in Alberta where less than 20% of the "tar sands" is suitable for extraction by surface mining (Moritis, 2004), it is highly unlikely that mining will ever gain traction for production of energy, as opposed to small pits extracting asphalt for road construction. The heavy oil and bitumen deposits in Utah tend to be located in areas with exceptional scenic quality and high environmental/conservation values. Many are in areas with very limited access to water resources that would be required for surface mining and for steam-based thermal *in situ* recovery processes. This report begins with the premise that future exploitation of the heavy oil and bitumen resources will require innovative application of *in situ* heavy oil recovery technology now in use or in development in other heavy oil accumulations worldwide. Throughout this paper the terms *oil, heavy oil* and *bitumen* may be used interchangeably, indicating the variable oil gravities that characterize most of the stranded, immobile oil accumulations in Utah.

In northeast Utah, the largest accumulations of heavy oil and bitumens are located along the southern margin of the Uinta Basin underlying vast portions of the gently north-dipping East and West Tavaputs Plateaus (Fig. 1). This highland surface above the Roan Cliffs on either side of the Green River (Desolation) Canyon is supported by sandstones and limestones of the

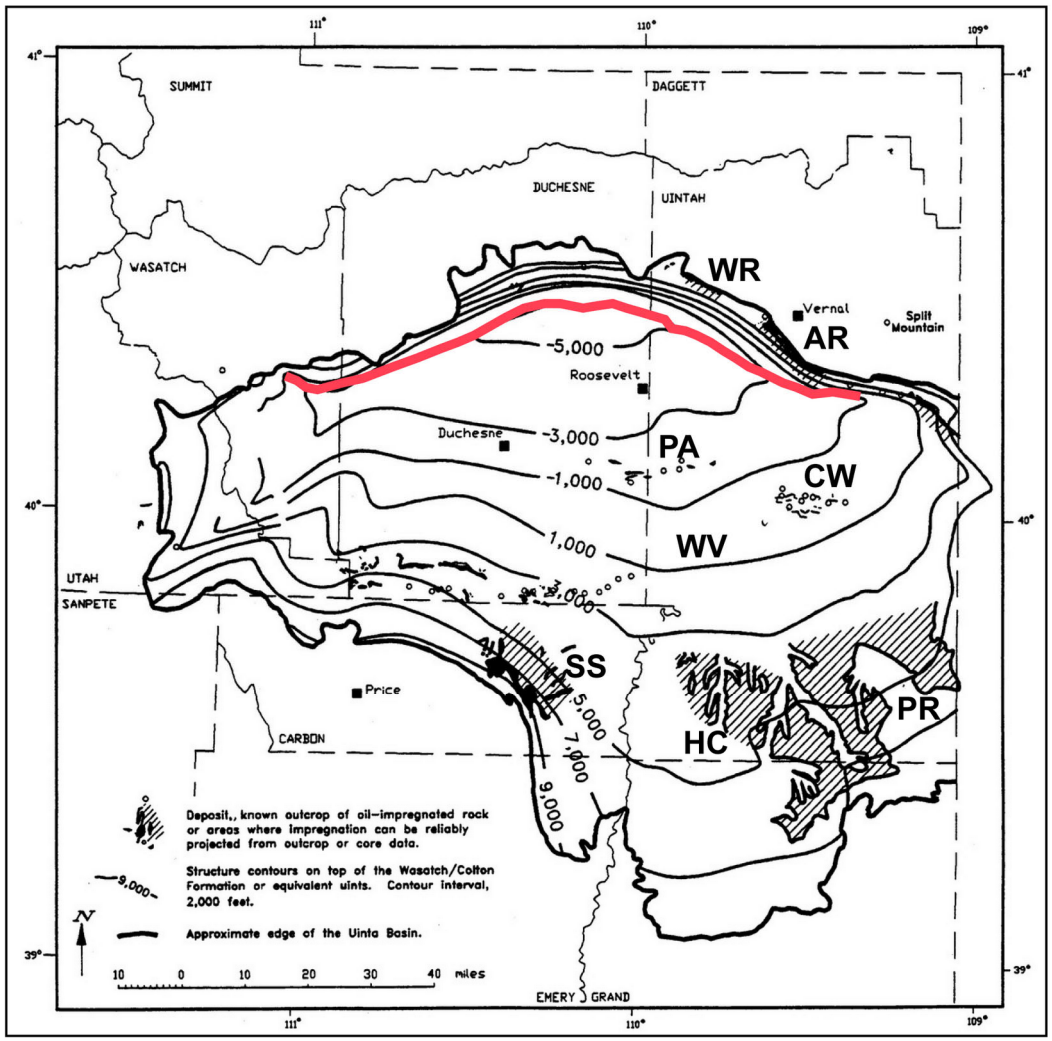

Figure 1: Structure contour map of the Uinta basin showing the location of the shallow, immobile reservoired oil deposits described in this paper. The datum is the base of the Eocene Green River Formation, or top of the Wasatch/Colton Formation. Map is modified from Blackett (1996). The red line is the approximate subsurface location of the buried Uinta Basin Boundary Fault.

Green River Formation (Eocene). There the original oil-in-place (OOIP) is at least 10 billion barrels. On the northern Uinta Basin margin, heavy oil accumulations occur in a variety of reservoirs on the hanging wall of the Uinta Basin Boundary Fault, the thrust that carries the Uinta Mountain uplift southward onto the depocenter of the strongly asymmetric Uinta Basin. The proven OOIP in these deposits is less than 2 billion barrels, but the potential for additional undiscovered oil is great. Additionally, immobile oil is known to exist in shallow, fluvial sandstone reservoirs throughout the central parts of the basin. They are documented overlying several of the conventional oil and gas fields. However, they may be far more widespread and would be better known if operators routinely well logged the shallow depths at which these pools commonly occur, hundreds to a few thousand feet.

Flanking the western half of the Paradox Basin, the only large bitumen accumulation that is potentially open for development is the Tar Sand Triangle in easternmost Wayne and Garfield Counties.

The focus of this report is:

a) the geologic setting and the character of the sandstone reservoirs,
b) the properties of the reservoired oils in these unconventional oil accumulations, and
c) appropriate methods for *in situ* recovery of these stranded oil resources.

There are a number of factors that are critical for determining if a particular *in situ* thermal recovery technology is appropriate for use in a specific oil pool or portion of an oil accumulation. The more important factors are:

- The concentration of oil in the reservoir, the volume of oil in a volume of rock, herein referred to as "oil grade."
- The distribution of oil-impregnated rocks within the oil reservoir section as measured by net pay to gross thickness and the thicknesses of the individual beds or bed clusters reservoiring the oil.
- The overall oil-in-place or oil resources available for development.
- The petrophysical properties of the rock influencing the success of an *in situ* thermal recovery process, principally permeability, porosity, and oil saturation.
- The physical properties of the oil at both ambient reservoir temperatures and at reservoir temperatures that could be obtained by an economically reasonable thermal recovery process. It is essential that oil be of sufficiently low viscosity when artificially heated to be capable of reasonably rapid Darcy flow from the sandstone reservoir.

If the oil is heavy or extra-heavy (bitumen), it is important that it is capable of upgrading to a marketable product.

The concentration of oil within the oil-impregnated sandstone was generally determined by Soxhlet extraction methods in which the weight (or volume) of oil extracted from a core sample was compared to the weight (or volume) of the sample. As the objective of most of the investigations was to assess the deposit for surface mining and retorting, the oil concentration or "grade" was reported in units of gallons of oil per ton of mined rock (gal/ton) or weight percent of oil compared to oil-impregnated rock (wt%). However, as the focus of this paper is the recovery of oil from a reservoir rock by means of oil wells, *oil grade* is reported in units of barrels of oil per acre-ft of reservoir rock (BO/ac-ft). The conversions used are: 1.0 gal/ton = 67.76 BO/ac-ft and 1.0 wt% = 169.40 BO/ac-ft. To convert from the oil fraction of rock volume: BO/ac-ft = 7758 x (decimal fraction of oil) or 7758 x (decimal porosity) x (decimal oil saturation).

If a test well has penetrated the entire oil-impregnated interval, the OOIP at the specific site of the well is determined by multiplying the oil grade by the net thickness of oil-impregnated reservoir penetrated. In this paper the oil-in-place is reported as thousands of barrels per acre (MBO/acre). As the recovery factors are unknown, only estimated oil resources, not oil reserves, are reported.

The larger heavy oil and bitumen deposits in Utah are best described in terms of their geologic setting, which influences the reservoirs and the oils contained within.

DEPOSITS ON SOUTH FLANK OF UINTA BASIN

In the latest Cretaceous through Eocene, following the onset of Laramide uplift initiating intermountain basin subsidence, large lakes formed throughout the region that previously was an extensive foreland basin, the Western Interior Seaway (Franczyk and others, 1992). In northeast Utah, in the general area of the Uinta Basin, there were two major lakes, Lake

Flagstaff of Paleocene age and Lake Uinta of Eocene age (Fouch, 1975). Light gray and varicolored biomicritics of the Flagstaff Limestone are the record of Lake Flagstaff and organic-rich lacustrine shales ("oil shales") of the Green River Formation were deposited in Lake Uinta (Fouch and others, 1994). During the dry period between Lake Flagstaff and Lake Uinta time, 800 to 1200 ft of continental red mudstone and sandstones were deposited in a fluvial-flood plain setting. This is the Colton or Wasatch Formation, which in part interfingers with both the underlying Flagstaff Limestone and the overlying Green River Formation. As Lake Uinta expanded during Green River time, the fluvial-flood plain setting was replaced by periodic sandy delta systems that emptied northward across marginal lacustrine carbonate muds and limestones (Picard and High, 1970; Ryder and others, 1976). These deltaic and shoreline sandstones (Figs. 2 and 3) are the reservoirs for the heavy oils on the south flank of the Uinta Basin.

The Sunnyside heavy oil deposit is located along the western face and dip slope of the Roan Cliffs (Fig. 1) east and north of the small coal-mining town of Sunnyside. The western margin of the deposit is well defined by topography, cliffs eroded into the bituminous-sandstones of the deposit. The northern, eastern, and southern boundaries are known principally by the end of bitumen outcropping in the canyon walls of streams incised into the West Tavaputs Plateau, the northeasterly dip slope of the Roan Cliffs.

In many parts of the deposit, the crest of the Roan Cliffs exceeds 9000 ft elevation. The high benches of the West Tavaputs Plateau overlying the deposit are higher than 8000 ft elevation. The many streams cut into the plateau tend to be deeply incised, with steep canyon walls that make the canyon floors virtually inaccessible from the plateau. With few exceptions, they also are inaccessible from their mouths in Desolation Canyon (Green River) to the east.

Figure 2: Stacked fluvial-deltaic sandstones in the lower Green River Formation in Nine Mile Canyon, immediately north of the Sunnyside deposit. Photograph by S. Schamel.

Figure 3: Small, lenticular distributary sandstone channels incised into lacustrine and shoreface deposits of the lower Green River Formation in Willow Creek Canyon. The thick planar light-gray beds are shoreface and sheet sandstones similar in lithology to that of the channel deposits, but with different internal structures. Photograph by S. Schamel.

The P.R. Spring-Hill Creek deposits have a similar topographic and geologic setting to the Sunnyside deposit, but they are on the higher portions of the East Tavaputs Plateau, above the Roan Cliffs east of the Green River canyon (Fig. 1). The P.R. Spring and Hill Creek deposits are separated by the deeply incised Willow Creek Canyon. Prior to canyon incision into the Tavaputs Plateau, it is likely that Sunnyside, Hill Creek, and P.R. Spring constituted a single, extremely large oil accumulation.

In addition to the giant Sunnyside and P.R. Spring-Hill Creek deposits, several considerably smaller deposits exist on the West Tavaputs Plateau (Ritzma, 1979; Blackett, 1996). Immediately downdip from Sunnyside is the 20-25 MMBO *Cottonwood-Jacks Canyon deposit* in the same reservoir intervals as Sunnyside. Some authors include this deposit within the limits of Sunnyside (e.g., Oblad and others, 1987). To the north of Sunnyside is the 5-10 MMBO *Nine Mile Canyon deposit*, a series of isolated Garden Gulch and Parachute Creek bituminous-impregnated sandstone outcrops along the canyon walls over a 17 mile length of the canyon (Ritzma, 1979). Just off of Nine Mile Canyon is the 50-70 MMBO *Argyle Canyon deposit* in deltaic and interfingering lacustrine shoreface sandstones in the Parachute Creek Member. The main part of the deposit in is the middle part of the canyon where the bitumen-impregnated interval is 400 ft thick. To the northwest of Sunnyside is the 10-15 MMBO *Minnie Maud Creek deposit*, which consists of only a few 5–15-ft-thick bitumen-impregnated intervals in the Garden Gulch and Parachute Creek Members. On strike to the west of Minnie Maud is the 10-15 MMBO *Willow Creek deposit* with a total thickness of bitumen-impregnated Parachute Creek channel sands on the order of 80 ft thick.

P.R. Spring-Hill Creek Deposit

The P.R. Spring-Hill Creek heavy oil deposit lies beneath almost the entirety of the East Tavaputs Plateau in southern Uintah and northernmost Grand Counties, Utah (Fig. 4). The southern and eastern limits of the deposit are the Roan Cliffs and the Douglas Creek arch, respectively, where the oil-impregnated sandstone reservoirs outcrop. The western limits are poorly defined, but the oil accumulation appears to end just east of the cliffs on the east flank of the Green River Canyon. At present, the downdip, northern limits are unknown (Sinks, 1985a) and for convenience are defined by the thickness of overburden. The estimated size of the

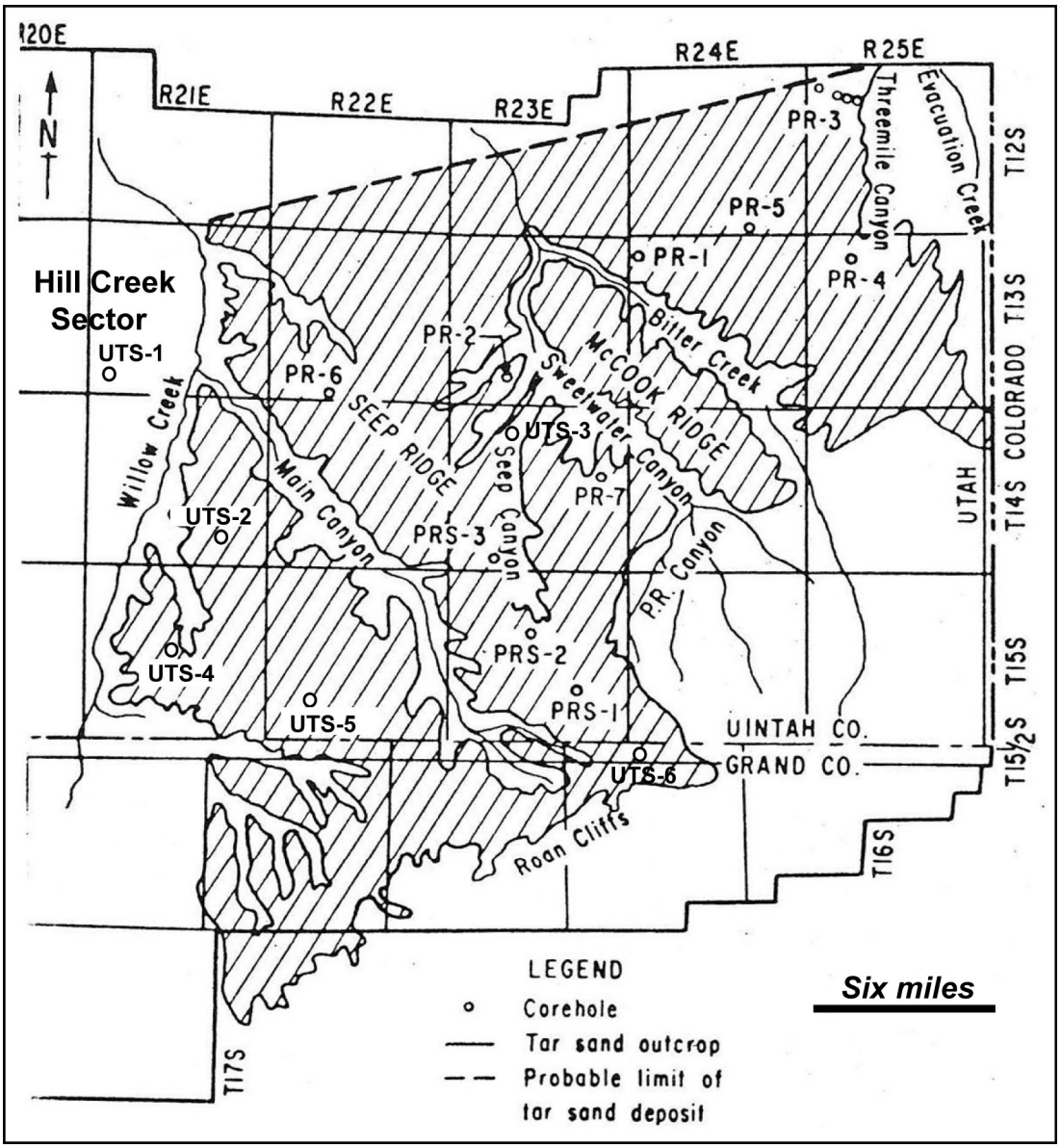

Figure 4: Extent of the P.R. Spring heavy oil deposit east of the Willow Creek Canyon on the eastern Tavaputs Plateau (modified after Johnson and others, 1976). Shown are the locations of U.S. Bureau of Mines and other cores discussed in this report. The four Sweetwater Creek wells not shown are located on Seep Ridge approximately between the PRS-3 and PR-2 wells. The northern boundary shown in a dashed line approximates 250 foot isopleths of overburden above the shallowest bitumenous sandstone, not an established limit of the deposit.

deposit is 470 sections (square miles), 350 sections in the P.R. Spring portion (Johnson and others, 1976) and 120 sections in the Hill Creek portion (Gwynn, 1985). Although normally treated as separate deposits, P.R. Spring and Hill Creek are parts of the same heavy oil accumulation. However, the deep Willow Creek Canyon is incised through the oil-impregnated sandstone reservoirs physically dividing the single deposit into a very large eastern part and a relatively small western sector. Less deep canyons divide the P.R. Spring deposit into various sectors (Fig. 4), none of which are completely separated from adjacent sectors. The U.S. Bureau of Mines estimated the deposit to contain 5.0 to 5.5 billion barrels of oil, measured and inferred (reported in Ritzma, 1979).

Oil-impregnated sandstone beds in up to five or six distinct zones are found in the lower two members of the Green River Formation (lower and middle Eocene). The intervals containing oil-impregnated sandstones are 150 to 350 ft thick; individual sandstone beds are up to 50-70 ft thick (Byrd, 1970), but more commonly they are only 1 to 10 ft thick. In most areas, it is the lowest member, the Douglas Creek Member, that contains most of the oil-impregnated sandstones. In the development of Lake Uinta in the area of the East Tavaputs Plateau, this member represents the transition from fluvial to lacustrine shoreline deposition. The Douglas Creek Member consists of intercalated sandstone, siltstone, shale, and limestone (algal and ostrocodal). The sandstones were deposited in marginal-lacustrine channels on or incised into near-shore, fine-grained open lacustrine sediments during lake lowstands (Fouch and others, 1992). Oil-impregnated sandstones occur also in the lower parts of the Parachute Creek Member, the unit deposited during the maximum extent of Lake Uinta and containing abundant "oil shales." The richest "oil shale," the Mahogany Bed, is the boundary between the Douglas Creek Member and the Parachute Creek Member. The sandstones are very fine to fine grained and arkosic (Sinks, 1985a).

Eighty-six shallow test wells have been drilled on the East Tavaputs Plateau to delineate the extent of the P.R. Spring-Hill Creek heavy oil deposit. A substantial number of these wells were cored and the core samples analyzed for oil richness, fluid saturations, and rock properties. A subset of 26 of the cores for which data is in the public domain have been selected to represent the character of the deposit (Tables 1 and 2). These cores are from seven separate sectors of the deposit, from the Threemile Canyon area near the Colorado state line on the east, to the Hill Creek area between Hill Creek and Willow Creek on the west.

Recognizing that the published averages of core properties are suspect, the raw data have been tabulated for presentation in this report. The analyses, for the most part, were done by Core Laboratories in the 1970s and early 1980s, and they should be considered to be reliable. The well locations are shown on Figure 4 and the average and median core properties are presented in Tables 1 and 2. In most instances, the core was sampled at 1 ft intervals only within the zones containing oil-impregnated sandstones. For the purposes of this report, which is focused on *in situ* recovery of the heavy oil, a 1-ft gap in oil-impregnated sands is treated as insignificant, but a 2-ft or greater gap is considered as separating different reservoir intervals. Table 1 reports the gross and net thicknesses of the oil-impregnated section and Table 2 reports the maximum bed (or interval) thickness and the number of individual beds (or intervals) penetrated in the well. A reservoir consisting of only one or a few thick oil-impregnated sandstone beds is more suitable for thermal recovery methods than one containing many thin beds, even if both have the same net sandstone thickness and sand-to-shale ratio.

The Asphalt Wash sector is located between Threemile Canyon and Bitter Creek. The three U.S. Bureau of Mines test wells in the sector illustrate the manner in which oil-impregnated sandstone beds are distributed in the stratigraphic section (Johnson and others, 1976). The oil

Table 1: Average properties of bituminous sandstones and reservoired oil determined from cores penetrating the P.R. Springs-Hill Creek deposit. The test wells are clustered geographically from northeast (Threemile Canyon) to southwest (Hill Creek). Refer to Fig. 4 for the locations of the well clusters (sectors). Average values for each sector are shown in red italics. Data are from Peterson and Ritzma (1974), Sinks (1985a), Covington and Young (1985), and Utah Geological Survey open-files. NA=none available.

	Well	T-R	Sec	Elev, ft	TD, ft	API°	Bbls/ac-ft	Gross thick	Net thick	Mbbls/acre
Threemile Cyn	PR-3A	12S-25E	8	6,302	95	10.9	1,335.9	25	25	33.40
Threemile Cyn	PR-3B	12S-25E	8	6,361	157	11.1	1,429.9	28	28	40.04
Threemile Cyn	PR-3C	12S-25E	8	6,430	317	10.0	1,635.3	26	26	42.52
Threemile Cyn	PR-3D	12S-25E	7	6,512	416	10.3	812.3	8	8	6.50
						10.6	*1,303.4*		*22*	*28.35*
Asphalt Wash	PR-1	13S-24E	6	6,210	326	11.1	994.9	87	35	34.82
Asphalt Wash	PR-5	12S-24E	34	6,437	274	11.6	1,162.3	86	13	15.11
Asphalt Wash	PR-4	13S-25E	5	7,187	195	11.2	1,247.6	19	19	23.70
						11.3	*1,134.9*		*22*	*25.35*
Sweetwater Cyn	PR-7	14S-23E	14	6,798	212	9.9	1,176.1	163	23	27.05
Sweetwater Cyn	UTS-3	14S-23E	8	6,693	229	na	675.5	118	45	30.40
Sweetwater Cyn	PR-2	13S-23E	29	6,346	202	14.6	801.0	70	14	11.21
						12.3	*884.2*		*27*	*24.17*
Sweetwater Ck	U 26-33	13S-23E	26	6,441	254	na	942.2	99	16	9.40
Sweetwater Ck	U 14-34	14S-22E	14	7,003	244	na	1,177.9	144	7	8.20
Sweetwater Ck	U 24-24	14S-22E	24	7,131	300	na	1,226.7	66	16	19.60
Sweetwater Ck	U 25-32	14S-22E	25	7,162	201	na	587.7	99	16	9.40
							983.6		*14*	*13.52*
M&E Mine	F bed	15.5S-24E	32	na	na	na	1,529.4	na	20	30.59
M&E Mine	E bed	15.5S-24E	32	na	na	na	2,039.1	na	35	71.37
							1,784.2		*55*	*101.96*
Seep Ridge	UTS-6	15.5S-24E	33	8,295	417	na	740.2	337	95	70.32
Seep Ridge	PRS-1	15S-23E	27	8,010	247	13.3	900.6	196	96	86.46
Seep Ridge	PRS-2	15S-23E	16	7,702	282	12.5	756.4	191	56	42.36
Seep Ridge	PRS-3	14S-23E	32	7,387	242	10.9	940.6	133	42	39.51
Seep Ridge	PR-6	13S-22E	33	6,707	423	11.0	728.2	227	65	47.33
						11.9	*813.2*		*71*	*57.57*
Meadow Creek	UTS-5	15S-22E	29	7,472	316	na	667.9	222	41	27.38
Meadow Creek	UTS-4	15S-21E	21	7,383	446	na	171.4	334	78	13.37
Meadow Creek	UTS-2	14S-21E	26	7,003	310	na	320.6	150	13	4.17
							386.6		*44*	*17.01*
Hill Creek	HC-1	14S-20E	31	7,261	268	9.4	720.7	187	63	45.40
Hill Creek	HC-2	14S-20E	33	7,483	488	6.6	566.8	131	27	15.30
Hill Creek	HC-3	15S-20E	3	7,409	500	10.9	407.7	152	37	15.08
Hill Creek	UTS-1	13S-21E	29	6,489	401	na	427.2	85	41	17.51
						9.0	*530.6*		*42*	*22.29*

reservoirs cluster in two zones which consist of several separate oil-impregnated sandstone beds, or less commonly a single relatively thick bed (Fig. 5). The reservoir units are laterally discontinuous as "zones," as shown in Zone 2, and as separate sandstone beds within a zone. Oil grades measured within the sandstones are shown in Fig. 6 for the two deeper test wells, PR-1 and PR-5. The clustering of oil-impregnated intervals is clear in the plots, as well as the vertical variability of oil-richness between individual beds and even within single beds. Although the thickness of the section containing oil-impregnated sandstones is comparable between the two wells, 87 and 86 ft, the net thickness of oil-impregnated sandstone is very different, 35 and 13 ft, leading to substantial difference in oil-in-place, 34.8 and 15.1 MBO/acre, for the two wells having similar oil grades (Table 1). Curiously, the PR-4 well, with just one oil-impregnated zone (Fig. 5), has larger oil-in-place (23.7 MBO/acre) than the nearby PR-5 well due to both a larger net thickness and a slightly higher oil grade (Table 1). These three wells demonstrate the vertical and lateral variability in reservoir properties controlling oil-in-place that characterizes all of the P.R. Spring-Hill Creek heavy oil deposit.

Table 2: Average and median petrophysical properties of the bituminous sandstones measured in core samples from the P.R. Spring-Hill Creek deposit. Average values for each sector are shown in red italics.

				Average:				Median:			
Area	***Well***	***Max, ft***	***Beds***	***Porosity***	***Perm, md***	***So, %***	***Sw, %***	***Porosity***	***Perm, md***	***So, %***	***Sw, %***
Threemile Cyn	PR-3A	25	1	29.2	1618	57.6	13.1	29.6	1716	59.5	13.2
Threemile Cyn	PR-3B	28	1	28.2	1590	62.4	13.8	28.6	1686	67.0	8.8
Threemile Cyn	PR-3C	26	1	25.4	1831	82.3	3.1	25.9	1732	84.3	2.7
Threemile Cyn	PR-3D	8	1	30.8	1987	32.9	35.8	31.4	1960	32.9	39.7
		21.8	***1.0***	***28.4***	***1757***	***58.8***	***16.5***	***28.9***	***1774***	***60.9***	***16.1***
Asphalt Wash	PR-1	13	6	25.0	439	52.7	4.1	25.5	290	52.3	2.8
Asphalt Wash	PR-5	3	4	26.0	419	58.4	6.3	25.9	330	58.3	5.8
Asphalt Wash	PR-4	19	1	26.8	614	60.2	7.6	27.2	468	65.5	5.8
		11.7	***3.7***	***25.9***	***491***	***57.1***	***6.0***	***26.2***	***363***	***58.7***	***4.8***
Sweetwater Cyn	PR-7	15	6	26.1	1362	57.3	13.2	27.1	1369	53.6	8.0
Sweetwater Cyn	UTS-3	15	8	22.0	270	37.8	14.8	23.4	90	38.4	11.4
Sweetwater Cyn	PR-2	4	6	20.3	169	54.0	3.5	19.6	100	51.9	3.1
		11.3	***6.7***	***22.8***	***600***	***49.7***	***10.5***	***23.4***	***520***	***48.0***	***7.5***
Sweetwater Ck	U 26-33	5	4	24.0	831	49.2	na	23.8	233	41.0	na
Sweetwater Ck	U 14-34	3	5	28.5	1903	53.4	na	28.8	1778	43.6	na
Sweetwater Ck	U 24-24	11	3	27.4	1664	57.2	na	26.7	790	51.2	na
Sweetwater Ck	U 25-32	12	4	26.5	2382	28.9	na	26.8	2075	24.0	na
		7.8	***4.0***	***26.6***	***1695***	***47.2***		***26.5***	***1219***	***40.0***	
Seep Ridge	UTS-6	15	14	24.5	891	35.0	11.3	25.4	116	34.4	8.8
Seep Ridge	PRS-1	22	9	28.3	1624	39.5	14.5	29.0	689	34.0	11.8
Seep Ridge	PRS-2	24	9	27.9	1169	35.5	20.3	28.5	853	32.9	19.3
Seep Ridge	PRS-3	21	9	27.8	910	43.6	21.3	28.1	693	39.3	18.2
Seep Ridge	PR-6	19	14	24.9	230	39.2	18.7	25.5	136	37.6	12.2
		20.2	***11.0***	***26.7***	***964.8***	***38.6***	***17.2***	***27.3***	***497.4***	***35.6***	***14.1***
Meadow Creek	UTS-5	25	6	24.0	1267	33.2	10.5	25.0	311	29.7	10.3
Meadow Creek	UTS-4	16	16	22.2	476	9.4	10.2	23.9	313	6.4	8.7
Meadow Creek	UTS-2	13	4	19.1	79	20.5	19.8	20.1	110	18.9	16.0
		18.0	***8.7***	***21.8***	***607***	***21.0***	***13.5***	***23.0***	***245***	***18.3***	***11.7***
Hill Creek	HC-1	10	6	21.6	288	45.1	9.6	22.1	156	42.2	8.3
Hill Creek	HC-2	11	10	22.6	340	34.5	15.9	23.5	244	30.4	13.2
Hill Creek	HC-3	12	6	23.6	380	24.3	29.4	24.2	235	15.9	27.9
Hill Creek	UTS-1	25	5	18.2	57	28.8	21.9	18.4	10	25.5	16.0
		14.5	***6.8***	***21.5***	***266***	***33.2***	***19.2***	***22.1***	***161***	***28.5***	***16.4***

Between the test wells in the Asphalt Wash sector, there is virtually no systematic variation in porosity, permeability, and fluid saturations (Figs. 7 and 8; Table 2). Porosity is in the general range of 20% to 30%, and averages 25.9% for the three wells. Permeability ranges over six orders of magnitude, but generally it is in the range of 100 md to 1000 md. The average for the three wells is 491 md, with well averages ranging from 419 md to 614 md. Oil saturations (So) cluster between 40% and 80%, averaging 57.1% and having little variation between wells. Water saturations (Sw) are very low, averaging just 6.0% for the sector. The very low Sw values are likely due to preferential drainage of water from the core during handling and storage. The highly viscous heavy oil is far less likely to drain from the core, so the values reported likely are very close to actual *in situ* values. Given the small variation in porosity of the reservoir sandstones, there is a very strong correlation between oil grade and oil saturation in the individual core samples analyzed (Fig. 9). API gravity of reservoired oil in the Asphalt Wash sector wells ranges from 13.1º to 7.5º (Fig. 6). A systematic increase in oil density (decrease in ºAPI) is observed down section. Zone 1 reservoirs have heavy oil, whereas Zone 2 reservoirs have bitumen. The gravity of oil at the top of Zone 1 in PR-4 is 11.2º.

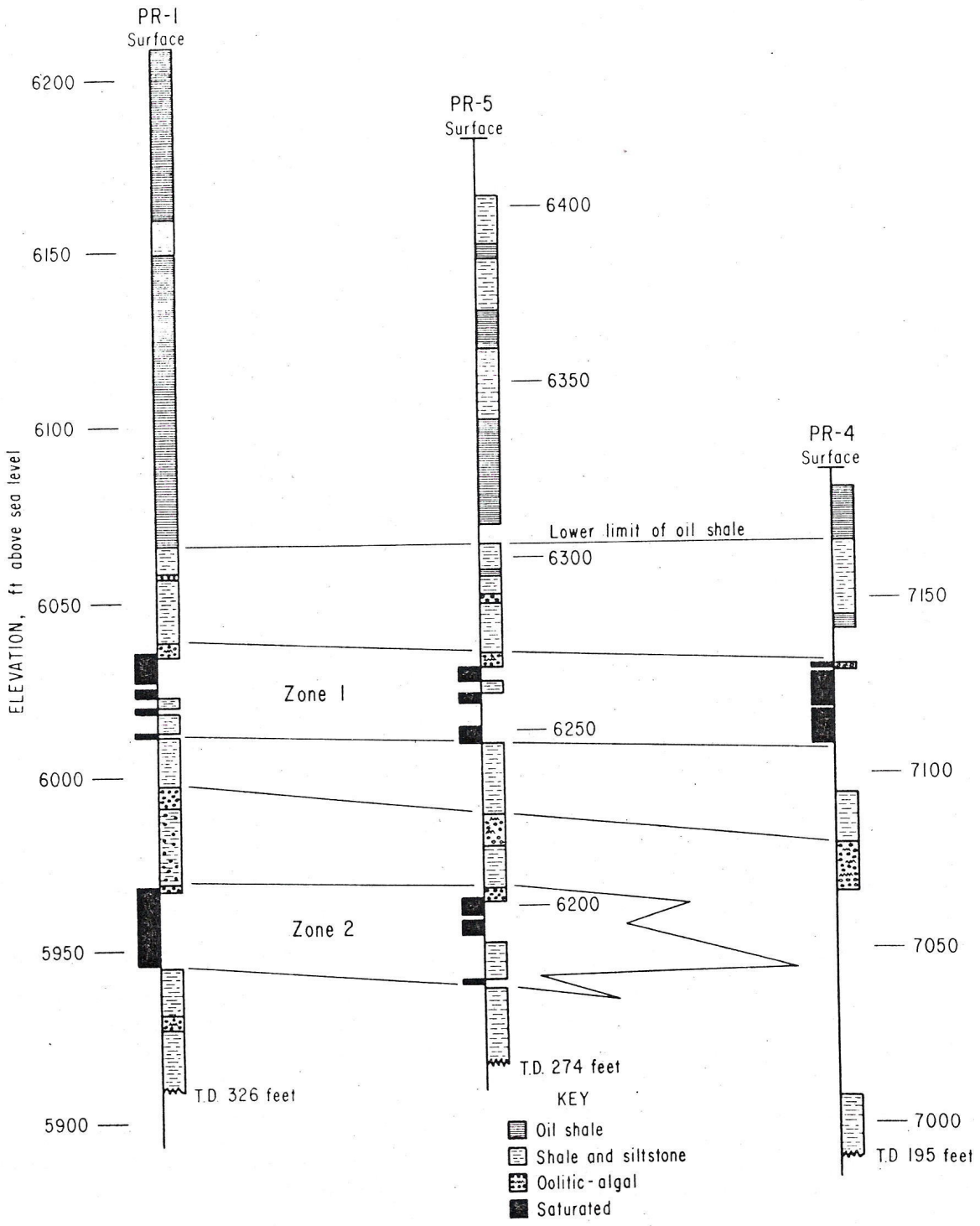

Figure 5: Representative stratigraphic sections showing the sporadic distribution of bitumenous sandstone lenses within the lower Green River Formation in the Asphalt Wash area of the P.R. Spring deposit (Johnson and others, 1976). Note that even within the two bitumenous sandstone zones penetrated, individual bitumenous sandstone lenses are separated by non-bitumenous layers. Refer to Figure 4 for the locations of the coreholes shown.

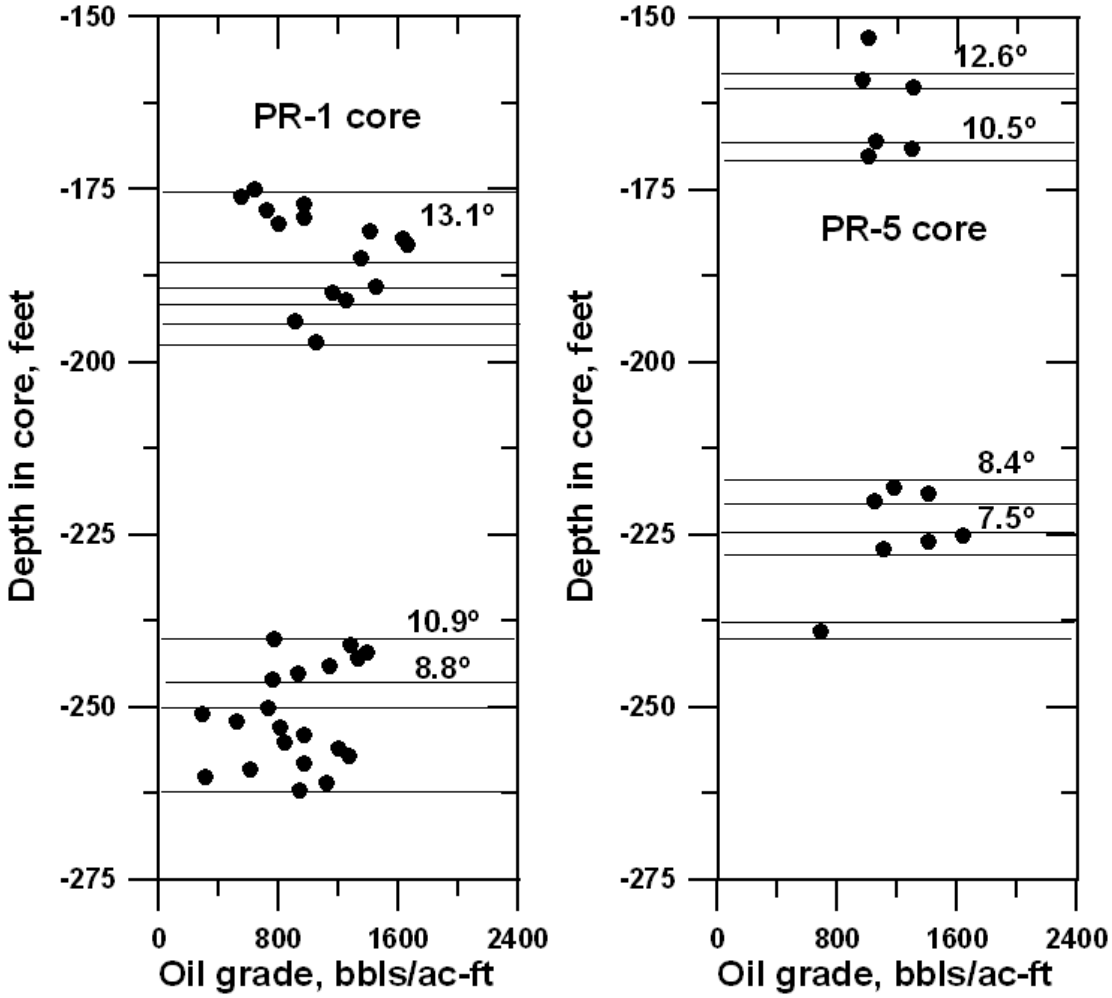

Figure 6: Grade of heavy oil in bitumenous sandstone intervals in the PR-1 and PR-5 cores (Asphalt Wash) plotted against depth of the samples in the wells. The clustering of values shows the thickness and spacing of the bitumenous sandstone lenses penetrated by the test wells. The gross and net thicknesses of the bitumenous sandstone deposit are presented in Table 2; the maximum bitumenous sandstone bed thickness and the number of oil-impregnated beds in the deposit are presented in Table 3. The net to gross ratios for PR-1 and PR-5 are 0.40 and 0.15, respectively. The API gravity of the heavy or extra-heavy oil extracted from the core is shown in the position of the sample in the well. Data from Peterson and Ritzma (1974).

The relatively close-spaced test wells in the Threemile Canyon sector penetrate a single, relatively thick (25-28 ft) oil-impregnated sandstone bed (Marchant and others, 1974). These wells document unusually high oil grades that average 1303.4 BO/ac-ft for the four wells and are as high as 1635.3 BO/ac-ft (Table 1). This single oil-impregnated bed dips northward and is encountered at increasing depths. Fig. 10 plots oil grade measured in the same sandstone bed in successive wells. Within this sandstone reservoir oil grade is observed to increase from an average of 1335.9 BO/ac-ft (PR-3A) to 1635.3 BO/ac-ft (PR-3C). However, at a depth greater than 370 ft (PR-3D), oil grade is diminished to 812.3 BO/ac-ft. The lateral variability in oil grade does not relate to differences in porosity (Fig. 11; Table 2), which actually are higher in PC-3D (30.8% average) than in PC-3C (25.4% average). Rather, the controlling factor is oil saturation (Fig. 12; Table 2), which varies systematically downdip. The average oil saturation measured in PC-3D core samples is 32.9%, but it is 82.3% in PC-3C. It is possible that PC-3D is penetrating the reservoir sandstone immediately above the oil-water contact.

Table 3: Chart showing for correlated heavy oil-impregnated sandstone intervals, the average interval thickness, average heavy oil grade as barrels per acre-foot, average OOIP in thousands of barrels per acre, the percentage of OOIP in each interval, and the number of well penetrations of each interval. Data from Rozelle Consulting Services (1989).

	Thickness	Bbls/ac-ft	MBO/acre	% Total oil	Penetrations
Interval 11	10.0	956.1	9.51	1.24	53
Interval 21	23.1	1074.7	24.80	3.23	61
Interval 23	17.8	1058.4	18.87	2.45	53
Interval 25	19.2	870.0	16.71	2.17	60
Interval 26	17.3	878.8	15.24	1.98	60
Interval 31	31.6	1209.5	38.20	4.97	76
Interval 32	14.8	1106.5	16.40	2.13	35
Interval 33	26.2	1113.3	29.19	3.80	77
Interval 35	36.2	1148.5	41.55	5.40	79
Interval 36A	47.6	1176.3	56.00	7.28	77
Interval 36B	78.2	1179.7	92.25	12.00	67
Interval 37	47.1	1256.3	59.16	7.69	59
Interval 38	49.4	1246.1	61.52	8.00	55
Interval 41	76.2	1192.6	90.81	11.81	42
Interval 42	60.7	1253.6	76.14	9.90	27
Interval 43	70.9	1168.9	82.87	10.78	15
Interval 45	35.9	1108.6	39.83	5.18	26

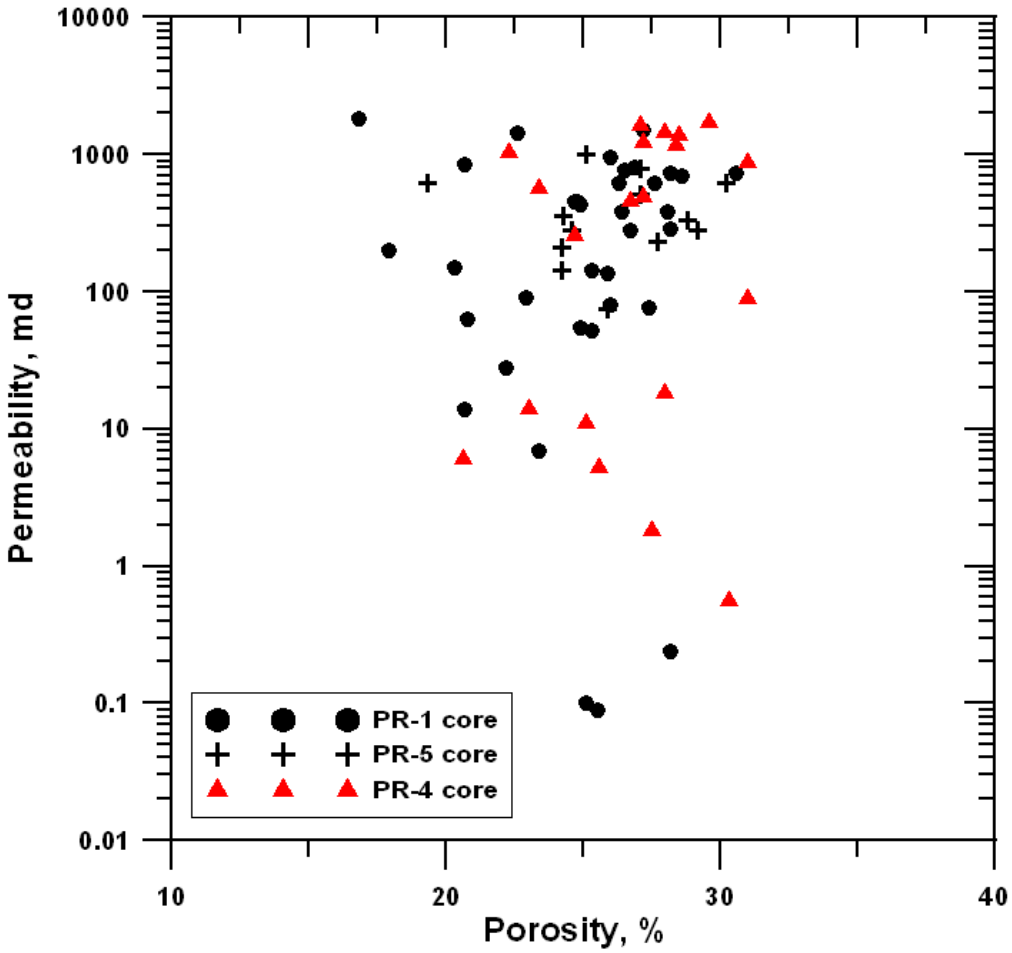

Figure 7: Variations in porosity and permeability measured in core from test wells in the Seep Ridge sector.

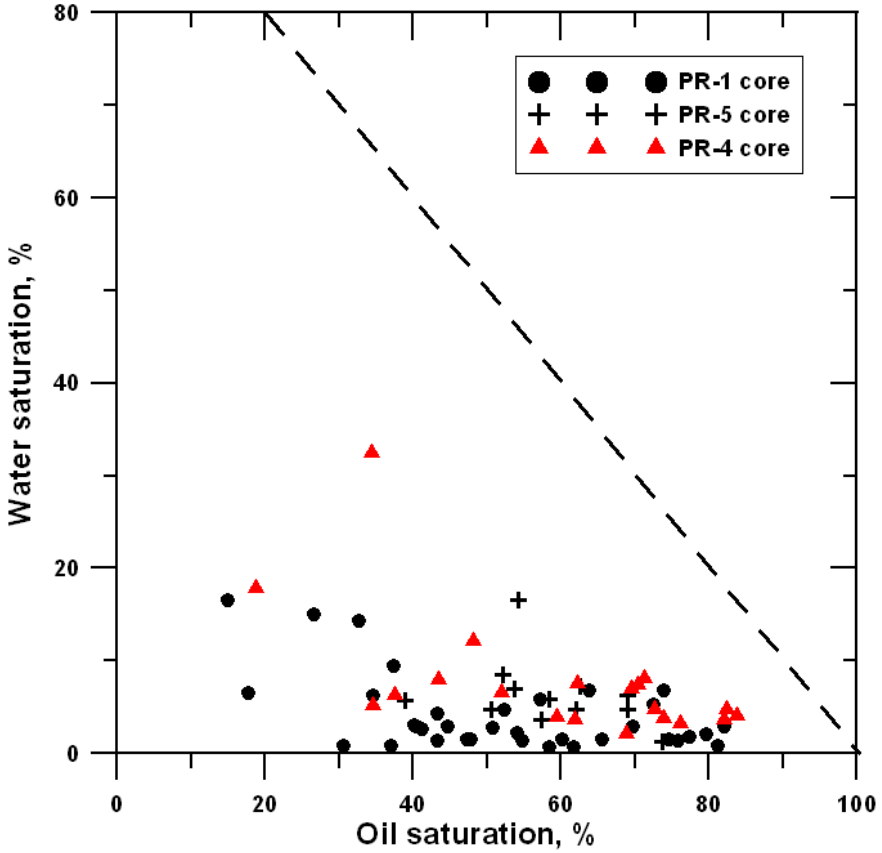

Figure 8: Fluid saturations measured in the three cores in the Asphalt Wash sector, wells PR1, PR-5, and PR-4. Note that none of the So + Sw values equal 100%, which is represented by the dashed line. Data from Peterson and Ritzma (1974).

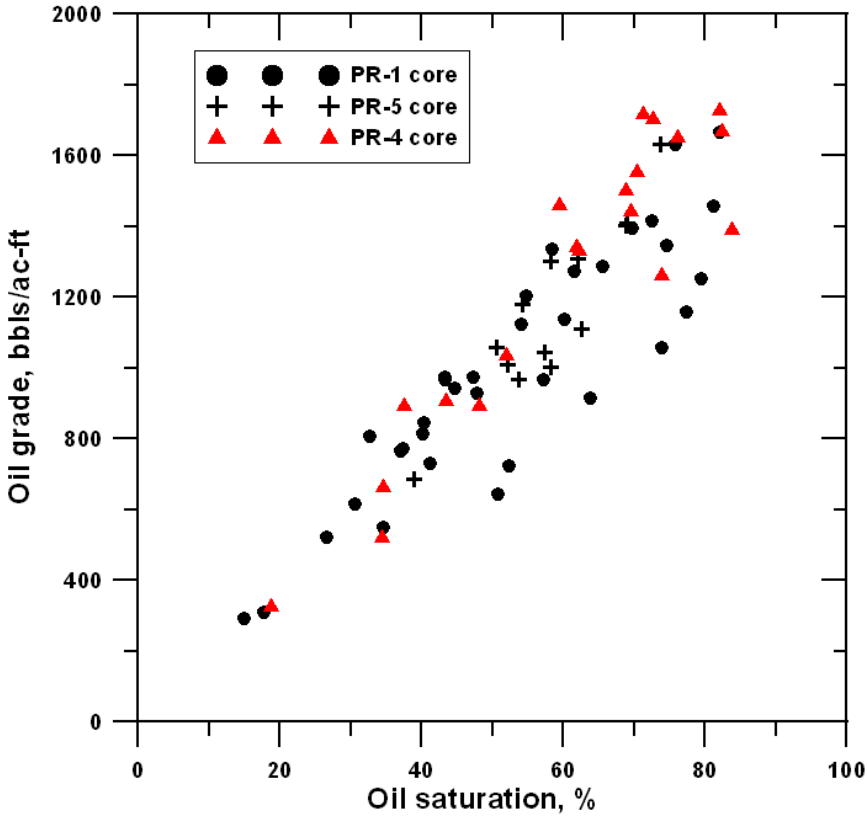

Figure 9: Fluid saturations measured in the three cores in the Asphalt Wash sector, wells PR1, PR-5, and PR-4. Note that none of the So + Sw values equal 100%, which is represented by the dashed line. Data from Peterson and Ritzma (1974).

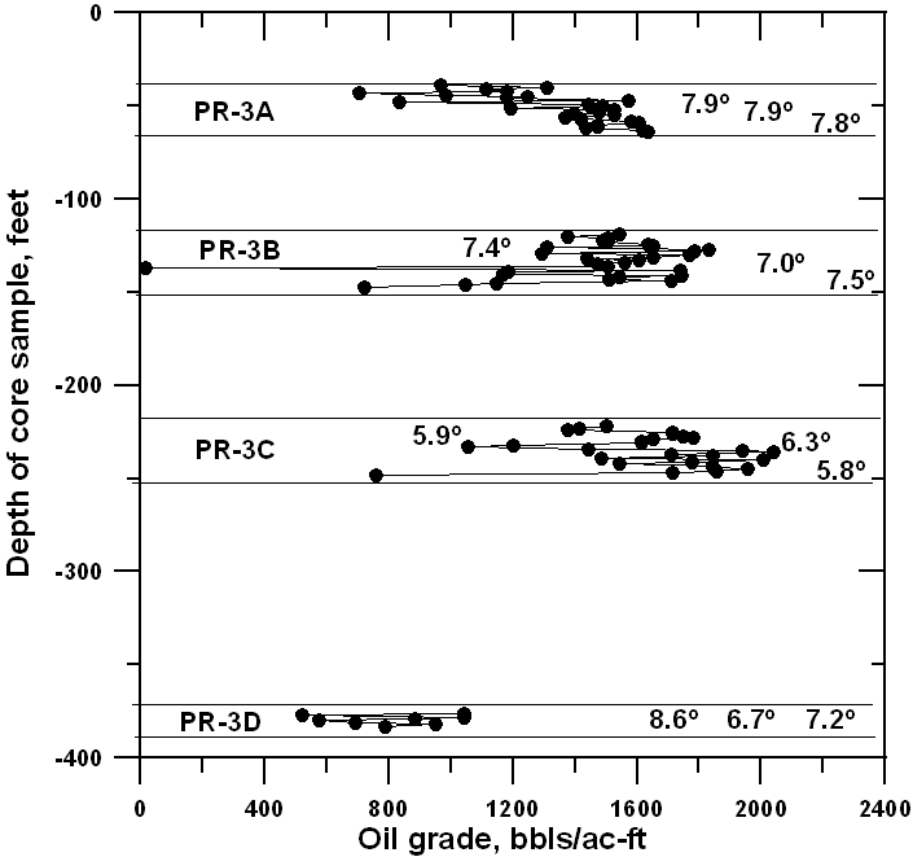

Figure 10: Composite oil grade profiles for the four test wells in the Threemile Canyon sector (Fig. 4; Table 2). A single, relatively thin oil-impregnated zone dips northward to progressively greater depths below the land surface. Each separate profile is from a different well penetrating this zone. API gravities measured in the core samples are shown on the profiles. Note that the oil grades increase with increasing depth until diminishing as the presumed bottom water region is approached in well PR-3D. Data from Peterson and Ritzma (1974).

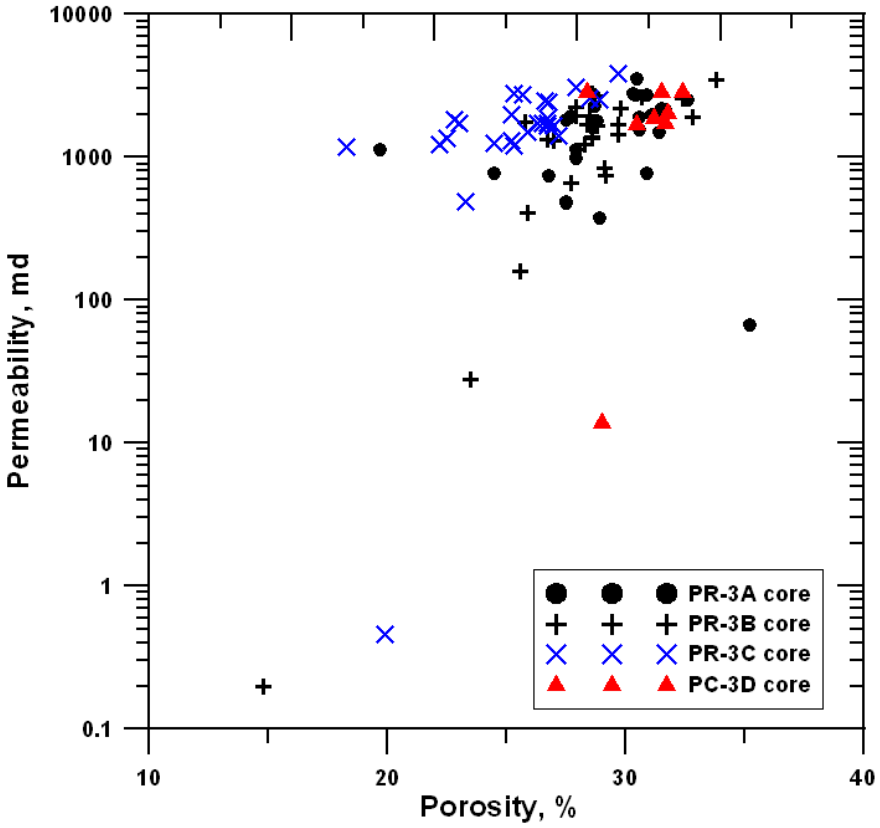

Figure 11: Porosity and permeability measured in cores from the four test wells in the Threemile Canyon sector (Fig. 4; Table 2). Note the distinct clustering of values from different wells penetrating the same sandstone reservoir unit. Data from Peterson and Ritzma (1974).

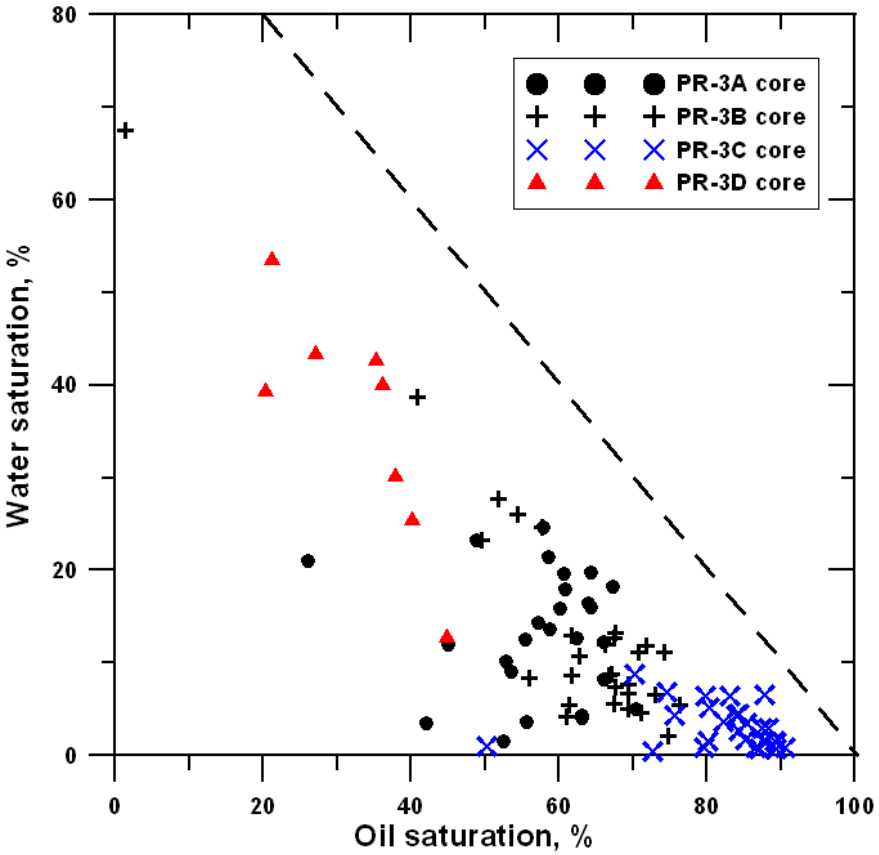

Figure 12: Variations in fluid saturations measured in cores from the four test wells in the Threemile Canyon sector (Fig. 4; Table 2). Note the distinct clustering of values from different wells penetrating the same sandstone reservoir unit, with the higher water saturations in the deeper core (PR-3D). Data from Peterson and Ritzma (1974).

In terms of OOIP, the Seep Ridge sector is the richest part of the deposit (Johnson and others, 1975), with an average 57.6 MBO/acre (see Table 1). In general, all of the five wells in this sector have higher than normal OOIP values, ranging from a high of 86.5 MBO/acre (PRS-1; Fig. 13) to a low of 39.5 MBO/acre. The overall richness is attributable to the unusually large net thickness of the oil-impregnated sands beneath Seep Ridge, which average 71 ft and range from 96 to 42 ft. It is in this sector that especially thick individual oil-impregnated sandstone beds are observed, ranging from 19 to 24 ft. However, the oil grades are not especially high. All are less than 940 BO/ac-ft and average just 831.2 BO/ac-ft. Higher grades are observed in all of the sectors to the east, but smaller net thicknesses result in generally smaller OOIP (Table 1).

The oil-impregnated sandstones penetrated by the test wells on Seep Ridge exhibit a higher degree of variability of porosity, permeability, and fluid saturations (Figs.14 and 15) than those of Asphalt Wash (Fig. 7 and 8). Both average porosity and average permeability diminish downdip (northward) from well PRS-1 to well PR-6: 28.3% to 24.9% and 1624 md to 230 md, respectively (Table 2). However, there is little difference between the wells in terms of fluid saturations despite the very large variability measured in each of the four wells (Fig. 15). The PR-6 well is in the downdip (northern) portion of Seep Ridge (Fig. 4). This well penetrated 13 separate oil-impregnated beds, the thickest of which is 19 ft. The net-to-gross ratio within the 227 ft interval containing oil-impregnated sandstones is 0.29. Oil grades diminish with depth and average 728.2 BO/ac-ft for the entire well. The oil density generally increases with depth.

Table 1 presents oil grade and OOIP values for two oil-saturated sandstone beds in and near the M&E Company mine above the Roan Cliffs at the head of Main Canyon and in the upper

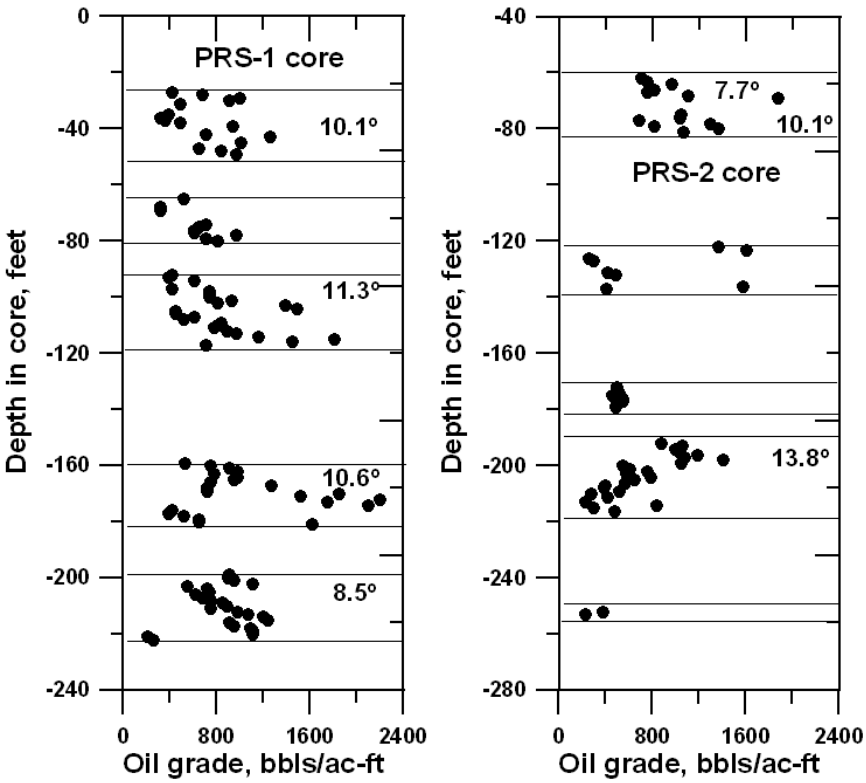

Figure 13: Grade of heavy oil in bitumenous sandstone intervals in the PRS-1and PRS-2 (Seep Ridge) cores plotted against depth of the samples in the wells. The clustering of values shows the thickness and spacing of the bitumenous sandstone lenses penetrated by the test wells. The gross and net thicknesses of the bitumenous sandstone deposit are presented in Table 1; the maximum bitumenous sandstone bed thickness and the number of oil-impregnated beds in the deposit are presented in Table 2. The net to gross ratios for PRS-1 and HC-1 are 0.49 and 0.29, respectively. The API gravity of the heavy oil and bitumen extracted from the core is shown in the position of the sample in the well. Data from Peterson and Ritzma (1974).

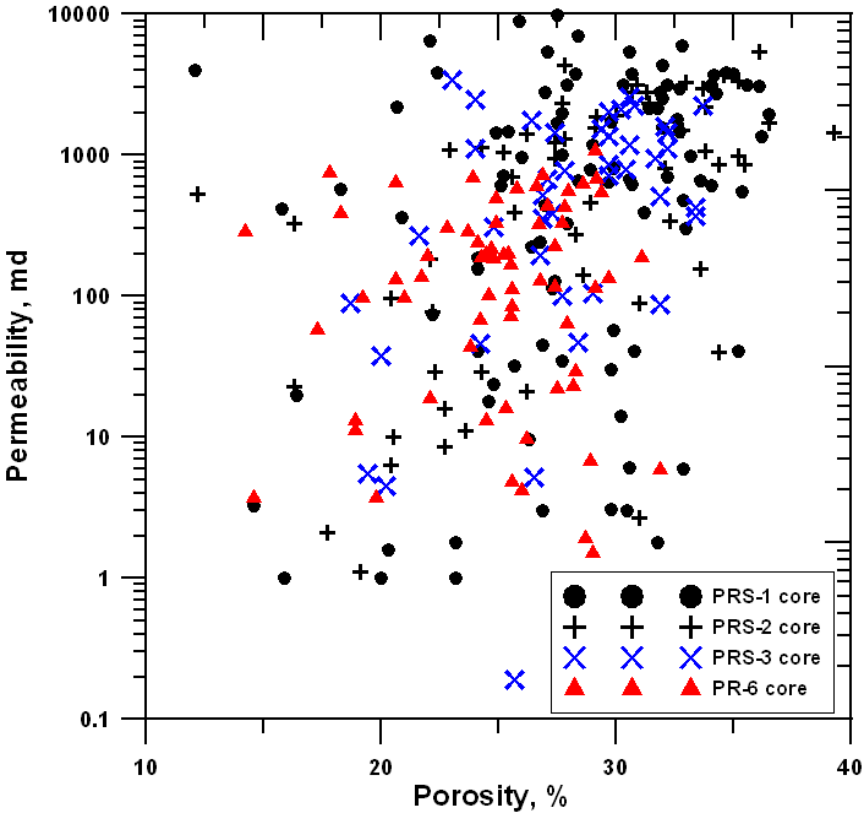

Figure 14: Variations in porosity and permeability measured in core from test wells in the Seep Ridge sector. Data from Peterson and Ritzma (1974).

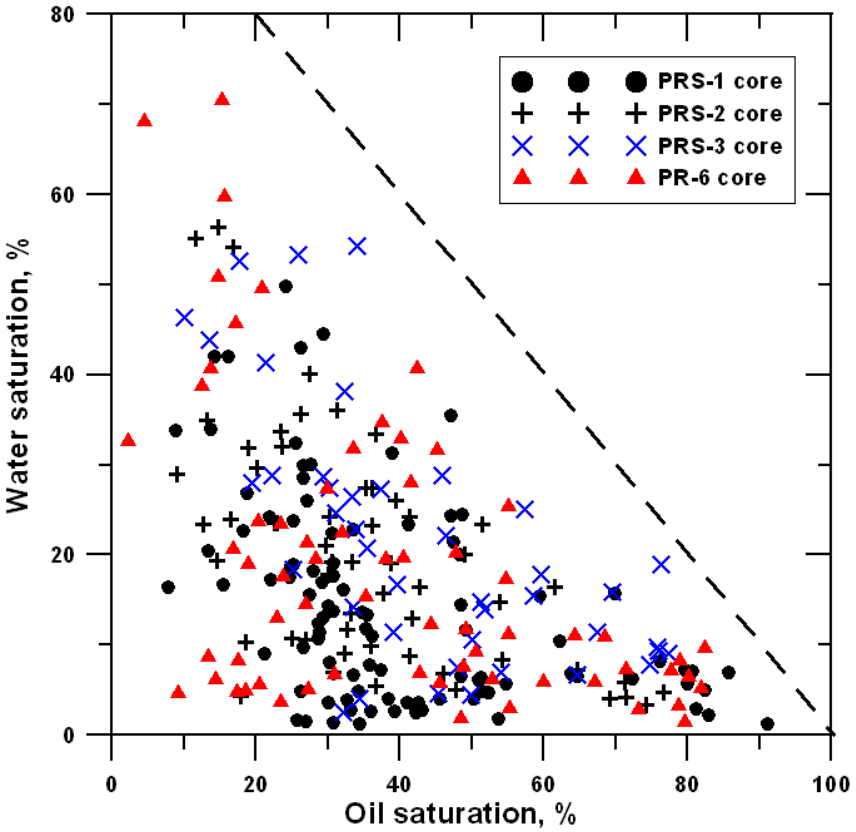

Figure 15: Variation in fluid saturations measured in core samples from test wells in the Seep Ridge sector. Data from Peterson and Ritzma (1974).

reaches of Seep Ridge. The values presented (1784.2 BO/ac-ft and 101.96 MBO/acre) are derived from average oil grade and bed thicknesses reported by Covington and Young (1985). Raw data from the two test wells were not available to independently confirm the average values reported.

The PR-7 well (Fig. 16) is in the updip (southern) portion of Sweetwater Canyon. This well penetrated only six beds, all of which, except one, are very thin. The single exception, near the top of the pay interval, is 15 ft thick and has the highest oil grades. The net-to-gross ratio within the 163-ft interval containing oil-impregnated sandstones is just 0.14. Due to the very high oil grades in the uppermost pay interval the average oil grade for the well is 1176.1 BO/ac-ft.

The Meadow Creek sector is situated on the plateau between Main Canyon and Willow Creek (Fig. 4). Well UTS-5 penetrated six oil-impregnated sandstone beds, the thickest of which is 25 ft (Fig. 17). The net-to-gross ratio in the 222-ft interval containing oil-impregnated sandstones is just 0.18 and the average oil grade is 667.0 BO/ac-ft. The 32-mile distant UTS-4 well penetrated 16 oil-impregnated sandstone beds, the thickest of which is 16 ft (Fig. 17). The net-to-gross within the 334-ft interval containing oil-impregnated sandstones is 0.23 and the average oil grade is only 171.4 BO/ac-ft. For the three wells in the sector, the average oil grade is 386.6 BO/ac-ft and the average OOIP is only 17.0 MBO/acre.

The Hill Creek sector is located northwest of the Meadow Creek sector on the west side of Willow Creek (Fig. 4). Both sectors are similar in having relatively low oil grades and low OOIP (Table 1). With the exception of well HC-1, the net thicknesses of oil-impregnated sandstones are low. This well has an estimated OOIP of 45.4 MBO/acre, which is three times that of the HC-2 and HC-3 wells farther to the west. In these two wells (Fig. 18) a single 11-

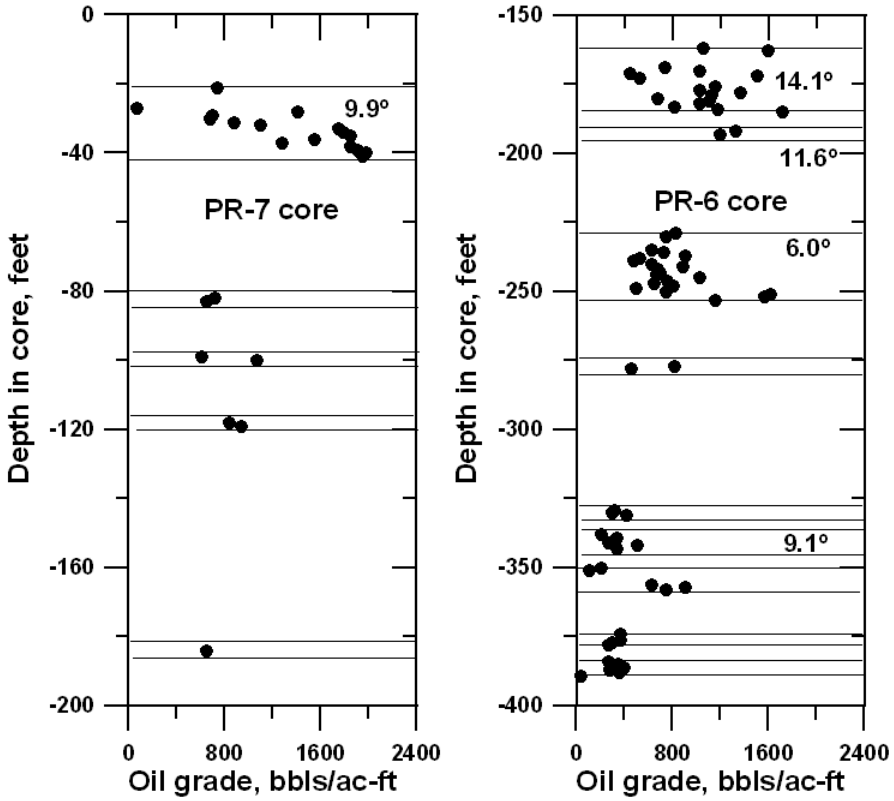

Figure 16: Grade of heavy oil in bituminous sandstone intervals in the PR-7 (Sweetwater Canyon) and PR-6 cores (Seep Ridge) plotted against depth of the samples in the wells. The clustering of values shows the thickness and spacing of the bituminous sandstone lenses penetrated by the test wells. The gross and net thicknesses of the bituminous sandstone deposit are presented in Table 2; the maximum bituminous sandstone bed thickness and the number of oil-impregnated beds in the deposit are presented in Table 3. The net to gross ratios for PR-7 and PR-6 are 0.14 and 0.29, respectively. The API gravity of the heavy or extra-heavy oil extracted from the core is shown in the position of the sample in the well. Data from Peterson and Ritzma (1974).

Figure 17: Grade of heavy oil in bituminous sandstone intervals in the UTS-5 and UTS-4 (Hill Creek) cores plotted against depth of the samples in the wells. The clustering of values shows the thickness and spacing of the bituminous sandstone lenses penetrated by the test wells. The gross and net thicknesses of the bituminous sandstone deposit are presented in Table 2; the maximum bituminous sandstone bed thickness and the number of oil-impregnated beds in the deposit are presented in Table 3. The net to gross ratios for UTS-5 and UTS-4 are 0.18 and 0.24, respectively. Data from Peterson and Ritzma (1974).

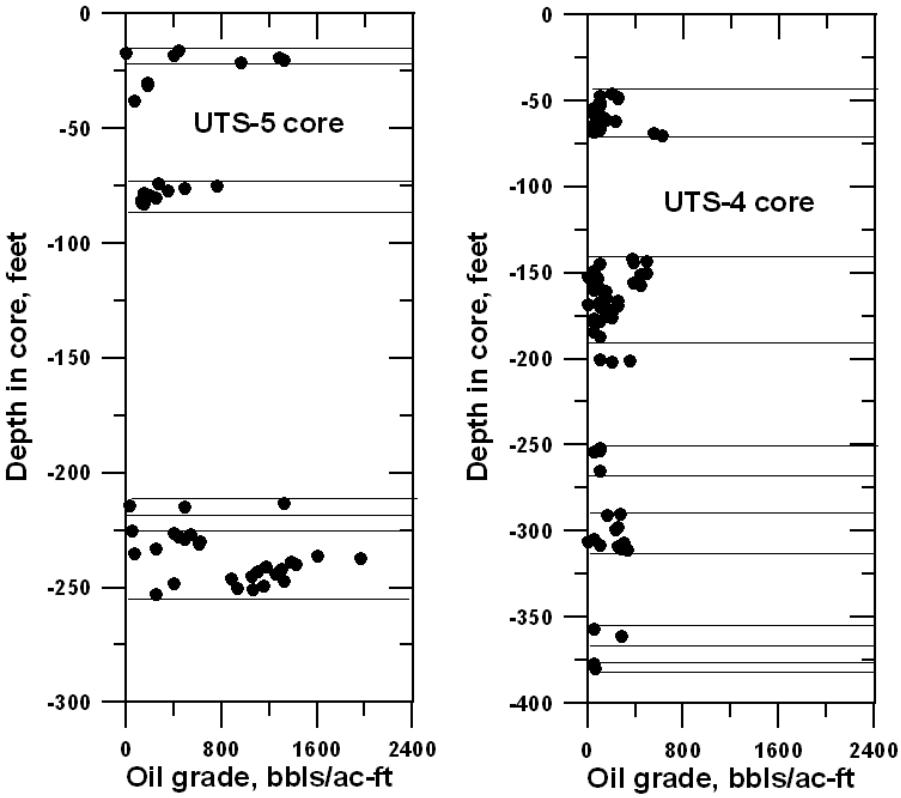

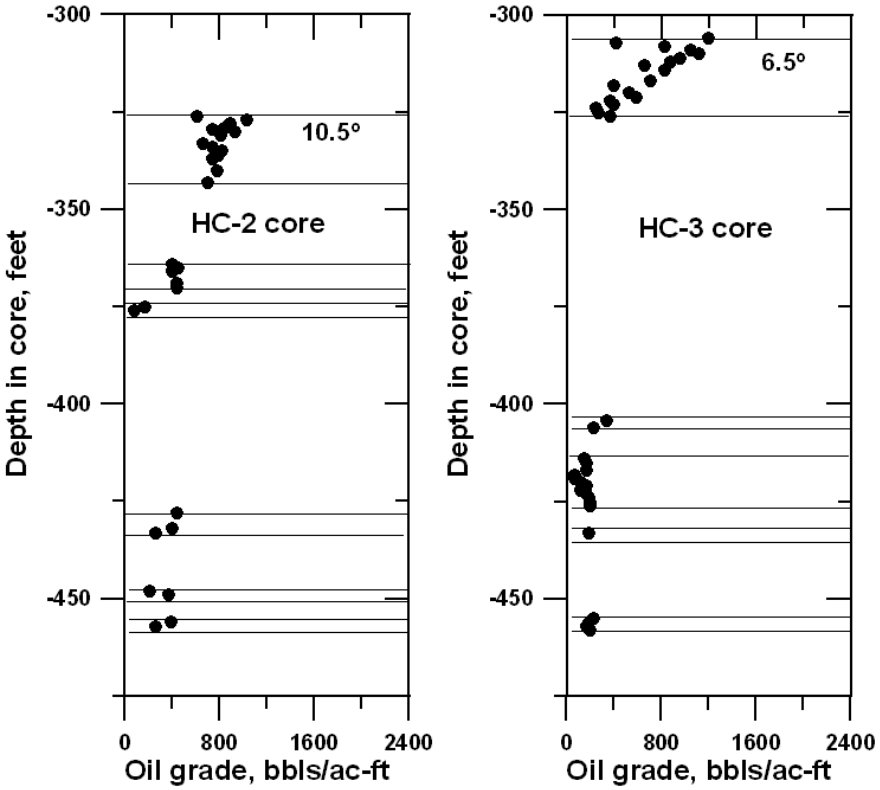

Figure 18: Grade of heavy oil in bitumenous sandstone intervals in the HC-2 and HC-3 (Hill Creek) cores plotted against depth of the samples in the wells. The clustering of values shows the thickness and spacing of the bitumenous sandstone lenses penetrated by the test wells. The gross and net thicknesses of the bitumenous sandstone deposit are presented in Table 2; the maximum bitumenous sandstone bed thickness and the number of oil-impregnated beds in the deposit are presented in Table 3. The net to gross ratios for HC-2 and HC-3 are 0.21 and 0.24, respectively. The API gravity of the heavy or extra-heavy oil extracted from the core is shown in the position of the sample in the well. Data from Peterson and Ritzma (1974).

12-ft-thick bed near the top of the section holds virtually all of the oil. Compared to most other sectors of the deposit, porosity, and permeability of the reservoir sandstones (Fig. 19) in the Hill Creek sector are systematically low, averaging 21.5% and 266 md, respectively. In general, oil saturations (Fig. 20) are lower than in other parts of the deposit (Table 2), averaging 33.2% as opposed to the normal 45% to 60% farther to the east. In the Hill Creek sector the reservoired oil is extra-heavy, ranging from 5.5º to 10.5º and averaging 7.9º.

The discussion above is intended to demonstrate the high degree of diversity within the P.R. Spring-Hill Creek heavy oil accumulation. However, with a sampling of just 26 wells, which is equivalent to one well per 18.1 sections, it is difficult to know how representative the data presented in Tables 1 and 2 are of the entire deposit. The ranges of sector averages may be the best indicator of the characteristics of the deposit as a whole. Sandstone porosity and permeability are 21.8% to 28.4% and 336 md to 1,757 md, respectively. The higher values are from the single thick sandstone bed in the Threemile Canyon area and the lowest values are from the Meadow Creek-Hill Creek sectors. Oil saturations vary considerably within sectors with 9.4% being the lowest value reported overall and 82.3% the highest. Broadly, average oil saturations decrease from east to west. Also within a given sector water saturations tend to decrease with increasing depth of the pay interval, perhaps indicating the presence of bottom water and/or the transition into the oil-water contact. These trends in oil saturation influence the general reduction in average oil grade from east to west, and in some sectors from shallow to deep (Tables 1 and 2).

The average sector OOIP values range from a high of 57.57 MBO/acre in Seep Ridge to a low of 13.52 MBO/acre in the adjacent Sweetwater Creek area. The average OOIP for all seven sectors is 26.89 MBO/acre or 17.212 MMBO/section. If this can be taken as a reasonable estimate for the entire 470 section (square mile) heavy oil accumulation, the size of the deposit

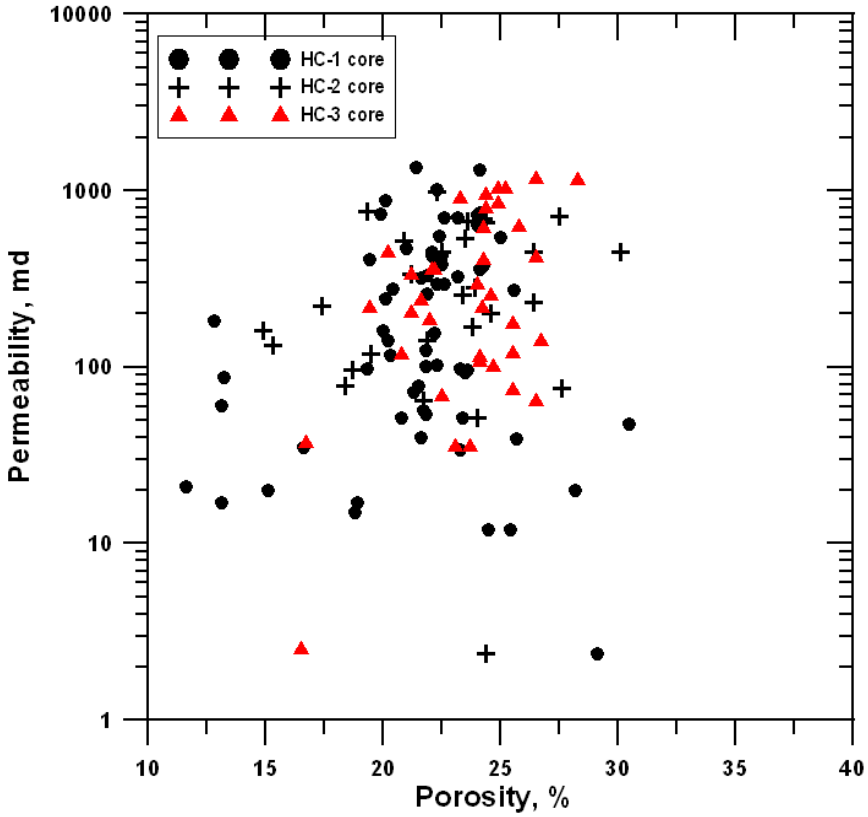

Figure 19: Porosity and permeability measured in oil-impregnated sandstones in the Hill Creek sectors wells. Data from Peterson and Ritzma (1974).

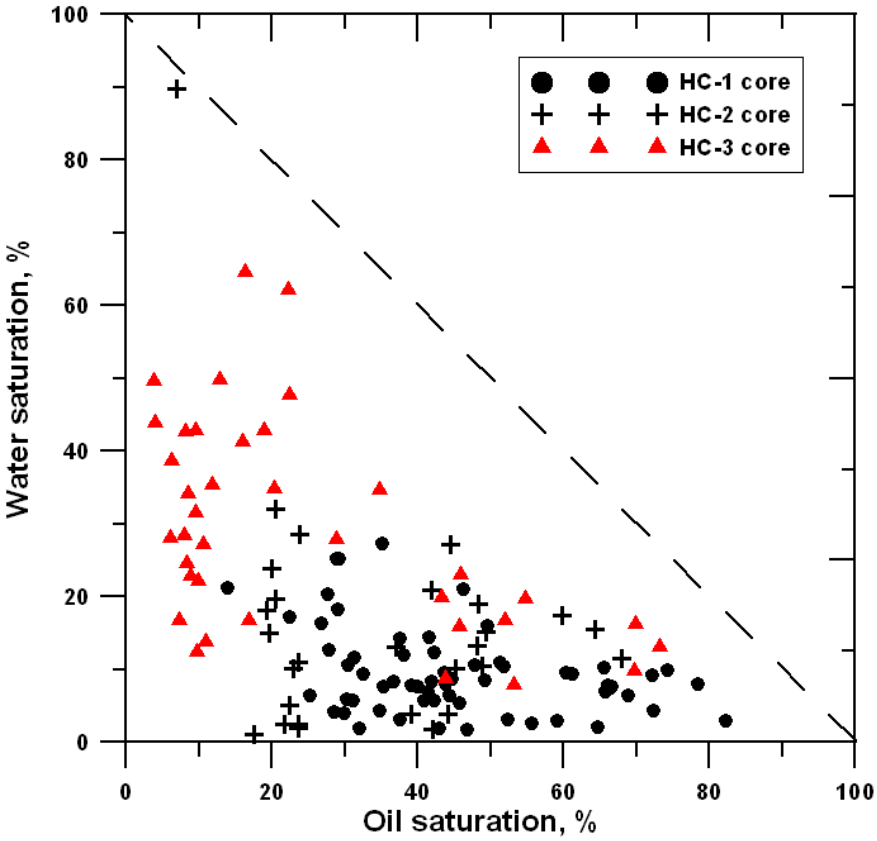

Figure 20: Fluid saturations measured in core samples of oil-impregnated sandstones in the Hill Creek sector. Note the decrease in oil saturation from the HC-1 well to the HC-3 well. Refer to Table 3 for the average values of fluid saturations in these three wells. Data from Peterson and Ritzma (1974).

is just under 8.1 billion barrels. This is a larger estimate than previously reported for the deposit (Ritzma, 1979). However, despite the very large size of this total oil accumulation, the important OOIP number is 26.9 MBO/acre, which is rather lean for commercial exploitation.

From the perspective of *in situ* recovery of the heavy oil, the P.R. Spring-Hill Creek accumulation presents multiple challenges, the most significant of which is not just the overall leanness of the deposit. The oil-impregnated sandstones are thin and highly discontinuous, and commonly they are intercalated with shales and carbonates that would inhibit all common recovery methods. Sandstone permeabilities and initial oil saturations generally are low compared to heavy oil reservoirs presently in production.

Sunnyside Deposit

The Sunnyside heavy oil accumulation (Holmes and Page, 1956) is found on the southern rim of the Uinta Basin where sandy Paleocene and Eocene strata support the West Tavaputs Plateau and its western erosional edge, the Roan Cliffs (Fig. 21). In the area of the deposit, strata dip at 7º to 14° to the northeast, flattening across Bruin Point-Mount Bartles flexure in the shallow monocline to about 3º to 4° (Fig. 22). The normal direction of dip along the south margin of the Uinta Basin is northward, but at Sunnyside the basin margin is deflected by the plunging nose of the Laramide-age San Rafael Swell where it intersects the reactivated WNW-trending Uncompaghre uplift, a late Paleozoic Ancestral Rockies basement uplift.

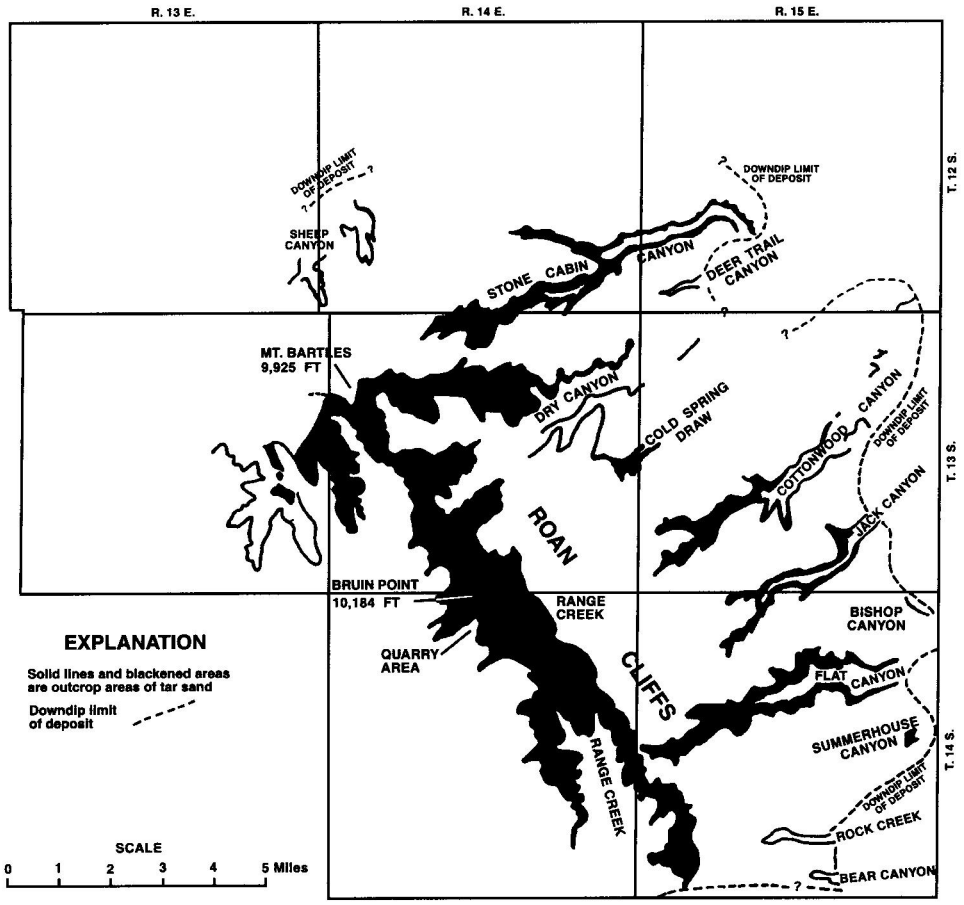

Figure 21: The surface exposures of bitumen-impregnated sandstones that define the known limits of the Sunnyside deposit (Gloyn and others, 2003). The tar sands are exposed in the steep western face of the Roan Cliffs and the several canyon walls incised into the dip slope to the northeast.

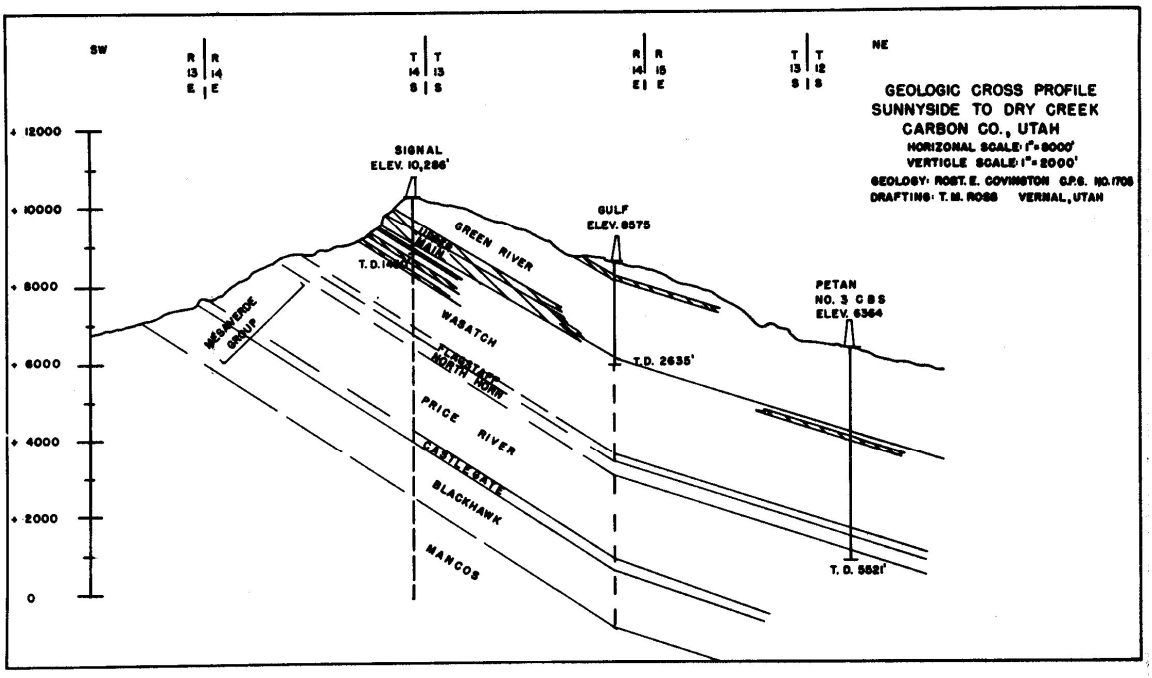

Figure 22: Geologic cross section through the Sunnyside heavy oil deposit from the town of Sunnyside northeast to Dry Canyon (Covington and Young, 1985).

Estimates of the oil-in-place within the Sunnyside heavy oil deposit have tended to be quite large, ranging from 3.5 to 5.8 billion barrels. Ritzma (1979) proposed 3500 to 4000 MMBO (1250 measured and 1750 indicated) of OOIP. Including the small Cottonwood-Jacks Canyon extension (see Fig. 21), Oblad and others (1987) estimated a considerably larger resource of 5200 to 5850 MMBO (1800 measured and 2200 indicated). The size of the deposit, though difficult to know with certainty, is at least 122 sections or 78,080 acres (Blackett, 1996). A uniform distribution of the estimated resources across an area of this size would yield an OOIP in the range of 45 to 75 MBO/acre. Such low oil-in-place values are hardly encouraging for the commercial development of the deposit. Fortunately, the bulk of the heavy oil in this accumulation is concentrated in a relatively small area (Gwynn, 1986).

The dip and strike sections in Fig. 23 depict the vertical and lateral variations in the density of bitumen-impregnated sandstone intervals (zones) near the crest of the Roan Cliffs. The cross sections intersect near Bruin Point (elev. 10,138 ft), where there is a maximum concentration of heavy oil resources.

In the area of the West Tavaputs Plateau, the Green River Formation has three distinct members (Fig. 23). At this position near the south shore of Lake Uinta, the lower unit, the *Douglas Creek Member*, is dominantly deltaic in character. The middle unit, the *Garden Gulch Member*, was deposited in a shoreline to shallow lacustrine setting. The upper unit, the *Parachute Creek Member*, represents an open lacustrine to marginal lacustrine depositional environment. It is this latter unit that contains the majority of the oil shale horizons of the Uinta-Piceance Basin. Deltaic activity was in decline during Garden Gulch time and was quite rare following deposition of the "Blue marker" in Parachute Creek time. The stratigraphy of the Green River Formation in the Roan Cliffs records the gradual expansion through the early Eocene of Lake Uinta southward across a major floodplain and delta system entering the lake from the south or southwest.

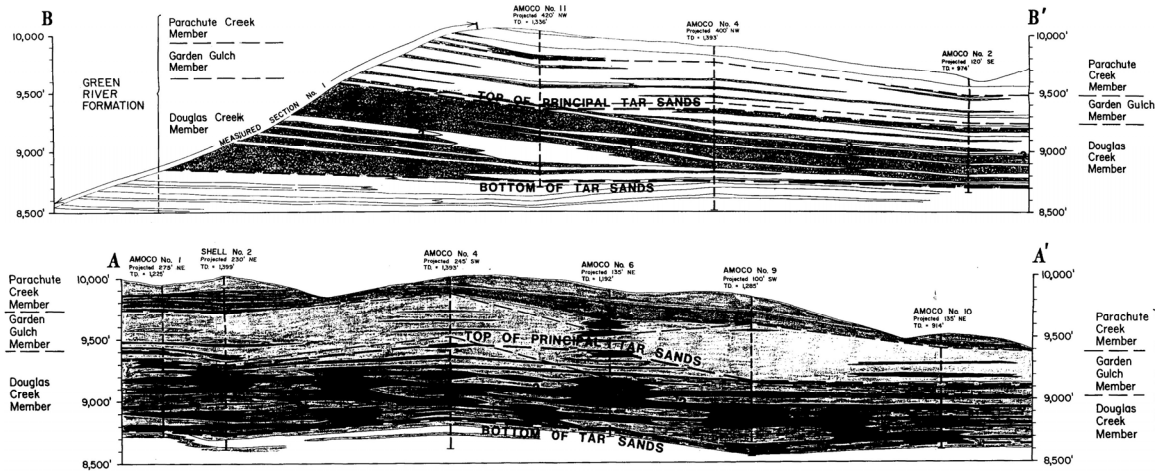

Figure 23: Dip section (B-B') through the Sunnyside heavy oil deposit showing the distribution of bitumen-impregnated sandstone intervals and a strike section (A-A') along the crest of the Roan Cliffs north and south of Bruin Point (Calkin, 1980).

In the West Tavaputs Plateau, the 1500-2000 foot thick Douglas Creek Member is divided into three informal units (Calkin, 1990). The middle and lower portions are divided by a prominent 80ï 100 ft red shale and limestone marker. The base of the lower portion (above the Colton Wasatch Formation) is taken to be the first occurrence of fresh-water ostracod coquina, but on the whole the Douglas Creek Member differs from the Colton in having light gray fine-grained sandstones, as opposed to reddish medium-grained sandstones (Calkin, 1991). However, the differences are subtle, so some authors (e.g., Ryder and others, 1976; Schenk and Polastro, 1987) have included the lower parts of this member in the Colton (Wasatch) Formation. The greater majority of the oil-impregnated sandstones (Zones 31ï 45) are located in the 800 ft upper portion of the Douglas Creek Member. The upper portion also contains numerous algal and ostracodal limestone intervals that generally form the tops of distinct 4th-order deltaic-lacustrine depositional sequences.

The 300ï 500-ft-thick Garden Gulch Member is characterized by a shallow lacustrine-shoreface green shale facies with abundant algal limestone and ostracod coquinas. In addition, there are intercalated beach and distributary channel mouth bar sandstones, some of which are oil-impregnated. However, little of the Sunnyside heavy oil deposit is reservoired in these sandstones. The 50ï 70-ft-thick *carbonate interval* forms the base of the member.

The Parachute Creek Member forms the crest of the Roan Cliffs and the higher benches of the West Tavaputs Plateau. In the area of the Sunnyside deposit, it is up to 600 ft thick. It is a black shale unit deposited under mainly deeper lacustrine conditions. There are numerous oil shale and tuff intervals, but no ostracod limestones. This is certainly the source rock unit for the Sunnyside deposit, yet it does not itself contain any of the oil-impregnated sandstone intervals (Calkin, 1989). Beneath the Tavaputs Plateau, the Parachute Creek Member is at too low a thermal maturity to have generated oil (Morgan and others, 2003).

Holmes and others (1948) mapped the surface exposures of the oil-impregnated sandstones in the western face of the Roan Cliffs. They identified 32 distinct tar sand intervals at the head of Water Canyon near Bruin Point. The thickest part of the deposit is at Bruin Point and in the Central Overlook and Southern Overlook immediately to the north and south, respectively, of Bruin Point. They observed that both the number of oil-impregnated intervals and net thickness

diminishes rapidly to the north of the Central Overlook at the head of Dry Creek Canyon and to the south of the Southern Overlook. Within a single sandstone interval, oil-saturation can change from heavy to none over a distance of just a few hundred feet (Holmes and Page, 1956; Clem, 1985).

Intensive coring during the late 1970s and early 1980s confirmed that the oil-impregnated sandstones are concentrated within a narrow northwest-trending belt that parallels the Roan Cliffs between the headwaters of Dry Creek Canyon and Range Creek and that is centered on Bruin Point (Calkin, 1981; Calkin, 1990). The belt is 6 to 8 miles long, 1 to 2 miles wide, and 300 to 1100 ft thick (Fig. 24). The volume of heavy oil decreases over a very short distance outside of this well-defined oil-rich area.

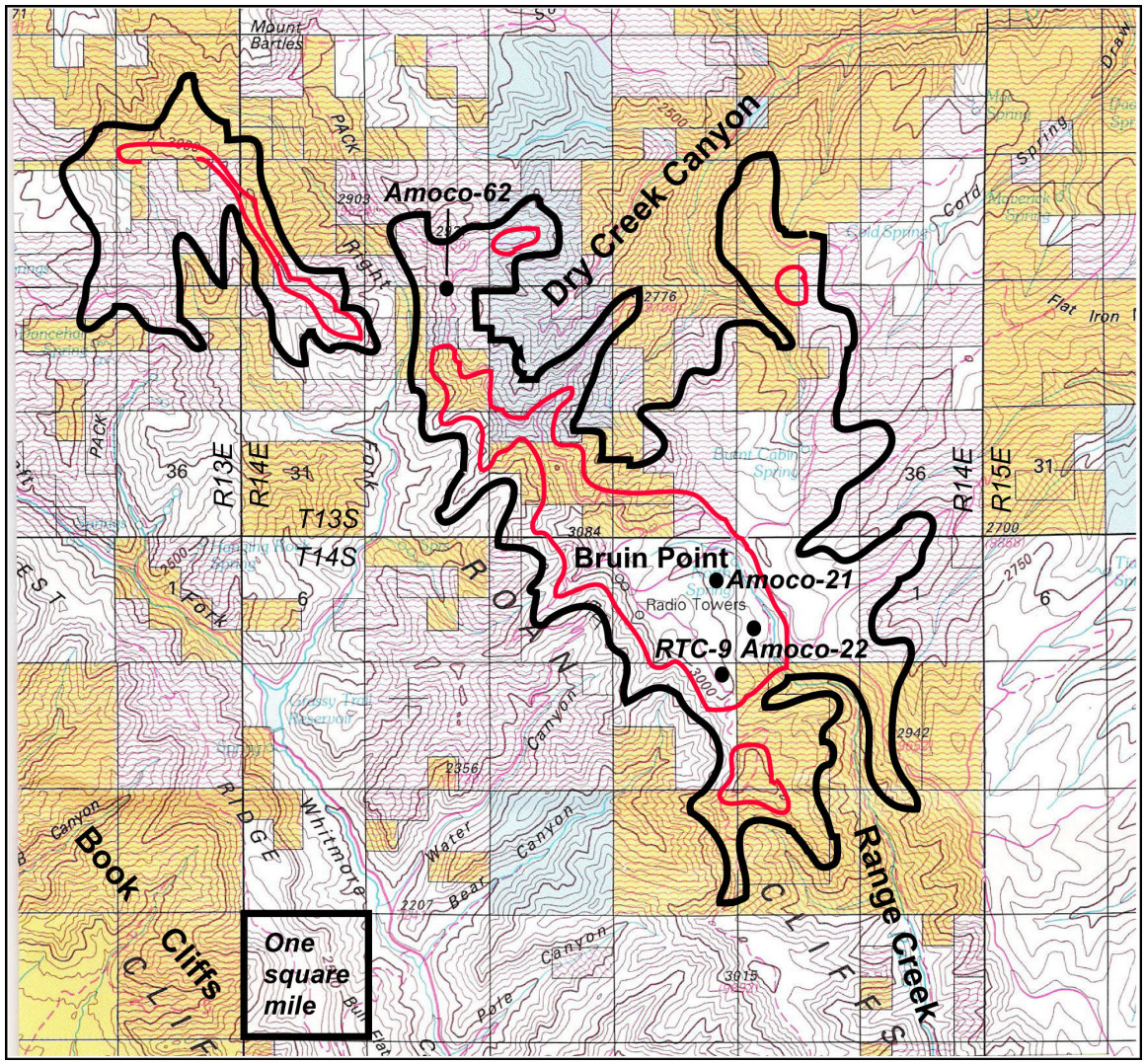

Figure 24: Areas of the Sunnyside deposit where the net thickness of oil-impregnated sandstone exceeds 50 feet (black line) and 200 feet (red line). Except for the broad plateau east of Bruin Point, the 100-foot net thickness isopleths are located very close to the 200-foot isopleths. A portion of the thickness variation is related to depositional thickness of the sandstones, but a substantial portion is due to erosional truncation of the oil-impregnated sandstones along canyon walls.

The West Tavaputs Plateau is traversed by an array of sub-parallel normal faults striking N65-70°W. These faults are the surface expression of the Laramide reactivation of the underlying Uncompaghre uplift, which shares the same strike trend. Along the northeast flank of the Uncompaghre uplift are a series of small anticlines formed along the bounding transpressional Garmesa fault (Stone, 1977). These anticlines are the traps for the Stone Cabin, Nine Mile Canyon, Jacks Canyon, and Flat Rock gas and oil fields in the lower Green River and Colton sandstones, and still deeper reservoirs. It is likely that the west northwest-trending normal faults are locally trapping structures for conventional oil beneath or downdip within the Sunnyside deposit. At shallower depths, the normal faults are likely open to the circulation of meteoric waters.

There are two dominant orthogonal joint sets in the Roan Cliffs (Calkin, 1991). The northwest set parallels the N20-40°W strike of bedding, which is controlled by the trend of the Bruin Point-Mount Bartles flexure. The northeast set parallels the regional dip direction. In the underlying Cretaceous strata of the Book Cliffs, there is a single dominant joint direction with an orientation of N66-68°E. The presence of the joint sets may adversely affect the application of thermal recovery methods in the lithified oil-impregnated sandstones.

The main portion of the Sunnyside deposit near Bruin Point is a combined stratigraphic-structural trap formed where the maximum thickness of stacked deltaic sandstones is overprinted by the Bruin Point-Mount Bartles monocline flexure (Figs. 22 and 23). The heavy oil is concentrated in the steeper, western segment where dips are 7° to 12°NE (Calkin, 1990). As the lower Green River Formation flattens to the northeast to dips of just 3° to 5° northeast, the sands become thinner, less abundant in the section, and considerably less oil-saturated.

The reservoir sandstones are generally a fine grained sub-arkose with just 6% cement and matrix. The average grain size distribution is 17% medium grained, 54% fine grained, 23% very fine grained, and 6% silt and clay. However, the actual grain-size distribution is highly dependent on depositional facies (Fig. 25), which in turn constrains the petrophysical properties and range of oil grades of oil-impregnated sandstones. The coarser grained, more porous and permeable sandstones (channel, bar finger, and sheet sands) normally have the larger concentrations of oil.

Sandstone porosity averages about 27%, ranging 24-29%, and average permeability is 812 md, ranging from 37 to 3300 md (Banks, 1981; Remy, 1984). Campbell and Ritzma (1979) reported the following values, all of which are comparable to those observed in the P.R. Spring-Hill Creek oil-impregnated sandstones:

Parameter	**Mean ± Std. Dev.**	**Range**	**Number of Samples**
Porosity	23 ± 6.5%	(3.7 – 35.6%)	1627
Permeability	570 ± 700 md	(0 – 5,370 md)	804
Oil saturation	51.8 ± 28.3%	(2.0 – 90.0%)	1404
Water saturation	20.9 ± 16.1%	(0.0 – 97.0%)	1404

The vertical and lateral variability of bitumen concentration within the reservoir units of the Sunnyside deposit are illustrated by comparing the richness in the RCT-9 core in the central part of the Bruin Point sub-delta with the Amoco-62 core (Fig. 26) in the Dry Creek Canyon sub-delta. Both cores penetrate the entire oil-impregnated interval and both sets of analyses are of Soxhlet extractions. Yet the overall *average* and *median* values of grade are quite different: 1,019.1 and 1,019.8 BO/ac-ft, respectively, for the RCT-9 core and only 365.8 and 254.1 BO/ac-ft, respectively, for the Amoco-62 core. The richness of the RCT-9 core generally increases

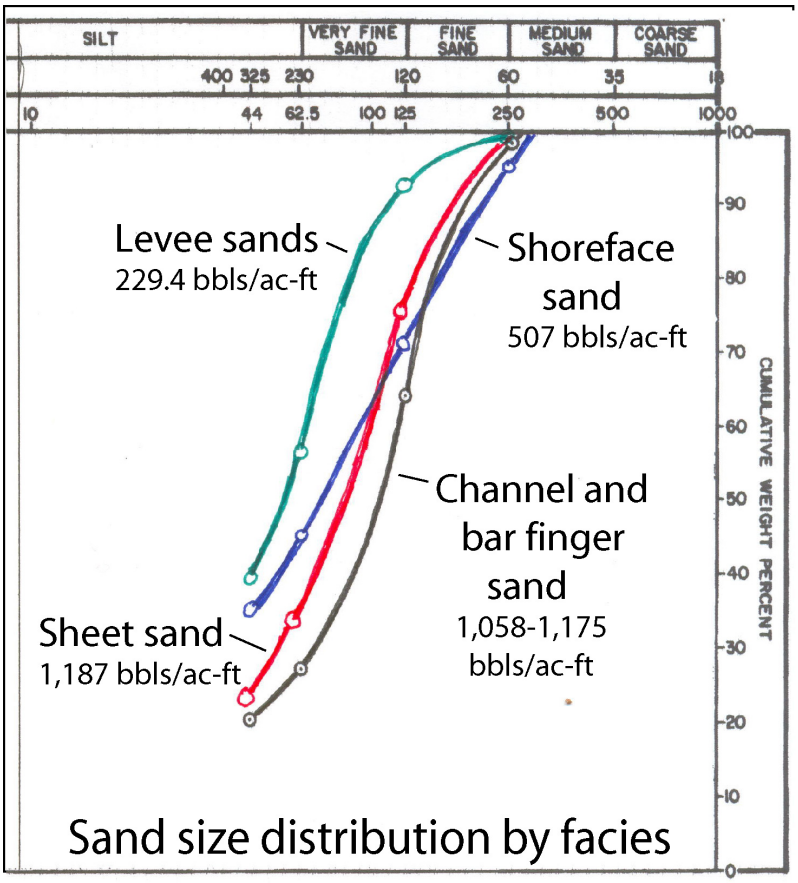

Figure 25: Average grain-size distribution within sandstones of differing depositional facies. Shown also is the average bitumen content within each depositional facies depicted in the set of cores in Figs. 27 and 32. Data from Calkin (1980).

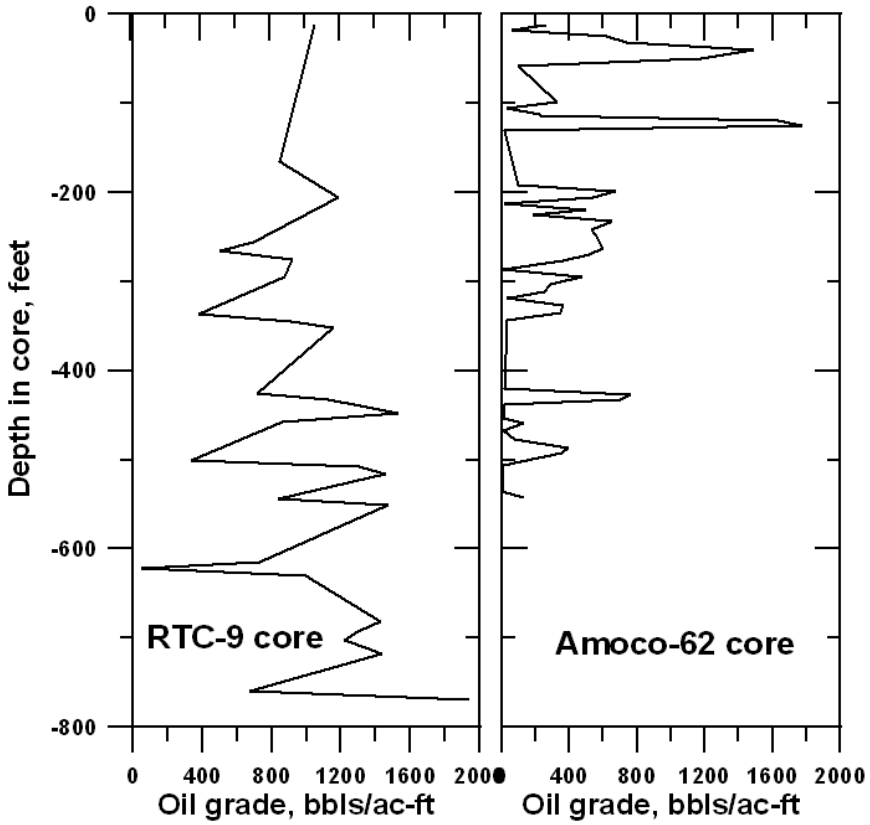

Figure 26: Vertical profile of oil grade of oil-impregnated sandstone intervals in the RCT-9 (NENE 10-T14S-R14E) and Amoco-62 (NWNE 3-T13S-R14E) cores. The RTC-9 core has 524.8 MBO/acre oil-in-place in a 515 foot net thickness; the apparent net-to-gross ratio is 0.49. The Amoco-62 core has 126.2 MBO/acre oil-in-place in a 343 foot net thickness; the net-to-gross ratio is 0.63.

with depth, whereas with the exception of two intervals near the top, the Amoco-62 core has relatively low values throughout. The Amoco-62 core penetrated just 343 ft of oil-saturated sandstones and has an estimated OOIP of only 126.19 MBO/acre. However, a prominent feature in both grade profiles is the presence of specific intervals that are appreciably richer in bitumen than the intervening intervals. This, of course, is tied to the fact that only the fluvial and littoral sandstones, not the interbedded mudstones and limestones, serve as reservoirs for the heavy oil.

The grade profile for Amoco-21 shows only the upper 800 ft of a 1068 ft core (Fig. 27). Beneath the profile shown in Figure 27 is a 184 ft continuous sandstone interval that is heavily oil-saturated, as well as two additional intervals of 4 and 7 ft thickness. The net thickness of oil-impregnated sandstone is 515 ft, which contains an estimated OOIP of 524.84 MBO/acre. The nearby Amoco-22 core (Fig. 32; SWSW 2-14S-14E) has an OOIP of 231.56 MBO/acre in a 469 ft net thickness; the net-to-gross is 0.57.

The relationship of oil grade to facies is shown in Figs. 27 through 34, in which the oil grade profiles are annotated with depositional facies interpreted by Calkin (1991) from sedimentologic features in the core. Amoco-21 and Amoco-22 cores are less than a mile apart on the west side of the upper reaches of Range Creek. Amoco-21 is to the north of Amoco-22, thus closer to Bruin Point. Within the Sunnyside deposit, the sandstone reservoir intervals represent either stream channel deposits, distributary channel deposits, distributary mouth bars,

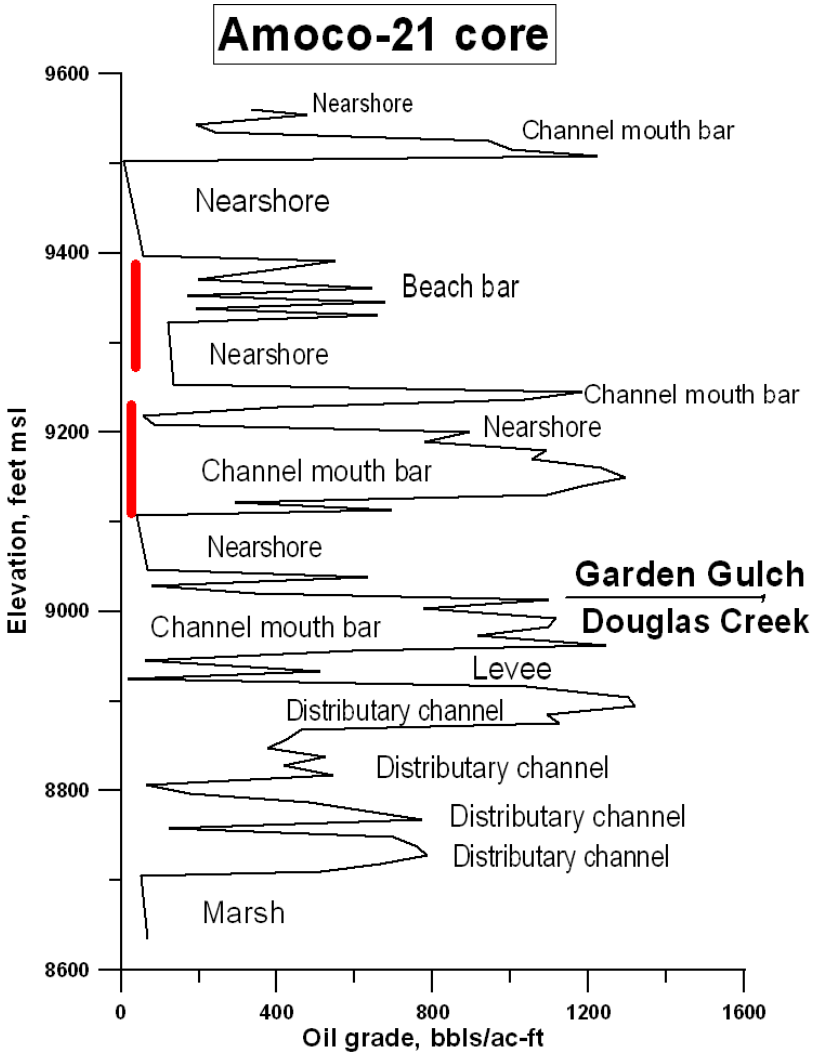

Figure 27: Vertical profile of grade of bitumen-impregnated sandstones in the Amoco-21 core (SENE 3-T14S-R14E). The depositional setting, as determined from interpretation of sedimentary structures in the core, is indicated. The core has an apparent 375.0 MBO/acre in 628 net thickness; the net-to-gross ratio is 0.68. Red bars indicate the locations of the core photographs in Figs. 28-31

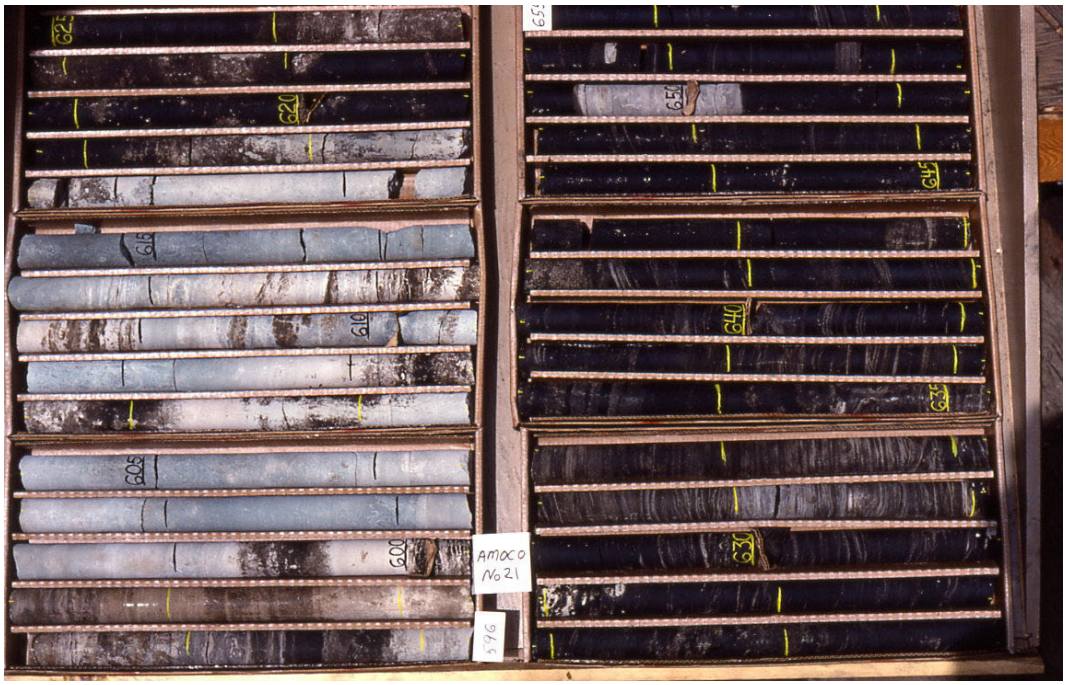

Figure 28: Core photograph of an oil-impregnated channel mouth bar deposit in Amoco- 21, 596-655 ft depth or elevation range 9,168 to 9,227 ft msl. Refer to this interval in the core profile in Fig. 27.

Figure 29: Core photograph of an oil-impregnated channel mouth bar deposit in Amoco- 21, 655-713 ft depth or elevation range 9,110 to 9,168 ft msl. Refer to this interval in the core profile in Fig. 27. This photograph continues the core shown in Fig. 28.

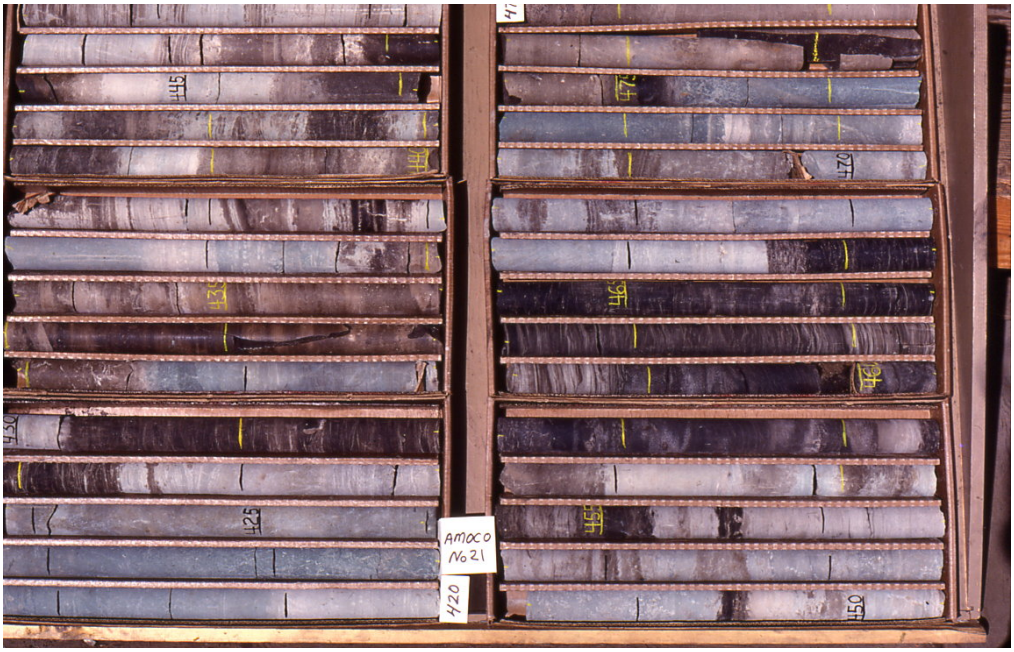

Figure 30: Core photograph of alternating beach bar sandstones and nearshore calcareous mudstone deposits in Amoco-21, 420-479 ft depth or elevation range 9,344 to 9,403 ft msl. This photograph is from the upper red interval indicated in the profile in Fig. 27.

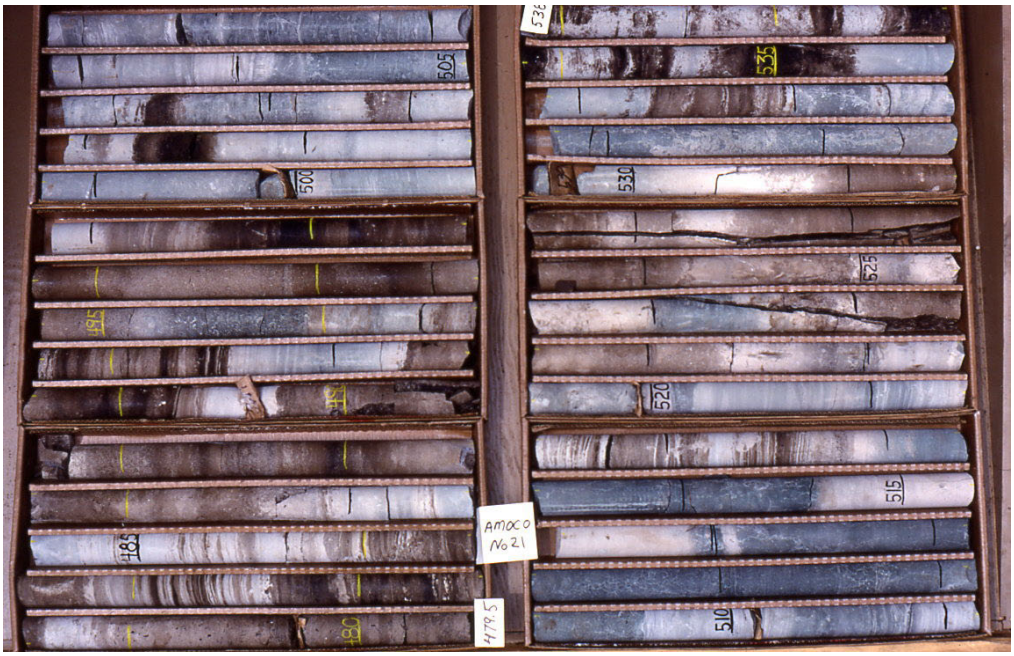

Figure 31: Core photograph alternating beach bar sandstones and nearshore calcareous mudstone deposits, in Amoco-21, 479-538 ft depth or elevation range 9,285 to 9,344 ft msl. This figure is the continuation of core shown in Fig. 30.

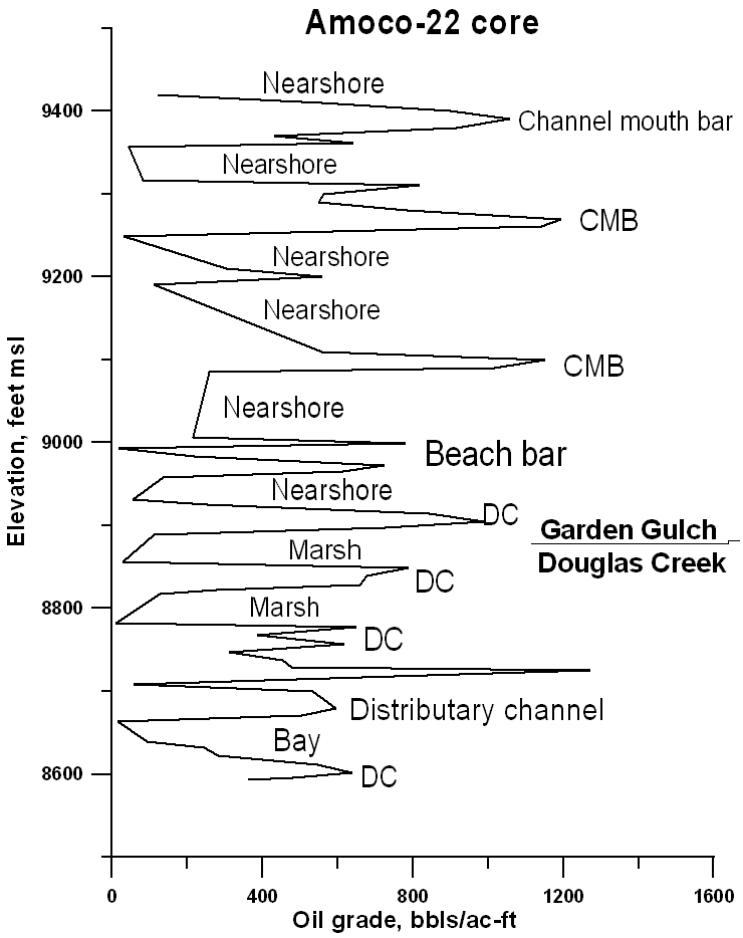

Figure 32: Vertical profile of grade of bitumen-impregnated sandstones in the Amoco-22 core (SWSW 2-T14S-R14E). The depositional setting, as determined from interpretation of sedimentary structures in the core, is indicated. The core has 231.56 MBO/acre oil-in-place in a 469 foot net thickness; the net-to-gross ratio is 0.57.

Figure 33: Core photograph of a distributary channel deposit flanked by levee deposits in Amoco-22, 559-618 ft depth or elevation range 8,871 to 8,930 ft msl. Refer to this interval in the core profile in Fig. 32.

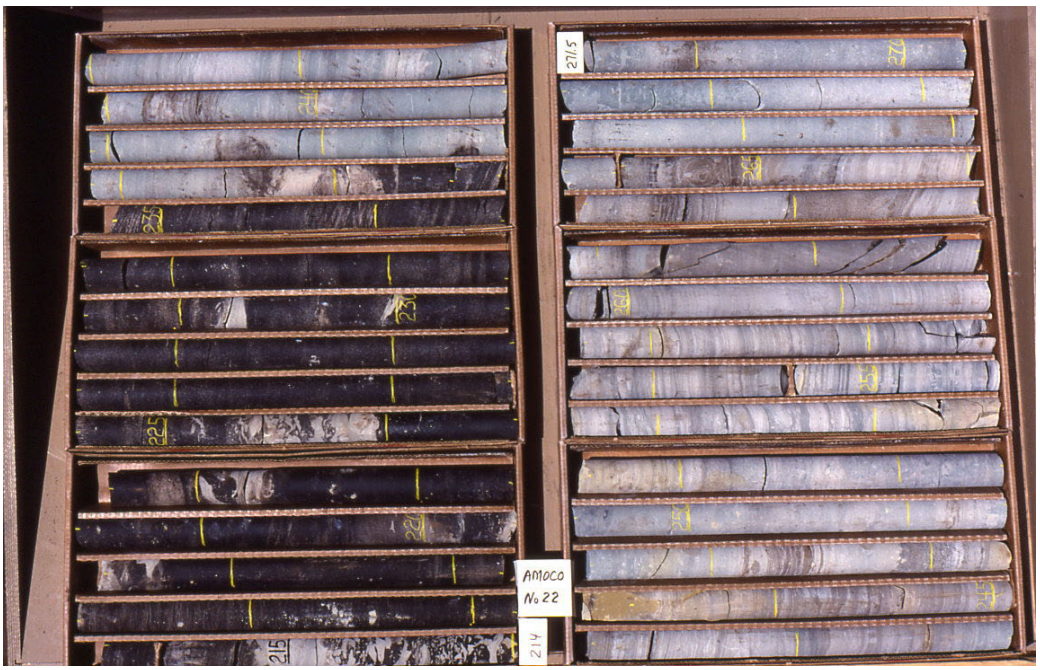

Figure 34: Core photograph of a channel mouth bar deposit in Amoco-22, 214-271 ft depth or elevation range 9,218 to 9,275 ft msl. Refer to this interval in the core profile in Fig. 32.

bar deposits, or beaches and dunes. As a consequence of different depositional settings, the sandstone thicknesses and spatial distributions are far from uniform. However, the sandstone bodies have a distinct direction reflecting the northeast to east orientation of the deltaic systems entering Lake Uinta.

The principal sandstone depositional facies are:

- *Stream channel deposits* – characterized by point bar deposits with epsilon cross bedding, shale lamination, and log fragments in channels superposed on muddy alluvial plain and upper coastal plain settings mainly in the lower parts of the oil-impregnated Douglas Creek Member.
- *Distributary channel deposits* – found throughout the Douglas Creek Member in a shoreline fringe setting and frequently scoured to depths of 1 to 5 ft into underlying shallow water lacustrine limstones; channel thicknesses can be as great as 80 to 120 ft.
- *Distributary mouth bar deposits* – located at the terminus of distributary channels with a spacing of 2000-4000 ft in the Douglas Creek Member and 3000-6000 ft in the Garden Gulch Member; this facies is rare in the Parachute Creek Member.
- *Beach and dune deposits* – generally less than 10 ft thick; despite a sheet-like geometry, a minor reservoir facies.

The reservoir sandstones are organized into 4th-order, fining- and shoaling-upward sequences that relate to climate-driven lake level cycles that shifted the shoreline in and out with a probable periodicity of about 100,000 years (Calkin, 1991). An erosional surface bounds each sequence, frequently associated with an intraformational conglomerate lag at the base of the overlying sandstone. Limestone intervals are present beneath nearly all sandstone zones. The sands are scoured into the limestone at the top of the preceding 4th-order sequence. These are apparently fluvial and/or distributary channels in the lake shore fringe or lower coastal plain. Thus, each lenticular sandstone interval which is several tens of feet thick, is bounded by effective shale and limestone seals of similar thickness.

In delineating the thickness, richness, and spatial distribution of the oil-impregnated sandstone intervals, Rozelle Consulting Services (1989) had access to data from 120 cores within the Dry Creek Canyon-Bruin Point-Range Creek area. In the Bruin Point-Dry Creek Canyon area about 87% of the heavy oil is reservoired in sandstone of the Douglas Creek Member and only 13% are in sandstone of the Garden Gulch Member of the Green River Formation. Insignificant quantities of heavy oil are found in the generally very fine grained sandstones of the Parachute Creek Member. The average thickness and oil grade of the oil-impregnated sandstone zones measured in each of the 120 cores are shown in Fig. 35.

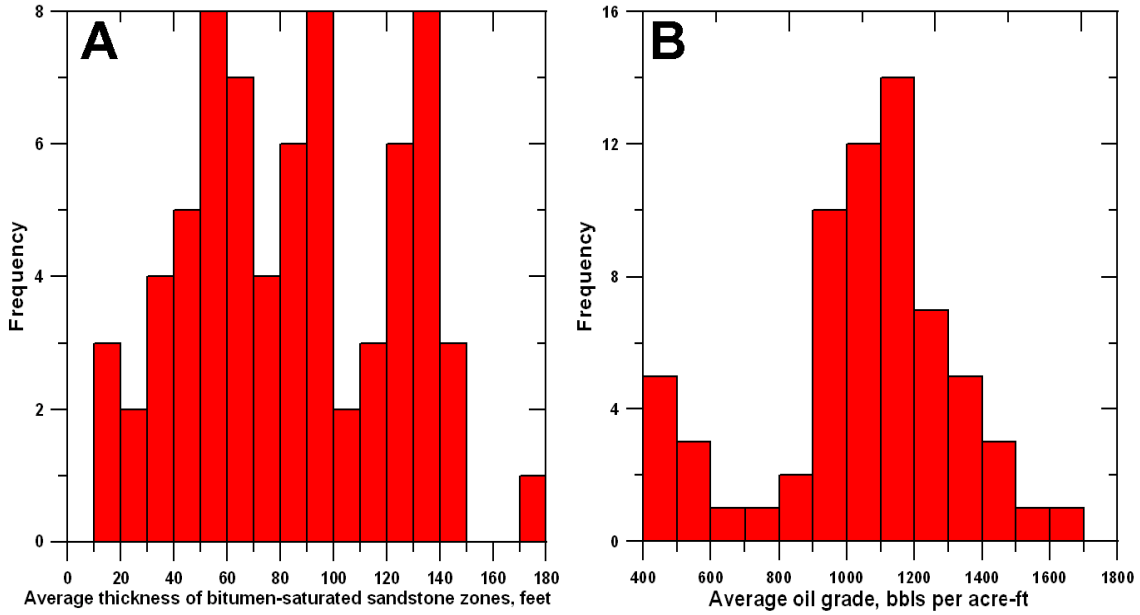

Figure 35: Histograms of average core data for cores in the Dry Creek Canyon-Bruin Point-Range Creek area (Rozelle Consulting Services, 1989). A) Average thickness of the bitumen-impregnated sandstone zones. Plotted is the average thickness of the several oil-impregnated zones in each individual core, not the distribution of thicknesses of each zone. Note that one of the cores penetrated a part of the deposit in which the average oil-saturated sandstone interval is 170-180 feet thick. B: Average heavy oil grade of bitumen-impregnated zones. Note that one of the wells penetrated a part of the deposit in which the average oil grade encountered is an extraordinary 1600-1700 bbls/ac-ft.

Isopach maps were generated for each of the 15 principal reservoir zones (Calkin, 1991). A description of just four of these zones, those holding the larger resources of the deposit (refer to Table 3), provides an indication of the spatial variability of the reservoir units in the Sunnyside deposit. The Central Overlook is on the ridge crest of the Roan Cliffs about 1 mile north of Bruin Point.

- Interval 31: Distributed across much of the study area; the average thickness is 31.6 ft, but it ranges from 3 to 90 ft. There are three major centers of deposition that are 5000 to 6000 ft apart. One "lobe" is near the Central Overlook, one near Bruin Point, and the third centered on well RCT-7 near Range Creek. Sites of high deposition have laterally adjacent lows, such that the inferred direction of sand influx is N65°E with thinning away from the Roan Cliffs.
- Interval 35: The average thickness is 36.2 ft with a range of 5 to 160 ft. As in Zone 31, there are three depocenters near the Central Overlook, Bruin Point, and beyond Range Creek. The larger lobe is at the Central Overlook, which appears to include a 45-ft-deep scour exposed on the Roan Cliff face. The trend of sand input is N50°E.

- Interval 36: The average thickness is 52.6 ft with a range of 14 to 125 ft. The main region of sand deposition is between Roan Cliff and Range Creek. Two lobes of maximum thickness (125 ft) are located at Bruin Point, but other minor depocenters exist across the Roan Cliffs, some of which suggest a "bird's foot" sandstone geometry. The inferred direction of sand input is N50°E.
- Interval 37: The average thickness is 47.1 ft with a range of 10 to 146 ft. The major sand lobes are near Bruin Point and the Central Overlook extending downdip toward Range Creek. This area has clusters of highs on the order of 120-130 ft thick that are about 2000-4000 ft apart separated by lows of 30-80 ft thickness. The stacking of depocenters in Zone 37 tend to be inverse from the lows in Zone 36, suggesting a shifting of delta lobes from one 4^{th}-order cycle to the next. This offset stacking pattern is described for many other zone pairs (Calkin, 1991). As with the previous two intervals, the inferred direction of sand influx is N50°E.

Just 17 oil-impregnated sandstone intervals in the lower Green River Formation hold virtually all of the OOIP. The average thickness and oil resources of these intervals as determined from cores are presented in Table 3. The median average interval thickness is 35.9 ft and the range is 10.0 to 78.2 ft. The median OOIP for the individual sandstone intervals is 39.8 MBO/acre and the range is 9.5 to 92.3 MBO/acre. Just four sandstone intervals having the greatest average thickness (60.7 to 78.2 ft) hold 44.5% of the total OOIP. These are intervals 36B, 41, 42, and 43, all in the lower part of the Douglas Creek Member. As each lenticular sandstone interval does not extend across the entire area investigated by cores (refer to Table 3), the total OOIP cannot be determined simply by adding the OOIP of all of the intervals. This analysis is most useful for identifying which oil-bearing sandstone intervals are suitable for commercial exploitation by alternative *in situ* recovery methods.

A resource assessment by Rozelle Consulting Service (1989) of the total oil-in-place in Amoco and adjacent non-Amoco properties in the core Dry Creek Canyon-Bruin Point-Range Creek area is 1151.31 MMBO. The median heavy oil grade assigned to the 11 properties for the purpose of computing total resources is 1156.7 BO/ac-ft and the range is 987.9 to 1275.2 BO/ac-ft. Outside of this oil-rich area, the oil grades and OOIP are sufficiently lean to discourage development. Also within the oil-rich area some portion of the resource is too close to the land surface to permit environmentally responsible and/or cost effective *in situ* recovery. The heavy oil resources in the Sunnyside deposit that may be available for commercial development cannot exceed 1.0 billion barrels.

Given the irregular thickness and lateral extent of the reservoir sandstone intervals and the relatively small net thickness and low grades reported in many wells outside of the oil-rich Bruin Point area, it is likely that large portions of the deposit cannot be developed commercially. This also is true due to the extremely rugged topography incised into much of the region underlain by the deposit.

DEPOSITS ON HANGING-WALL OF UINTA BASIN BOUNDARY FAULT

The heavy oil deposits along the north and northeast margin of the Uinta Basin are reservoired on the south flank of the Uinta anticlinorium (Stone, 1993) in a variety of stratigraphic units. These deposits are on the hanging-wall of the Uinta Basin Boundary Fault, the high-angle reverse or transpressional thrust that separates the Uinta Mountain basement

uplift from the deep north edge of the Uinta structural depression. Along most of the hanging-wall, strata of Late Phanerozoic through Eocene age strata dip southward or southwestward towards the Uinta Basin. Locally strata are subvertical or even overturned. Everywhere along its length the tip-line Uinta Basin Boundary Fault is buried beneath Eocene and younger basin sediments. Along much of the south flank of the Uinta Mountains (north edge of the basin) the up-turned strata are buried beneath Oligocene-Miocene clastic fans shed off of the mountain range. Only where river canyons have cut through this thin, late-Tertiary cover are the oil-impregnated sandstones observed.

The largest heavy oil accumulations are Asphalt Ridge, reservoired in Upper Cretaceous Mesaverde paralic and upper Eocene fluvial sandstones, and Whiterocks, reservoired in a Triassic-Jurassic eolian sandstone (Fig. 1). Both deposits are near the northeast corner of the Uinta Basin, immediately west of Vernal. Between Asphalt Ridge and Whiterocks is a small deposit, Littlewater Hills (10-12 MMBO), in which heavy oil occurs in fluvial sandstone of the upper Eocene Duchesne River Formation. Between the Whiterocks and Duchesne Rivers there are three smaller deposits, all in Duchesne River fluvial sandstones: Spring Branch, Lake Fork, and Tablona (Ritzma, 1979).

Southeast of the Green River and on strike with Asphalt Ridge is a chain of very small heavy oil deposits (Spring Hollow, Upper Kane Hollow, Cow Wash, and Rimrock) that tie the Asphalt Ridge deposit with the Raven Ridge deposit (75-100 MMBO; Ritzma, 1979). For the most part, heavy oil is reservoired in progressively older formations from the Uinta Formation at Spring Hollow to the several members of the Green River Formation and the Wasatch Formation at Rim Rock and Raven Ridge. Southeast of the Green River, increasingly older Eocene strata emerge at the land surface beneath the base of the regionally extensive Duchesne River unconformity. It is known that these same units are commonly oil-impregnated in the subsurface west and south of Asphalt Ridge. Refer to Blackett (1996) for a full description of these smaller heavy oil deposits.

Asphalt Ridge Deposit

Asphalt Ridge is situated on the forelimb of the broad Ashley Valley anticline (Figs. 36 through 39) where the Mesaverde Group strata dip 12° to 28° to the southwest (Kayser, 1966). The anticline is the hanging wall structure of the Uinta Basin Boundary Fault, the position of which is constrained by deeper exploration wells and a 2-D seismic survey conducted across the Ashley Valley oil field and southern Asphalt Ridge in July 1967 (Fesker, 1967). These data pin the location of the fault tip line at the level of Tertiary strata at the sharp northwest jog in the Green River in T6S-R22E. This also is the position of the Uinta Basin synclinal axis (Fig. 36) mapped by Untermann and others (1964). It is not known how deep the oil deposits extend on this hanging wall of the thrust sheet carrying the Ashley Valley anticline or whether there is a distinct oil-water contact forming the floor of the deposit. However, the tip line of the south Uinta Boundary fault must be the effective maximum down-dip limit to the extent of the Asphalt Ridge deposit. Southwest of the tip line, the Mesaverde sandstone reservoir is in the footwall of the thrust at depths greater than 12,000 ft.

The Asphalt Ridge heavy oil deposit (Fig. 40) occurs within (1) sandstones of the Duchesne River and Uinta Formations (Eocene), both representing fluvial, intermountain basin fill contemporaneous with the closing stages of the Laramide orogeny in the central Rocky Mountains, and (2) sandstones in the Mesaverde Group (Campanian), a prograding shoreline to

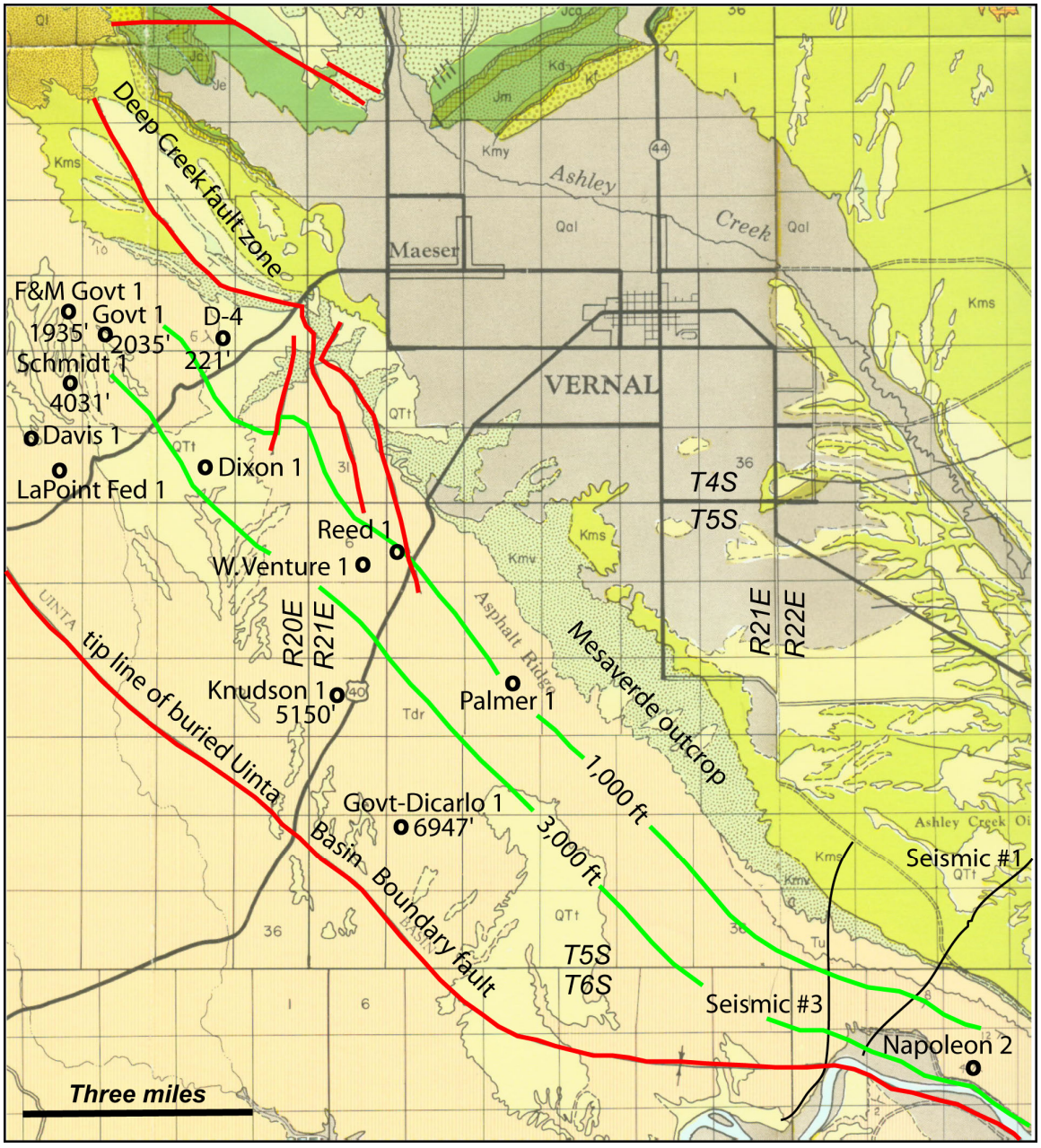

Figure 36: Geologic base map of the Asphalt Ridge area showing the depths to the top of the Mesaverde sandstones at five wells penetrating into the Cretaceous and other shallower wells penetrating oil-impregnated Eocene sandstones (Kayser, 1966). Also shown are 2-D seismic lines that constrain the position of the South Uinta Boundary Fault near the Green River. The Uinta Basin syncline shown on the map is the approximate trace of the buried tip line of the fault. The Napoleon 2 well penetrates the leading edge of the fault (Stone, 1993). Key to stratigraphic units: Tdr, Duchesne River Formation; Tu, Uinta Formation; Kmv, Mesaverde Group; Kms, Mancos Shale. The base map is derived from Untermann and others (1964).

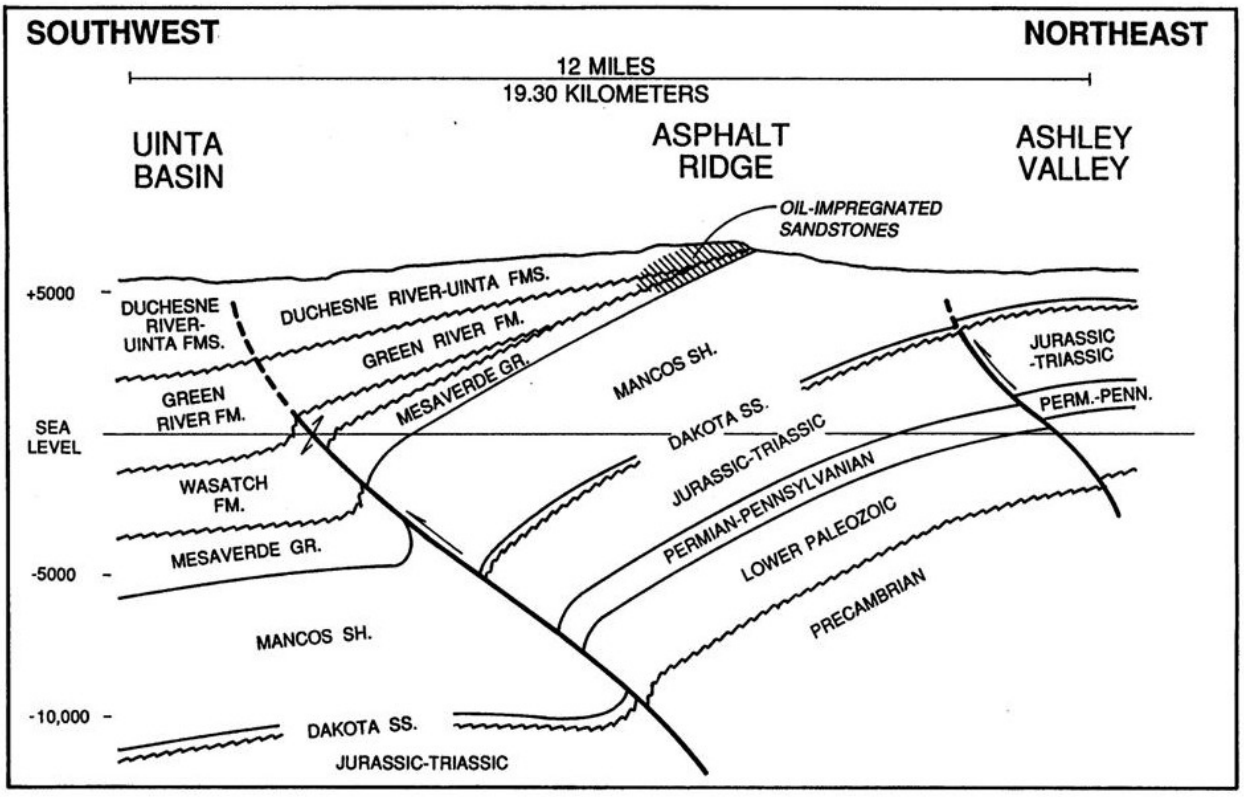

Figure 37: Cross section showing the forelimb of the Ashley Valley anticline, the Uinta Basin Boundary Fault beneath the Uinta Basin, and the location of oil-impregnated sandstones at Asphalt Ridge (Blackett, 1996).

Figure 38: North end of Asphalt Ridge west of Vernal with County asphalt mine at the base of the cliff in the middle ground. Photograph by S. Schamel.

Figure 39: Asphalt Ridge looking west into the stratigraphic section near the north end. The upper half of the slope is Duchesne River Formation. The oil-impregnated Mesaverde sandstones are the gray ledges forming the lower half of the slope. The uppermost Mancos Shale is exposed at the base of the slope and beneath the plain in the foreground. The Uinta County tar sand pit and the Crown Asphalt plant are immediately to the left of the field of view. Photograph by S. Schamel.

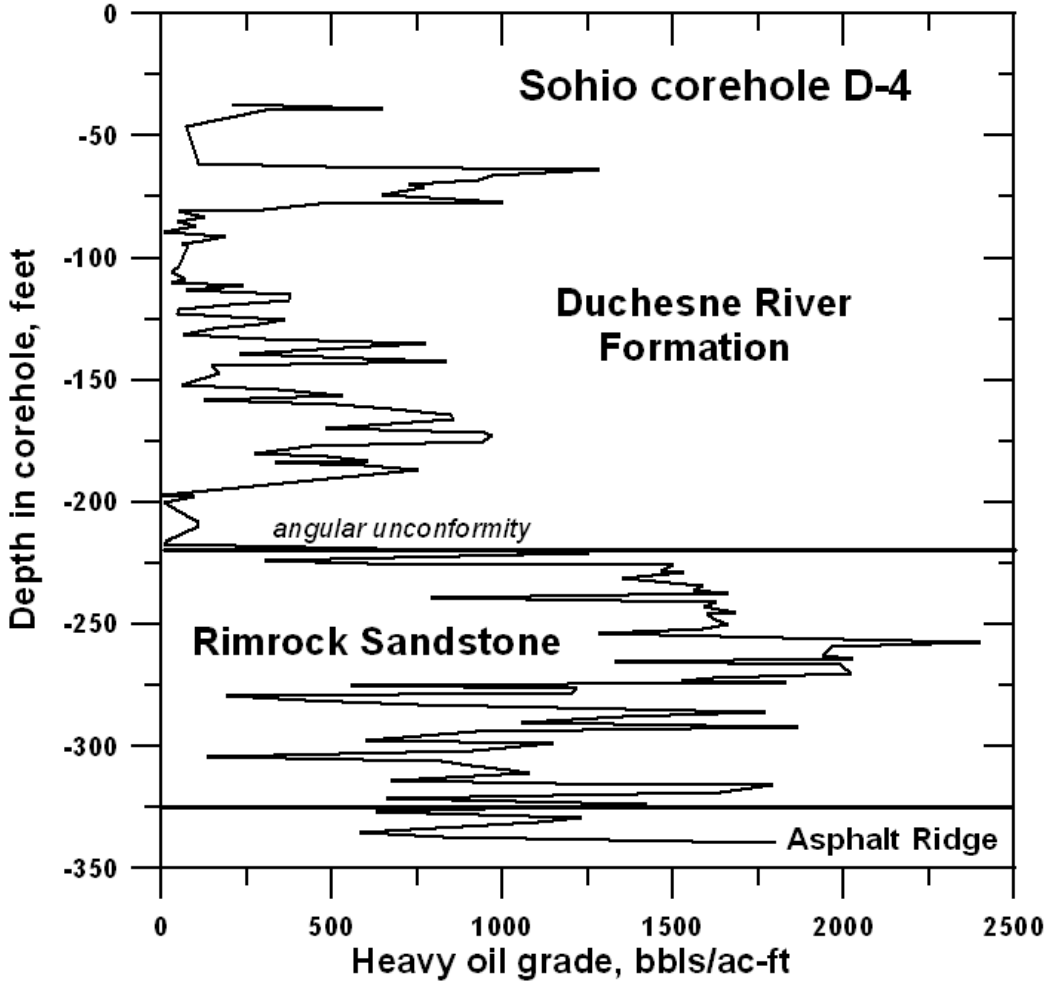

Figure 40: Distribution of oil-saturated sandstones within the upper Eocene Duchesne River Formation and Upper Cretaceous Mesaverde Group in the Sohio D-4 core in northwest Asphalt Ridge (SE 23-T4S-R20E). Data from unpublished record in Utah Geological Survey files.

delta plain succession deposited in the foreland basin to the Sevier orogeny (Franczyk and others, 1992). The Mancos Shale underlying the Mesaverde Group is nowhere oil-impregnated. At Asphalt Ridge, the Duchesne River and/or Uinta Formations rest with an angular unconformity of 3° to 8° on moderately tilted Mesaverde strata (Kayser, 1966). However, at the northwest end of Asphalt Ridge, the Mesaverde dips at about 45º and the average dip on the Eocene unconformity is about 25º (Tom Brown, Inc., 1974). To the southeast of Asphalt Ridge, the Green River and Wasatch/Colton Formations are present below the angular unconformity. These units also are oil-impregnated at shallow depths. Ritzma (1979) estimated the deposit to hold 1175 MMBO.

At Asphalt Ridge, the Mesaverde Group contains three stratigraphic units. Conformably overlying the Mancos Shale is the 100+-ft-thick Asphalt Ridge Sandstone, very fine to fine-grained friable sandstones heavily impregnated with heavy oil, but with few surface exposures. This is overlain by the Rim Rock Sandstone (Figs. 41 through 47), a fine- to medium-grained quartz arenite. This unit is the principal oil-impregnated reservoir in the northern part of the deposit, where it is about 200 ft thick (Sinks, 1985b). To the southeast the unit thins to less than 100 ft (Kayser, 1966). These two formations contain equivalents to the Sego Sandstone, Buck Tongue of the Mancos Shale, and the Castlegate Sandstone (Sprinkel, 2002). The upper unit, the Williams Fork Formation, a nonmarine succession of shales, fluvial sandstones, and thin coals, is very poorly exposed and commonly missing beneath the Eocene unconformity. From a limited number of samples, Kayser (1966) reports the Mesaverde sandstones have porosities in the range of 26% to 34%, permeabilities of 4 md to 402 md, and oil saturations of 19% to 73% (Table 4).

Table 4: Properties of Asphalt Ridge oil-impregnated sandstone core samples analyzed by Core Labs (Kayser, 1966).

Formation	*Perm md*	*Porosity %*	*So %*	*Bbls/ac ft*	*Description*
Duchesne River	70	28.8	52.7	1287.4	Moderate-rich
Duchesne River	4.7	17.9	69.2	928.3	Moderate
Duchesne River	745	32.2	65.0	1585.6	Rich
Uinta	*na*	31.6	71.2	1870.2	Very rich
Uinta	4.2	24.4	63.5	1179.0	Rich
Uinta	239	22.2	51.8	928.3	Moderate
Mesaverde	*na*	35.0	58.3	1775.3	Very rich
Mesaverde	402	34.1	46.7	1389.1	Rich
Mesaverde	90	26.0	19.2	433.7	Poor
Lower Mesaverde	30	29.5	72.6	1741.4	Rich

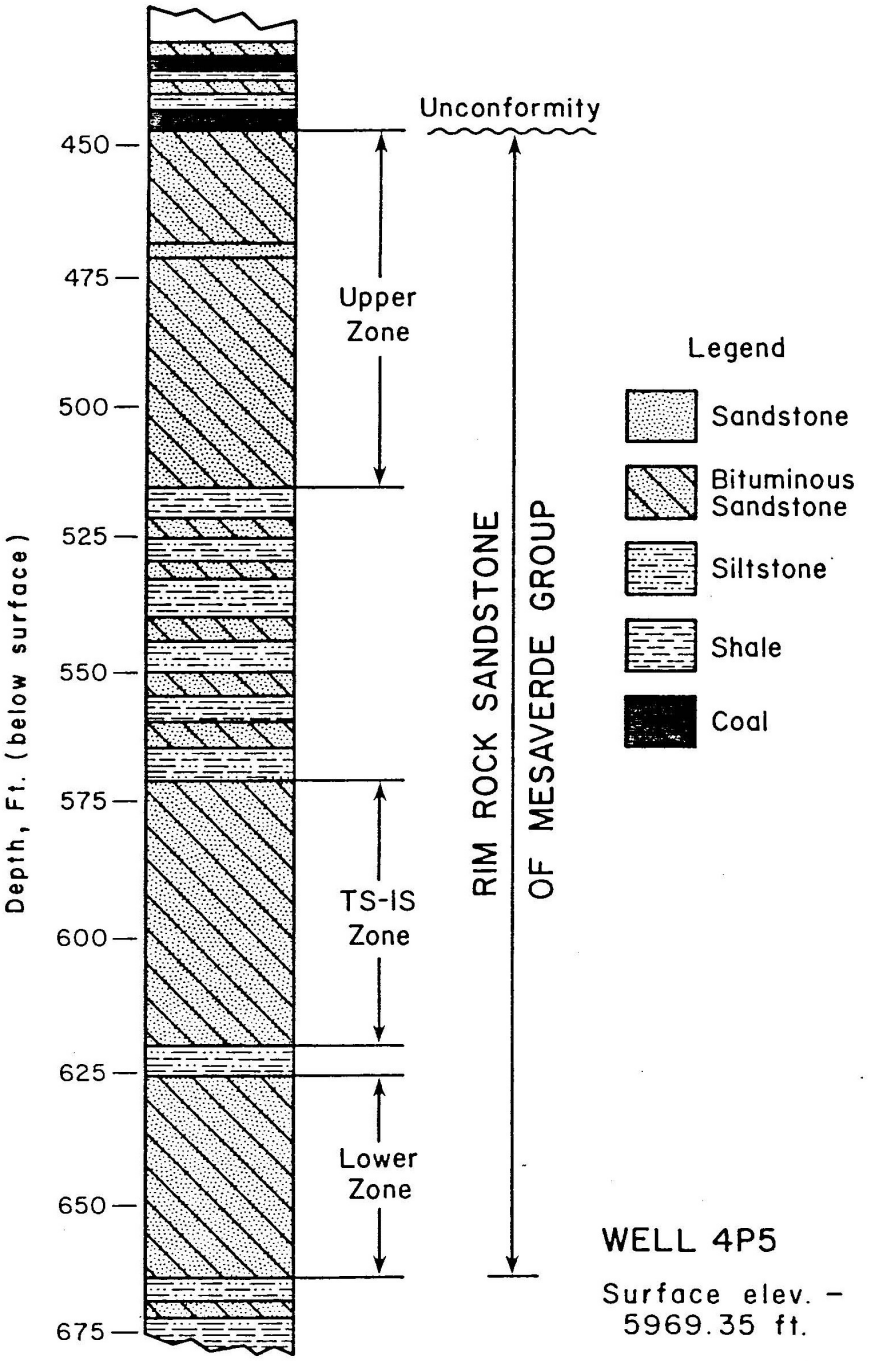

Figure 41: Lithologic section of the Rim Rock Sandstone reservoir in Asphalt Ridge Northwest area (SE 23-T4S-R20E) showing the bitumen-impregnated intervals (Sinks, 1985b). This corehole, 4P5, is within the stratigraphic profile shown as Fig. 42.

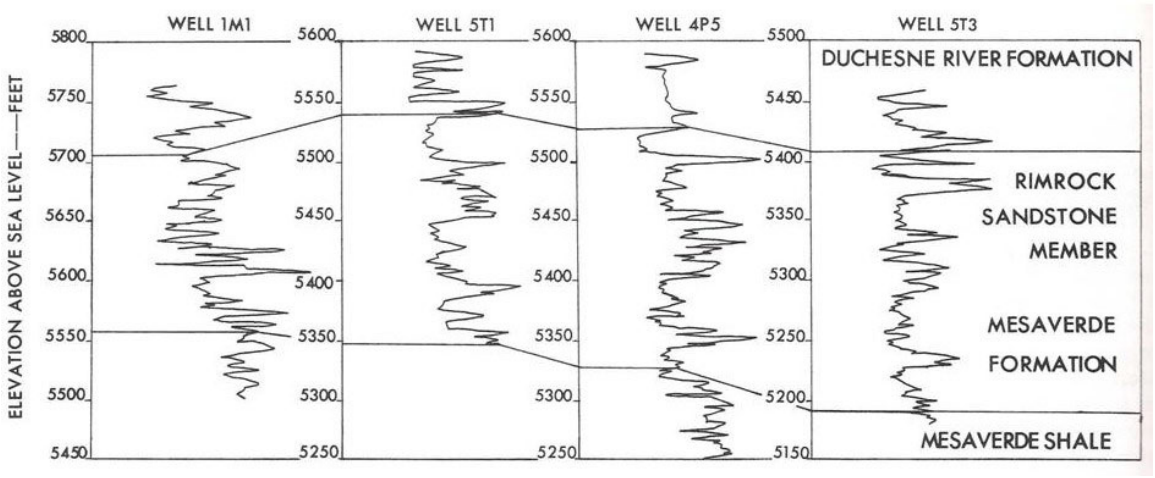

Figure 42: Gamma-ray logs in test wells on the LETC research site in 32 through 35 northwest Asphalt Ridge (SW 23-T4S-R20E) showing the internal heterogeneity of the Mesaverde Group heavy oil reservoir (Merriam and Fahy, 1985). The distance represented in the stratigraphic section is about 1000 feet. Mesaverde Formation and Mesaverde Shale should read Asphalt Ridge Sandstone and Mancos Shale, respectively. Lithologies for well 4P5 are shown in Figure 41.

Figure 43: Rim Rock Sandstone overlain unconformably by red mudstones and sandstone lenses of the Duchesne River Formation in exposures south of Highway 45. At this location in the southern Asphalt Ridge, the Rim Rock Sandstone is dipping at 20° and the Uinta Formation at about 10°, both to the southwest. Photograph by S. Schamel.

Figure 44: Massive 50 ft+ thick cross-bedded sandstone at the top of the preserved Mesaverde Group northeast of Collier Pass. This unit is immediately overlain unconformably by red mudstones of the Eocene Duchesne River Formation (see Fig. 42). Photograph by S. Schamel.

Figure 45: Cross-bed sets in the uniform, poorly lithified, medium-grained "salt and pepper" Rim Rock Sandstone at the base of the cliff in Fig. 43. Photograph by S. Schamel.

Figure 46: Large-scale, tabular cross-bed sets in Mesaverde sandstone in the road cut on south side of Highway 45 in general area of Fig. 42. The black camera case is 4 x 6 inch size. Photograph by S. Schamel

Figure 47: Oil-impregnated Rim Rock Sandstone in the Temple Mountain mine near the south end of Asphalt Ridge (36-T5S-R21E). Note the lower degree of oil-saturation in the conglomeratic lenses compared to the lithified sandstone beds above. The sandstone beds are "bleeding" heavy oil. Photograph by S. Schamel.

The Eocene-age Duchesne River and Uinta Formations are similar intercalated lithic sandstone, siltstone, claystone, and conglomerate successions (Sprinkel, 2002). The lower part of the sandier Duchesne River Formation is observed to intertongue with the muddy Uinta Formation south of Vernal. The porosity of the two upper Eocene units at Asphalt Ridge (Table 4) ranges from 18% to 32%, permeabilities are 5 md to 745 md, and oil saturations are 52% to 71%, all values within the range observed in the Cretaceous sandstones.

In January 1974, Tom Brown, Inc. drilled six test wells into oil-impregnated Mesaverde Group sandstones beneath their lease in Asphalt Ridge Northwest, due west of Vernal (Fig. 36). The wells are located immediately east of the cluster of three Mesaverde well penetrations shown in Fig. 36. The deepest Mesaverde top reported is 1521 ft (well # 8) and the shallowest is 396 ft (well #7). All wells were logged and core samples were recovered from four of the wells (Tom Brown, Inc., 1974). From a total of 1175 ft of recovered core, 332 oil-impregnated sandstone samples were analyzed for porosity, permeability, and fluid saturations (So and Sw). The results of the analyses are reported in Table 5.

For the Rim Rock Sandstone, the principal reservoir unit, the average sandstone porosity and permeability are 30.3% and 524.5 md, respectively. So and Sw are 63.5% and 7.5%, respectively. For the Asphalt Ridge Sandstone, the average sandstone porosity and permeability are slightly higher, 30.6% and 610.7 md, respectively, as are So and Sw, 65.6% and 12.0%, respectively. The average net pay for the Rim Rock Sandstone and the Asphalt Ridge Sandstone is 119.8 ft and 71.4 ft, respectively. Thus, the total Mesaverde sandstone net pay is about 200 ft. However, in some wells the top of the Rim Rock Sandstone is truncated by the Eocene unconformity, and in one deep well the Asphalt Ridge sandstones are water-wet, perhaps indicating the presence of an oil-water contact. The Eocene sandstones have an average porosity of 20% and an average oil saturation of 53.5% through a net pay thickness of 35.5 ft (Table 5).

Table 5: Data gathered from six test wells in Asphalt Ridge Northwest (Tom Brown, Inc., 1974). Values reported for each test wells are averages of 40 to 87 core samples for each reservoir unit; values in italics are derived from open-hole log analysis. Original oil-in-place is calculated from porosity and So. Averages for each stratigraphic interval are shown in red. The routine core analyses were done by Core Labs, Denver.

	Corehole	Net pay	Porosity%	Perm, md	So, %	Sw, %	bbls/ac-ft	MBO/acre
Eocene	1	35	*18*	na	69	na	963.5	33.72
	2	14	*21*	na	44	na	716.8	10.04
	5	41	*19*	na	53	na	781.2	32.03
	6	38	*20*	na	50	na	775.8	29.48
	7	37	*20*	na	59	na	915.4	33.87
	8	48	*22*	na	46	na	785.1	37.69
		35.5	**20.0**		**53.5**		**830.1**	**29.47**
Rimrock	2	36	*22*	na	*51*	na	870.4	31.34
	5	149	37	534	69	6	1980.6	295.11
	6	111	40	515	74	9	2296.4	254.90
	8	183	*22*	na	*60*	na	1024.1	187.40
		119.8	**30.3**	**524.5**	**63.5**	**7.5**	**1490.2**	**178.45**
Asphalt Ridge	1	118	*22*	na	*82*	na	1399.5	165.15
	5	50	37	752	66	3	1894.5	94.73
	6	68	36	637	62	11	1731.6	117.75
	7	92	41	443	53	22	1685.8	155.09
	8	29	17	na	65	na	857.3	24.86
		71.4	**30.6**	**610.7**	**65.6**	**12.0**	**1557.3**	**111.19**

The vertical and lateral variability of the Mesaverde sandstones is demonstrated in the gamma-ray logs for four test wells in the Laramie Energy Technology Center (LETC) experiment site in Asphalt Ridge Northwest (Fig. 42). Distinct sandstone packets 20 to 60 ft thick are separated by silty and/or shaly intervals, as shown also in the stratigraphic cross section in Fig. 42. It is difficult to correlate these sandstone packets laterally, even over the very short distance represented in the wells (Fig. 42). The profile and bedding features shown in Figs. 44 through 47 are suggestive of stacked fluvial channels.

In Asphalt Ridge Northwest, shallow 2-D seismic lines have revealed an array of northwest-southeast trending normal faults in a horst and graben configuration that cut the Upper Cretaceous and Eocene reservoirs (Sinks, 1985b). These faults are demonstrated to have been dominant factors adversely affecting the *in situ* recovery experiments carried out in the area by LETC (Merriam and Fahy, 1985). Both injected steam and air were lost through the faults. This fault system is at the southern end of the Deep Creek fault zone mapped by Haddox and others (2005), but the geologic map (Fig. 36) suggests that the system might extend farther, bending southward into the dip-slope of the northern part of Asphalt Ridge.

Unfortunately, there is little well control on the dip-slope of Asphalt Ridge to permit assessment of the extent and grade of the oil-impregnated sandstone southwest of the ridge crest. Table 6 lists all conventional wells on this dip slope; Fig. 36 shows the location of key wells that are discussed below.

Several wells drilled on the dip-slope of Asphalt Ridge penetrated Upper Cretaceous strata. These are shown on Fig. 36 with the depth in feet to the top of the Mesaverde sandstones indicated; see Table 6 for details. It is not recorded if these sandstones are oil-impregnated. However, Spieker (1930, p. 95) reports that two wells drilled in the 1910s, one of which is Dixon 1 and the other is near Western Venture 1, penetrated "black oil that was too viscous to be pumped." He also mentions that the Western Venture 1 well penetrated an oil-impregnated sandstone bed at 1279 ft and at depths of 1300 to 1500 ft the well was making gas.

Table 6: Wells in the area immediately downdip from Asphalt Ridge and its extension to the southeast that may serve to constrain the limits of the deposit. Data from Utah Division of Oil, Gas and Mining well files and Kayser (1966).

API No.	Well name	Operator	T-R	Sec	Elev.msl	TD ft	Top MV	Year
4304710371	Govt 1	Feldt & Maytag	4S-20E	21	6282	2140	1986	1962
4304720372	Union Oil Company 1	Union Oil	4S-20E	21	6275	2222	2035	1942
4304720374	Schmidt 1	Carter Oil	4S-20E	28	6086	6370	4,030	1948
4304710101	Lapoint-Fed 1	Belco Petroleum	4S-20E	33	5830	7446	na	1960
4304720378	Davis 1	Carter Oil	4S-20E	33	5840	8001	na	1947
na	#1	Western Venture	5S-21E	6	5700	1515	na	1927
na	W. Venture 1	Home Oil	5S-21E	8	5500	1165	na	1930
4304720404	#3	Uinta Dev. Co.	5S-21E	17	5395	1749	na	1912
4304710583	Knutsen 1	Carter Oil	5S-21E	18	5393	6013	5150	1947
4304710631	Government-Dicarlo 1	King Stevenson	5S-21E	29	5394	7265	6947	1961
4304710584	Vernal U1 (Nelson 1)	Carter Oil	5S-21E	33	5333	7884	na	1949
4304720434	USA 1	Carter Oil	6S-21E	9	5022	9002	na	1952
4304733871	Horseshoe Bend Fed 26-3	Westport	6S-21E	26	4991	3885	na	2001
4304734683	Shuffleboard 3-27	Rosewood	6S-21E	27	4814	3850	na	2002
4304731668	Shuffleboard Federal 1	Rosewood	6S-21E	27	4763	3810	na	1985
4304730031	Napoleon 2	Toledo Mining	6S-22E	9	4875	5640	na	1968
4304731563	Walker Hollow U77	Citation	7S-23E	1	5185	5700	na	1984
4304731579	Walker Hollow U79	Exxon	7S-23E	1	5151	5576	na	1986
4304731645	Walker Hollow U78	Exxon	7S-23E	1	5176	5563	na	1985
4304731665	Walker Hollow U69	Citation	7S-23E	2	5327	5698	na	1985
4304734757	Walker Hollow U80	Citation	7S-23E	3	5337	5520	na	2003
4304732606	N Walker Hollow 6-1	Riata Energy	7S-23E	6	5858	2926	na	1995

In 1957, Gulf Oil drilled two shallow wells on its fee property in NE 16-T5S-R21E to assess the suitability of the reservoir for *in situ* recovery methods (Terwilliger, 1957). The wells cored and tested the Duchesne River Formation only. The Palmer well penetrated a bitumen-impregnated zone (avg. 5.5 wt % or 931.7 bbls/ac ft) at a depth of 610-652 ft, but in drilling to total depth at 855 ft no additional impregnated zones were penetrated. The report concluded that the significant deposit is in the Mesaverde sandstone (not penetrated), which is both porous and uniform in its properties, not the Duchesne River sandstones. The Eocene sandstones tend to be lenticular and shaly.

Given the very large amount of attention that the Asphalt Ridge deposit has received over the past half century, it is surprising that so little information exists in the public domain about the OOIP. Fortunately, there are several sources of data, most unpublished and widely scattered about the deposit.

Kayser (1966) examined in detail with numerous test wells, two areas, one in the north part of Asphalt Ridge and the second in the south. The north area of 1750 acres is centered on the Uintah County asphalt pit and is within sections 25 and 36, T4S-R20E; sections 30, 31, and 32, T4S-R21E; and sections 5 and 6, T5S-R21E. Based on 20 coreholes uniformly distributed across the test area, a total resource of 330 MMBO was estimated. The average net thickness of oil-impregnated Rim Rock Sandstone is 90 ft. This calculates to an average oil grade of 2095.2 bbls/ac-foot and an average OOIP of 188.57 MBO/acre.

The south area of 3500 acres is within sections 25, 26, and 36, T5S-R21E; sections 31 and 32, T5S-R22E; and sections 5 and 6, T6S-R22E. Based on 14 coreholes, most in the south half of the test area, total resources is estimated to be 367 MMBO. The average net thickness of oil-impregnated Rim Rock Sandstone is 50 ft, yielding an average oil grade in this area of 2097.1 BO/ac-ft or an OOIP of 104.86 MBO/acre.

An unpublished report by Sohio Petroleum (1974) includes data tables for three test cores (Fig. 48). The average oil grade and maximum oil-in-place determined from the cores are:

- Sohio CE-3: 172.53 MBO/acre in a 146.5 ft interval; median grade of 1347.5 BO/ac-ft.
- Sohio CE-2: 131.53 MBO/acre in a 140.5 ft interval; median grade of 903.4 BO/ac-ft.
- Sohio F-1: 118.12 MBO/acre in a 140.0 ft interval; median grade of 857.5 BO/ac-ft.

The 1957 Sohio core, D-4, taken from Asphalt Ridge Northwest (Fig. 40) has average oil grades for the Duchesne River Formation, the Rim Rock Sandstone, and the Asphalt Ridge Sandstone of 359.9 BO/ac-ft, 1312.1 BO/ac-ft and 1028.3 BO/ac-ft, respectively. The estimated OOIP in the Duchesne River Formation is 53.15 MBO/acre in a 145 ft net interval. The Mesaverde Group sandstones have an estimated OOIP of 171.24 MBO/acre in a 137 ft thick net interval --- 140.39 MBO/acre in the Rimrock Sandstone and 30.85 MBO/acre in the thinner and slightly leaner Asphalt Ridge Sandstone.

The estimates of OOIP in Mesaverde sandstones derived from the Kayser (1966) core data bracket the estimates from other specific cores, 104.9 to 188.6 MBO/acre. In an area of just 5250 acres, the two test areas, Kayser (1966) estimates 697 MMBO of heavy oil within just the Rim Rock and Asphalt Ridge Sandstones, excluding younger bitumen-impregnated intervals. If this resource grade can be applied as the average through the approximately 16 sections (10,240 acres) of the Asphalt Ridge deposit where the Mesaverde sandstones are sufficiently shallow for surface mining or shallow *in situ* exploitation, the total resource for the deposit is 1359.5 MMBO. But it is highly likely that the heavy oils continue southwestward to greater depths within the dip slope of the cuesta. Doubling or tripling the down-dip area in which heavy oils could be recovered by *in situ* methods would increase the resource to 2.72 or 4.08 billion barrels of oil, respectively, or possibly greater if the Eocene reservoirs can be exploited commercially.

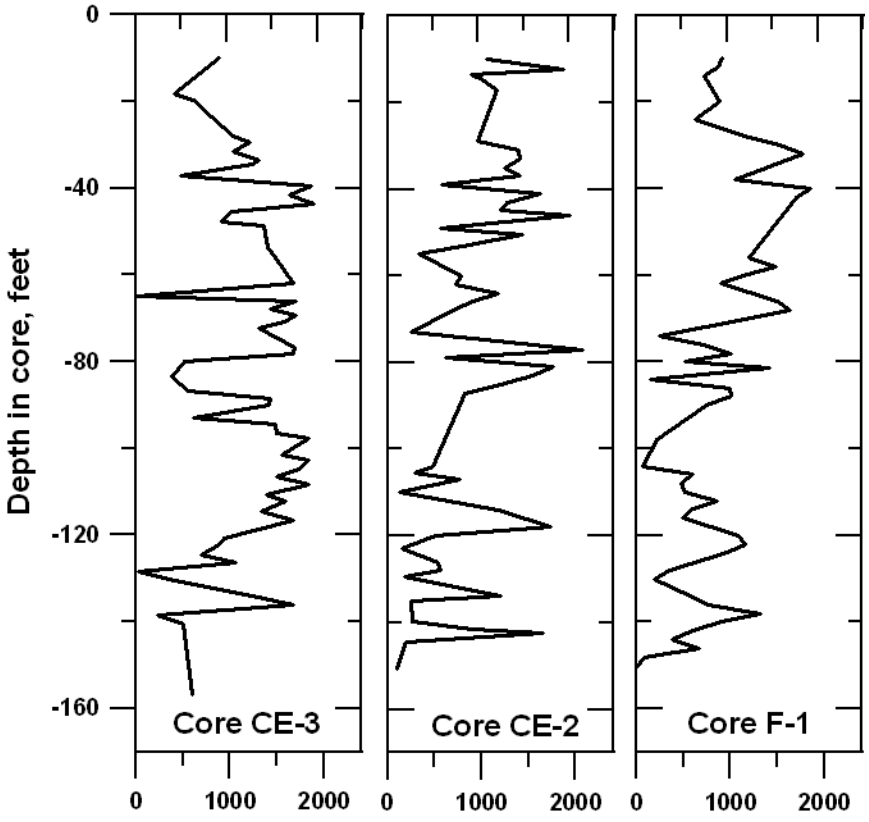

Figure 48: Measured oil grades in Sohio cores near the southern end of Asphalt Ridge (Source of data: Sohio, 1974). Core CE-3: a 146.5 foot oil-impregnated section has 172.53 MBO/acre oil-in-place. Core CE-2: a 140.5 foot oil-impregnated section has 131.53 MBO/acre oil-in-place. Core F-1: a 140.0 ft thick oil-impregnated section has 118.12 MBO/acre oil-in-place.

Whiterocks Deposit

The Whiterocks heavy oil deposit is located within a steeply upturned section of the south flank of the Uinta Mountains anticlinorium (Fig. 49). The known limits of the deposit are at the crest of the sub-vertical Whiterocks anticline, which is situated immediately to the west of the 5-mile wide Little Mountain fault zone, a major structural feature in the eastern Uinta Basin (Haddox and others, 2005). The anticline is likely the product of late Eocene-Oligocene transpressional movement on the fault zone. The Whiterock River cuts through the crest of the anticline (Fig. 49). The stratal dips near its crest are 75° SE to subvertical. The west flank of the anticline has lower dips within the exposed Paleozoic section. Lower dips exist also east of Mosby Mountain (Fig. 50).

The heavy oil is reservoired in the Nugget Sandstone of Late Triassic-Early Jurassic age (Sprinkel, 2002), an eolian sandstone equivalent to the Navajo Sandstone of central and southern Utah and the principal reservoir unit in the Utah-Wyoming thrust belt. It is an important oil and gas reservoir throughout Utah and adjacent states. The Nugget Sandstone rests unconformably on the varicolored mudstones of the Chinle Formation (Upper Triassic) and is unconformably overlain by 30-118 ft of red, green and gray sandy shale, sandstone, siltstone, limestone, and bedded gypsum of the Carmel Formation (Middle Jurassic). Both units are effective lateral seals in the upturned section at Whiterocks Canyon.

The Nugget Sandstone is near the middle of a thick packet of Mississippian through Upper Cretaceous strata folded by the Uinta Mountains anticlinorium. These strata are overlain with an angular unconformity along the north edge of the Unita Basin by varicolored lithic sandstone, siltstone, claystone, and conglomerate of the Duchesne River Formation (upper

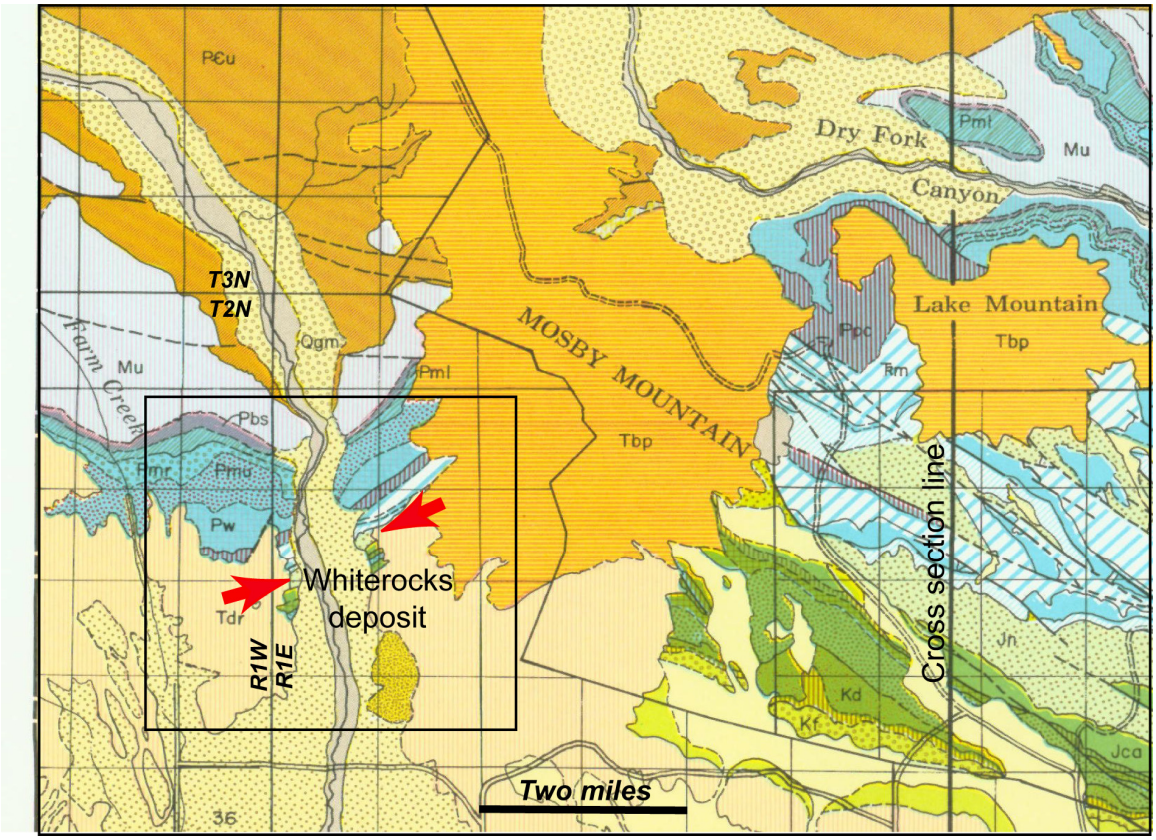

Figure 49: Geologic map of the southern flank of the Uinta Mountains in westernmost Uintah County. The Whiterocks deposit is located southwest of Mosby Mountain along the Whiterocks River (between red arrows). The deposit is on the nose of the steeply plunging Whiterocks anticline. The box indicates map view in Fig. 51. Key to units: Jn, Nugget Sandstone; Tdr, Duchesne River Formation; Tbp, Bishop Conglomerate. Modified from Untermann and others (1964).

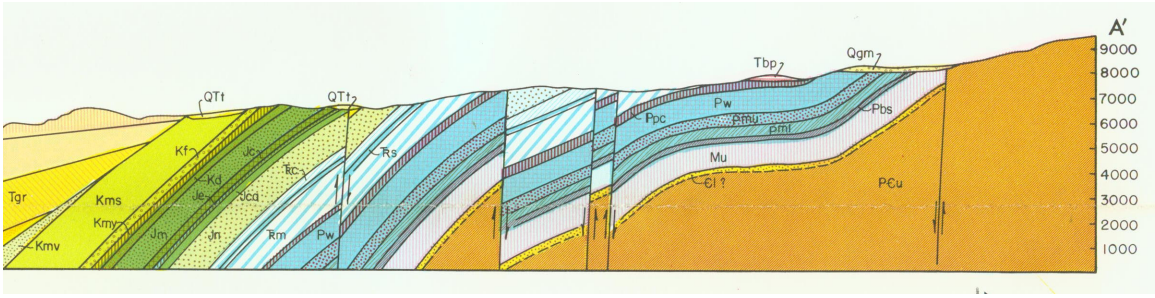

Figure 50: North-south structural cross section (location shown in Fig. 49) showing the variable dips of Paleozoic-Mesozoic strata on the south flank of the Uinta Mountains. The Tertiary fill of the Uinta Basin rest with sharp angular unconformity on Cretaceous and older strata. Modified from Untermann and others (1964).

Eocene). Above the Whiterocks deposit, the Duchesne River strata dip less than 10° basinward, and they are generally less than 500 ft thick. In turn, the Eocene sediments are overlain by the Bishop Conglomerate (Oligocene), light-gray friable sandstone and poorly sorted boulder to pebble conglomerate representing the proximal debris created by erosional unroofing of the rapidly rising Uinta Mountains. The Bishop Conglomerate forms a debris apron on the south slope of the Uinta Mountains that is partially incised by the major rivers, such as the Whiterocks and Dry Fork (Fig. 49). Mosby Mountain, Lake Mountain and Little Mountain are erosional remnants of the Bishop Conglomerate (Fig. 49; orange overprint). On the geologic map of Uintah County (Untermann and others, 1964), this unit has been misidentified as the Browns Park Formation (Tbp) of Miocene age, but Sprinkel (2002) identifies it as the slightly older Bishop Conglomerate based on K-Ar age dating of interbedded tuffs. Where present on the flanks of the Whiterocks Canyon, the muddy Tertiary sediments appear to constitute an effective top-seal to the upturned Nugget Sandstone. Evidence points to charging of the reservoir following deposition of the Duchesne River Formation (Blackett, 1996).

Southeast of Mosby Mountain in the Little Mountain fault zone, the Nugget Sandstone (Jn) generally is exposed at the surface. However, to the west of the fault zone it is buried beneath the Duchesne River Formation and locally the Bishop Conglomerate. It is exposed only in small outcrops along the Whiterocks River (Figs. 51 and 52).

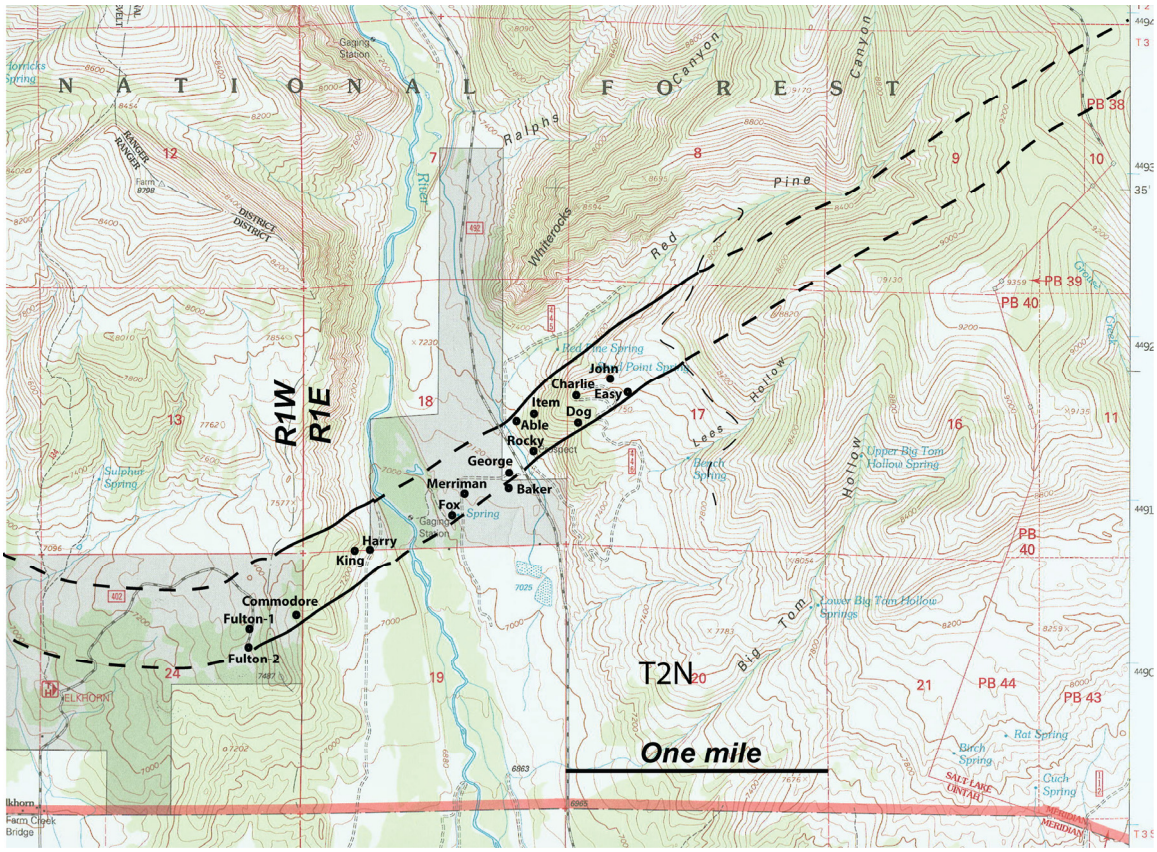

Figure 51: Location of coreholes (black dots) penetrating the Whiterocks heavy oil deposit, the limits of which are shown in the heavy and dashed overprint on the U.S.G.S. Ice Cave Peak 7.5' quadrangle map. Well locations from Peterson (1982).

Figure 52: Outcrop of heavy oil-impregnated Nugget Sandstone on the east side of the Whiterocks Canyon. Note the quarry in subvertical, large-scale cross-bedded sandstone on the south (right) side of the ridge. Photograph by S. Schamel.

The 900-ft-thick Nugget Sandstone is a porous and relatively permeable reservoir unit bounded stratigraphically above and below by clay-rich, relatively impermeable, sealing units. Bedding ranges from massive cross-bedded to planar thin-bedded characteristic of alternating dune and interdune deposits. The rock is a well sorted, fine-grained to very fine grained, quartz arenite (Fig. 53) containing less than 5% feldspar and heavy minerals. Clay-sized material is common in the matrix. Cements include authigenic quartz, calcite, and iron oxide, but the rock is generally non-calcareous. Near the center of the formation there are thin beds of shale and limestone, which have very low oil saturations (Peterson, 1982, 1985).

At least in the near-surface cored intervals, gypsum and clay fill small fractures and displaced bedding surfaces. It is not clear from the core descriptions if gypsum and clay veins are so prevalent as to interfere with fluid flow through the reservoir. In quarries on the east flank of the canyon the sandstone is cut by anastomising calcite veins and a structural fabric (Fig. 53). If common and laterally extensive, the veins and structural fabric could inhibit thermal recovery processes.

Peterson (1982) reports porosity measured in the Merriman Ranch 1 well (Figs. 51 and 54) to average 16.8% and range between 6% to 21%. Permeability averages 237 md; the range is 4 md to 400 md. The Fulton Whiterocks 1 well (Fig. 54A) has higher porosity (average 32.1%), but lower permeability (average 63.3 md). Oil saturation in the Merriman and Fulton cores average 25.7% and 29.4%, respectively. Corresponding water saturations are 65.4% and 55.4%, respectively. As can be seen in Fig. 54B, the range of fluid saturation values is quite large. These petrophysical and fluid saturation values first reported in Polumbus Jr. and Associates (1961) may be suspect given the considerable discrepancy between the Merriman and Fulton cores. No other petrophysical data are in the public domain for the Whiterocks reservoir.

The vertical variability found in the Nugget Sandstone reservoir is represented in the oil grade profile of the Rocky-slant well (Fig. 55) for which numerous close-spaced core measurements are reported in Peterson (1982). The profile shows a general increase in oil richness with depth in the core, which samples less than a half of the full oil column at the well site. This “slant well” is oblique to bedding. All of the other test wells are vertical and sub-parallel to oblique to bedding.

Figure 53: Partially oil-impregnated, large-scale cross-bedded eolian sandstone cut by thin, anastomosing calcite veins and a subtle structural fabric. Location is the quarry on the east side of the Whiterocks Canyon visible in Fig. 52. The camera case is 6 in. wide. Photograph by S. Schamel.

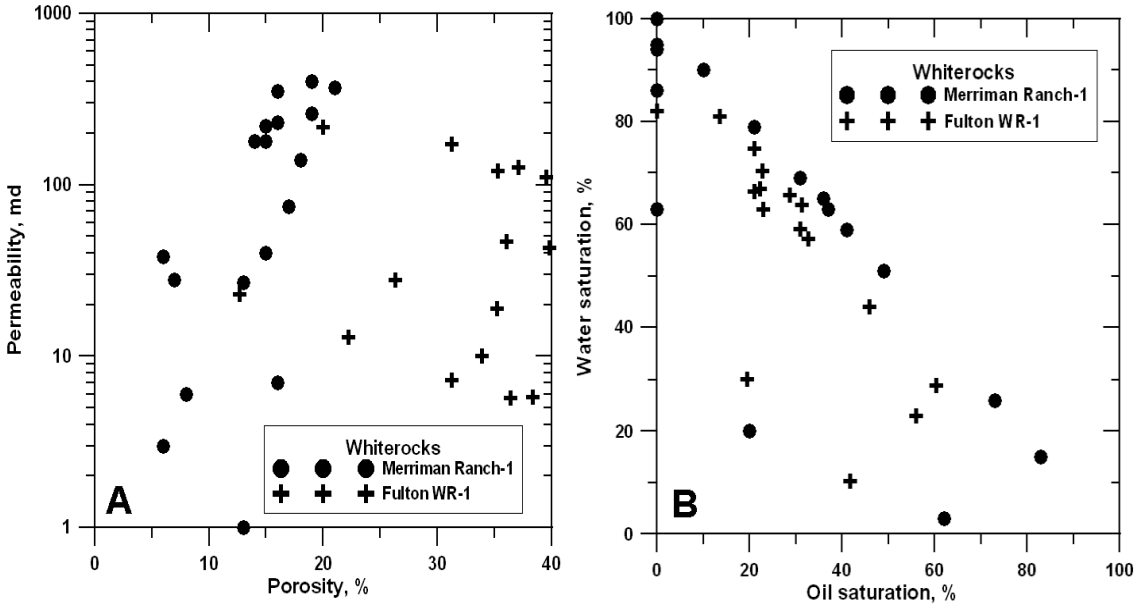

Figure 54: Nugget Sandstone petrophysical properties (A) and fluid saturations (B) measured in core from the Merriman Ranch 1 and Fulton Whiterocks 1 wells (for locations see Fig. 28). Data from Polumbus Jr. and Associates (1961).

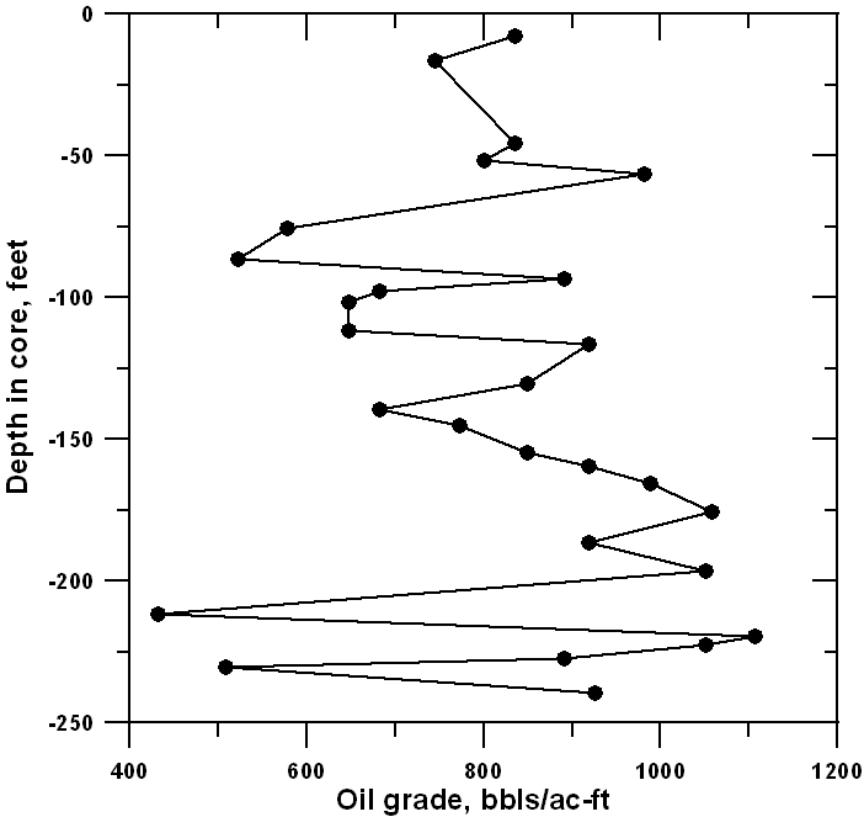

Figure 55: Vertical variability of oil grade measured in Nugget Sandstone core from the Rocky-slant well. The average grade in the 230-foot interval cored is 817.4 bbls/acre-ft with a range 431.2 to 1105.9 bbls/acre-ft. Data from Peterson (1982).

Outside of the Whiterocks River valley, where erosion has not cut deep into the Nugget Sandstone reservoir, the oil columns are rather thick (Fig. 56). The thickness of the oil-impregnated interval or oil column is in the range 500 to 675 ft on the west side of the valley and 599 to 781 ft on the east side. In general, the oil resource (Fig. 57) correlates with thickness of the oil column. The oil resources are in the range 426 to 547 MBO/acre on the west side of the valley and 250 to 576 MBO/acre on the east side.

In many of the coreholes, Peterson (1985) divides the zone of oil saturation into three intervals: a "shallow" zone, a middle "lean" zone, and a "deep" zone (Table 7). The shallow zone has an average thickness of 145 ft (range 88-241 ft) and an average OOIP of 90.5 MBO/acre. It contains an estimated 27% of the total oil resource in the deposit. The lean zone averages just 37 ft thick (range 17-54 ft) and has an average OOIP of only 6.7 MBO/acre, just 3% of the total. The deep zone averages 365 ft thick (range 88-583 ft) and as a consequence it accounts for an estimated 70% of the resources of the deposit. The average OOIP for the deep zone alone is 211.1 MBO/acre. The average OOIP for the portion of the Whiterocks deposit sampled by the cores penetrating the full oil column is 343.8 MBO/acre.

The average oil grades, thickness of oil-impregnated sandstones, and estimated OOIP as tabulated from data in Polumbus Jr. and Associates (1961) and Peterson (1982) are reported in Table 8. Two of the wells, Item and Rocky, did not penetrate the full oil-impregnated zone. Predictably, the higher OOIP values are on the valley slopes where the total thickness of the oil column is greater. It is significant that the higher grades are located near the ends of the region investigated. The deposit shows no indication of playing out along trend.

Covington and Young (1985) report that the average oil saturation in the Commodore well (see Fig. 51 for location) is 897.4 bbls/acre-ft. Given the 530 ft oil column reported in the well, this oil grade would yield an OOIP of 475.6 MBO/acre, a value consistent with other wells in the deposit.

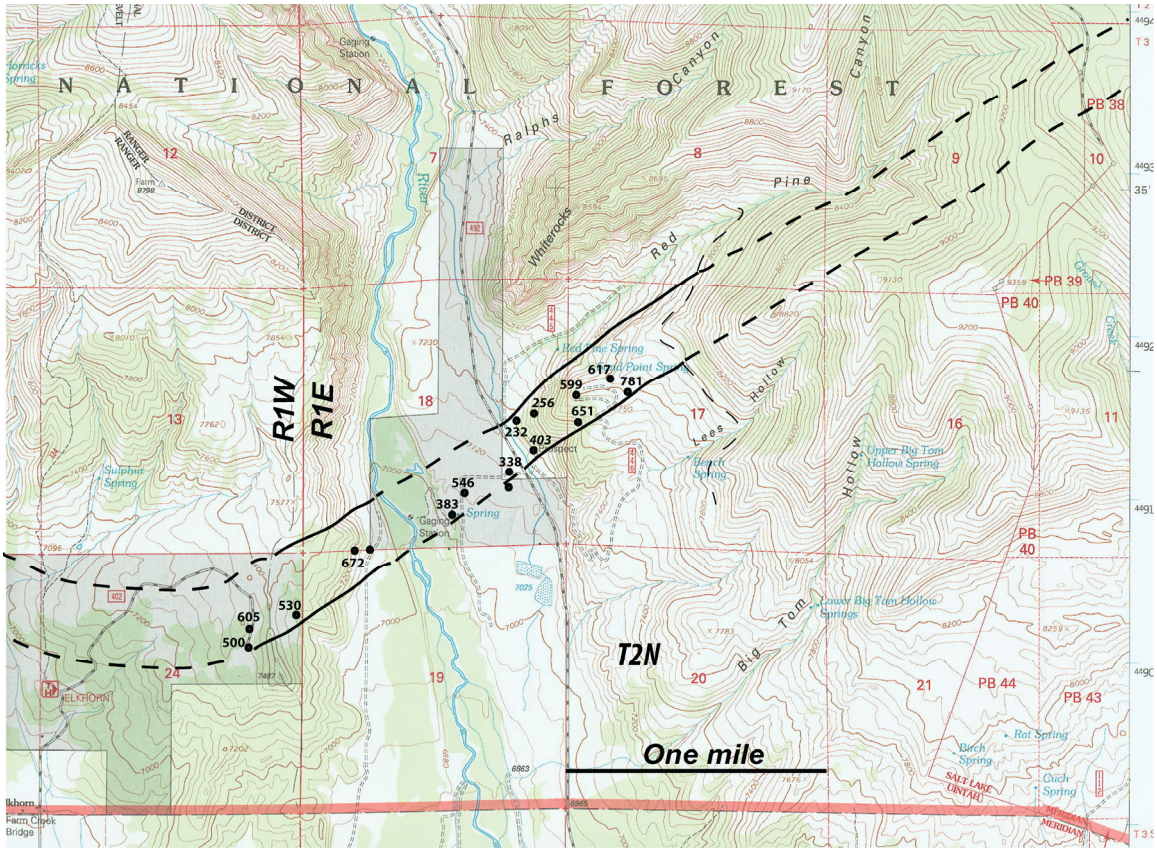

Figure 56: Map showing thickness in feet of the oil-impregnated interval, the oil column, at the various coreholes (black dots). Refer to Table 8 for the data and sources. Data from Peterson (1982).

Based on a simple calculation using the average oil grade for the 10 full-penetration wells shown in Table 8 plus the Commodore well and the number of acres underlain by reservoir encompassing those wells (Fig. 57), the estimated OOIP in the cored ("proven") segment of the deposit is 290 acres x 338.0 MBO/acre = 98.02 MMbbls. This value is in line with previous estimates of oil resource presented in Table 9. However, this number should be seen as the minimum oil resource value for the Whiterocks deposit.

If oil-impregnated Nugget Sandstone extends both to the west and to the east beyond the cored segment adjacent to Whiterocks River, the deposit's oil resource will be considerably larger. Using just the probable trace of the reservoir shown in Fig. 56, we can calculate the proven plus probable oil resource to be:

SW plateau segment:	250 acres x 486.5 MBO/acre =	121.6 MMBO
Whiterock valley segment:	120 acres x 246.3 MBO/acre =	30.8
NE plateau segment:	400 acres x 454.0 MBO/acre =	181.6
	Total oil-in-place:	334.0 MMBO.

The actual resource could be as great as 450-500 MMBO if the oil-impregnated sands continue westward as far as the Uintah-Duchesne county line and eastward to the Little Mountain fault zone.

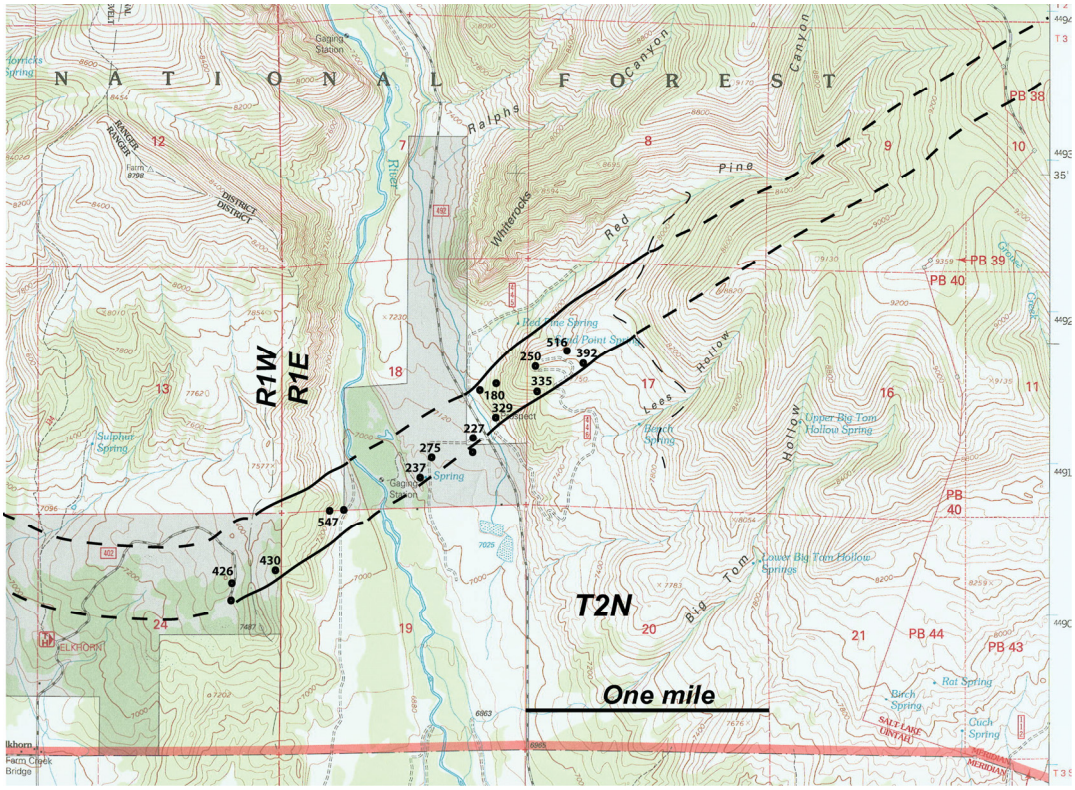

Figure 57: Map showing the distribution of the original oil-in-place (MBO/acre) determined from wells penetrating oil-impregnated Nugget Sandstone. Refer to Table 8 for the data and sources. Note that high oil grades correlate closely with thickness of the oil-saturated intervals shown in Fig. 56. Data from Peterson (1982).

Table 7: Oil-in-place per acre is in thousands of barrels MBO/acre in cores at the Whiterocks deposit differentiated by shallow, lean, and deep zones within the oil-impregnated interval. The Item and Rocky vertical wells did not penetrate the full oil-impregnated zone and therefore represent a minimum of possible total oil in place per acre. Data from Peterson (1985).

Well:	*Easy*	*John*	*Dog*	*Charlie*	*Item*	*Able*	*Rocky Vert.*	*George*	*Fox*	*King*	*Average*
Shallow zone:	114.0	117.0	52.0	68.0	64.0	57.0	82.0	53.0	159.0	139.0	90.5
Lean zone:			5.5		6.0	2.5	4.0	12.0	13.0	4.0	6.7
Deep zone:	288.0	367.0	320.5	282.0	14.0	85.5	143.0	154.0	66.0	391.0	211.1
Total:	402.0	484.0	378.0	350.0	84.0	145.0	229.0	219.0	238.0	534.0	306.3

Table 8: Average and median oil-in-place measured in cores taken from the Whiterocks heavy oil deposit. Values are calculated from unpublished data in Polumbus Jr. and Associates (1961) and Peterson (1982), and are compared against grades for the same wells reported in Peterson (1985).

	Bbls/acre-ft:		Feet:	MBO/acre:		
Well:	*Average*	*Median*	*Total saturated*	*Average*	*Median*	*Peterson (1985)*
Easy	501.8	462.2	781	391.9	361.0	402
John	835.8	863.2	617	515.7	532.6	484
Dog	514.9	479.2	651	335.2	312.0	378
Charlie	417.8	455.4	599	250.2	272.8	350
*Item**	301.0	278.7	*256*	*77.1*	*71.3*	*84*
Able	775.7	788.5	232	180.0	182.9	145
*Rocky Vert.**	817.4	848.5	*403*	*329.4*	*341.9*	*229*
George	670.4	598.1	338	226.6	202.2	219
Fox	618.2	734.1	383	236.8	281.2	238
King	813.6	815.7	672	546.7	548.1	534
Merriman-1	504.2	489.4	546	275.3	267.2	NA
Fulton-1 WR	703.9	660.0	605	425.8	399.3	NA
Fulton-2 WR	NA	NA	500	NA	NA	NA

** grade from Rocky-slant; incomplete penetration of saturated zone in italics.*

Table 9: Reported estimates of oil-in-place in the known extent of the Whiterocks heavy oil deposit.

Source	*Total (MMBO)*	*Proven*	*Possible*	*Explanation*
Severy (1943)	9.52			For exposed portions; based on mapping.
Shirley (1961)	105	57	27	Based on 11 coreholes extending deposit beyond outcrop.
Covington (1963)	about 50			Based on existing corehole data.
Lewin & Assoc (1984)	120	60	60	Separated into 200 acre tracts; 600 ft saturation zone.
Campbell (1975)	37.3			Based on 182 acre and 500 ft saturation zone.
Ritzma (1979)	65-125			Based on previous work.
Peterson (1985)	>100			Based on previous work and new corehole data.

SHALLOW IMMOBILE OIL DEPOSITS WITHIN UINTA BASIN

Within the interior of the Uinta Basin, Ritzma (1979) identified a belt of shallow "tar sand" accumulations in the Uinta Formation that extended from east of Duchesne to Natural Buttes gas field. These accumulations are shown on the Energy Resources Map of Utah (Gurgel, 1983) principally as clusters of single well occurrences that Ritzma (1979) assigned to two oil fields (Fig. 1): Pariette (12-15 million barrels of OOIP; T8S, R15-18E) and Chapita Wells (7.5-8.0 million barrels of OOIP; T9S, R20-21E).

The full extent of shallow oil pools in the central part of the Uinta Basin is difficult to determine because most operators do not begin logging until well within the Green River Formation. The oil within these shallow Uinta Formation sandstone reservoirs is either heavy or high pour point oil considered noncommercial due to its inability to flow freely from the cool reservoirs. On the whole, these shallow oil pools have received scant attention in the past, yet they may constitute a large untapped oil resource accessible through thermal *in situ* recovery methods.

In Brennan Bottoms field, several operators have encountered a mixture of mobile/ immobile oil, condensate and natural gas (commonly biogenic) in shallow Uinta Formation sandstones at depths of 2500 to 3000 ft (personal communication, James Emme, March, 2008). The Brennan Fed 4-15 well (API#4304731332; NE SE 15-T7S-R20E), drilled and completed in the Uinta Formation (upper Eocene) in 1984, initially tested 575 Mcfgpd, but no oil or water. However, in a 20 month period in 2003-2004, this well produced 132 barrels of oil without reservoir stimulation from the same 3025 to 3067 ft deep Uinta Formation sandstones that had been completed in 1984 (Utah Division of Oil, Gas and Mines public records).

In 1982, Gulf Oil investigated the potential for oil recovery from the shallow Uinta Formation sandstones in Wonsits Valley field (Nettle, 1982). This shallow, immobile oil resource was reexamined by Chevron U.S.A. in 1990, but no action was taken. The reports prepared in assessing this stranded oil resource are the basis for the following discussion.

Wonsits Valley Field

Wonsits Valley oil field is located in the southeast Uinta Basin, immediately east of the Green River and north of the White River (Figs. 58 and 59). The field occupies 10 sections in the northeast portion of T8S-R21E, 5 sections in the northwest portion of T8S-R22E, and extends slightly into T7S-R22E, where the producing trend becomes Wonsits oil field. Current production is from lenses of medium-grained, calcareous, quartz arenite and fine-grained, sandy, ostracodal limestone in the lower Green River Formation (Schuh, 1993). The pay zones are at depths of about 5500 ft, where reservoir temperatures exceed 150ºF. The high-paraffin crude has an API gravity of 29-30º, a pour point of 90ºF, and a viscosity in the reservoir near 4.0 cp. Reservoir energy is provided by solution gas drive.

The lacustrine Green River Formation is conformably overlain by the upper Eocene Uinta Formation, a red-brown mudstone succession containing fluvial channel sandstones. In the area of Wonsits Valley field at a depth of 800 to 1600 ft, the lenticular sandstone beds in the Uinta Formation contain immobile oil. Immobility is due to high viscosity and/or reservoir temperatures lower than the pour point of the oil. Knowledge of the deposit is derived from an unpublished industry report (Nettle, 1982) which describes the sandstone reservoir properties in three test wells and the characteristics of oil samples swabbed from one of the test wells. Additional information on the distribution of net sandstone thickness is from Chalcraft (1990).

Figure 58: Satellite image of Wonsits Valley field between the Green River to the west and the White River to the south. Note the many close-spaced well pads that delineate the extent of the field. Source: GoogleEarth.

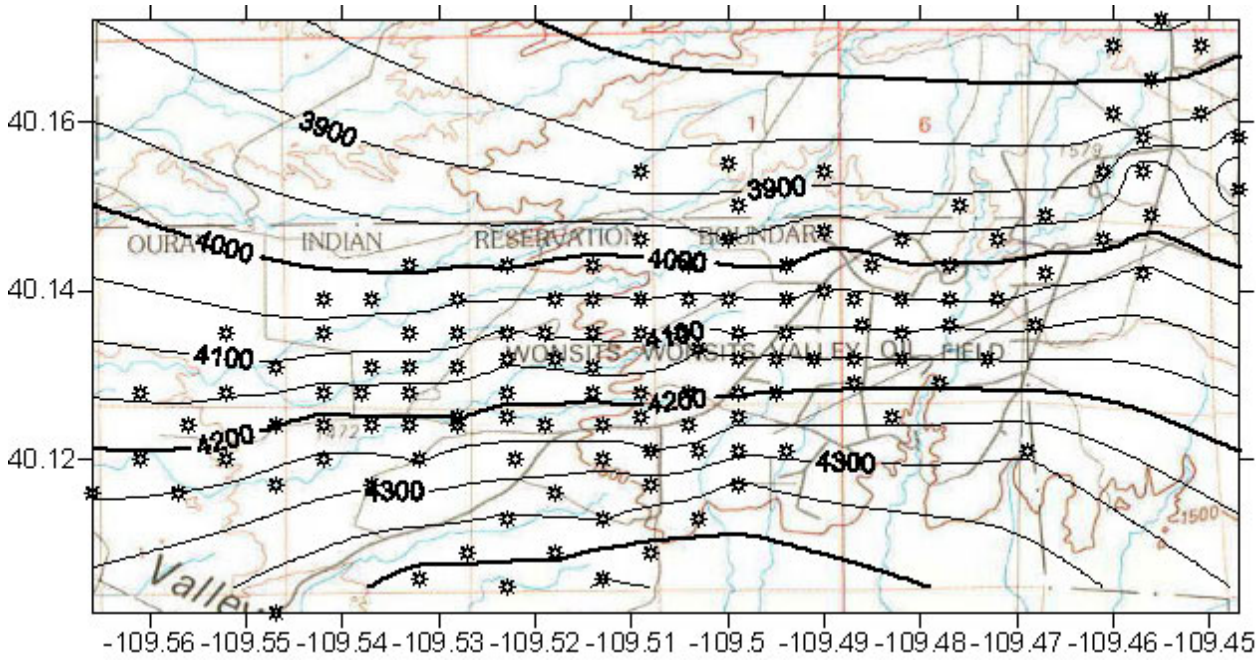

Figure 59: Structure map of the top of the Uinta Formation in the Wonsits Valley field. This datum dips northward at about three degrees, or a 500 ft drop over 2 miles. The contours are feet elevation relative to mean sea level; the interval is 50 feet. The map is six miles (sections) wide. Data for constructing map from Nettle (1982).

The Uinta Formation is nearly flat-lying in Wonsits Valley field (Fig. 59), dipping very gently northward with a drop of only 500 ft over a distance of 2 miles. The lenticular nature of sandstone beds in the Uinta Formation is well illustrated by their spatial variability in the three test wells (Fig. 60). The correlations assigned to each sandstone bed are from Nettle (1982), but they could well have been assigned differently by other log interpreters. Clear in these test wells is the great lateral variability in thickness and in the relative proportion of sandstone beds. Table 10 shows the variations between the test wells in thickness of the sandstone beds and the proportion of sandstone to mudstone (sand-shale ratio).

Whereas the overall range of thickness is 43.2 ft vs. 6.1 ft, median thicknesses between the test wells is just 21.1 ft vs. 16.3 ft. The variations in sandstone bed thickness in all three test wells are depicted as a histogram in Fig. 61A.

Table 10: Summary of sandstone bed thicknesses observed in the three test wells, Wonsits Valley field.

	Test well 1	Test well 2	Test well 3
Total sandstone thickness	230.6	271.0	133.4
Sand-shale ratio	0.298	0.360	0.184
Average thickness	23.1	22.6	16.7
Median thickness	19.4	21.1	16.3
Maximum thickness	43.2	33.7	32.5
Minimum thickness	8.6	10.5	6.1

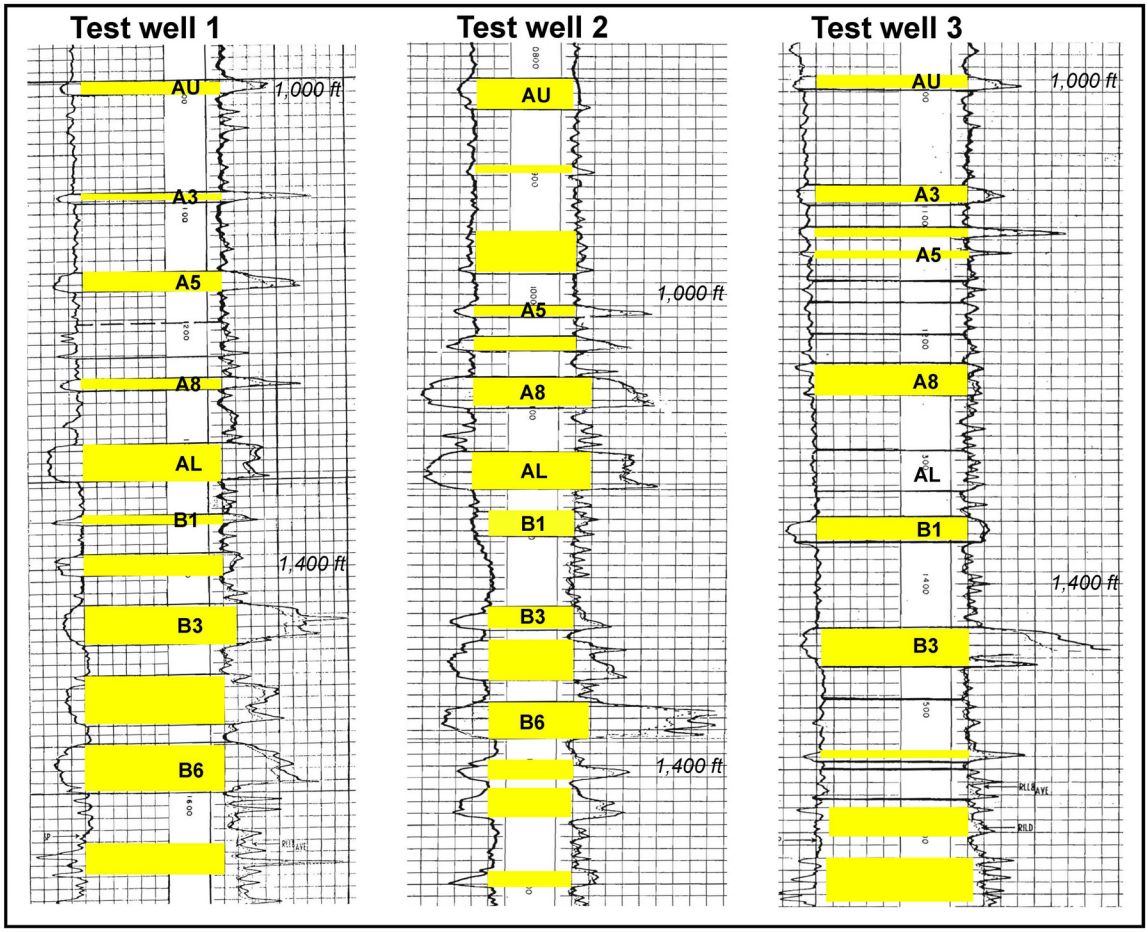

Figure 60: Sandstone intervals in three test wells. The identification of specific sandstone beds, or their sandy mudstone equivalents, is after Nettle (1982). They could not be independently verified as reasonable correlations. The log traces are SP on the left and resistivity on the right.

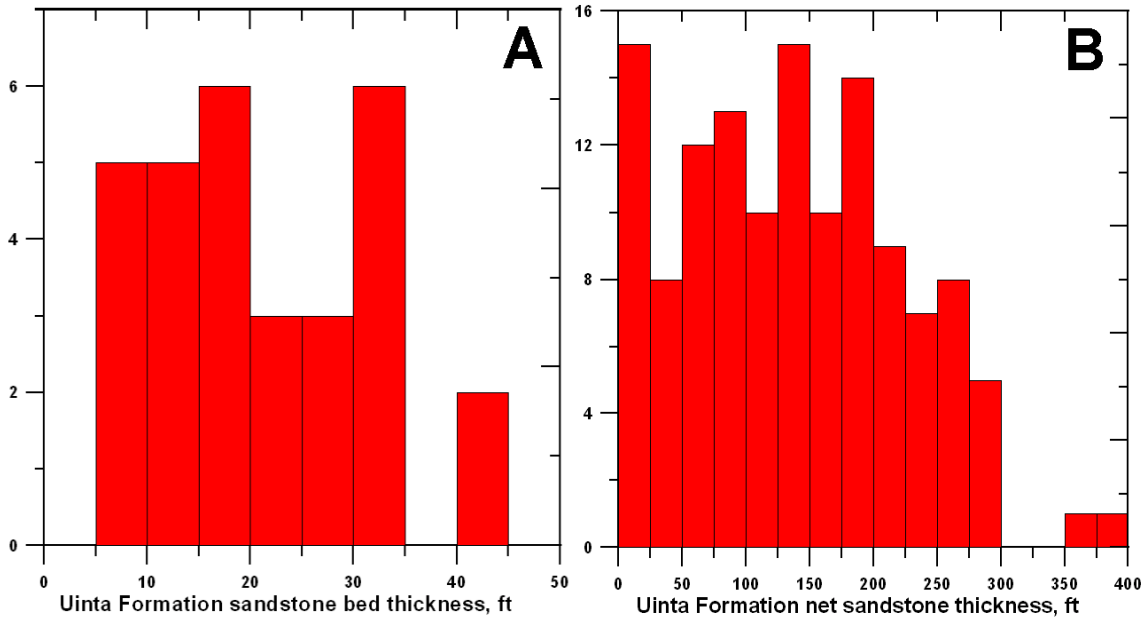

Figure 61: Histograms of sandstone bed thicknesses observed in the three test wells (A) and the net thickness of oil-impregnated sandstone within the entire field (B). Data from Nettle (1982).

The sandstones are described as fine-grained feldspathic sandstone with moderate to high clay content, 5 to 35% (Nettle, 1982). Authigenic chlorite is the dominant clay mineral, but illite, kaolinite and smectite are also observed. Cements include quartz, analcite, calcite, and anhydrite. The high proportion of clay and cement results in relatively low porosity and permeability for such a shallow deposit (Table 11, Fig. 62A). Porosity ranges between 21.1% and 12.2%; the median values are 18.0% to 16.0%. Permeability to air ranges from 194 md to 0.1 md; the median values are just 12.5 md to 0.6 md. Laboratory tests showed the sandstone to be highly sensitive to both brine and distilled water, which could cause clay swelling and reduction of permeability (Nettle, 1982). The test wells had been drilled and cored using fresh-water mud.

For a commercially viable oil reservoir, the sandstones have low oil saturations (Table 11) averaging 42.6% to 53.9%, after normalization, So + Sw = 100%. However, there is a wide range of oil saturations observed in these rocks (Fig. 62B).

Table 11: Summary of petrophysical properties of sandstone beds in the three test wells, Wonsits Valley field.

	Test well 1	***Test well 2***	***Test well 3***
Porosity, %, average	18.1	17.4	16.5
Porosity, %, median	18.0	16.5	16.0
Porosity, %, max	21.0	21.1	21.2
Porosity, %, min	16.0	13.6	12.2
Permeability, md, average	18.0	50.7	61.2
Permeability, md, median	12.5	10.5	0.6
Permeability, md, max	56.0	194.9	297.0
Permeability, md, min	1.0	0.1	0.1
So, %, average	53.9	42.6	43.1

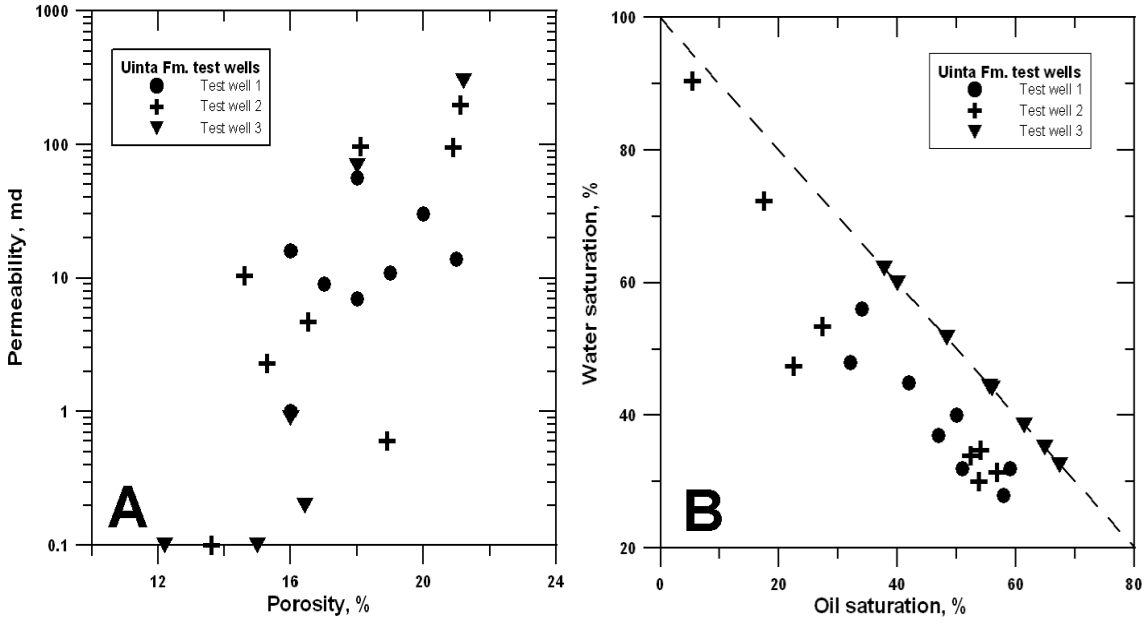

Figure 62: Values of porosity and permeability (A) and fluid saturations (B) measured in test well cores from the Uinta Formation lenticular sandstone beds. Data from Nettle (1982).

The total net thickness of sandstone beds in the Uinta Formation range from 382 ft to 1 ft, averaging 139 ft. The median net thickness is 140 ft. A histogram of the total net thickness determined for 159 wells in the field shows a generally uniform distribution of values less than 280 ft (Fig. 61B). The larger net sandstone thicknesses are clustered near the center of Wonsits Valley field, but as would be anticipated in these highly lenticular fluvial sandstones, the net thickness values are spatially irregular.

Calculation and mapping of OOIP in the Uinta Formation sandstone reservoirs was based on the net thickness of the sandstones and an average oil grade of 300 thousand barrels per section-foot applied uniformly across the field (Nettle, 1982). This oil grade is the equivalent of 470 barrels per acre-foot. The median OOIP is 65.8 MBO/acre, but it is as great as 180 MBO/acre. The spatial distribution of estimated OOIP (Fig. 63) corresponds to the net sandstone thickness distribution. An approximate 4420 acres of Wonsits Valley field has OOIP greater than 50 MBO/acre. The total estimated OOIP in this richer part of the Uinta Formation is 310 MMBO.

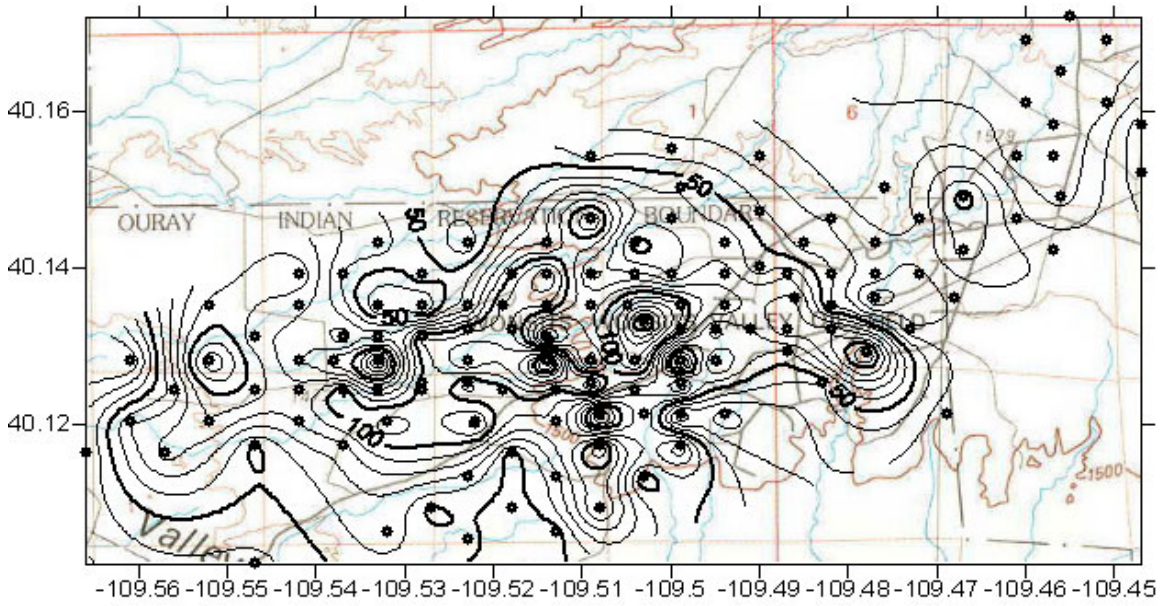

Figure 63: Distribution of estimated oil in place within shallow Uinta Formation sandstone lenses in units of MBO/acre. The values are calculated directly from the net sandstone thickness assuming a uniform oil concentration of 470 bbls/ac-ft in sandstone beds. The map is six miles (sections) wide. Net thickness data for constructing map from Nettle (1982).

DEPOSITS WITHIN AND MARGINAL TO THE PARADOX BASIN

In the southeast quadrant of Utah, there exists an array of shallow bitumen accumulations along the western margin and within the interior of the Pennsylvanian-Permian Paradox basin. Most are relatively small and/or of very low grades, but the largest deposit in Utah (Ritzma, 1979), the Tar Sand Triangle, is part of this group. Nearly all of the accumulations appear to be remnants of giant exhumed oil fields, recognized to be portions of breached oil traps, either anticlinal or combined structural-stratigraphic. Normally, the oils are heavier than 10º API and have high sulfur content in the range 1.6 to 6.3 wt%. They are heavily biodegraded.

Bitumen accumulations are found throughout the crest of the San Rafael Swell in Emery County (Table 12). The principal reservoir unit is the Triassic Moenkopi Formation, nearshore and tidal flat sandstones, limestones and mudstones. These strata rest unconformably on the Permian late orogenic sedimentary fill of the Paradox basin. Minor bitumen deposits occur also in Triassic-Jurassic sandstones overlying the Moenkopi Formation. All San Rafael Swell accumulations collectively contain an estimated 450-550 MMBO (Table 12). However, the deposits are very lean and spread over a very large area. Even one of the larger deposits, Black Dragon (Tripp, 1985), has an average grade of only 300 BO/ac-ft and an average OOIP of a mere 4.26 MBO/acre.

Table 12: Shallow bitumen accumulations within the San Rafael Swell on the northwest margin of the Paradox basin (Ritzma, 1979).

Oil accumulation	Twp	Rng	Reservoir unit(s)	MMBO
Black Dragon	21-22S	12-14E	Moenkopi	100-125
Family Butte	22-24S	9-11E	Moenkopi	100-125
Cottonwood Draw	21S	11-12E	Moenkopi	75-80
Red Canyon	20-21S	10-13E	Moenkopi	60-80
Wickiup	21-22S	10-11E	Moenkopi	60-75
Chute Canyon	24-25S	10-11E	Moenkopi	50-60
Flat Top	24S	11E	Chinle	0.25-0.50
Justensen Flats	23S	9E	Navajo + Kayenta	very small
Temple Mountain	24-25S	10-11E	Chinle + Wingate	very small

South and southeast of the San Rafael Swell, the scattered small heavy oil occurrences (Table 13) are near-surface oil seeps commonly overlying light oil and gas fields in the Mississippian Leadville Limestone. This is definitely true for Salt Wash and Ten Mile Wash fields in northern Grand County (Smouse, 1993). The large Circle Cliffs field occupies a breached anticlinal trap (Ritzma, 1980). It straddles the boundary of the Capitol Reef National Park and the Grand Staircase-Escalante National Monument, where it is off limits to development. The only bitumen accumulation of economic consequence in the region is in the Tar Sand Triangle.

Table 13: Shallow bitumen accumulations within and marginal to the Paradox basin (Ritzma, 1979).

Oil accumulation	Twp	Rng	Reservoir unit(s)	MMBO
Tar Sand Triangle	29-33S	14-17E	White Rim + Moenkopi	12,500-16,000
Circle Cliffs	33-36S	14-17E	Moenkopi	860
White Canyon	34-35S	15-16E	Hoskinni Mbr. (Moenkopi)	12 to 15
Ten Mile Wash	23-24S	18-19E	Burro Cyn + Morrison	6
Salt Wash	22-23S	16-17E	Morrison + Entrada	0.2-0.25
Sweetwater Dome	26S	14E	Curtis + Entrada	0.10-0.12

Tar Sand Triangle deposit

The Tar Sand Triangle bitumen deposit is located on the Colorado Plateau in Garfield and Wayne Counties, southeast Utah. It lies beneath a deeply dissected plateau bounded on three sides by deep canyons, the Green River to the northeast, the Colorado River to the southeast, and the Dirty Devil River to the West (Fig. 64). The highest surface, supported by the Navajo Sandstone (Jurassic) and having an elevation of about 7000 ft, is preserved along a long, sinuous ridge west of the Orange Cliffs (Fig. 65). Below this surface are several benches, with the principal ones supported by the Moenkopi Formation (Triassic) and the Cedar Mesa Sandstone (Permian). The encircling rivers are at elevations of 3700-4000 ft.

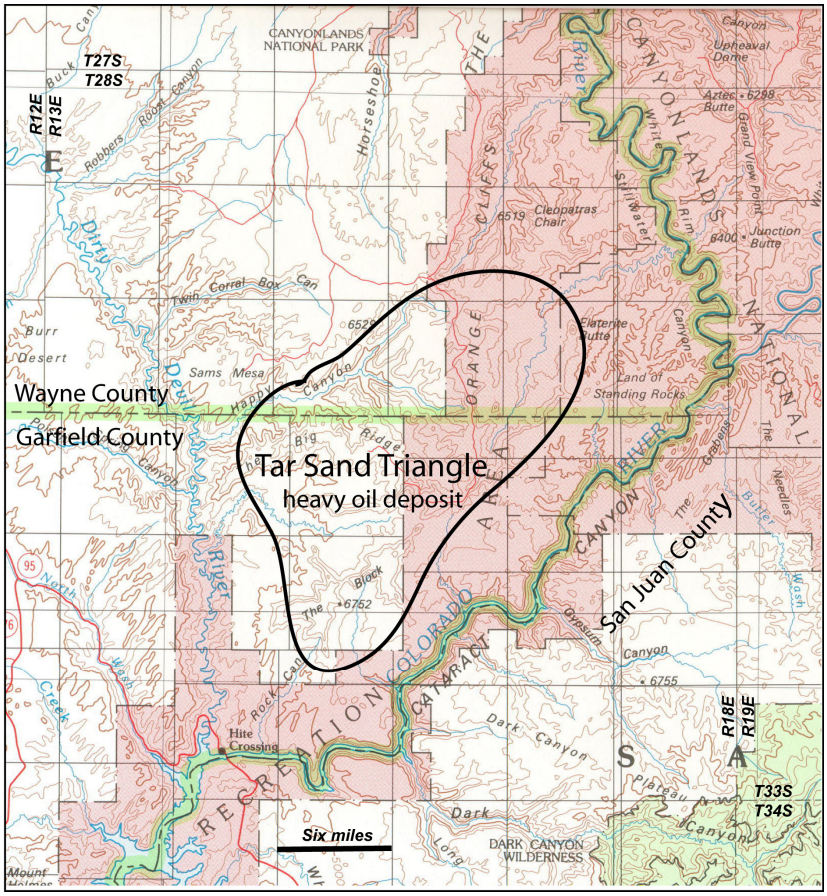

Figure 64: Topographic map showing the limits of the Tar Sand Triangle deposit as defined by the zero thickness isopleth of bitumen-impregnated sandstone reservoir. The deposit is situated in mesa country bounded by deeply incised canyons of the Green River to the northeast, the Colorado River to the southeast, and the Dirty Devil River to the west. Roughly half the deposit lies within the boundaries of the Glen Canyon National Recreation Area and the Canyonlands National Park. The map shows the principal unimproved road accessing the Orange Cliffs-The Big Ridge plateau overlying the deposit.

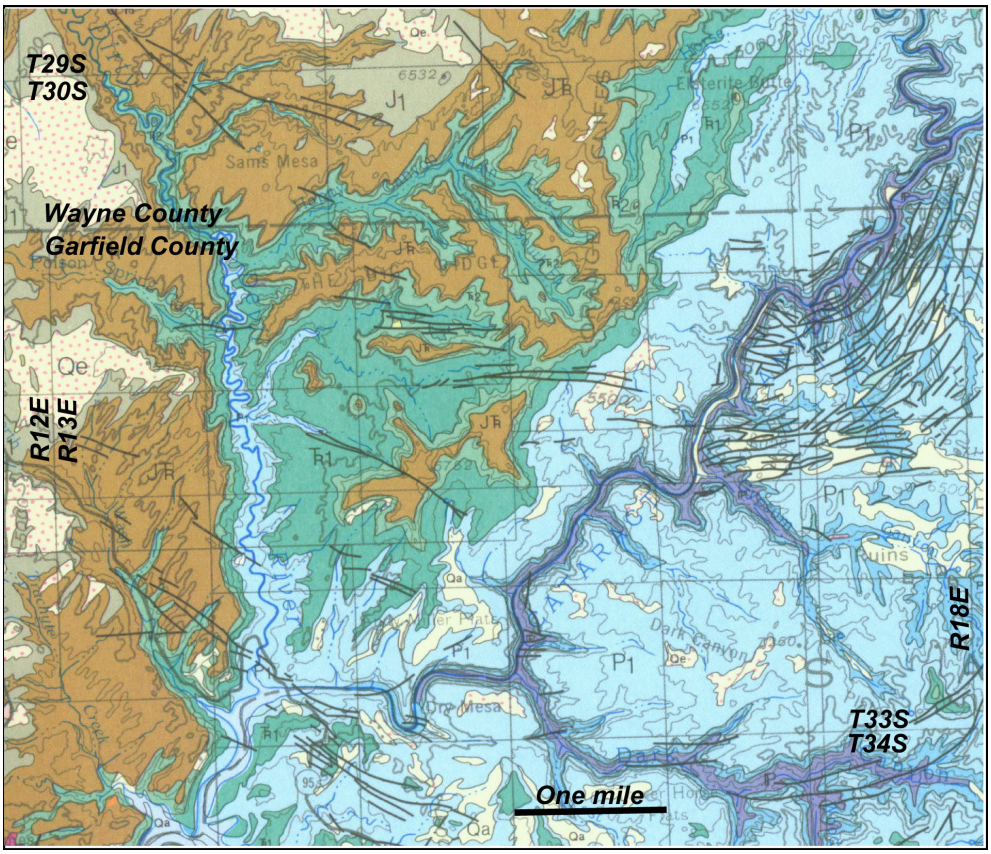

Figure 65: Geologic map of the Tar Sand Triangle area between the Colorado and Dirty Devil Rivers (extracted from Geologic Map of Utah; Hintze, 1980). The high sinuous plateau supported by the Navajo Sandstone (JTr) containing Gordon Flats, Flint Flat, and The Big Ridge are in brown just north and south of the Garfield-Wayne county line in the upper center part of the map.

The deposit covers an area of about 200 square miles (126,720 acres) within all or parts of 8 townships (Fig. 64): T30S-R15E, T30S-R16E, T30S-R17E, T31½S-R16E, T31S-R14E, T31S-R15E, T31S-R16E, and T32S-R15E. About 40% of the deposit is within the Glen Canyon National Recreation Area (NRA) and a very small part (less than 200 acres) is in the Horse Canyon area on the western edge of the Canyonlands National Park (NP). The remaining part of the deposit is on public lands administered by the Bureau of Land Management (BLM) and Utah School and Institutional Trust Lands Administration (SITLA). No part of the deposit is on fee land.

The Tar Sand Triangle is located near the southwest margin of the Paradox basin immediately outside of the region underlain by Pennsylvanian evaporites. This is an area of essentially flat-lying, undeformed strata of Permian to Jurassic age forming a stepped landscape incised by steep-walled canyons (Fig. 66). The highest bench is supported by the Navajo Sandstone (Jurassic); various Triassic sandstones and the Cedar Mesa Sandstone form the lower

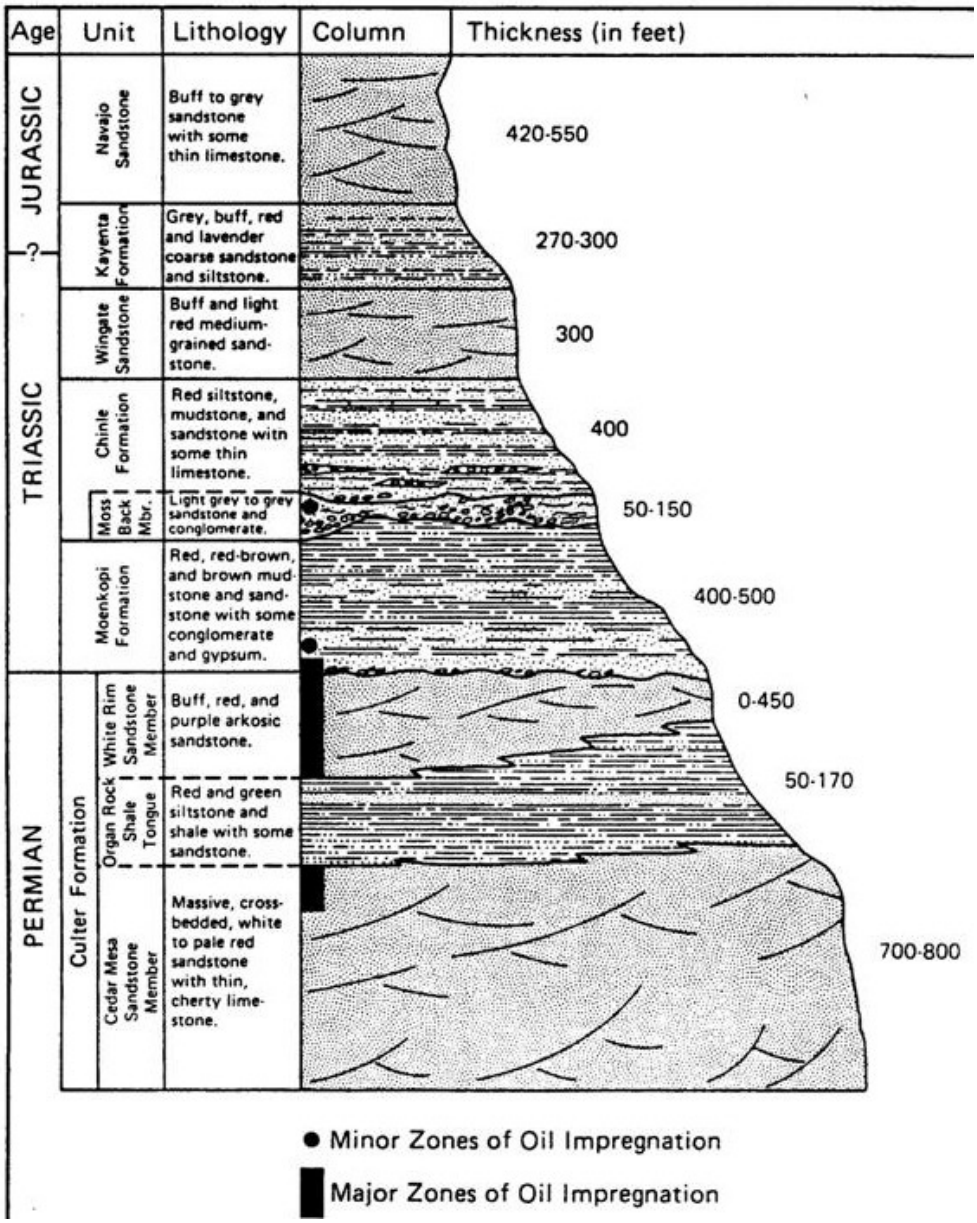

Figure 66: Stratigraphy of the Tar Sand Triangle showing the major and minor zones of bitumen-impregnation (Dana and others, 1984).

benches (Fig. 67). The Moenkopi Formation (Triassic) rests with an angular unconformity on the Cutler Formation (Upper Permian). Heavy oil is found principally in the White Rim Sandstone, the uppermost member of the Lower Permian Cutler Formation. However, at a few locations the upper Cedar Mesa Sandstone and the sandy basal part of the Moenkopi Formation, the Hoskinni Member, also are bitumen-impregnated (Fig. 66). The Cedar Mesa and White Rim Sandstone members are similar eolian deposits separated in the Tar Sand Triangle by the Organ Rock Shale Tongue projecting southwestward out of the Paradox basin. The White Rim Sandstone is encased in less permeable strata, the Moenkopi Formation red mudstones above and the Organ Rock Shale below.

The bitumen in the White Rim Sandstone occupies a conventional stratigraphic trap (Campbell and Ritzma, 1981; Huntoon and others, 1994) in which the updip edge is truncated by the basal-Triassic unconformity (Fig. 68). Within this trap, a distinct oil-water contact has been recognized that establishes the western tapered edge of the deposit. The eastern edge is defined by the unconformity cut-off, or the modern land surface in the canyon of the Colorado River. The deposit strata are nearly flat-lying, dipping to the northwest at just 120 ft per mile (Fig. 69).

The combination of erosional beveling and stratigraphic position above the westward thinning tongue of the Organ Rock Shale (Fig. 70) has resulted in the thinning of the White Rim Sandstone towards the southeast and east (Fig. 71). In the area of the Tar Sand Triangle, the White Rim Sandstone is less than about 350 ft thick. Most authors, principally Huntoon and others (1994), assume that the westward thickening of the White Rim Sandstone indicates that it only could have been charged from that direction, but in fact the source of the oil and the direction of charge are unknown.

Figure 67: View to the southwest of the Upper Permian-Jurassic stratigraphy exposed along the Colorado River in the Canyonlands National Park immediately north of the Tar Sand Triangle. The White Rim Sandstone is indicated by the red arrow. Photograph by S. Schamel.

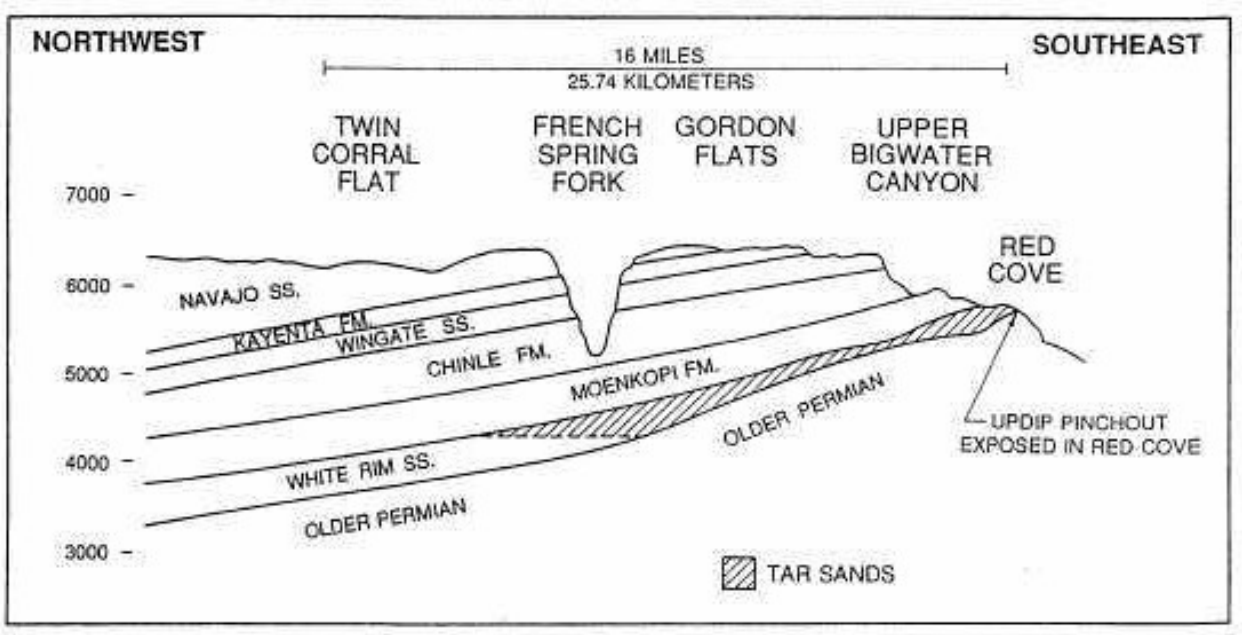

Figure 68: Generalized cross section of the Tar Sand Triangle heavy oil deposit showing the stratigraphic position of the principal reservoir, the White Rim Sandstone (Bishop and Tripp, 1993).

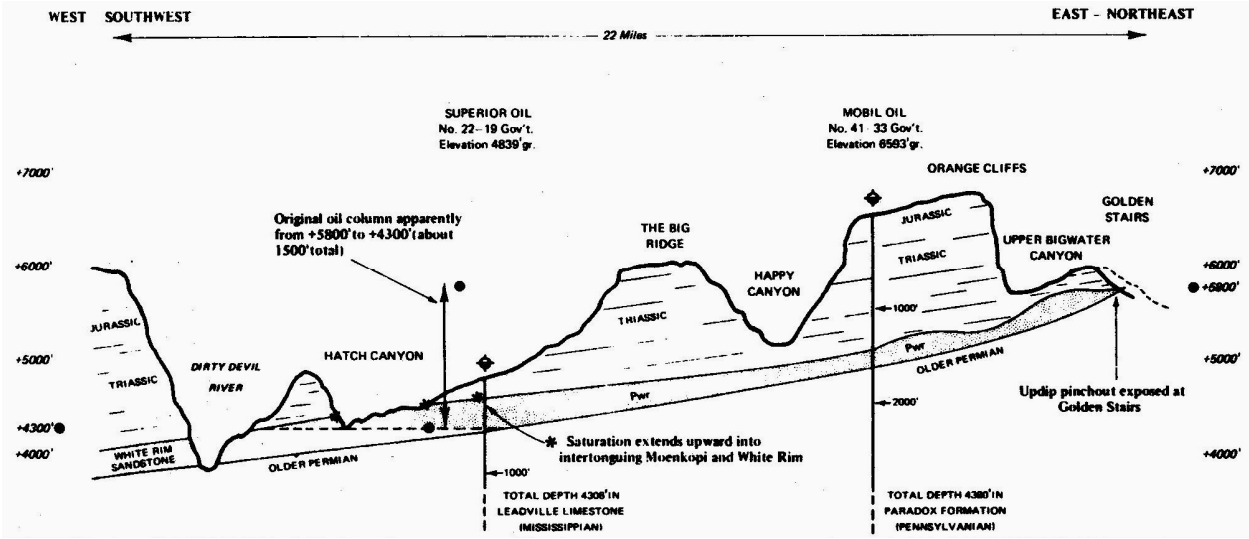

Figure 69: Cross section from Dirty Devil Canyon to the Orange Cliffs above the Colorado River showing the lateral extent of the Tar Sand Triangle deposit and the position of the oil-water contact east of the Dirty Devil River (Dana and others, 1984).

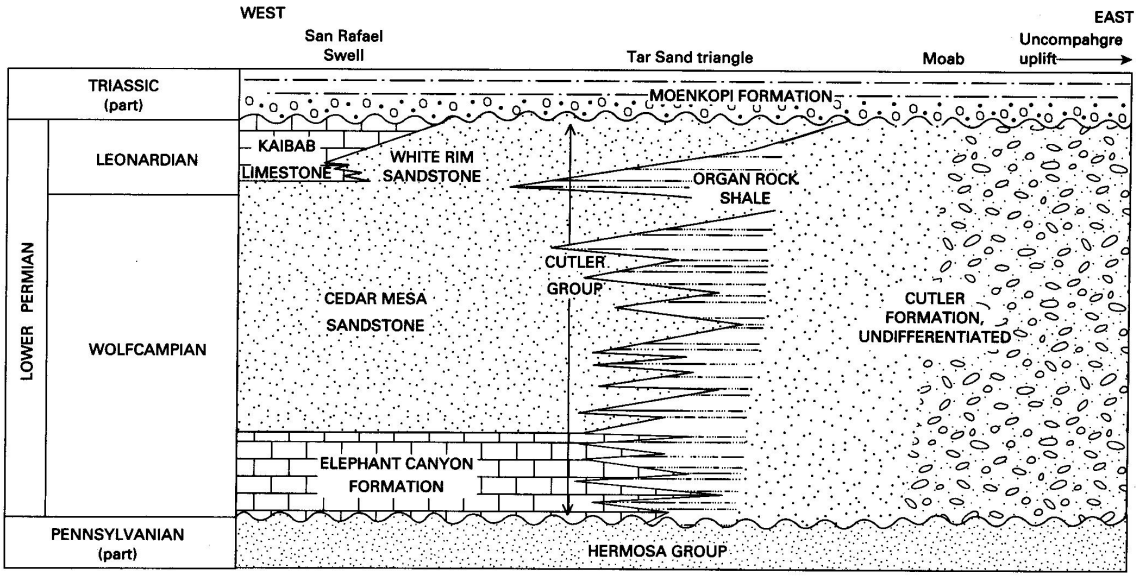

Figure 70: Lower Permian stratigraphy in central Utah showing the truncation of the White Rim Sandstone beneath the Moenkopi Formation (Triassic) giving rise to the updip stratigraphic trap controlling, in part, the Tar Sand Triangle deposit (Hansley, 1995).

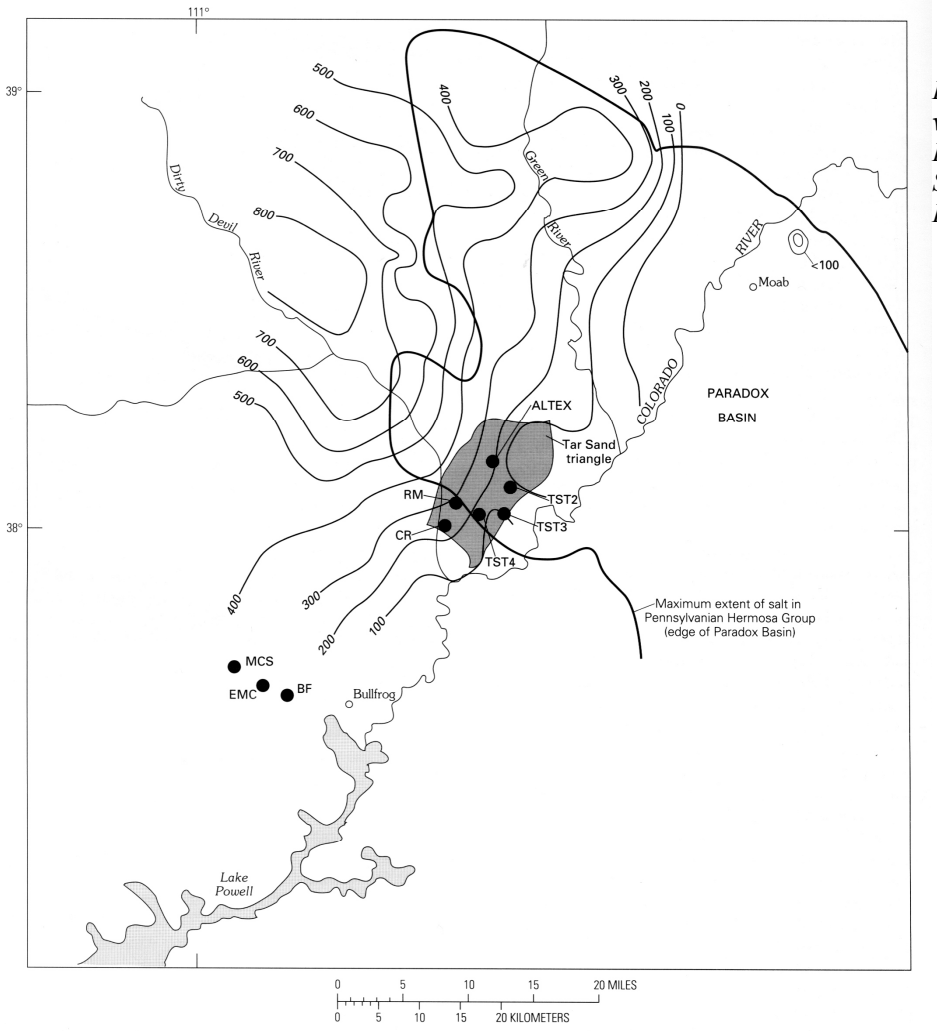

Figure 71: Isopach thickness variation in feet of the White Rim Sandstone across the Tar Sand Triangle (extracted from Hansley, 1995).

The Tar Sand Triangle deposit is thought to be part of a much larger oil accumulation on the Colorado Plateau in the tectonic position of either the south rim of the Paradox basin or the updip edge of the Sevier foredeep basin, or both. It may be a remnant of a 30-40 BBO oil field (Hansley, 1995) in which the normal oil evolved into a heavy oil within the reservoir after emplacement by a combination of biodegradation, water washing, and oxidation. The degradation of the oil probably occurred as the Colorado Plateau uplifted in the late Cenozoic and the deposit was exhumed. Fluid inclusion closing temperatures infer that the White Rim Sandstone had been buried to a depth of about 11,500 ft at the time of reservoir filling, most likely in the mid-Tertiary and just prior to erosional unroofing (Huntoon and others, 1999).

The principal reservoir in the Tar Sand Triangle, containing about 99% of the OOIP, is the White Rim Sandstone of Early Permian (Leonardian) age. It is composed of white, subrounded to well-rounded, fine to very fine grained quartzarenite (Huntoon and others, 1994) and is dominated by large-scale, high-angle cross-stratification (Fig. 72). The White Rim Sandstone is mainly eolian in origin, but the top of the unit was modified by erosional marine processes as the sea transgressed across the dune field (Huntoon, 1985; Huntoon and Chan, 1987). It is not known to what extent this upper part of the unit is preserved in the Tar Sand Triangle, as detailed lithologic descriptions are not available for the wells drilled in the deposit.

Figure 72: Outcrop of the White Rim Sandstone along the Dirty Devil River showing the large-scale planar cross-bed sets and overall uniformity in lithology that characterize this eolian deposit (Huntoon and Chan, 1987).

The White Rim Sandstone has had a complex diagenetic history (Schenk, 1988; Hansley, 1995) that has involved calcite cementation of primary pores, calcite and potassium feldspar dissolution forming a secondary porosity, kaolinite-illite-quartz precipitation in the secondary porosity, and minor Fe-carbonate growth. The diagenesis is related to a long history of fluid migration through the sandstone (Sanford, 1995), including reactive organic acids derived from migrating hydrocarbons (Hansley, 1995). The diagenesis predates the entry of meteoric waters under the modern arid conditions of the region (Schenk, 1988). It is principally the secondary porosity that reservoirs the heavy oil.

Twenty-eight wells provide control on the thickness of the White Rim Sandstone in the Tar Sand Triangle and the minimum thickness of the bitumen-impregnated interval (Fig. 73; Table 14). The average unit thickness is 230.0 ft (median = 236.8 ft), which is consistent with the regional isopach map (Fig. 71) showing the unit thinning southeastward toward the Colorado River.

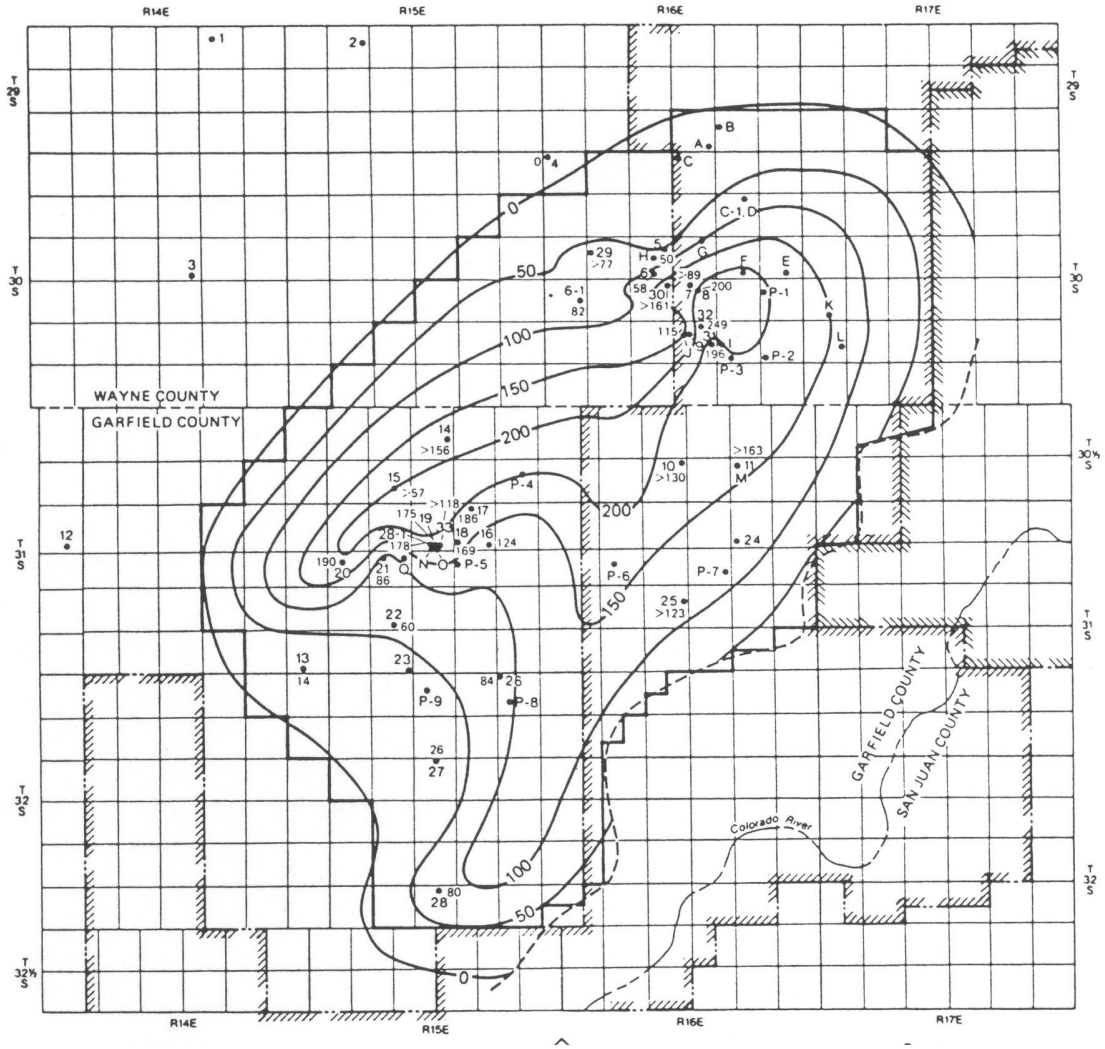

Figure 73: Thickness of the bitumen-impregnated interval within the White Rim Sandstone superposed on the township-range grid (Dana et al., 1984). Wells providing control on interval thickness are shown on the map and named in Table 14. Each of the squares on the map represents one section or one square mile. The isopleth interval is 50 feet.

Table 14: Wells in the Tar Sand Triangle penetrating the White Rim Sandstone and providing control on the thickness of the bitumen-impregnated interval and the heavy oil grade of eight control wells. The symbol ">" indicates wells not fully penetrating the White Rim Sandstone; the thickness is greater than that listed in the table. Data from Dana and others (1984).

Company	Well	T	R	Sec.	loc.	Elev (ft)	Top WRSs	Thick ft	Sat. ft	>	Mbbls/acre
Sagadahoc O&G	Skyline State 1	30S	16E	16	SE NE	6362	1470	240	50		29.00
Oil Dev. Co. of Utah	Gordon Flats 16-1	30S	16E	16	SW SE	6298	1420	230	58		
Oil Dev. Co. of Utah	Gordon Flats 19-1	30S	16E	19	NE NE SE	6231	1530	210	82		
Sagadahoc O&G	Skyline State 2	30S	16E	22	NE NW	6381	1344	240	89	>	
Oil Dev. Co. of Utah	Gordon Flats 22-1	30S	16E	22	NW SW NE	6542	1392	264	200		113.42
Phillips	French Seep 1	30S	16E	27	SE NW	6465	1390	228	115		
Mobil Oil	Robbers Roost 41-33	30.5S	16E	33	NE NE	6604	1425	185	185		
LETC/DOE	TST-2	30.5S	16E	35	SE NW NW	6812	1412	168	163		61.45
Kirkwood O&G	Technology 14-36	31S	14E	36	NE SE SW	4823	200	235	14		
Kirkwood O&G	White Rim 44-4	31S	15E	4	SE NE SE	6034	1400		156	>	
Kirkwood O&G	Magnum 23-8	31S	15E	8	SE NW SE	5084	483	371	57	>	
Kirkwood O&G	Garfield 44-15	31S	15E	15	SW SE SE	5321	507	303	124		
Kirkwood O&G	Winfield 21-15	31S	15E	15	NE NE NW	6127	1424		186		
Kirkwood O&G	Remington 14-15	31S	15E	15	NW SW SW	5307	529	301	169		
Kirkwood O&G	State 34-16	31S	15E	16	SW SE	5058	325	295	175		
Superior Oil	Utah S-Govt 22-19	31S	15E	19	SE NW	4850	244	333	190		103.55
Kirkwood O&G	Monroe 22-20	31S	15E	20	NE SE NW	4988	307	336	86		
Kirkwood O&G	Cromwell 33-29	31S	15E	29	NW SW SE	5060	228	259	60		
LETC/DOE	TST-4	31S	16E	16	NE SE NE	6895	1395	130	123		56.58
Kirkwood O&G	State 11-2	32S	15E	2	NW NW NW	5320	140	180	84		
Kirkwood O&G	State 31-16	32S	15E	16	NE NW NE	5535	397	188	26		
Texas Pacific	USA-Rock Canyon 1	32S	15E	33	C NW NE	5400	130	160	80		
Kirkwood O&G	State 34-16B	31S	15E	16	SW SE	5058	287		178	?	
Shell Oil	#7	30S	16E	17	SW NW	6163	1481	167	77	>	33.21
Shell Oil	#1	30S	16E	21	NE NE NE	6333	1375	197	161	>	
Oil Dev. Co. of Utah	Gordon Flats 27-1	30S	16E	27	NE SE	6567	1432	213	196		244.00
Shell Oil	#9	30S	16E	27	NW NE	6540	1428	249	249		85.83
Kirkwood O&G	State 34-16A	31S	15E	16	SW SE	5088	319		118	>	

The average bitumen-impregnated interval constitutes only about half of total unit thickness, 123.3 ft (median = 123.0 ft). The range of thicknesses of the bitumen-impregnated interval encountered in the wells (Table 14) is 14-249 ft. The bitumen thickness map defines a central core of the deposit with interval thickness in excess of 150 ft, which passes outward in all directions to the region of no oil-saturation within the White Rim reservoir (Fig. 74). Thinning of the bitumen-impregnated zone to the southeast is related to stratigraphic thinning. The zone thins to the northwest due to the low-angle intersection of the horizontal oil-water contact with the gently northwest-dipping reservoir.

For wells spudded on the high plateau, the depth to the top of the White Rim Sandstone is generally in the range 1400-1500 ft. It is considerably less for wells located on the intermediate benches and box canyons incised into the plateau. Except along the cliff line over the Colorado River and in the deeper canyons of the Dirty Devil River drainage, the deposit is rarely exposed at the surface.

Based on 121 core samples from four Santa Fe Energy wells in Wayne County (T30S-R16E), Campbell and Ritzma (1981) reported the following petrophysical characteristics for the White Rim Sandstone:

- Porosity median = 19.8%; range of 9.7-31.7%,
- Permeability median = 340 md; range 0.07-2790 md after oil extraction,
  median = 268 md; range 0.03-2580 md before oil extraction,
- So median = 32.2%; range 5.8-85.4%,
- Sw median = 4.9%; range 0.9-31.4%.

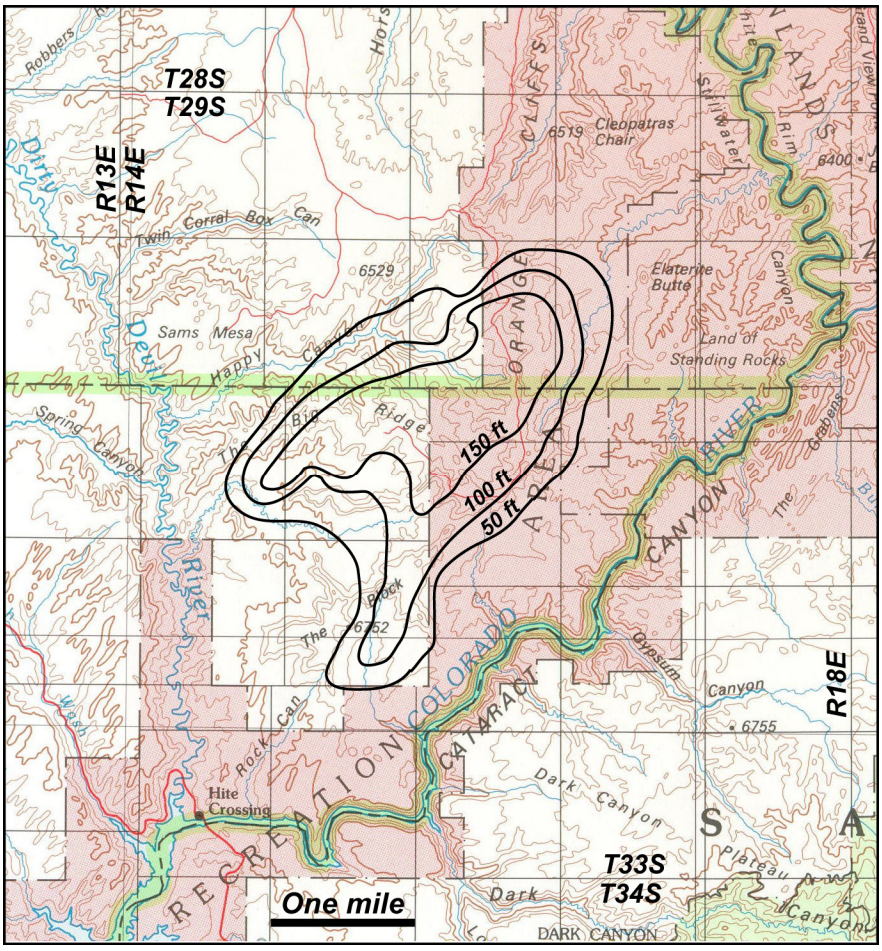

Figure 74: Thickness of the bitumen-impregnated interval of the White Rim Sandstone superimposed on a topographic map. Shown are the 50, 100 and 150 ft isopleths of the map in Figure 74. Shown in pink are northern portions of the Glen Canyon National Recreation Area and the Horse Canyon, Land of Standing Rocks, and The Grabens sections of the Canyonlands National Park.

However, the most reliable information on petrophysical properties of the White Rim Sandstone comes from three cores taken by the Western Research Institute in the early 1980s. The data are reported in tables accompanying Dana and others (1984). Only two of the wells (TST-2 and TST-4) were successful in penetrating and coring nearly the entire bitumen-impregnated interval, 163 and 123 ft, respectively. The third well, TST-3, sampled only 70 ft of the oil zone. The TST-2 and TST-3 wells were spudded on Flint Flat, whereas the TST-4 well is located at the southeast corner of The Big Ridge. The specific locations are given in Table 14.

As might be expected of an eolian sandstone, the porosity and permeability of the White Rim reservoir is good (Fig. 75; Table 15), with average porosity in the range 15.3 to 17.4% and permeability averaging between 200 and 500 md. There is, however, substantial vertical variability in porosity values (Fig. 76), which might have some influence on the overall effectiveness of thermal recovery. For unknown reasons, the variability is much more expressed in TST-2 than in TST-4. Lithology logs are not available for these wells. However, for all three cores a good correlation exists between porosity and permeability (Fig. 75). Note that the majority of core samples have porosity in excess of 15% and permeabilities greater than 100 md. Although the number of control samples differ, the permeability distribution (Fig. 75) is similar in all three cores.

The values reported herein are for core samples with bitumen extracted. The porosity and permeability measured in core with the original bitumen in place are only 20-30% of the bitumen-extracted values. These values also are tabulated in Dana and others (1984).

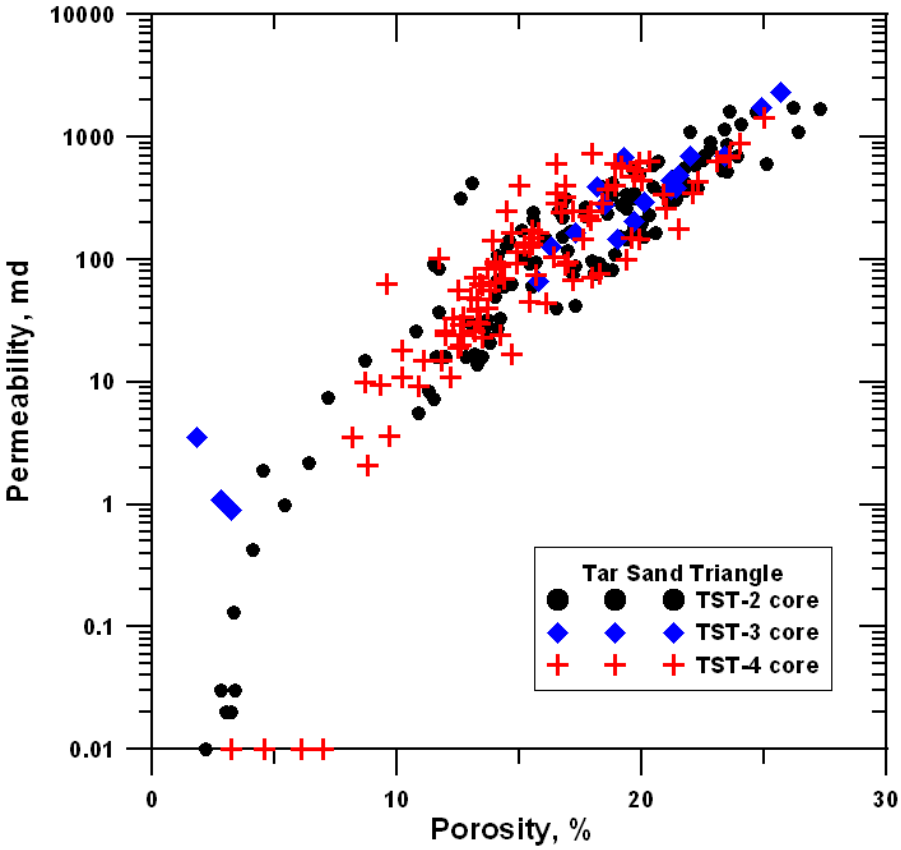

Figure 75: Porosity and permeability measured in core samples from the TST-2, TST-3, and TST-4 test wells. Data from Dana and others (1984).

Table 15: Average porosity and permeability values for the LERC test well cores.

	TST-2	TST-3	TST-4
Average:	17.2 ± 5.5%	17.4 ± 6.3%	15.3 ± 4.1%
Median:	18.2%	18.6%	15.2%
Average:	293 md	476 md	192 md
Median:	162 md	335 md	93 md

Fluid saturations measured in the TST-2 and TST-4 cores are summarized in Table 16. For TST-2, the average oil and water saturations are 27.4% and 22.0%, respectively. The values for TST-4 are slightly higher, 35.6% and 25.9%, respectively. Oil saturation profiles are presented in Fig. 77. The sum of oil + water saturations are very low in the two cores, just 49.9% and 61.5%. In both cores, the oil saturations are higher than water saturations, despite the overall low So (Fig. 77). These observations lead to the conclusion that either (a) the reservoir is situated above the local water table, within the vadose zone, and air also is present in the pore space, or (b) the handling of the cores was such that substantial fluid loss occurred before the cores were analyzed. Fluid drainage during handling is supported by the observation that samples with the highest So+Sw values (Fig. 78) also have exceptionally low permeabilities, generally less than 0.1 md.

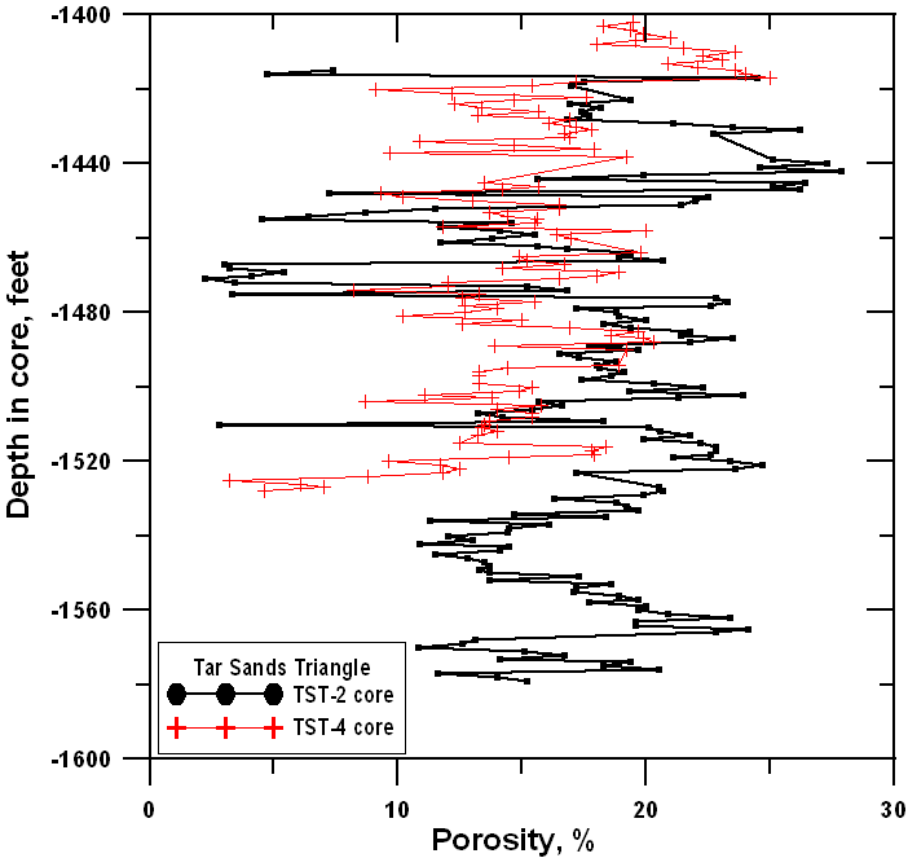

Figure 76: Porosity profiles showing systematic vertical variations in White Rim Sandstone petrophysical properties. Data measured in core from the TST-2 and TST-4 test wells (Dana and others, 1984).

Table 16: Average and median values of oil and water saturations observed in the TST-2 and TST-4 cores (Dana and others, 1984). The Ekberg correction normalizes the saturation values to sum to 100% assuming proportional drainage of both oil and water.

	Average of observed values (%)			Ekberg corrected (%)	
	So	Sw	So+Sw	So	Sw
TST-2	27.4 ±11.8	22.0 ±14.1	49.4 ±14.9	57.2 ±16.0	42.8 ±16.0
TST-4	35.6 ±14.7	25.9 ±8.5	61.5 ±15.3	58.0 ±16.4	42.3 ±16.5

	Median values observed (%)			Ekberg corrected (%)	
	So	Sw	So+Sw	So	Sw
TST-2	27.8	17.8	46.6	59.4	40.6
TST-4	38.7	24.7	63.3	60.9	39.1

The standard adjustment for fluid drainage from the core, the Ekberg correction, involves normalizing the total fluids to 100% according to the proportion of oil to water in the original analysis. The resulting Ekberg corrected values, Soe and Swe, are given in Table 16. If valid, the actual oil saturations would be about 60%, well within the range favorable for *in situ* recovery processes to be effective. However, it is more likely that the water drained from the core preferentially to the viscous heavy oil. This would mean that the values of So reported closely reflect the actual oil saturations in the reservoir, that is 40% or less. If these So values are characteristic of the entire prime area of the deposit, then standard *in situ* recovery processes could not operate efficiently in the Tar Sand Triangle.

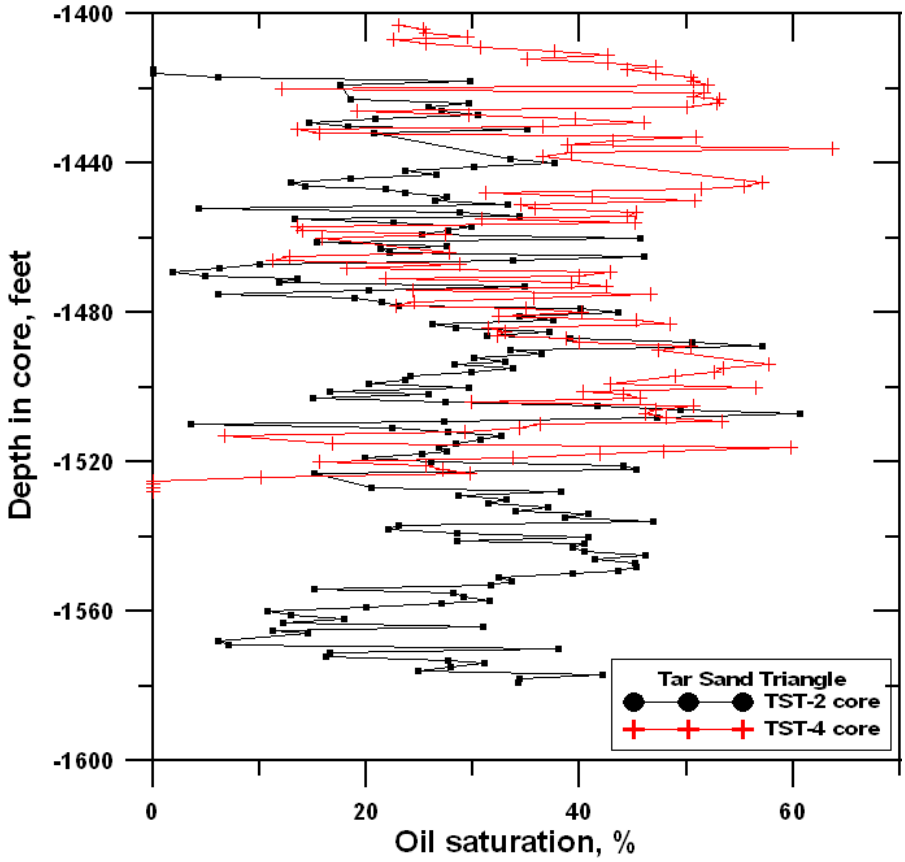

Figure 77: Oil saturation profile in the TST-2 and TST-4 cores. Data from Dana and others (1984).

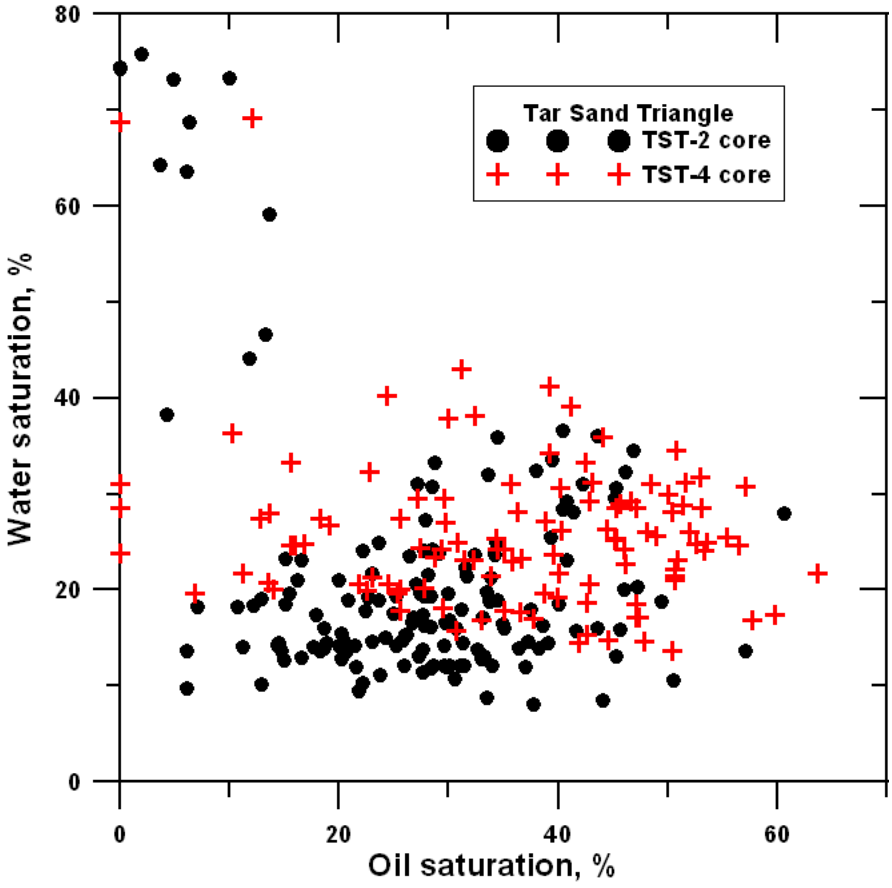

Figure 78: Oil versus water saturation cross plot for TST-2 and TST-4 core samples, uncorrected. The isolated cloud of high Sw values are all samples with exceptionally low permeability values generally less than 0.1 md. Note that most samples do not sum to 100% indicating loss of fluids from the rock either in the reservoir or during handling of the core. Data from Dana and others (1984).

Curiously, for all of the test drilling that was done in the Tar Sands Triangle deposit in the 1970s and early 1980s, there are only limited data in the public domain documenting the volume of original oil in place. However, the published estimates are remarkably consistent. Campbell and Ritzma (1979) cite a richness of 482.5 BO/ac-ft based on 121 core samples from four Santa Fe Energy wells in the Gordon Flats area. Phillips (1987) reports a grade of 487.9 BO/ac-ft from the Black Ledge (T32S-R16E, sec. 18) sector of the Tar Sand Triangle. The median grades in the TST-2 and TST-4 cores reported in Dana and others (1984) are 355.7 and 423.5 BO/ac-ft, respectively. Taking these values as representative of the "core" area of the deposit, the OOIP in a 150-ft-thick impregnated interval is in the range 53.36 to 73.49 Mbbls/ acre.

Fig. 79 shows the vertical variability of bitumen grade in the TST-2 and TST-4 test wells. This variability is considerable in both wells, with the richness of individual core samples changing over a short distance from less than 200 BO/ac-ft to more than 800 BO/ac-ft. As stated above, the median (and average) grade differs between the two wells, as do the thicknesses of the bitumen-impregnated intervals. The TST-2 core has 59.05 MBO/acre of heavy oil in a 165 ft interval and the TST-4 core has 52.04 MBO/acre in a 126 ft interval. However, neither the TST-2 or TST-4 well is in the prime central portion of the deposit where the bitumen-impregnated interval is greater than 150 ft.

Dana and others (1984) report values for OOIP from only eight wells in the deposit (see Table 17). These values are cross plotted against the reported thickness of the bitumen-impregnated interval in each well (Fig. 80). Except for either one (or three) "outlier(s)" in the data, a linear relationship is suggested in the cross plot. "Best-fit" linear regressions of subsets of the data are used to predict the OOIP for the 28 wells for which thickness of the oil interval is reported (Table 17).

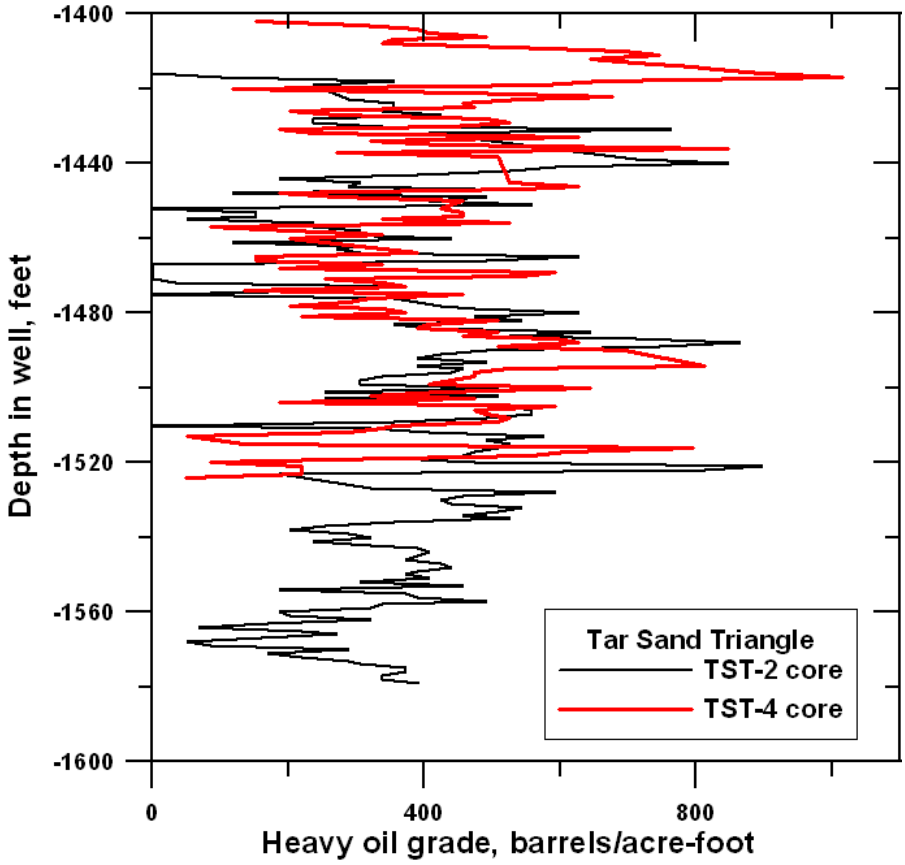

Figure 79: Profile of bitumen grade measured in cores in north-central Tar Sands Triangle. The median grade observed in the LERC TST-2 core is 355.7 bbls/ac ft and the arithmetic average is 360.1 bbls/ac-ft. The oil-in-place of the 164 ft cored section is 59.05 MBO/acre. The median grade observed in the LERC TST-4 core is 423.5 bbls/ac-ft and the arithmetic average is 413.0 bbls/ac ft. The oil-in-place of the 126 ft cored section is 52.04 MBO/acre. Data from Dana and others (1984).

Table 17: Estimated heavy oil resource in the Tar Sand Triangle deposit based on correlations of grade with thickness of the bitumen-impregnated interval in the Tar Sand Triangle. Data from Dana and others (1984).

Company	Well	T	R	Sec.	loc.	Top WRSs	Sat. ft	Mbbls/acre	R=0.92	R=0.73
Sagadahoc O&G	Skyline State 1	30S	16E	16	SE NE	1470	50	29.00	19.23	23.53
Oil Dev. Co. of Utah	Gordon Flats 16-1	30S	16E	16	SW SE	1420	58		22.31	27.30
Oil Dev. Co. of Utah	Gordon Flats 19-1	30S	16E	19	NE NE SE	1530	82		31.54	38.60
Sagadahoc O&G	Skyline State 2	30S	16E	22	NE NW	1344	89		34.23	41.89
Oil Dev. Co. of Utah	Gordon Flats 22-1	30S	16E	22	NW SW NE	1392	200	113.42	76.92	94.14
Phillips	French Seep 1	30S	16E	27	SE NW	1390	115		44.23	54.13
Mobil Oil	Robbers Roost 41-33	30.5S	16E	33	NE NE	1425	185		71.15	87.08
LETC/DOE	TST-2	30.5S	16E	35	SE NW NW	1412	163	61.45	62.69	76.72
Kirkwood O&G	Technology 14-36	31S	14E	36	NE SE SW	200	14		5.38	6.59
Kirkwood O&G	White Rim 44-4	31S	15E	4	SE NE SE	1400	156		60.00	73.43
Kirkwood O&G	Magnum 23-8	31S	15E	8	SE NW SE	483	57		21.92	26.83
Kirkwood O&G	Garfield 44-15	31S	15E	15	SW SE SE	507	124		47.69	58.37
Kirkwood O&G	Winfield 21-15	31S	15E	15	NE NE NW	1424	186		71.54	87.55
Kirkwood O&G	Remington 14-15	31S	15E	15	NW SW SW	529	169		65.00	79.55
Kirkwood O&G	State 34-16	31S	15E	16	SW SE	325	175		67.31	82.37
Superior Oil	Utah S-Govt 22-19	31S	15E	19	SE NW	244	190	103.55	73.08	89.43
Kirkwood O&G	Monroe 22-20	31S	15E	20	NE SE NW	307	86		33.08	40.48
Kirkwood O&G	Cromwell 33-29	31S	15E	29	NW SW SE	228	60		23.08	28.24
LETC/DOE	TST-4	31S	16E	16	NE SE NE	1395	123	56.58	47.31	57.90
Kirkwood O&G	State 11-2	32S	15E	2	NW NW NW	140	84		32.31	39.54
Kirkwood O&G	State 31-16	32S	15E	16	NE NW NE	397	26		10.00	12.24
Texas Pacific	USA-Rock Canyon 1	32S	15E	33	C NW NE	130	80		30.77	37.66
Kirkwood O&G	State 34-16B	31S	15E	16	SW SE	287	178		68.46	83.78
Shell Oil	#7	30S	16E	17	SW NW	1481	77	33.21	29.62	36.24
Shell Oil	#1	30S	16E	21	NE NE NE	1375	161		61.92	75.78
Oil Dev. Co. of Utah	Gordon Flats 27-1	30S	16E	27	NE SE	1432	196	244.00	75.38	92.26
Shell Oil	#9	30S	16E	27	NW NE	1428	249	85.83	95.77	117.20
Kirkwood O&G	State 34-16A	31S	15E	16	SW SE	319	118		45.38	55.54
							Median:	73.64	46.35	56.72

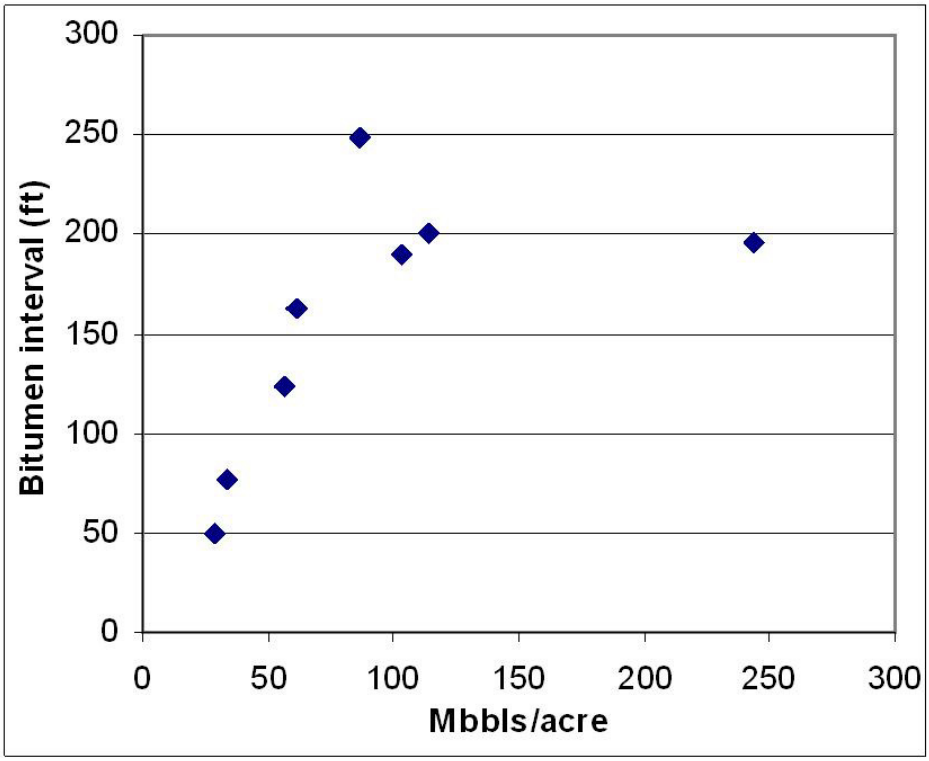

Figure 80: Cross plot of heavy oil grade in MBO/acre versus the thickness of the heavy oil-impregnated interval within the White Rim Sandstone reservoir. Data from Dana and others (1984). Excluding the three "outliers" in the data set, a conservative prediction of grade is expressed by MBO/acre = thickness in feet/2.6 with a correlation coefficient, R^2, of 0.92. Excluding only one outlier, a less conservative prediction with a R^2 of just 0.73 is MBO/acre = thickness in feet/2.1245.

A linear regression using all eight data points in Fig. 80 results in a function that greatly overestimates the reported OOIP for all but the high value (244 MBO/acre) well. It is rejected as unreliable. Excluding only the single "outlier," the linear regression yields a correlation of:

MBO/acre = Thickness in ft/2.1245, with a correlation coefficient, R^2, of 0.73.

However, excluding three "outliers" the linear regression yields a more conservative

MBO/acre = Thickness in ft/2.6, with a correlation coefficient, R^2, of 0.92.

For a 150-ft-thick bitumen-impregnated interval, the more conservative estimator predicts an oil grade of 57.7 MBO/acre; the less conservative estimator predicts 70.6 MBO/acre.

These numbers are lower than the estimates of Dana and others (1984), perhaps because the authors factored the 244 MBO/acre value into their estimator, the "outlier" value excluded herein. Consequently, they assign an average value of 110.0 MBO/acre to 16,640 acres in the prime part of the deposit where they also project, on only two control points, a bitumen-impregnated interval greater than 200 ft thick. The actual OOIP of the Tar Sand Triangle deposit, while large, is not known with any degree of certainty.

Character of Utah Heavy Oil and Bitumen

Reliable data on the physical and chemical properties of Uinta Basin immobile oils is mixed. Some individual oil samples have been intensely investigated, and in some deposits there is an abundance of information of a single type, such as oil density. Fortunately, sufficient data can be assembled from published and unpublished sources to document the variations in the immobile reservoired oils from one part of the basin to another.

The *P.R. Spring-Hill Creek deposit* contains both heavy oil and bitumen (Fig. 81), with a range of values from 5.5º to 15.4º. The average API is 9.4º±2.62º. Two sectors, Threemile Canyon and Hill Creek, appear to have only bitumens, but in the other sectors the heavy oil tends to be in the shallower portions of the pay interval and bitumens in the deeper portions. These oils have very low sulfur content averaging 0.45±0.09 wt%.

For the *Sunnyside deposit*, Campbell and Ritzma (1979) report an average gravity of 8.6º with a range from 7.6º to 9.2º. Soxhlet extracts from the Amoco cores are in the range 7.1º to 10.1º.

Asphalt Ridge appears to have a high quality heavy oil with reported API gravity in the range of 10° to 14.4°, a relatively high H/C atomic ratio, low asphaltene content, and exceptionally low sulfur, nitrogen, and metals content for a heavy oil (Table 18). The heavy oil also has a relatively high volatility content, which together with its low Conradson carbon residue, makes it an ideal heavy oil for upgrading by a broad range of refining processes (Oblad and others, 1987; Thomas and others, 1994; Yeh, 1997). This oil has been thoroughly analyzed and is very well characterized (Oblad and others, 1985; Rose and others, 1992; Tsai and others, 1993; Drelich and others, 1994). Viscosity data reported by Yeh (1997) are used to predict that a viscosity of 50 cp to 10 cp is reached in the temperature range 283ºF to 328°F, which is well within the operating range of a mature steamflood or cyclic steam stimulation recovery project and actually below that of an *in situ* combustion project.

Laboratory tests (Thomas and others, 1994) have determined that the Asphalt Ridge bitumen meets ASTM specifications as an AC-5 viscosity-graded asphalt. Furthermore, the +412°C (+775°F) distillation residue meets all specifications as an AC-10 grade asphalt. In

addition, the residue is resistant to moisture-induced loss of strength. The corresponding -412° C distillate has significant reductions in API gravity (22.8° vs. 19.1°), molecular weight (220 vs. 690), and viscosity (just 15 cp at 60°F) compared to the original oil. It is composed primarily of 3-ring saturates and 2- and 3-ring aromatics. Upon hydrogenation, the aromatic compounds could yield a high-density jet fuel. With modern refining methods and catalysts virtually all other petroleum products could also be produced effectively from the Asphalt Ridge heavy oil.

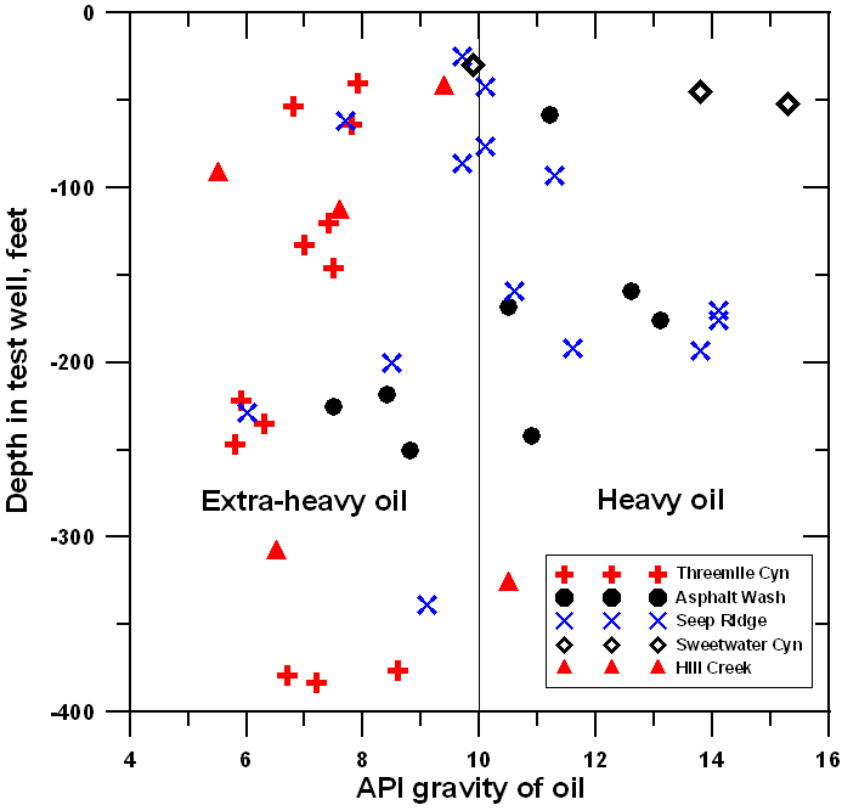

Figure 81: API gravity of the heavy and extra-heavy oils extracted from oil-impregnated sandstones in various sectors of the P.R. Spring-Hill Creek deposit. Source of data: Peterson and Ritzma (1974).

Table 18: Chemical and physical properties of Asphalt Ridge heavy oil (Yeh, 1997). Temperatures have been converted from Kelvin to Fahrenheit.

Gravity:	11.4° API
Conradson carbon residue:	11.0 wt%
Asphaltenes:	10.1 wt%
H/C atomic ratio:	1.58
Simulated distillation:	
Volatility:	45.2 wt% (mostly distillate and gas oil fractions)
Residuum:	54.8 wt%
Carbon:	84.9 wt%
Hydrogen:	11.2 wt%
Sulfur:	0.42 wt%
Nitrogen:	0.97 wt%
Metals:	91 ppm
Pour point:	155.9°F
Viscosity at 139.7°F:	37,590 cp
at 157.7°F:	11,750 cp
at 166.7°F:	8,227 cp
at 175.7°F:	5,583 cp

The reported API gravity of the heavy oil extracted from the *Whiterocks* deposit is 11.4° to 13.5°, averaging 12.5°. The oil contains a large percentage of saturates and aromatics, and it has a very low sulfur content, just 0.4% (Oblad and others, 1987). Its composition is very similar to that of Asphalt Ridge, making it relatively easy and inexpensive to upgrade.

It is instructive to compare the Sunnyside crude with that from Asphalt Ridge (Table 19). The Sunnyside crude, being more intensely biodegraded, is heavier, with a lower H/C atomic ratio and consequently larger molecular weight. It is richer in asphaltenes, and consequently less rich in saturates, aromatics, and resins. However, it is much like the Asphalt Ridge crude in nitrogen and sulfur content, both relatively low for a heavy oil. API gravities are variable from one surface location or core to another.

Table 19: Chemistry and physical properties of the Sunnyside heavy oil compared with that of the Asphalt Ridge crude. Data from Bukka and others, 1991; Oblad and others, 1987.

Property	***Sunnyside crude***	***Asphalt Ridge crude***
API gravity	5.5	14.4
H/C ratio	1.45	1.56
Molecular weight	588	490
Viscosity at 122º F (cp)	1,500,000	80,000
Nitrogen (wt. %)	0.90	1.06
Sulfur (wt. %)	0.50	0.44
Fractional composition		
Saturates	24.9	32.4
Aromatics	18.6	22.4
Resins	30.6	37.6
Asphaltenes	23.7	7.3

A single sample of a Sunnyside bitumen extract from a mined sandstone was analysed by gas chromatography-mass spectrometry (Dolcater, 1988). The analysis showed an *absence* of n-alkanes, branched alkanes, cyclohexanes, benzenes, naphtalenes, and penanthrenes, all common components of a "normal" crude oil. The absence of this large group of compounds, together with the presence of demethylated terpanes indicates a high level of biodegradation of this particular Sunnyside bitumen sample. Furthermore, the preserved biomarkers, including terpanes and steranes, indicate the oil was likely sourced at a low degree of thermal maturity from the Green River black shales. The apparent absence of steranes in the biomarker suite of P.R. Spring bitumens (Reed, 1977) suggests a slightly higher degree of biodegradation than in the Sunnyside deposit.

Compared with all other heavy oils in Utah, the Sunnyside crude is particularly viscous (Fig 82). At 122º F, its viscosity is 1,500,000 cp, compared to 80,000 cp for the Asphalt Ridge (Table 19) and just 7000 cp for the Athabasca crudes at the same temperature. A standard Andrade plot of viscosity vs. temperature predicts that a viscosity appropriate for Darcy flow recovery of oil from the sandstone, 50 to 10 cp, is reached only at temperatures on the order of 326º to 367 °F. For most thermal recovery methods to be effective, this would require raising formation temperature *artificially* by at least 250 °F, an expensive proposition. The higher viscosity of Sunnyside crude relates to the relatively larger proportion of compounds with carboxylic groups in the crude, rather than to the relative proportion of asphaltenes alone (Bukka and others, 1991). The larger content of the carboxylic groups lead to more extensive hydrogen-bonding of aromatics and resins with the asphaltenes in the composite bitumen, increasing the resistance to flow of the oil.

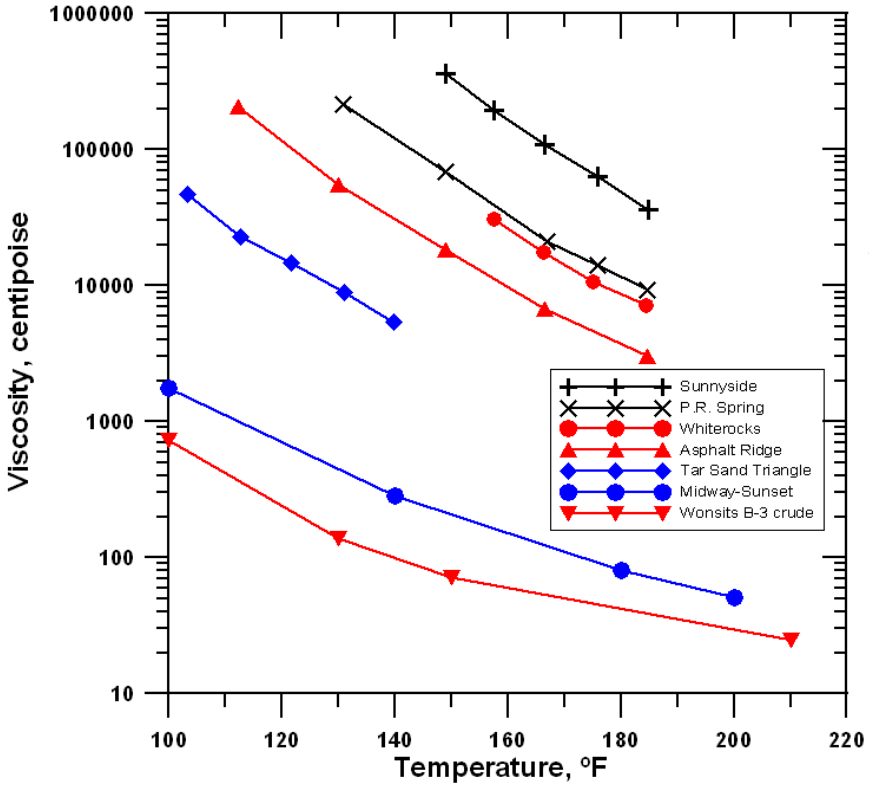

Figure 82: Viscosity dependence on temperature for bitumen and heavy oils from Uinta Basin heavy oil deposits, the Tar Sand Triangle and, for comparison, the Midway-Sunset field in the San Joaquin basin, California. Data from Oblad and others (1987), Nettle (1982), and Schamel and others (2002).

In the shallow *Wonsits Valley field*, crude oil samples were collected by swabbing three sandstone beds at different depths in test well 1 (refer to Fig. 60). In terms of oil composition and physical properties there is a sharp contrast between the oils related to depth of the oil pool in the Uinta Formation (Table 20). The shallowest two oils, at depths of 1160 and 1450 ft, have API gravities of 17.5º and 16.5º, just moderately heavy. Both have relatively high asphaltene contents, 15.0 and 8.2 wt%, respectively, and low wax contents 14.7 and 17.6 wt%, respectively. In contrast, the B-6 crude oil at 1580 ft depth, just 130 ft deeper than the B-3 crude, is a normal waxy Uinta Basin oil with an API gravity of 24.6º, a low asphaltine (4.1 wt%), and a high wax (33.2 wt%) content. The density of the B-6 oil is just at the low end of the range of normal Uinta Basin oils (Stowe, 1972). Predictably, the pour points of the three oils are observed to increase with wax content from >75ºF for the shallow A-5 crude to 100ºF for the deeper B-6 crude.

Table 20: Chemical composition and physical properties of Uinta Formation crude oils.

	A-5 crude	***B-3 crude***	***B-6 crude***
Depth, ft	1160	1450	1580
BHT, ºF	75	80	81
Pour point, ºF	>75	90	100
API gravity	17.5	16.5	24.6
Wax content, wt %	14.7	17.6	33.2
Asphaltene, wt %	15.0	8.2	4.1
Sulfur, wt %	0.24	0.27	0.30
Heating value, Btu/lb	18,491	18,489	19,346

The A-5 crude oil is considerably more viscous than the B-3 and B-6 oils (Fig. 83). The B-6 oil has viscosities equivalent to that reported for oils produced from the main Green River oil pools (Stowe, 1972).

In all instances, the reservoir temperature is lower than the pour point temperature of the crudes, by as much as nearly 20ºF (Table 20). For this reason, as well as the relatively high viscosity of the A-5 and B-3 crudes (Fig. 83), these oils are immobile in reservoir. Attempts to produce oil from the test wells were unsuccessful, even after circulating hot water at approximately 200ºF in an enclosed system in each well. Oil samples were recovered only after injecting 270ºF water and swabbing the well (Nettle, 1982). Commercial production of oil will require application of cyclic steam stimulation for a prolonged period or the use of an alternative unconventional oil recovery technique.

Quantitative hydrous pyrolysis data from the lower Green River, black-shale facies and Mahogany zone support progressive stages of hydrocarbon generation with increasing thermal maturation in the Uinta Basin: first bitumen (high molecular weight molecules), then immiscible or "normal" oil, and finally natural gas and pyrobitumen (Ruble and others, 2001). In these experiments, the initial liquid hydrocarbons are rich in aromatics and asphaltines. At higher levels of thermal maturity or higher temperatures, saturates are generated from the asphaltines. The low-maturity aromatic-intermediate and aromatic-asphaltic oils in the Uinta Basin are considered to be expelled bitumens (Ruble and others, 2001). The two groups of oils, low-maturity, heavier and aromatic-rich versus higher-maturity, lighter and saturate-rich are observed in the Uinta Basin to be segregated by depth (Figs. 84 and 85). The provenance biomarker ß-carotene is present in oil generated from hydrous pyrolysis of the Mahogany zone, but not in oil generated from the black shale facies. ß-carotene is an abundant biomarker in the bitumen in both the P.R. Spring and the Sunnyside deposits (Reed, 1977; Dolcater, 1988).

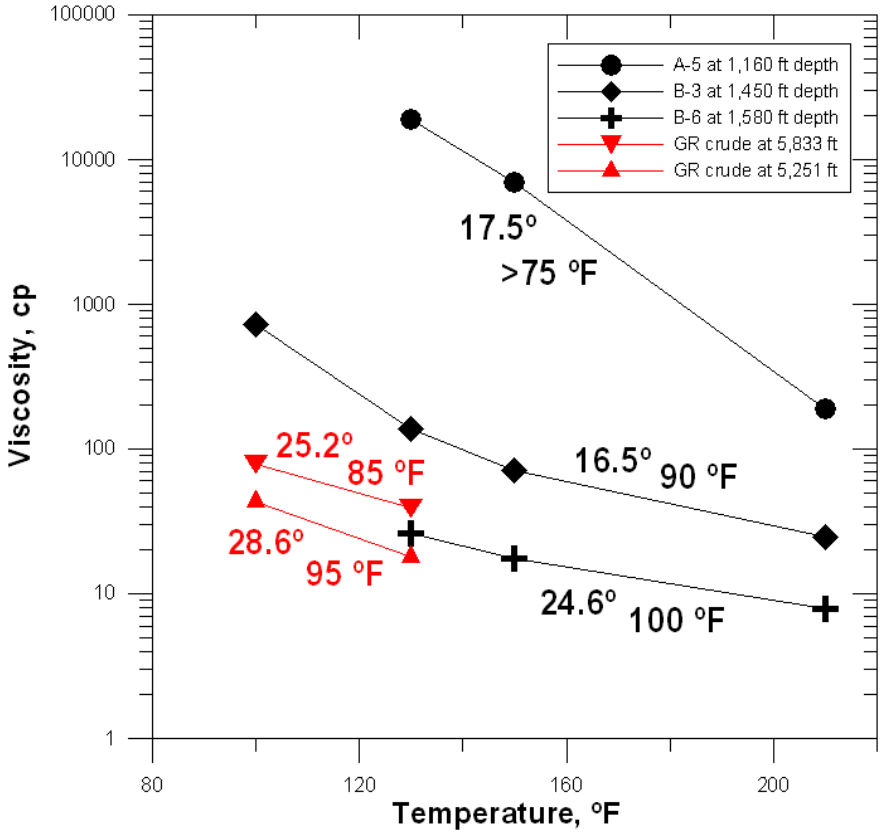

Figure 83: Viscosity of shallow-immobile and "conventional" waxy crude oil in the Wonsits Valley field. Oils represented by black symbols are from shallow Uinta Formation sandstone reservoirs, whereas those represented in red are from deeper Green River sandstone reservoirs. Indicated are the API gravity and the pour point of the oils. Refer to the legend for the reservoir depths of the oils plotted. Data from Nettle (1982) and Stowe (1972).

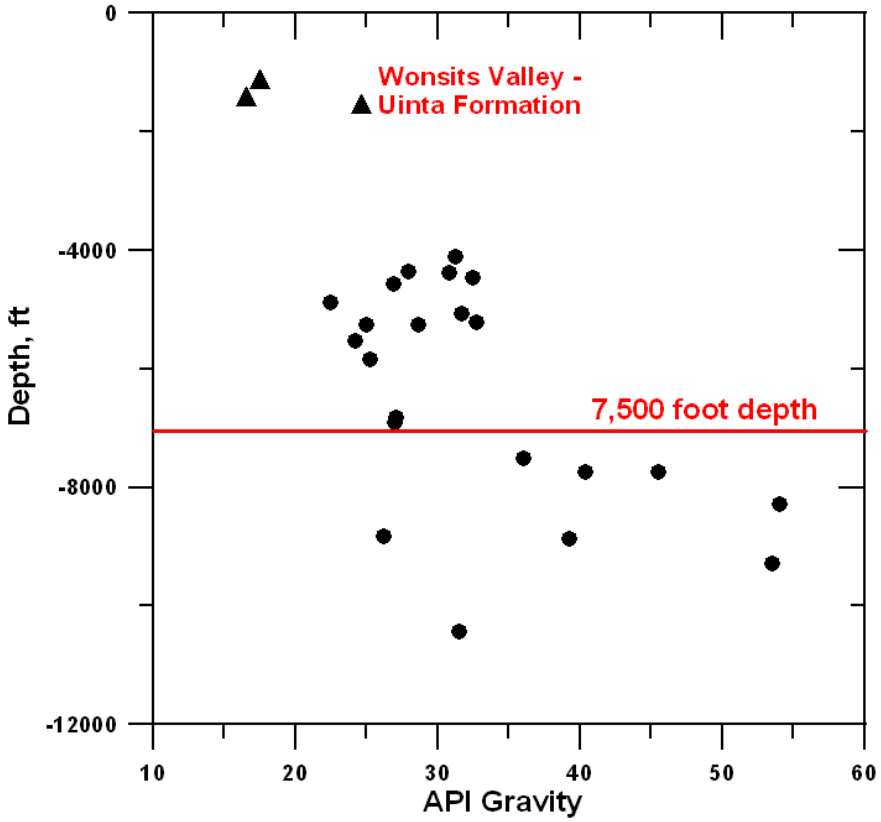

Figure 84: Variations in API gravity of Uinta Basin oils as a function of depth of the producing reservoir. Note that the lighter oils (>35° API) are found only below a depth of 7500 ft. Oils from the Uinta Formation in Wonsits Valley field are only slightly heavier than the shallow-produced (4000-7500 ft) oil in the basin. Data from Nettle (1982) and Stowe (1972).

Figure 85: Variations in ratio of saturates-to-aromatics of Uinta Basin oils as a function of depth of the producing reservoir. Note that the saturate-rich oils (ratio greater than 12) are found only below a depth of 7500 ft. An oil from the Uinta Formation in Wonsits Valley field falls into the same cluster of low saturates-to-aromatics ratios that characterizes the shallow-produced (4000-7500 ft) oil in the basin. Data from Lillis and others (2003).

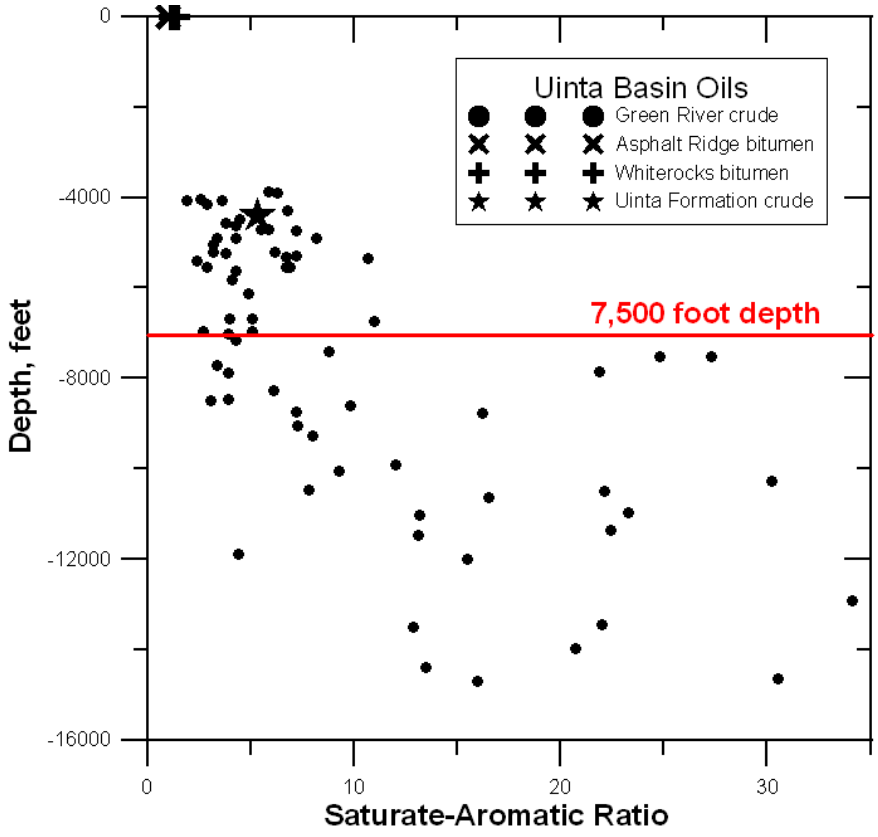

Beneath the West and East Tavaputs Plateau, the source rock intervals of the Green River Formation have not reached the oil maturation window (Morgan and others, 2003). However, beneath the central and northern parts of the basin, the Green River source rocks have generated oil, including the high saturate (waxy) oils that are characteristic of the Uinta Basin (Fouch and others, 1994).

The water chemistry of the Uinta Basin indicates large-scale fluxing of young meteoric waters into the up-turned edges of the basin, particularly the southern margin. Formation waters from the deeper oil and gas reservoirs in the basin are brackish to moderately saline, as one might expect given that the reservoirs are non-marine fluvial or lacustrine sandstones. Total dissolved solids (TDS) range between 5000 and 40,000 mg/l, averaging about 20,000 mg/l (Gwynn, 1992). This is less than sea water, which is about 35,000 mg/l, and considerably less than normal oil field brines that generally exceed 150,000 mg/l. Through a variety of mechanisms, formation waters tend to become more saline as they mature and are more deeply buried. Also, local dissolution of the "saline facies" at the top of the Green River Formation may be contributing to the higher TDS values observed. The pattern of dissolved species in the formation "brines" is consistent with significant infiltration of meteoric water into the producing formations from recharge areas ringing the basin. All of the currently productive reservoir units are exposed on the south flank of the basin and are close to the surface elsewhere on the basin margins. TDS, chlorine, and sodium decrease outward from the basin center. Magnesium, calcium and, most importantly, bicarbonate decrease inward towards the basin center (Gwynn, 1992). Bicarbonate, being diagenetically unstable, is a strong indicator of young meteoric waters. Sulfate, also diagenetically unstable, decreases away from the southeast basin margin towards the basin center.

The bitumens of the Sunnyside and P.R. Spring deposits have characteristics of an immature aromatic-asphaltic oil or bitumen representing the first liquids expelled from Green River kerogen as the oil generative window was initially reached to the north of the deposits. Perhaps the bitumen is derived mainly from the Mahogany zone, which is in close stratigraphic proximity to the reservoir sandstones. This viscous bitumen migrated laterally updip into a region that later in the history of the basin was subjected to major influx of young meteoric waters that degraded the immature oil. The heavy and immobile oils in the center and northern parts of the basin are likely slightly to moderately biodegraded, normal, saturate-rich oils that migrated vertically into the existing deposits.

From the standpoint of oil quality, the shallow stranded oil resources in the interior of the Uinta Basin and perhaps also the heavy oil resources of the Asphalt Ridge and Whiterocks deposits appear to be the more favorable targets for early *in situ* thermal recovery projects. However, the low quality of the bitumen in the Sunnyside deposit presents a serious barrier to development of this resource, even in the oil-rich Dry Creek Canyon-Bruin Point-Range Creek "core" zone where large-scale *in situ* thermal recovery projects might otherwise be feasible.

Most of the analyses of the Tar Sand Triangle bitumen were carried out on samples from surface seeps, the most degraded of the oil in the deposit. Thus, Wood and Ritzma (1972) report a range of API gravity for surface samples from 9.6° to -3.6°; the average of the 12 samples is 4.3°. Chevron analyzed a single surface sample from the Tar Sand Triangle (Black Ledge; T32S-R16E, sec. 18) with a reported grade of 487.9 BO/ac ft (Phillips, 1987). The sulfur content was a high 3.87% and the SARA analysis was as follows: saturates, 18.7%; aromatics, 3.4%; NSO, 28.8%; and asphaltenes, 45.5%. The ^{13}C isotopic ratio was -29.9 per mill. This surface sample may be considered representative of the bitumen at depth within the reservoir.

The surface bitumen samples are much heavier and more degraded than the 11.1° API oil from core that was analysed by Bunger and others (1979) (Table 21). The Tar Sand Triangle bitumen is very close in composition and physical properties to the Athabasca bitumen used for comparison, but it differs substantially from the more saturate-rich heavy oil from Asphalt Ridge Northwest. It has a relatively low H/C ratio (1.44) and high asphaltine (26.0%) and sulfur (4.38%) content, as well as a very high carbon residue. All of these factors will make upgrading the heavy oil difficult and expensive. However, the oil does have a favorable nitrogen and metals contents.

Table 21: Properties of the Tar Sand Triangle (TST) bitumen compared with those of Asphalt Ridge Northwest (AR NW) and the Athabasca tar sands. Data from Bunger and others, 1979).

Property	***TST***	***AR NW***	***Athabasca***
API gravity	11.1	14.4	11.6
H/C atomic ratio	1.44	1.64	1.48
Saturated HC (wt %)	25.7	21.6	27.8
Aromatic HC (wt %)	31.9	38.1	26.9
Asphaltines (wt %)	26	6.3	16.4
Carbon residue (wt %)	21.6	3.5	16.1
Sulfur (wt %)	4.38	1.02	4.85
Nitrogen (wt %)	0.46	0.59	0.47
Va + Ni (ppm)	161	145	292
Dyn. viscosity (poise)	12,990	29,500	6380
Heating value Btu/lb)	17,900	18,800	17,700

The viscosity of the Tar Sand Triangle oil is the lowest of any heavy oils in Utah (Fig. 82), although it is slightly more viscous than the Athabasca oil (Table 21). At a reservoir temperature of 100°F, the viscosity of the oil is about 50,000 cp. By conventional Andrade extrapolation, a viscosity of 100 cp would be reached in this oil at just 230°F and 10 cp would be reached at 290°F. These temperatures are well within the range of normal thermal recovery processes.

Based on biomarker analysis of many heavy oils in southern Utah (Tar Sand Triangle, Circle Cliffs, San Rafael, and others), Dembicki and others (1986) and Wenrich and Palacas (1990) conclude that all oils have been derived from the same carbonate source rock(s). They note as evidence for the carbonate source the low disterane concentrations and the predominance of norhopane over hopane, pristine-phytane ratios less than 1, the predominance of even alkanes, $C_{35} > C_{34}$, and the high sulfur content.

Both the black calcareous shales of Paradox Formation (Pennsylvanian) in the Paradox basin and the Manning Canyon-Doughnut Shale (Mississippian-Pennsylvanian) in western Utah, are plausible source rocks for the Tar Sand Triangle bitumen. Both nearby source rock units contain interbedded limestone. The Paradox black "shales" are known to be the source for hydrocarbons in the Paradox basin (Nuccio and Condon, 1996). Huntoon and others (1999) propose the Delle Phosphatic Member of the Deseret Limestone (Mississippian) in western Utah as the source rock, but this unit is thin, discontinuous, and very distant. The source of the oil remains uncertain.

IN SITU THERMAL AND NON-THERMAL RECOVERY TECHNOLOGY

Stranded immobile oils, such as those described in this report, owe their immobility to either a high viscosity at ambient reservoir temperatures or they have pour points that are higher than ambient reservoir temperature, commonly by only a few degrees. In either case, the oil is unable to flow from pores within the sandstone reservoir to the production well at commercially reasonable rates. The relatively low permeabilities that characterize most of the Utah heavy oil sandstone reservoirs, which are consolidated, only exacerbates the resistance to Darcy flow. All thermal recovery methods strive to increase the temperature of the reservoir, heating the oil to the temperatures required to permit Darcy flow at reasonable rates. Although this threshold viscosity is different for different oils and reservoir systems, the objective is normally to lower the viscosity to at least 50 to 10 cp. High pour point oils need only be heated to a few degrees above their pour point to liquefy them, thus facilitating Darcy flow.

A variety of delivery systems can be used to transfer heat from the surface to the reservoir or to generate heat *in situ*. The thermodynamic properties of water are such that steam is a very effective and commonly used medium for thermal recovery projects worldwide. With a latent heat of vaporization at the atmospheric boiling point (212 ºF) of 970.3 Btu/lb (2257 kJ/kg) a relatively small volume of water converted to steam can carry a very large amount of heat energy when injected into the target reservoir (Prats, 1982). This contrasts with the specific enthalpy or heat content of liquid water at 212 ºF of just 180.07 Btu/lb (419.1 kJ/kg). In addition, water for generating steam is inexpensive, readily available, environmentally benign, and easy to handle. However, the cost of steam generation normally is the highest cost factor in any steam recovery project. All standard steam-based processes require large investments in infrastructure, have large surface footprints, and need to be large-scale operations to be optimally economic (Figs. 86 through 88). Even in the most efficient operations, large quantities of heat are lost through pipes at the surface leading from the steam generator to the injector well and then downhole before the target reservoir is reached. The most commonly used steam-based recovery technologies are cyclic steam stimulation (CSS), steam drive (steam flood), and steam-assisted gravity drainage (SAGD), and variants of these processes that introduce organic solvents into the steam and/or injection stream (VAPEX).

Figure 86: View of a small steam drive project in the Midway-Sunset field, southwest San Joaquin basin, California. An injector well is in the immediate foreground; adjacent producers with pumpjacks are in the middle ground. A pair of steam generators and insulated pipe racks are on the distant bench. Photograph by S. Schamel.

Figure 87: Network of insulated steam delivery pipes leading from the two mid-size (10,000 bspd) steam generators to the clusters of injection wells in this 40 acre project. The operations in the middle and distant view are those seen in Fig. 91. Photograph by S. Schamel.

Figure 88: Aerial view of a small portion of the Midway-Sunset field showing the density of surface facilities supporting only a few of the many thermal recovery projects that are currently operating in this giant heavy oil field. The satellite image is centered on 35.1187° N and 119.4755°W and is approximately one-half mile wide. Source: GoogleEarth

An alternative thermal recovery process is to generate the heat within the reservoir itself. This can be accomplished by burning some portion of the reservoired oil under controlled conditions (*in situ* combustion), by inserting electrodes in the oil-impregnated sandstones for electrical resistance heating, or by radio frequency (RF) heating. All three methods have been tried experimentally in heavy oil deposits with varying degrees of success, but at the present time none have broad application in the industry. However, electrical and RF heating methods are in advanced stages of development for environmental cleaning of petrochemicals in the vadose zone from leaking storage tanks and surface spills.

Two additional processes have been proposed for recovery of heavy oils: CO_2 flood and microbial enhanced oil recovery (MEOR). Both are now used widely for recovering oils that are normal or near-normal in composition and properties, but as yet neither have found acceptance in actual heavy oil deposits.

Cyclic steam stimulation

Cyclic steam stimulation (CSS) is the most simple of all of the steam-based thermal recovery processes. An array of vertical wells is drilled into the oil-impregnated sandstone reservoir and completed by perforating the casing at closely spaced intervals in the pay zone (Fig. 89). Steam is injected into the wells for a period of several weeks at rates approximating one to two barrels of steam (barrel of water converted to steam) per day per well. The wells are allowed to "soak" for a period of weeks to allow the injected heat to convect/conduct out into the reservoir. Then the same wells are pumped until the wells begin to water out as a cone of

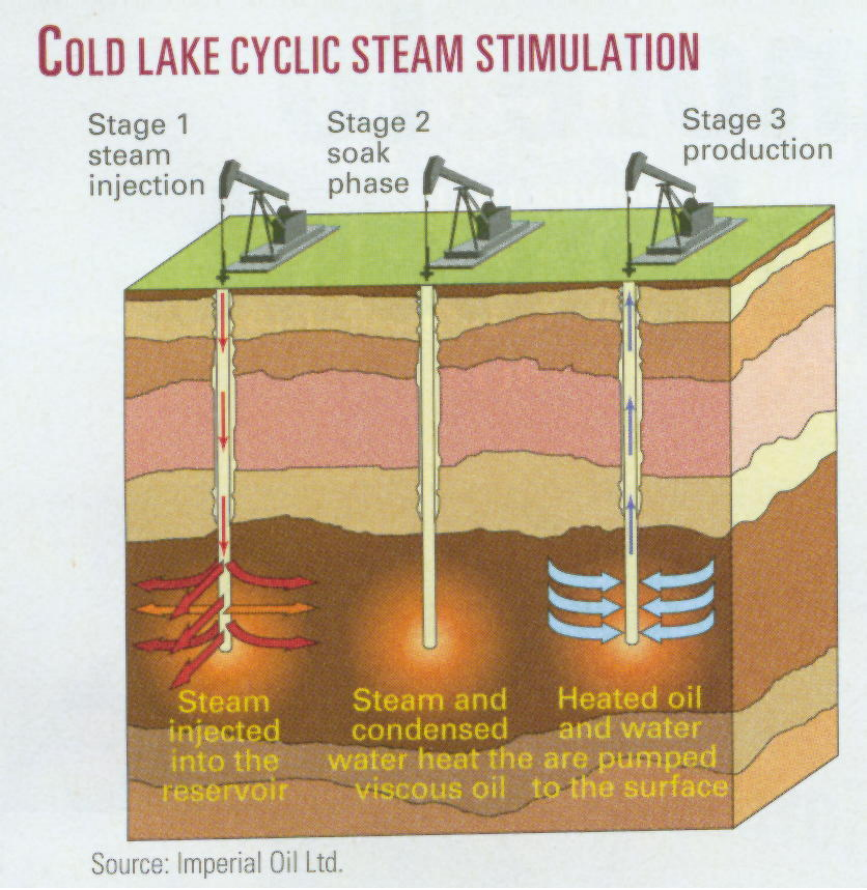

Figure 89: Diagram illustrating the three stages of the cyclic steam stimulation process (Moritis, 2004).

depression develops around the well. The only drive mechanism is gravity drive. Then the entire 6 to 12 month cycle is repeated. With each cycle the initial oil rates are normally lower than the previous cycle, the average oil-water ratios for the production phases drop off, and the steam-oil ratio (SOR) increases, indicating a reduction in recovery process efficiency.

Although the well configurations and management are simple, an efficient conventional CSS project requires a large investment in steam generators, insulated pipe arrays, as well as the pump jacks, water knock-out facilities, water purification plants, and oil gathering systems of any oil field. Efficiency and profitability improves with increasing scale of operation. Even the most efficient and long-lived CSS projects leave large volumes of stranded oil in the reservoir between wells. Most CSS projects eventually are converted to steam drive projects.

The largest CSS project in Canada is the Cold Lake operation of Imperial Oil. The project was started in 1985 and now has oil rates of 150,000 bopd (from a peak of 540,000 bopd) from about 4000 active wells operating at pressures in excess of the reservoir fracture pressure. After about 12 cycles over the past 20-25 years, the field is now mature and production is in decline. Plans for renovation of the field involve conversion to steam drive recovery either by (a) converting alternate CSS injectors/producers to injectors, which is inexpensive, yet minimally effective in simulations or (b) more effectively, by placing new horizontal injectors midway between the rows of existing vertical wells. The later method places steam in previously cold oil volumes, which can result in a simulated 115% improvement in oil rates over non-improved oil recovery (IOR) CSS methods alone, that is, doing nothing different.

Also performed at Cold Lake is an Imperial Oil pilot using CSS with a 5% volume of C5+ condensate to aid in reducing the viscosity of the heavy crude, a process referred to as LASER. The pilot is showing that the method is best initiated in the middle cycles of the life of a CSS project.

Steam drive

To increase recovery factors from a bitumen or heavy oil reservoir, the steam drive (steam flood) technology pushes steam under pressure from a vertical injector well toward adjacent vertical producer wells (Fig. 90). This permits sweeping of oil from portions of the reservoir that in CSS would be stranded beneath the adjacent cones of depression. Steam drive is essentially a normal water flood EOR process with a thermal (steam) component.

In the usual configurations, each steam injector is surrounded by either four (inverted 5-spot) or eight (inverted 9-spot) production wells. Normally, the producers are positioned in an orthogonal grid with the injectors located at the centers of each square. The injectors are completed with solid casing cemented in place and perforated in the lower half of the reservoir to facilitate placement of steam near the bottom of the oil-impregnated region. The producers are completed with slotted pipe held in place with gravel pack through all, or nearly all, of the pay interval. Above the pay zone, the producer is solid pipe cemented in place to prevent fluid leakage into higher strata. Wells in the array generally have four-acre to two-acre spacing (Fig. 91), so the injectors and producers are clustered very close to one another.

Where a bottom-water aquifer exists in the reservoir unit, it is normal to have a transition zone above the actual oil-water contact in which water saturation (Sw) gradually decreases to the values characteristic of the main part of the reservoir. This transition zone can be several tens of feet thick. In recovery of heavy oil by steam drive, efficiencies can be realized by limiting the placement of steam to just those portions of the reservoir with lowest Sw, thus

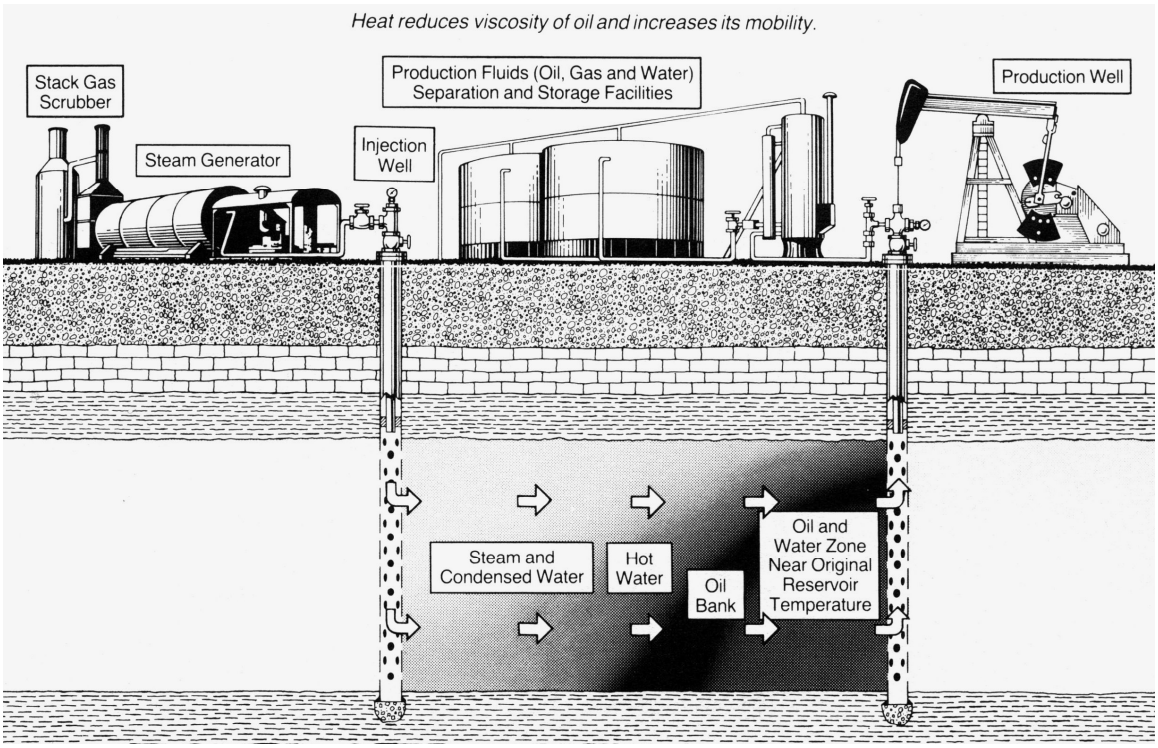

Figure 90: Components of the steam drive process (Stosur and Slater, 1987

Figure 91: Typical two-acre spacing of a steam injector well and an adjacent producer in a mature steam drive project, Midway-Sunset field, California. Photograph by S. Schamel.

reducing the disproportionate loss of heat to connate water (Schamel and Deo, 2003). The specific heat of heavy oil is less than half that of water, about 0.44 lb-1F-1 (1.83 kJkg-1K-1) versus 1.0 Btu lb-1F-1 (4.18 kJkg-1K-1), respectively (Burger and others 1985). This mandates avoiding placement of steam into the water-rich transition zone.

There is a tendency in steam drive projects for the steam or hot water to rise towards the top of the reservoir, thus overriding and by-passing large portions of the reservoir near the producers. Where this occurs, the sweep efficiency can be very low and premature steam break-through is a serious risk. This problem is less common in heterogeneous reservoirs in which discontinuous lenses of low-permeability beds serve as sub-horizontal barriers to steam, preventing override (Schamel and others, 2002). On the other hand, discontinuous lenses of high-permeability sand or sandstone may act as flow units that create *cul-de-sacs* within the reservoir restricting mobility of steam and effectiveness of the flood. Sands with high permeability contrasts can experience extreme fingering of the steam through the reservoir leading to premature break-through.

In a mature steam drive project, the rates of steam injection are on the order of 1.0-1.2 barrels of steam per foot of pay per well per day, or somewhat higher in pay intervals less than 100 ft thick. Target SORs are on the order of 2.0 to 4.0, but the project may be economic at SORs of up to 6.0-8.0 depending on overall operating expenses (OPEX). Steam drive projects have very large surface footprints (Figs. 86 through 88) and large greenhouse gas emissions, comparable to those of CSS projects.

Steam-assisted gravity drive (SAGD)

Steam-assisted gravity drainage, or SAGD, is a recovery method developed in the 1990s expressly for the Athabasca tar sands (Butler, 1991). This technique is the *in situ* technology that ultimately may recover more than two-thirds of remaining non-mined tar sand crude in northern Alberta. The tar sand of the Athabasca deposit is in the 100-ft-thick McMurray Formation, two-thirds of which are a quality bitumen reservoir.

In the standard SAGD well configuration the horizontal steam injector lies directly above the horizontal producer. The spacing of the two parallel wells depends on the thickness of the sub-horizontal reservoir, but both are intentionally in the lower half of the reservoir to allow sufficient space above the injector for the rise of the roughly cylindrical steam chest (Fig. 92). Ideally, the steam chest is wide at the top and narrow at the bottom near the producer. Typically the horizontal injector and producer are 15 to 30 ft apart and 3000 to 3500 ft long. In a full field operation the well pairs are about 300 ft apart. The wells are primed by cycling steam through them until the entire volume of reservoir between them is heated. Then steam is injected continuously. Heavy oil contacted by the rising steam, and heated to a low viscosity, drains downward towards the producer well. The steam gives up most of its heat through condensation of steam to hot water. The difference in temperature between the steam-(hot water) chest and the producer well is referred to as the "subcool." Steam chest growth is necessary for oil production. The rate of oil drainage is directly proportional to the square root of the height and the permeability of the steam chamber (Butler, 1991). Normally it takes several years for the steam chamber to become fully developed and oil rates to peak.

SAGD has advantages over steam drive in that it depends only on gravity as the driving mechanism, resulting in stable oil displacement and potentially better recovery from the reservoir. Steam override, a serious problem in some steam drive operations, is not an issue in

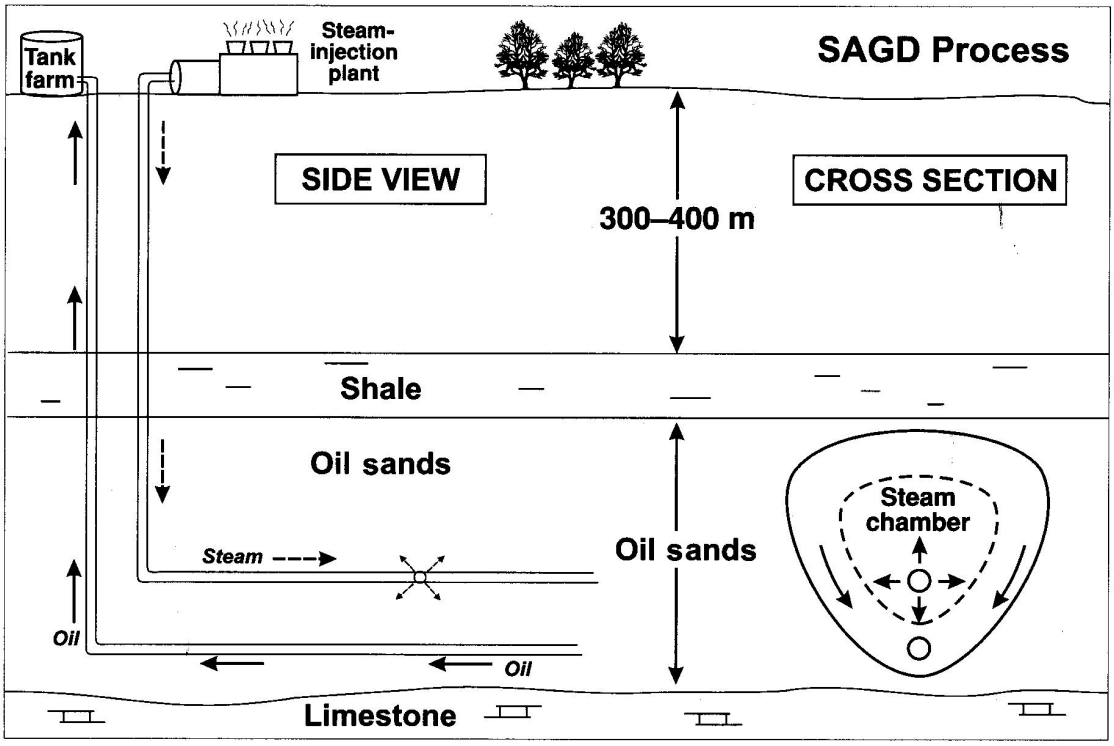

Figure 92: Block diagram illustrating the steam-assisted gravity drainage process. (Skipper, 2001)

SAGD. Also, in contrast with steam drive, the oil remains hot and fluid as it drains to the production well. A SAGD operation normally has a much smaller surface footprint than does CSS or steam drive projects (Rach, 2004). However, SAGD can be relatively less effective in heterogeneous reservoirs in which the presence of impermeable beds blocks the vertical rise of steam, thus limiting the height of the steam chest (Chen and others, 2007). Also, a successful SAGD requires constant management of temperatures in the steam chamber.

The SAGD must be operated so as to avoid, or at least minimize, "flashing" of water to steam in the producer well. When flashing occurs, there can be damage to the well, sanding out of the reservoir, and a sudden drop of temperature in the steam chest as heat is transferred to momentary in-well steam generation. The two options for managing the SAGD to avoid flashing are (a) "steam-trap control," which maintains the steam chest well above the producer well, or (b) "subcool control," which maintains the production fluids below the saturation or "flash" temperature for water. In normal operations, for safety reasons, a subcool of 20-30°C is the target, but SAGD simulations suggest that production rates and stability decrease for subcool greater than 3°C. A 5°C subcool is thought "unsafe" at low-pressures, but also at low pressures, the alternative "steam-trap control" is more difficult to attain than "subcool control." Because temperature varies from toe (cool) to heel (hot) of the SAGD well pair, proper management of the steam-trap or subcool along the length of the operation is especially difficult to attain.

In additional to the "conventional" SAGD described above, there are now several variants, including: (a) hybrid or solvent-assisted SAGD (ES-SAGD), and (b) low-pressure SAGD (LP-SAGD). The variations, when applied appropriately to different reservoir conditions, are intended to lower operating costs. Optimization of operating costs relative to recovery is becoming increasingly more critical as the price of natural gas needed to fuel the generation of steam increases.

The capital costs (CAPEX) involved in the different SAGD recovery processes are similar, regardless of the variant used, because all use nearly the same horizontal wells and surface facilities. It is only the artificial lift system used that leads to differences in CAPEX. However, LP- and ES-SAGD can be run at considerably lower SORs, which lowers the OPEX. The OPEX energy savings can be as much as 45%. However, operating at lower pressure or with a solvent- or vapor-assist, has a variety of operational trade-offs that could outweigh the efficiency and total OPEX of the alternative SAGD methods over "conventional."

ES-SAGD: The viscosity of reservoired bitumen can be lowered by raising the reservoir temperature by insertion of heat carried in steam or by adding large fractions of solvents, such as C_2-C_{10}, or ideally both. In ES-SAGD the solvent is added to the steam, so the steam carries both heat and solvent to contact the bitumen-saturated reservoir. Optimization involves use of a solvent that has a condensation temperature close to that of steam at the ambient pressure of the reservoir, which is most commonly septane (C_7) or octane (C_8). Even though most of the solvent can be recovered and recycled in a ES-SAGD operation, there can be as much as 15% or greater loss within the reservoir. This becomes an added component to the OPEX. Additional issues involve developing an understanding of how to effectively impact the bitumen along the cold bitumen interface to make this recovery method most efficient. This is still a recovery technique in development with only four, full-field tests underway at present. The Alberta Research Center (ARC) has been the leading organization for this research.

LP-SAGD: Based on operational experience with SAGD projects in northern Alberta, it is generally accepted that there is a monotonic, virtually linear, relationship between the operational pressure of the SAGD and its SOR. At about 1000 kPa, the SOR is approximately 2.0, which is very economic. But at 10,000 kPa, the SOR is 4.0-6.0, which requires much higher energy consumption for a barrel of oil produced. At pressures greater than about 2000 kPa, it is possible to use gas lift for the lift system. The higher pressure approach has both a low CAPEX and OPEX, and it is the lift system most widely used in northern Alberta SAGD operations. At operating pressures lower than 2000 kPa, it is necessary to use another artificial lift system, beam pumps or electrical submersible pumps (ESP). At present there are serious concerns with the advantages and difficulties of these alternative artificial lift systems in a SAGD operation that could facilitate LP-SAGD. For instance, some operators describe problems inserting the ESPs for doglegs on the order of 15°, but Schlumberger claims successful pump runs at these conditions. Also, few ESPs now available can operate successfully at the high temperatures typical of SAGD. Most are rated to just over 200°C. However, Weatherford has a new gas-driven pump that solves many of the problems encountered with the ESPs. This new pump style could open LP-SAGD to wider adoption.

An advantage of "conventional" or elevated-pressure SAGD is the geomechanical boost to oil recovery. Thermal expansion and the lowering of effective stress through the injection of fluid into the reservoir at high pressure, the sand reservoir experiences both dilation on a grain-to-grain scale and shear fracturing at a scale of millimeters to decimeters. High pressure injection has the effect of decreasing the "effective pressure" in the reservoir, thereby moving the stress field towards the fracture strength envelop. The effect of these geomechanical alterations is to increase the effective permeability and flow rates of fluids within the modified reservoir. If there is a horizontal regional stress field, as exists in northern Alberta and the Uinta Basin of Utah, the fracture strength envelop is reached at lower fluid pressure than otherwise would be the case. Both extensional and shear fractures can be induced, that together with grain-to-grain dilation improve the petrophysical properties of the reservoir. Obviously,

the advantages resulting from geomechanical effects are less with LP-SAGD than in "conventional" SAGD. This may be a serious trade-off, even at higher natural gas price. But the magnitude of the trade-off depends on the mechanical properties of the reservoir sand/ sandstone.

The production improvements resulting from geomechanical effects have been simulated by Advanced Technology using a coupled SAGD and geomechanical (FLAC) numerical simulator. The simulations showed a two-fold improvement in recovery rates at high injection pressures (5000 and 7500 psi) and a two-fold improvement where a horizontal residual stress exists. Thermal and pressure induced dilation can result in a 60% increase in permeability of the reservoir. The thermal- and pressure-induced dilation (swelling of the reservoir) is currently being monitored in the McMurray unconsolidated tar sands as a measure of the growth of the steam chest and SAGD optimization using InSAR satellite surface telemetry, and by downhole tiltmeters and seismic arrays (Pinnacle). From these data it is shown that the pressure (stress) front associated with the growth of the steam chest can be 40 ft (or 6 months) out in advance of the thermal front (Pat Collins, personal communication, Petroleum Geomechanics, March 2006). Also, convection transfer of heat through the reservoir precedes conduction at the steam interface, resulting in a more efficient heating of the oil-saturated reservoir. These methods now have wide adoption in SAGD recovery projects northern Alberta.

Chen and others (2007) describe how pressure-induced fractures, especially vertical fractures, can overcome the barriers to the upward rise of steam in a heterogeneous bitumen reservoir. The fractures permit the steam chamber to grow vertically through fractured impermeable strata that otherwise would have been barriers to the growth of the steam chamber. In numerical simulations using the conditions found in the McMurray bitumen reservoir, but with shale lenses, the presence of vertical fractures can double oil recovery factors (Chen and others, 2007). The vertical fractures aid both the upward growth of the steam chamber and the downward flow of heated oil to the producer well. The optimal fracture orientation is vertical and parallel to the direction of injector and recovery wells.

For very shallow heavy oil pools, heating of the oil can be accomplished by placement of a series of horizontal wells beneath the oil pool through which steam is circulated, but not injected (Osterloh and Jones, 2003). This avoids the problems that can be caused by escape of the steam to the surface. Other strategies may be available for production of heavy oil from ultra-shallow reservoirs (Dunn-Norman and others, 2002).

Geothermal Hot-Water Flood

The use of hot water in the place of steam has many drawbacks if it needs to be heated at the surface prior to injection into the bitumen or heavy oil reservoir. At present, only a few hot water recovery projects are active in California and Texas (Koottungal, 2008). However, if hot water (or its heat content) produced from either a steam-based recovery project or primary oil production is available, the water may need no further heating to employ in a successful hot-water flood. Otherwise, the heat content will be lost to surface cooling or into the water disposal wells. Alternatively, an effective source of hot water can be a deep aquifer (Fig. 93), a geothermal hot-water source (Pederson and Sitorus, 2001). The use of hot water from geothermal sources eliminates the need to burn fossil fuels to recover oil, thus lowering OPEX and greenhouse gas emissions and potentially reducing substantially CAPEX and the surface footprint of the EOR project.

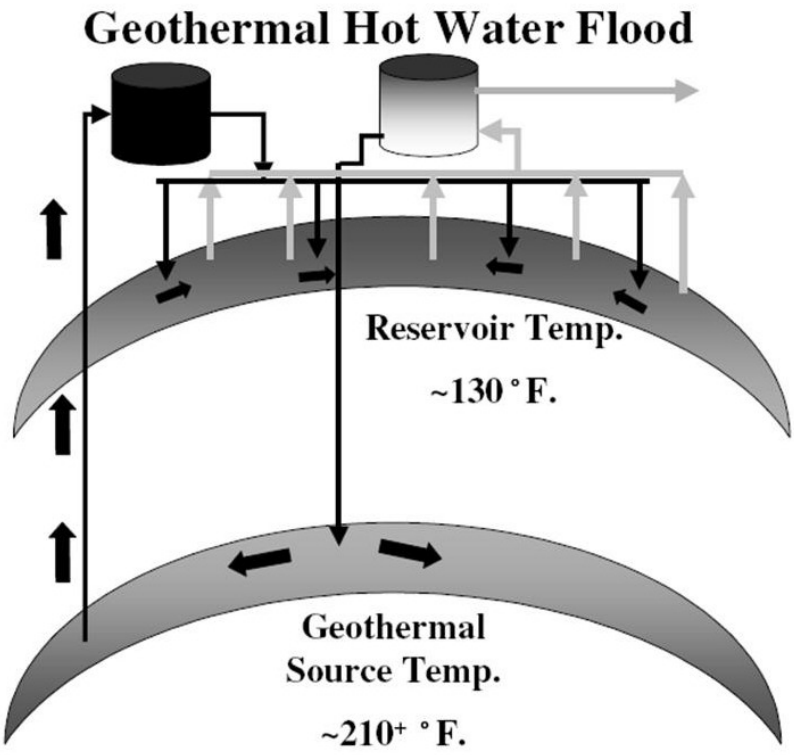

Figure 93: Components of a geothermal hot-water flood project (Pederson and Sitorus, 2001).

In Balam South field on Sumatra, this method was found to be effective in shallow, high viscosity waxy oil deposits where the geothermal hot water has low concentration of dissolved solids (Pederson and Sitorus, 2001).

Solvent Vapor Extraction (SVX)

Several of the steam extraction technologies, such as ES-SAGD, add small quantities of a petroleum solvent to the steam injection stream to aid in mobilizing the bitumen. In the solvent vapor extraction (SVX) methods no heat or water is used, but rather only the solvent is injected into the reservoir (Yazdani and Maini, 2005). In the VAPEX (vapor extraction) method gas condensates (C_5-C_{10}) are injected in either vertical or horizontal wells in CSS, steam drive or, most commonly, SAGD configurations (Fig. 94). VAPEX was initially proposed as a solvent-based analog of the SAGD process (Butler and Mokrys, 1991). This extraction method requires no natural gas for steam generation, so it may have a lower OPEX. This also means that it has considerably lower greenhouse gas emissions than steam-based thermal recovery, and it has minimal process water requirements. However, effectiveness depends on achieving a high degree of contact of the solvent with virgin oil and economics are highly dependent on successful recovery and cycling of the solvents used.

Recently, the Petroleum Technology Research Centre (PTRC) in Regina has organized a consortium to develop a similar recovery process that uses a solvent gas mixture of propane, butane, methane, and CO_2 (Collison, 2007). The concept is that in less permeable consolidated rock, in contrast to the highly permeable McMurray sands, a gas can result in a better sweep of the reservoir and higher recovery rates than can the liquid solvent used in VAPEX.

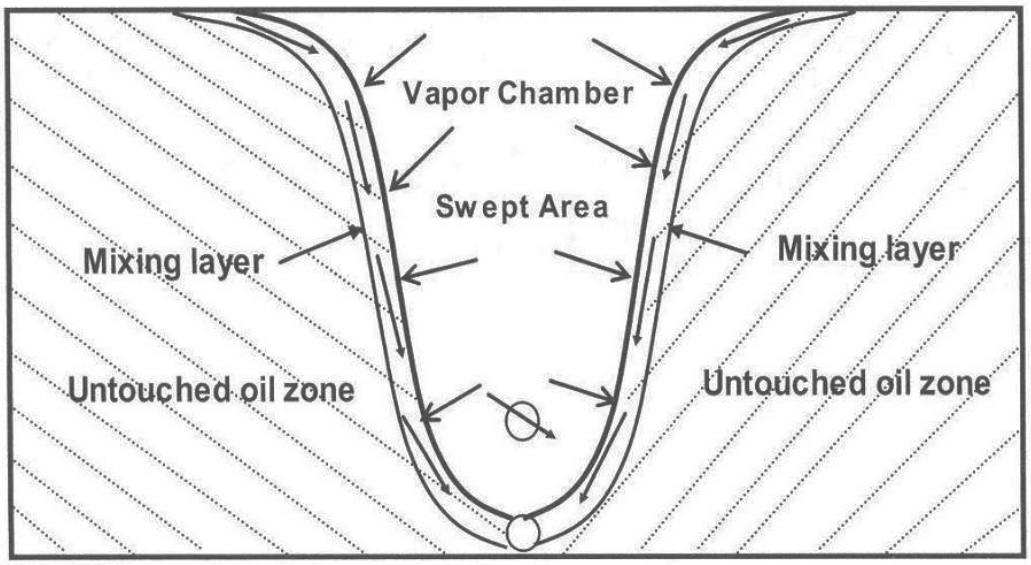

Figure 94: Components of a Vapex project in which liquid solvents are injected with steam in a normal SAGD well configuration (Yazdoni and Maini, 2005).

In Situ Combustion

The reservoired oil may serve as the fuel for generating heat required to facilitate the oil recovery process. In the "conventional" *in situ* combustion method, air is injected into the reservoir, auto-igniting the heavy oil or bitumen. This creates a high temperature combustion zone with temperatures as high as 750º to 1,290º F that is sustained as long as oxygen is supplied through pressurized injection of air (Fig. 95). The hot, combusted air contacts cold, viscous oil in front of the combustion zone causing the lighter oil components to mobilize and the heavier fractions to be converted to coke, which becomes the fuel that sustains ongoing combustion in the reservoir. Under ideal conditions, the lighter oil fraction, combustion gases, and reservoir water converted to steam are swept forward towards nearby vertical production wells.

When successful, *in situ* combustion offers many advantages over steam-based thermal recovery. The process results in substantial upgrading of the produced oil, leaving behind in the reservoir the undesirable heavy fractions that become the fuel propelling oil recovery. The process eliminates the need for large steam generators and the network of insulated pipes at the surface; both CAPEX and OPEX are substantially lower. The only addition to the production facilities beyond what is part of a steam-based project is a unit for processing combustion gases. The produced gas is dominantly nitrogen (about 75%) and CO_2 (about 15%) with small quantities of methane and C_2-C_5. Once the N_2 and very small amounts of H_2S have been removed, the remaining gas can be sold as a low-Btu fuel (Chris Bloomer, personal communication, June, 2008). Potentially, the surface footprint, greenhouse gas emissions, and water requirements of an *in situ* combustion project are much smaller than those for any steam-based operations. However, this method is very difficult to control in the subsurface and premature break-through of the combustion front from injector to producers doomed nearly all previous air injection projects. In general, the method has been abandoned by industry for heavy oil recovery, except for a few small projects in Gujarat, India (13.5º-17.0º API), Louisiana (19º API), the Battrum field, Saskatchewan (18º API), and reservoir pressure

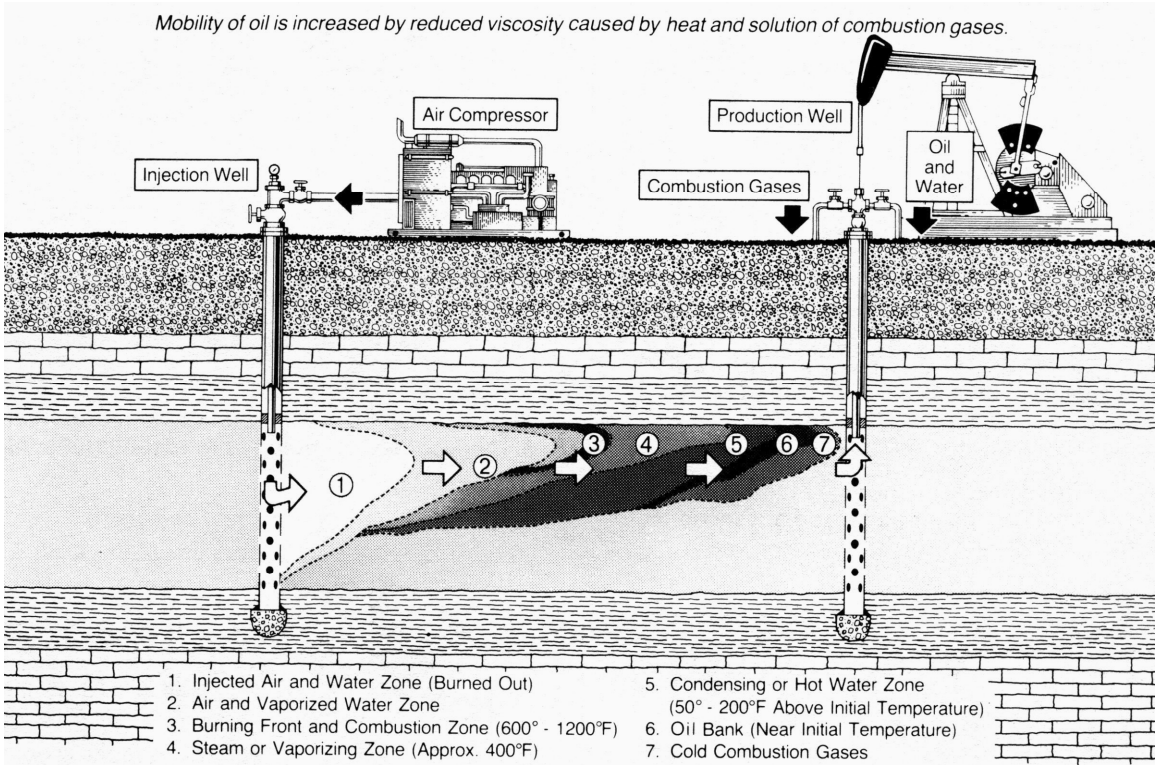

Figure 95: Components of the in situ combustion process (Stosur and Slater, 1987).

maintenance applications in North Dakota (Koottungal, 2008). However, the Suplacu de Barcău heavy oil field in Romania, which has operated successfully under *in situ* combustion since 1964 with a recovery factor of 56% in the reservoir, is swept by the combustion front (Paduraru and Pantazi, 2000).

THAI™, toe-to-heel air injection (Xia and others, 2002), is an alternative *in situ* combustion technology that is intended to mitigate the likelihood of premature break-through of the combustion front by combining a vertical air injector with a horizontal producer (Fig. 96). The "toe" of the producer is placed very close to the bottom of the injector so as to create a very short initial distance for the sweep of hot oil. The "heel" of the horizontal well is over 1000 ft distant from the point of air injection, enabling a large volume of reservoir to be produced.

The Whitesands pilot project in the Athabasca tar sand deposit has demonstrated the viability of the THAI™ technology for economic recovery of bitumen from the 46-to 85-ft-thick middle McMurray sand reservoir (Petrobank, 2007). The pilot consists of three horizontal producers 1640 ft long and 328 ft apart, paired with three vertical air injection wells. Operations began in late March 2006 with a three-month, pre-ignition, steam heating of the wells to bring the reservoir temperature to an ignition temperature of 200º-212º F. Then air was injected to ignite the combustion front and heating the cold bitumen in advance of the combustion front to over 750º F, enabled by the forward migration of the hot combustion gases. The lighter fraction of the bitumen moves towards the horizontal producer by a combination of gravity drainage and high pressure combustion gas drive. Once steady-state is reached in the combustion cell (Fig. 97), the combustion front advances at a rate of 0.5 to 1.0 ft per day or up to 335 ft per year. After one full year of operation, the pilot had an average oil rate of 200 to 500 bopd per producer. In 2008-2009, Petrobank is installing another three THAI™ well pairs on its Whitesands property.

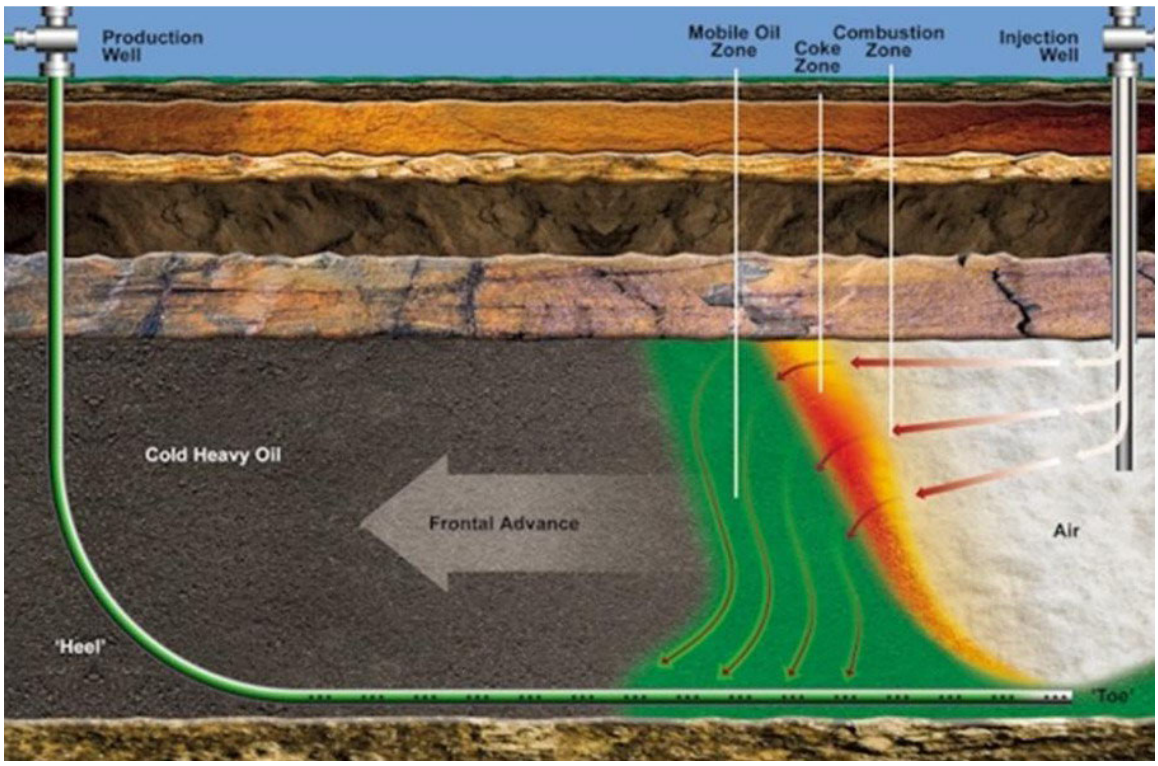

Figure 96: Components of the THAI™ (toe-to-heel air injection) technology. Source: www.petrobank.com, Petrobank, 2007

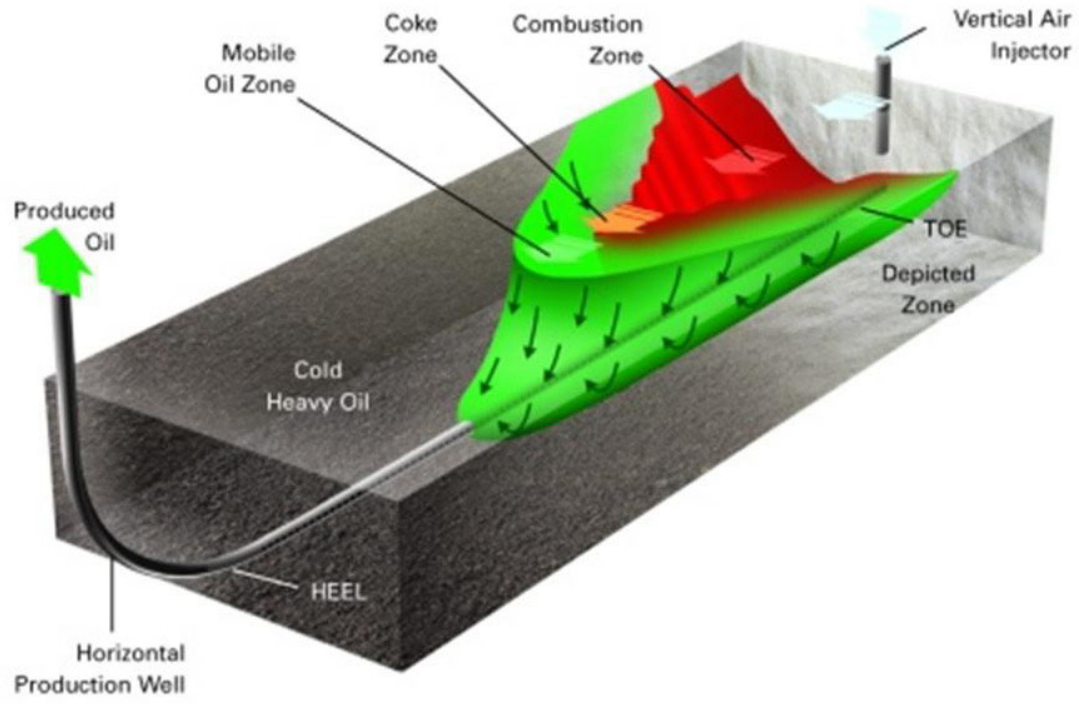

Figure 97: Steady-state configuration of THAI™. Source: www.petrobank.com, Petrobank, 2007.

The McMurray sand reservoir at the Whitesands property is unconsolidated, having average porosity, permeability, and oil saturation of 34%, 6610 md, and 80%, respectively. It is a relatively homogeneous, estuarine bayfill, very fine to medium grained sand deposit with scattered mud drapes. The average oil grade is 2110 BO/ac-ft and the OOIP is 90 to 210 MBO/ acre. Although the McMurray sand is an ideal reservoir for implementation of the THAI™ technology, laboratory studies indicate that it can work successfully in reservoirs with a So and permeability as low as 30% and 500 md, respectively (Chris Bloomer, personal communication, June, 2008). As an alternative to cycling steam in the pre-ignition phase, the wells could have been heated with down-hole electrical heaters.

Electrical Heating

Electric heating, in which electrodes are placed in the reservoir to raise temperature, is still in the development stage. The heating occurs by electrical resistance adjacent to the two paired electrodes, not in the rock volume in between, and it is highly dependent on the magnitude of reservoir electrical resistivity. Normally operators have been using the technology on a relatively small scale for cleanup of surface spills of hydrocarbons into the shallow vadous zone. However, one small operator, E-T Energy, is operating an electrical heating pilot covering only one acre on the outskirts of Ft. McMurray. Here the tar sand is very shallow making it possible to space the heater wells at just 16 meters, the maximum spacing considered effective to heat the oil-saturated reservoir. The company claims that the operating cost for electricity to drive the recovery is 70kwhr/barrel or about C$7.00/bbl. Furthermore, the company claims that electrical heating can cause unplugging of clays from reservoir pore throats, thus improving recovery over the history of the operation. This process is described on the web site www.e-tenergy.com.

Electromagnetic Radio-Frequency Heating

The electromagnetic radio-frequency (RF) heating process is comparable to embedding a microwave oven within an oil-impregnated reservoir. In a configuration developed and field tested by the Illinois Institute of Technology (IIT) three parallel banks of vertical electrodes are placed into wells drilled into the oil reservoir. Electrical power is applied to the central "exciter" row of electrodes, which then establish an electromagnetic field with the flanking "guard" electrodes (Sresty and others, 1986). Some portion of the electromagnetic energy within the oil and water saturated sandstone in the field is converted to heat. However, only that portion of the reservoir enclosed by the electrode array, referred to as a "triplate line geometry" (Sresty and others, 1986), is heated.

In 1981, the IIT carried out a very small RF heating pilot in the Rim Rock Sandstone reservoir in Asphalt Ridge Northwest (Sresty and others, 1986). A triplate line array of 20-ft long electrodes was installed in a 33-cubic-yard volume of the reservoir. For 20 days, 40 to 70 KW of RF power was applied to the array heating the shallow reservoir to as much as 392º F. The heated oil was allowed to drain by gravity drive into a collection chamber mined out for that purpose immediately beneath the electrode array. A total of 8.0 barrels of oil was captured, representing about 35% of the OOIP. Furthermore, that oil saturation profile appeared to have been shifted downward, suggesting gravity drainage throughout the reservoir volume heated. Sresty and others (1986) claim that if the experiment had continued for 6 months, the oil recovery would have been 50-75% of OOIP. While intriguing, this pilot project was too small

in size and duration to demonstrate the viability of this technology. An obvious drawback is the need to drill an array of very closely spaced wells into the reservoir for the placement of the electrodes, and for the construction of a gathering sump or system of horizontal producers beneath the heated zones. While perhaps economic for near-surface oil recovery, it is unlikely to be feasible for heavy oil or bitumen reservoirs at normal operating depths of many hundreds or thousands of feet. This approach remains unproven, but it could have niche applications.

Carbon Dioxide Injection

When a gas is dissolved in crude oil, the oil experiences both a volume expansion (swelling) and a reduction of oil viscosity. This is true regardless of the gas, whether methane, nitrogen, or carbon dioxide. However, CO_2 is more effective than other gases for causing oil swelling and viscosity reduction (Burger and others, 1985). This is the chemical basis for the CO_2 injection EOR process. The penetration of CO_2 into the oil is by diffusion. For the process to be effective, a large contact area is necessary in the reservoir. Furthermore, at lower reservoir pressures less CO_2 can be dissolved in the crude oil. Swelling and viscosity reduction are directly proportional to the oil saturation pressure, which normally is proportional to depth of burial. Laboratory experiments (Combe and others, 1997) have shown that viscosity reduction of a fully CO_2 saturated oil is a factor of 8 at 1000 psi (2325 ft depth) and a factor of 20 at 2175 psi (about 5000 ft depth).

The only long-term commercial CO_2 injection recovery program for recovering heavy oil is in Bati Raman field (Combe and others, 1997) in southeast Turkey, operated by the Turkish Petroleum Corporation (TPAO). Initially, the field contained 1.85 BBO having a gravity of 9-15º API and a viscosity of 200 to 2000 cp. The reservoir is a 4300-ft-deep limestone having both matrix and fracture porosity. Permeability is in the range 400 to 2,000 md. A continuous, 210-ft-thick, oil-impregnated zone extends over an area of 16.7 square miles. The CO_2 for the operation is derived from Dahan field just 50 miles from Bati Raman. After several unsuccessful attempts to produce the heavy oil by water flood, cyclic steam stimulation, and steam drive, a successful CO_2 injection EOR program was started by TPAO in 1986. To date, a cumulative production of 50.8 MMBO is attributed to CO_2 injection (TPAO online report). The expected recovery factor from the CO_2 injection project is 6% (Combe and others, 1997).

CO_2 immiscible flood technology is used successfully in numerous fields in Trinidad to recover 17º to 29º API oils in reservoirs 2000 to 4000 ft deep (Koottugal, 2008). The sandstone reservoirs have permeabilities in the range 30-300 md.

Other non-thermal EOR technologies that have been proposed for recovery of heavy oil and bitumen from sandstone reservoirs include: microbial enhanced oil recovery (MEOR; Mokhatab and Giangiacomo, 2006) and alkali-surfactant flooding (Bryan and Kantzas, 2007). These and other similar approaches seek to alter the properties of the heavy oil or the oil-sand interface so as to facilitate Darcy flow of the heavy oil. All are still in development and, as yet, they should be considered unproven technologies for recovery of bitumen and heavy oil.

RECOVERY STRATEGIES

In assessing the likelihood of successful *in situ* recovery projects in Utah it is useful to examine the general reservoir and oil characteristics of successful projects elsewhere in the world (Moritis, 2008). Table 22 shows the average properties for 94 individual fields or

projects declared by their operators to be commercial. The largest number of projects is in the southern San Joaquin basin, Alberta, Venezuela, China, and Trinidad. Many of the reservoirs are unconsolidated or poorly consolidated sands, and the remainder are in sandstones. Nearly all are EOR projects that followed initial primary production from the same reservoir. In the Midway-Sunset field, San Joaquin basin, steam-based recovery was preceded by many decades of gradually declining primary production with the reservoir energy provided by solution gas drive (Schamel and others, 2002).

Table 22: General reservoir and oil properties of successful thermal in situ recovery projects in California (San Joaquin basin), Canada, Venezuela, and elsewhere. Data from the Oil & Gas Journal 2008 worldwide EOR survey (Koottungal, 2008). The numbers in the table are average values for the number of individual fields/ projects indicated. Viscosity is that at the reservoir temperature shown in the table.

Region	ºAPI	Porosity%	Perm, md	Visc, cp	Temp, ºF	Soi, %	Depth, ft	# fields
San Joaquin	13	33	2,259	6,850	96	60	1306	37
Alberta	10	32	3,650	671,300	59	78	1467	10
Venezuela	11	32	4,511	1,986	129	83	2789	14
Trinadad	14	30	305	2,061	105	70	1556	9
China	17	29	2,700	16,893	95	65	2602	15
Indonesia	22	36	1,600	350	100	61	550	1
Brazil	16	25	2,113	1,381	112	76	1850	4
Colombia	13	28	1,200	2,965	108	57	2100	1
Germany	25	30	7,850	175	100	50	2600	1
Wyoming	18	22	100	20	54	85	900	2
Overall average:	**16**	**30**	**2629**	**70,398**	**96**	**68**	**1772**	

Compared to an average of worldwide successful thermal *in situ* recovery projects, Utah's deposits generally have heavier (lower ºAPI) and more viscous oils, substantially lower permeability, and lower initial oil saturations. Only the Athabasca oil is comparable to those of Utah, but that reservoir is highly permeable, unconsolidated sand.

The previous *in situ* field experiments performed in Utah's bitumen and heavy oil deposits were all too small and short-lived to serve as adequate indications of which technologies could be successful for commercial recovery operations. Most were performed at a time when the technologies themselves were still in development and could have easily failed for technical reasons unrelated to the inherent applicability of the method to the reservoir.

In the Sunnyside deposit as part of an exploration program in 1955-1965, Signal Oil & Gas Company drilled a stratigraphic test well in sec. 4, T14S-R14E to a depth of 1450 ft, encountering a gross and net thickness of bitumen-saturated sandstone of 645 and 366 ft, respectively (Covington, 1976). The average porosity, permeability, and oil saturation were 25%, 750-1750 md, and 55%, respectively. This well also tested the presence of liquid hydrocarbons downdip from the area of known tar sands. In addition, in 1966-1967, Signal drilled three horizontal holes in the face of the Utah Rock Asphalt quarry for steam flood extraction tests. The pilot consisted of a central producer and two adjacent steam injectors, each only 370 ft long. The test was abandoned as uneconomic after producing only 560 barrels of oil with a very high SOR of 23.8 (Lewin & Associates, 1984; Marchant, 1988).

Exploration continued in the Sunnyside deposit with core holes drilled in 1965 by Shell Oil Company and Atlantic Refining Company (Covington, 1964). The six holes drilled by Shell in sec. 3, T14S-R14E were used in 1966 to conduct a 5-spot, steam-flood pilot (Marchant, 1988). The test was terminated in 1967 when it was determined that the natural fracture system interfered with the steam flood (Thurber and Welborn, 1977; Lewin & Associates, 1984). Pan-American Petroleum Corporation conducted a steam-flood pilot in 1966, but little is known about the test or its results.

From 1971 to 1982, the DOE Laramie Energy Technology Center (LETC) carried out several, small, thermal-recovery pilots (cyclic steam stimulation and reverse combustion) in Asphalt Ridge Northwest on a Sohio Oil lease (Land and others, 1977; Johnson and others, 1982; Johnson and others 1984; Johnson and Thomas, 1988; Merriam and Fahy, 1985; Holmes and others, 1986; Johnson and Lyle, 1994). The inconclusive electromagnetic RF heating experiment performed by the IIT in 1981 (Sresty and others, 1986) was discussed in the previous section.

Without actual *in situ* production experience to serve as a guide to applicability of various technologies for the heavy oil and/or bitumen deposits of Utah, one can only use the characteristics of successful projects elsewhere. In nearly every instance, the lithified sandstone reservoirs in Utah have petrophysical properties, thicknesses, oil saturations, and resource concentrations (OOIP) at the low end of economically viable *in situ* recovery projects. Therefore, the applicability assessments presented in Table 23 and the discussion below are speculative and optimistic. Only by initiating pilot projects that test alternative heavy oil-bitumen recovery technologies can we know if this very large energy resource can be developed successfully.

Table 23: Applicability of various technologies for in situ recovery of heavy oil and/or bitumen from the principal deposits in Utah. See text for explanation of applicability categories. Key to deposits: PR, P.R. Spring-Hill Creek; SS, Sunnyside "core" area; AR, Asphalt Ridge; WR, Whiterocks; WV, Wonsits Valley and other analogous deposits in the central Uinta Basin; TST, Tar Sand Triangle.

Technology	PR	SS	AR	WR	WV	TST
Cyclic steam stimulation	C	B	A	B	B	B
Steam drive	D	B	A	B	C	B
Steam-assisted gravity drive	D	B	A	A	C	B
Geothermal hot-water flood	D	D	D	D	A	D
Solvent vapor extraction	C	B	B	B	B	B
THAI™ in situ combustion	D	A	A	A	C	A
Electrical heating	C	B	B	B	D	C
Carbon dioxide injection	D	D	D	D	B	D

The applicability categories in Table 23 are as follows:

Category A: The technology may have general application with only moderate modifications to conform to specific reservoir and/or operational/regulatory challenges.

Category B: The technology may have site-specific application or may require major modifications to conform to specific reservoir and/or operational/regulatory challenges.

Category C: The technology probably cannot be applied at the present time, but it is worthy of further reconsideration as the technology matures or as understanding of the deposit improves.

Category D: The technology is considered to be unsuitable.

On the south flank of the Uinta Basin, lenticular distributary channel and marginal lacustrine sandstones intercalated within the lower parts of the Green River Formation are the principal reservoir across more than 600 square miles of the West and East Tavaputs Plateau. Although the sandstones are relatively porous and permeable, averaging 25.1% and 948 md, respectively, they tend to have both low oil saturations (45.4%) and oil-impregnated net

thickness (40.7 ft). Consequently, the volume of OOIP per unit area in these deposits is very small, averaging 25.9 MBO/acre in the P.R. Spring-Hill Creek deposit. All indications are that OOIP is similar in the Sunnyside deposit outside of the exceptional several square mile Dry Creek Canyon-Bruin Point-Range Creek "core" area. In this area, stacked fluvial channels in the Douglas Creek Member, many over 100 ft thick with gross thickness of many hundreds of feet, locally contain OOIP that is more than an order of magnitude greater than the other parts of the south flank deposits. Throughout, the reservoired oils are extra-heavy to heavy, averaging less than 10º API. Biomarkers indicate that these are immature Green River oils that have been heavily biodegraded. These oils are asphaltine-rich, saturate-poor, and very viscous.

Outside of the "core" area of the Sunnyside deposit there appears to be little incentive to develop the bitumen resources. Despite the many logistic and potential regulatory challenges to operating in this bitumen-rich area, the "core" area of the Sunnyside deposit is an obvious candidate for testing a variety of *in situ* recovery technologies. THAI™ *in situ* combustion may prove to be successful, as it has low demands on external energy and water resources and it can be operated with a relatively small surface footprint. As much of the deposit is very shallow, solvent vapor extraction and electrical heating could be effective. Given the presence of thick continuous sand units, steam-based recovery methods could be technically successful, although in this setting perhaps uneconomic or impractical. For the thicker and most bitumen-rich sandstone beds outside of the "core" area in Sunnyside and P.R. Spring-Hill Creek, small-scale, electrical heating, solvent extraction and/or cyclic steam stimulation projects could be effective and economic if properly designed and managed.

On the north flank of the Uinta Basin, heavy oil is reservoired in Mesozoic sandstones on the up-turned hanging-wall of the Uinta Basin boundary fault, and in fluvial and marginal lacustrine sandstones of the Eocene strata that unconformably onlap the thrust fault. The only known deposits of consequence are Asphalt Ridge and Whiterocks, although exploratory drilling within buried portions of the thrust sheet could reveal others. The main reservoir at Asphalt Ridge is stacked fluvial channels of the Mesaverde Group, which contains OOIP in the range 120 to 190 MBO/acre. At Whiterocks, the Nugget Sandstone (Triassic-Jurassic) is the only reservoir. This eolian sandstone is porous (16 to 32%), moderately permeable (50 to 250 md), and relatively homogeneous. As the reservoir is subvertical, the height of the oil column, not the 90 ft thickness of the unit, determines the OOIP, which is in the range 450-485 MBO/ acre. The heavy oil in both deposits has API gravity in the 10º to 14º range, and it has the composition of a moderately biodegraded normal Uinta Basin oil. It is relatively high in saturates, low in asphaltines, and thereby easily upgraded to marketable products. Viscosities are considerably lower than those of the south flank oils.

At both Asphalt Ridge and Whiterocks, steam-based recovery methods should be technically successful. However, the need for a small surface footprint and minimal air emissions at Whiterocks, which is in the Ashley National Forest, might preclude the use of CSS and steam-drive. Both deposits are excellent candidates for THAI™ *in situ* combustion. In specific parts of the deposits, solvent extraction and electrical heating might have application. The presence of an oil industry infrastructure in the northeast Uinta Basin should encourage early development of these deposits.

The shallow-oil pools in the central portion of the Uinta Basin present an immediate opportunity for development of a stranded, immobile oil resource. Here lenticular, fluvial channel sandstones in the upper Eocene Uinta Formation reservoir both moderately biodegraded heavy oil and normal oil having a pour point that is greater than the ambient

reservoir temperature. If the Wonsits Valley shallow oil pools are representative of the many similar accumulations scattered across the basin, the oils change down section from degraded heavy oil to immobile normal oil to mobile normal oil at current production, which is produced from depths below about 4000 ft. Many of these deposits produce small volumes of biogenic gas (Rice and others, 1992), indicating active biodegradation of the shallow, reservoired oil.

Several factors indicate that geothermal hot-water flood could be successfully implemented in the shallow parts of Wonsits Valley field and in similar shallow-oil deposits overlying active oil/gas fields in the basin. First, there is a ready supply of hot, low salinity water recovered from normal field operations, hot water that otherwise would be discarded in disposal wells. Second, in at least some parts of the pools only a small increase in temperature is required to mobilize the now-immobile oil. Additionally, the shallow oil is of the same, or nearly the same, quality as the oil produced from the deeper Green River Formation. The gathering system is in place to handle this oil and it has a ready market. The principal challenge will be to design a hot-water flood project that can adequately sweep the highly lenticular sandstone bodies within the Uinta Formation. Alternative technologies for recovery of these relatively light oils include CO_2 injection, solvent vapor extraction, and small-scale cyclic steam stimulation.

The bitumen in the Tar Sand Triangle is reservoired in a several-hundred-foot-thick eolian sandstone, the White Rim Sandstone. Across an area of 88 square miles, the thickness of the bitumen-impregnated sandstone exceeds 100 ft. The strata are gently dipping and otherwise unstructured. Porosity and permeability of the sandstone reservoir are in the range 15-19% and 200-500 md, respectively. The oil saturation is in the range 30-35%. The bitumen is heavy (< 8º API), has a high asphaltane and sulfur content, and is saturate-poor. However, compared to other Utah heavy oils, it has a low viscosity.

A large area in which the bitumen-impregnated interval is in excess of 100 ft, an apparently homogeneous, relatively porous reservoir, and relatively low viscosity of the oil all would indicate that steam-based recovery methods could be successful in the Tar Sand Triangle. However, the close proximity to a national park and national recreation area, as well as limited access to water resources, would favor a recovery process that has little water demand, has a very small surface footprint, and generates minimal air pollutants. THAI™ *in situ* combustion might be applied very effectively in this deposit, particularly as the deposit has an exceptionally low oil saturation. Solvent extraction is an alternative technology, and electrical heating might prove effective on the intermediate benches where the deposit is relatively close to the surface. The overall remoteness of the deposit, limited water resources (Pyper, 1983), lack of essential infrastructure, large distance to oil refineries, and generally poor quality of the bitumen could delay its development for several decades. In-reservoir upgrading possible with *in situ* combustion might solve the last of these impediments.

Given the current knowledge of Utah's heavy oil and bitumen deposits, none are adequately characterized to design an *in situ* oil recovery program. There is a critical need to fully characterize the deposits in terms of spatial variability of reservoir and oil properties. For instance, at Whiterocks we do not know how much farther the deposit might continue along strike. At the very large Asphalt Ridge deposit we do not know the position of the oil-water contact or the quality of oil downdip. A comprehensive effort to fully characterize these oil-rich deposits in terms of their suitability for *in situ* recovery processes is needed to encourage the large private investments required for their development. The oil resource is there, but at present it is stranded. Our challenge is to develop creative ways to recovery it.

ACKNOWLEDGEMENTS

This study was partly funded by the Utah Geological Survey "Characterization of Utah's Hydrocarbon Reservoirs and Potential New Reserves" program. Appreciation is expressed to professional associates who have generously contributed information, advice and other material support to this project: Chris Bloomer, James Emme, Wally Gwynn, Terry Massoth, Craig Morgan, Tom Chidsey (reviewer), David Tabet, Gene Van Dyke, and Staffan Van Dyke.

REFERENCES CITED

Banks, E.Y., 1981, Petrographic characteristics and provenance of fluvial sandstone, Sunnyside oil-impregnated sandstone deposits, Carbon County, Utah: Salt Lake City, University of Utah, M.S. Thesis, 112 pages.

Bishop, C. E., and B. T. Tripp, 1993, An overview of tar sand of Utah. Utah Geological Survey, American Association of Petroleum Geologists Rocky Mountain Section meeting brochure, September 1993, 28 p.

Blackett, R. E., 1996, Tar-sand resources of the Uinta Basin, Utah: Utah Geological Survey Open-File Report 335, 122 p.

Bryan, J. and A. Kantzas, 2007, Enhanced heavy-oil recovery by alkali-surfactant flooding. Society of Petroleum Engineers Paper 110738, 13 p.

Bukka, K., J.D. Miller, and A.G. Oblad, 1991, Fractionation and characterization of Utah tar sand bitumens - influence of chemical composition on bitumen viscosity: Energy & Fuels, v. 5, p. 333-340.

Bunger, J. W., K. P. Thomas, and S. M. Dorrence, 1979, Compound types and properties of Utah and Athabasca tar sand bitumens: Fuel Science and Technology International, v. 58, p. 183-195.

Burger, J., P. Sourieau, and M. Combarnous, 1985, Thermal methods of oil recovery. Paris, Èditions Technip, 430 p.

Butler, R. M., 1991, Thermal recovery of oil and bitumen. Englewood Cliffs, N.J., Prentice Hall, 527 p.

Butler, R.M., and I. J. Mokrys, 1991, A new process (VAPEX) for recovering heavy oils using hot water and hydrocarbon vapor. Journal of Canadian Petroleum Technology, v. 30, no. 1, p. 97-106.

Byrd, W. D., Jr., 1970, P.R. Spring oil-impregnated sandstone deposits, Uintah and Grand Counties, Utah. Utah Geological and Mineralogical Survey Special Publication 50, 34 p.

Calkin, W. S., 1980, Sandstone size analysis from the Sunnyside tar sands project. Utah Geological Survey open files, 23 p.

Calkin, W. S., 1981, Geologic summary report of the Sunnyside tar sands project, Carbon County, Utah. Utah Geological Survey open files, 153 p.

Calkin, W. S., 1989, Summary of field activity, 1989 exploration program, Sunnyside tar sands, Carbon County, Utah. Utah Geological Survey open files, 12 p.

Calkin, W. S., 1990, Geologic summary report of the 1990 exploration program, Sunnyside tar sands project, Carbon County, Utah, Golden, CO, 189 pages.

Calkin, W. S., 1991, Geologic summary report of the 1990 exploration program, Sunnyside tar sands project, Carbon County, Utah, Golden, CO, 133 pages.

Campbell, J. A., 1975, Oil-impregnated sandstone deposits of Utah: Mining Engineering, v. 27, p. 47-53.

Campbell, J. A., and H. R. Ritzma, 1979, Geology and petroleum resources of the major oil-impregnated sandstone deposits of Utah: Utah Geological and Mineral Survey Special Studies 50, 24 p.

Campbell, J. A., and H. R. Ritzma, 1981, Geology and petroleum resources of the major oil-impregnated sandstone deposits of Utah, *in* R. F. Meyer, and C. T. Steele, eds., The future of heavy crude oil and tar Sands: Conference on June 4-12, 1979, Edmonton, AB, p. 237-253.

Chalcraft, R. G., 1990, Wonsits Valley, Utah – Tar sand deposits: unpublished Chevron USA report, Utah Geological Survey open-file, 4 p.

Chen, Q., M. G. Gerritsen, and A. R. Kovscek, 2007, Effects of reservoir heterogeneities on the steam-assisted gravity drainage process. Society of Petroleum Engineers Paper 109873, 10 p.

Clem, K., 1985, Economic potential of state-owned lands in the Sunnyside Special Tar Sand Area, Carbon County, Utah: Utah Geological and Mineral Survey Report of Investigation 196, 22 pages.

Collison, M., 2007, Solvents on track. Oilsands Review, v. 3, no. 1, p. 43-44.

Combe, J. F. Faure, K. Issever, and I. Topkaya, 1997, Bati-Raman heavy oil field -reservoir management of CO2 injection in fractured limestone formations. Proceedings of the Offshore Mediterranean Conference and Exhibition, Ravenna, Italy, March 19-21, 1997, 15 p.

Covington, R. E., 1963, Bituminous sandstone and limestone deposits of Utah, *in* A. L. Crawford, ed., Oil and gas possibilities of Utah, Re-evaluated. Utah Geological and Mineral Survey Bulletin 54, p. 225-248.

Covington, R. E., 1964, Bituminous sandstones in the Uinta Basin, *in* Intermountain Association of Petroleum Geologists, 13th Annual Field Conference, p. 227-242.

Covington, R. E., 1976, Oil impregnated rocks of Utah. Brigham Young University Geology Studies, v. 22, p. 143-150.

Covington, R. E., and K.J. Young, 1985, Brief history and recent developments in tar sand deposits of Uinta Basin, *in* M. D. Picard, ed., Geology and energy resources, Uinta Basin of Utah. Utah Geological Association Publication 12, p. 227-241.

Dana, G. F., R. L. Oliver, and J. R. Elliott, 1984, Geology and resources of the Tar Sand Triangle, southeastern Utah: Laramie, WY, Western Research Institute, DOE/ FE/60177-1625, 50 p.

Dembicki, H., Jr., M. J. Anderson, and R. P. Diedrich, 1986, Oil-to-oil correlation in northwestern Colorado Plateau. American Association of Petroleum Geologists Bulletin, v. 70, p. 1033.

Dolcater, D. L., 1988, Sunnyside tar sand - comments on source, degradation, and maturity of the heavy oil. Unpublished Amoco Production Company report T88-G-1, January 11, 1988, Utah Geological Survey open-file, 7 p.

Drelich, J., K. Bukka, J. D. Miller, and F. V. Hanson, 1994, Surface tension of toluene-extracted bitumens from Utah oil sands as determined by Wilhelmy plate and contact angle techniques: Energy & Fuels, v. 8, p. 700-704.

Dunn-Norman, S., A. Gupta, D.A. Summers, L. F. Koederitz, and D. T. Numbere, 2002, Recovery methods for heavy oil in ultra-shallow reservoirs. Society of Petroleum Engineers Paper 76710, 6 p.

Fesker, R., 1967, Geophysical report, seismograph survey of the Asphalt Ridge prospect, Uintah County, Utah for Utah State Geological Survey, Salt Lake City, Utah. Petty Geophysical Engineering Company, November 1997, Utah Geological Survey public files, 17 p., 4 plates.

Fouch, T. D., 1975, Lithofacies and related hydrocarbon accumulations in Tertiary strata of the western and central Uinta Basin, Utah, *in* D.W. Bolyard, ed., Deep drilling frontiers of the central Rocky Mountains: Rocky Mountain Association of Petroleum Geologists Symposium, Denver, p. 163-174.

Fouch, T. D., V. F. Nuccio, J. C. Osmond, L. MacMillan, W. B. Cashion and C. J. Wandrey, 1992, oil and gas in uppermost Cretaceous and Tertiary rock, Uinta Basin, Utah, *in* T. D. Fouch, V. F. Nuccio and T. C. Chidsey, Jr., eds., Hydrocarbon and mineral resources of the Uinta Basin, Utah and Colorado. Utah Geological Association 1992 Field Symposium, p. 9-47.

Fouch, T. D., V. F. Nuccio, D. E Anders, D. D. Rice, J. K. Pitman, and R. F. Mast, 1994, Green River (!) petroleum system, Uinta Basin, Utah, U.S.A. *in* L. B. Magoon and W. G. Dow, eds., The petroleum system - from source to trap. American Association of Petroleum Geologists Memoir 60, p. 399-421.

Franczyk, K. J., T. D. Fouch, R. C. Johnson, C. M. Molenaar, and W. A. Cobban, 1992, Cretaceous and Tertiary paleogeographic reconstructions for the Uinta-Piceance Basin study area, Colorado and Utah. U. S. Geological Survey Bulletin 1787, p. Q1-Q37.

Gloyn, R. W., D.E. Tabet, B.T. Tripp, C.E. Bishop, C.D. Morgan, J.W. Gwynn, and R.E. Blackett, 2003, Energy, mineral, and ground-water resources of Carbon and Emery Counties, Utah: Salt Lake City, Utah Geological Survey Bulletin 132, 161 p.

Gurgel, K. D., 1983, Energy resources map of Utah. Utah Geological and Mineral Survey Map 68, 1:500,000.

Gwynn, J. W., 1985, The Hill Creek oil-impregnated sandstone deposit. Utah Geological and Mineralogical Survey Report of Investigation 201, 40 p.

Gwynn, J. W., 1986, Overburden map and thickness determinations, Sunnyside oil-impregnated sandstone deposit, Carbon and Duchesne Counties, Utah: Utah Geological and Mineral Survey Report of Investigation, 7 p.

Gwynn, J. W., 1992, The oil well saline-water resources of the Uinta basin, Utah: Their character and distribution, *in* T. D. Fouch, V. F. Naccio, and T. C. Chidsey, Jr., eds., Hydrocarbon and Mineral Resources of the Uinta Basin, Utah and Colorado. Utah Geological Association Guidebook 20, p. 289-311.

Haddox, D. A., B. J. Kowallis, and J. D. Shakespeare, 2005, Mapping and kinematic analysis of the Deep Creek fault zone, south flank of the Uinta Mountains, Utah *in* C.M. Dehler, J. L. Pederson, D. A. Sprinkel, and G. J. Kowallis, eds., Uinta Mountain Geology: Utah Geological Association Publication 33, p. 321-333.

Hansley, P. L., 1995, Diagenetic and burial history of the Lower Permian White Rim Sandstone in the Tar Sand Triangle, Paradox Basin, southeastern Utah: U.S. Geological Survey Bulletin 2000-I, 41 p.

Hintze, L. F., 1980, Geologic Map of Utah. Utah Geological and Mineral Survey, 1:500,000, two sheets.

Holmes, C. N., B. M. Page, and P. Averitt, 1948, Geology of the bituminous sandstone deposits near Sunnyside, Carbon County, Utah. U.S. Geological Survey Preliminary Oil and Gas Map 86, 1:24,000, one sheet.

Holmes, C. N., and B. M. Page, 1956, Geology of the bituminous sandstone deposits near Sunnyside, Carbon County, Utah, *in* J. A. Peterson, ed., Geology and economic deposits of east central Utah: Intermountain Association of Petroleum Geologists Seventh Annual Field Conference: Salt Lake City, p. 171-177.

Holmes, S. A., J. Romanowski, Leo J., and K. P. Thomas, 1986, Impregnated hydrocarbon distribution in bitumens and in oils recovered by thermal processes: DOE Tar Sand Symposium: Jackson, WY, Western Research Institute, July 7-10, 1986, p. 20.

Huntoon, J. E., 1985, Depositional environments and paleotopographic relief of the White Rim Sandstone (Permian) in the Elaterite basin, Canyonlands National Park and Glen Canyon National Recreation Area, Utah: University of Utah M.S. Thesis, Salt Lake City, 143 p.

Huntoon, J. E., and M. A. Chan, 1987, Marine origin of paleotopographic relief on eolian White Rim Sandstone (Permian), Elaterite Basin, Utah: American Association of Petroleum Geologists Bulletin, v. 71, p. 1035-1045.

Huntoon, J. E., J. C. Dolson, and B. M. Henry, 1994, Seals and migration pathways in paleogeomorphically trapped petroleum occurrences: Permian White Rim Sandstone, Tar-Sand Triangle area, Utah, *in* J. C. Dolson, ed., Unconformity-related hydrocarbons in sedimentary sequences: Denver, Rock Mountain Association of Geologists, p. 99-118.

Huntoon, J. E., P. L. Hansley, and N. D. Naeser, 1999, The search for a source rock for the giant Tar Sand Triangle accumulation, southeastern Utah. American Association of Petroleum Geologists Bulletin, v. 83, p. 467-495.

Johnson, J., and A. Lyle, 1994, *In situ* combustion simulation testing of tar sand, Research Investigations in Oil Shale, Tar Sand, Coal Research, Advanced Exploratory Process Technology, and Advanced Fuels Research Volume 1, DOE/MC/11076-5057, Department of Energy Office of Fossil Energy, p. 47-53.

Johnson, L.A., L.C. Marchant, and C.Q. Cupps, 1975, Properties of Utah tar sands – South Seep Ridge area, P.R. Spring deposit. U.S. Bureau of Mines Report of Investigations 8003, 14 p.

Johnson, L.A., L.C. Marchant, and C.Q. Cupps, 1976, Properties of Utah tar sands – Asphalt Wash area, P.R. Spring deposit. U.S. Bureau of Mines Report of Investigations 8030, 11 p.

Johnson Jr., L. A., L. J. Fahy, L. J. Romanowski Jr., and H. L. Hutchinson, 1984, A steamflood in a Utah tar sand, U.S.A., *in* R. F. Meyer, J. C. Wynn, and J. C. Olson, eds., The future of heavy crude and tar sands: New York, McGraw-Hill, p. 727-736.

Johnson Jr., L. A., L. J. Fahy, L. J. Romanowski, R. V. Barbour, and K. P. Thomas, 1982, An echoing in-situ combustion oil recovery project in a Utah tar sand, *in* D. Ball, L. C. Marchant, and A. Goldburg, eds., Tar Sands: The IOCC Monograph Series: Oklahoma City, Interstate Oil Compact Commission, p. 151-162.

Johnson Jr., L. A., and K. P. Thomas, 1988, Comparison of laboratory and field steamfloods in tar sand, *in* R. F. Meyer, ed., The Third UNITAR/UNDP International Conference on

Heavy Crude and Tar Sands: Edmonton, AB, Alberta Oil Sands Technology and Research Authority, p. 805-811.

Kayser, R. B., 1966, Bituminous sandstone deposits, Asphalt Ridge: Utah Geological and Mineralogical Survey Special Studies 19, 62 p.

Koottungal, L., 2008, 2008 worldwide EOR survey. Oil & Gas Journal, v. 106, no. 15, p. 47-59.

Kuuskraa, V. A., E. C. Hammerschaimb, and M. Paque, 1987, Major tar sand and heavy-oil deposits of the United States, *in* R. F. Meyer, ed, Exploration for heavy crude oil and natural bitumen. American Association of Petroleum Geologists Studies in Geology 25, p. 123-256.

Land, C.S., C.Q. Cupps, L.C. Marchant, and F.M. Carlson, 1977, Field experiment of reverse combustion oil recovery from a Utah tar sand: DOE/LERC/R1-77/5, 18 p. (microfiche document at University of Utah library).

Lewin & Associates, 1984, Major tar sand and heavy oil deposits of the United States. Interstate Oil Compact Commission, January 1984, 272 p.

Lillis, P. G., A. Warden, and J. D. King, 2003, Petroleum Systems of the Uinta and Piceance Basins – geochemical characteristics of oil types, *in* Petroleum systems and geological assessment of oil and gas in the Uinta-Piceance Province, Utah and Colorado: U.S. Geological Survey Digital Data Series DDS-69-B, 25 p.

Marchant, L.C., L.A. Johnson, and C.Q. Cupps, 1974, Properties of Utah tar sands – Thirteenmile Canyon area, P.R. Spring deposit. U.S. Bureau of Mines Report of Investigations 7923, 14 p.

Marchant, L. C., 1988, U.S. tar sand oil recovery projects - 1985, *in* R. F. Meyer, ed., The Third UNITAR/UNDP International Conference on Heavy Crude and Tar Sands: Edmonton, AB, Alberta Oil Sands Technology and Research Authority, p. 933-940.

Merriam, N.W., and L.J. Fahy, 1985, LETC tar sand research – North Asphalt Ridge, *in* M. D. Picard, ed., Geology and energy resources, Uinta Basin of Utah: Utah Geological Association Publication 12, p. 253-256.

Meyer, R. F., and C. J. Schenk, 1988, An estimate of world resources of heavy crude oil and natural bitumen, *in* R. F. Meyer, ed., The Third UNITAR/UNDP International Conference of Heavy Crude and Tar Sands: July 22-31, 1985, Long Beach, CA, p. 73-83.

Mokhatab, S., and L. A. Giangiacomo, 2006, Microbial enhanced oil recovery techniques improve production. World Oil, v. 227, no. 10, p. 85-93.

Moritis, G., 2004, Oil sands drive Canada's oil production growth. Oil & Gas Journal, v. 102, no. 21, p. 43-52.

Moritis, G., 2008, More US EOR projects start but EOR production continues to decline. Oil & Gas Journal, v. 106, no. 15, p. 41-46.

Morgan, C. D., T.C. Chidsey Jr., K. P. McClure, S. R. Bereskin and M. D. Deo, 2003, Reservoir characterization of the Lower Green River Formation, Uinta Basin, Utah. Utah Geological Survey Open-File Report 411.

Nettle, R. L., 1982, Evaluation of the Uinta sands, Wonsits Valley field, Uintah County, Utah: unpublished Gulf Oil report, Utah Geological Survey open-file, 12 p.

Nuccio, V. F., and S. M. Condon, 1996, Burial and thermal history of the Paradox Basin, Utah and Colorado, and petroleum potential of the Middle Pennsylvanian Paradox Formation: U.S. Geological Survey Bulletin 2000-O, 41 p.

Oblad, A. G., J. W. Bunger, F. V. Hanson, J. D. Miller, and J. D. Seader, 1985, Studies of Utah's and other domestic tar sands. Proceedings of the First Annual Oil Shale/Tar Sand Contractors Meeting, p. 73-89.

Oblad, A. G., J.W. Bunger, F.V. Hanson, J.D. Miller, H.R. Ritzma, and J.D. Seader, 1987, Tar sand research and development at the University of Utah, *in* J.M. Hollander, H. Brooks, and D. Sternlight, eds., Annual Review of Energy, v. 12: Palo Alto, CA, p. 283-356.

Osterloh, W. T., and J. Jones, 2003, Novel thermal process for recovery of extremely shallow heavy oil. Society of Petroleum Engineers Reservoir Evaluation & Engineering, v. 6, no. 2, p. 127-134.

Paduraru, R., and I. Pantazi, 2000, IOR/EOR: Over six decades of Romanian experience. Proceeding of European Petroleum Conference, Paris, 24-25 October, 2000, p. 489-497.

Pederson, J. M., and J. H. Sitorus, 2001, Geothermal hot-water flood – Balam South Telisa Sand, Sumatra, Indonesia. Society of Petroleum Engineers Paper 68724, 7 p.

Peterson, P. R., 1982, An analysis of the tar sand deposit on the Rocky Mountain Exploration Company Whiterocks Federal lease, Uintah County, Utah. Unpublished consulting report, Denver, CO, 16 p.

Peterson, P. R., 1985, The Whiterocks tar sand deposit, *in* M. D. Picard, ed., Geology and energy resources, Uinta Basin of Utah. Utah Geological Association Publication 12, p. 243-252.

Peterson, P. R., and H. R. Ritzma, 1974, Informational core drilling in Utah's oil-impregnated sandstone deposits, southeast Uinta Basin, Uintah County, Utah. Utah Geological and Mineralogical Survey Report of Investigation 88, 85 p.

Petrobank, 2007, Whitesands project expansion application. www.petrobank.com , unpaginated.

Phillips, S. T., 1987, Transmittal of geochemical results - Tar Sand Triangle, Circle Cliffs, and San Rafael Swell outcrop samples: La Habra, CA, Chevron Oil Field Research Co., unpaginated, unpublished.

Picard, M. D., and L. R. High Jr., 1970, Sedimentology of oil-impregnated lacustrine and fluvial sandstone, P.R. Spring area, southeast Uinta Basin, Utah. Utah Geological and Mineralogical Survey Special Studies 33, 32 p.

Polumbus Jr and Associates, 1961, Core hole and well data summary, White Rocks Oil, Uintah County, Utah. Unpublished report, Utah Geological Survey.

Prats, M., 1982, Thermal Recovery. Society of Petroleum Engineers Monograph, Henry L. Doherty Series, v. 7, 283 p.

Pyper, G. E., 1983, Tar Sand Triangle and White Canyon special tar sand areas, *in* K. L. Lindkov, ed., Potential hydrologic impacts of a tar-sand industry: U.S. Geological Survey Water-Resources Investigations Report 83-4109, p. 98-113.

Rach, N. M., 2004, SAGD drilling parameters evolve for oil sands. Oil & Gas Journal, v. 102, no. 21, p. 53-55.

Reed, W. E., 1977, Molecular compositions of weathered petroleum and comparison with its possible source. Geochimica et Cosmochimica Acta, v. 41, no. 2, p. 237-247.

Remy, R. R., 1984, Report on the composition, texture, diagenesis, and provenence of the Sunnyside tar sands, Carbon County, Utah. Amoco Minerals Company in-house report, December 4, 1984, Utah Geological Survey open-file, 35 p.

Rice, D. D., T. D. Fouch, and R. C. Johnson, 1992, Influence of source rock type, thermal maturity, and migration on composition and distribution of natural gases, Uinta Basin, Utah, *in* T. D. Fouch, V. F. Nuccio and T.C. Chidsey, Jr. (eds.), Hydrocarbon and mineral resources of the Uinta Basin, Utah and Colorado. Utah Geological Association Guidebook 20, p. 95-109.

Ritzma, H. R., 1979, Oil-impregnated rock deposits of Utah. Utah Geological and Mineralogical Survey Map 47, 1:1,000,000, 2 sheets.

Ritzma, H. R., 1980, Oil-impregnated sandstone deposits, Circle Cliffs uplift, Utah, *in* M. D. Picard, ed., Henry Mountain Symposium. Utah Geological Association Guidebook 8, p. 341-351.

Rose, P. E., K. Bukka, M. D. Deo, F. V. Hanson, and A. G. Oblad, 1992, Characterization of Uinta Basin oil sand bitumens: 1992 Eastern Oil Shale Symposium, p. 277-282.

Rozelle Consulting Services, 1989, Final report on 1989 update of the computerized geologic model to include the 1988 drill hole data, Sunnyside tar sand project, Sunnyside, Utah: Golden, CO, Rozelle Consulting Services, unpaginated.

Ruble, T. E., M. D. Lewan, and R. P. Philp, 2001, New insights on the Green River petroleum system in the Uinta Basin from hydrous pyrolysis experiments. American Association of Petroleum Geologists Bulletin, v. 85, p. 1333-1571.

Ryder, R.T., T.D. Fouch, and J.H. Elison, 1976, Early Tertiary sedimentation in the western Uinta Basin, Utah: Geological Society of America Bulletin, v. 87, p. 496-512.

Sanford, R. F., 1995, Ground-water flow and migration of hydrocarbons to the Lower Permian White Rim Sandstone, Tar Sand Triangle, southeastern Utah: U.S. Geological Survey Bulletin 2000-J, 24 p.

Schamel, S., M. Deo, and M. Deets, 2002, Reactivation of an idle lease to increase heavy oil recovery through application of conventional steam drive technology in a low dip slope and basin reservoir in the Midway-Sunset field, San Joaquin basin, California. Final report for U.S. Department of Energy Contract No. DE-FC-95BC14937, 146 p.

Schamel, S., and M. Deo, 2003, Role of small-scale variations in water saturation in optimization of steam flood heavy oil recovery in the Midway-Sunset field, California. Society of Petroleum Engineers Paper 83499, 10 p.

Schenk, C. J., 1988, Petrology and diagenesis of the bitumen- and heavy-oil-bearing White Rim Formation (Permian), Tar-Sand Triangle area, southeastern Utah, *in* R. F. Meyer, and E. J. Wiggins, eds., The Fourth UNITAR/UNDP International Conference on Heavy Crude and Tar Sands, volume 2: Geology, Chemistry. Edmonton, Alberta Oil Sands Technology and Research Authority, p. 155-172.

Schenk, C.J., and R.M. Pollastro, 1987, Preliminary geologic analysis of the tar sands near Sunnyside, Utah, in R.F. Meyer, ed., Exploration for Heavy Crude Oil and Natural Bitumen: American Association of Petroleum Geologists Studies in Geology 25, p. 589-599.

Schuh, M. L., 1993, Wonsits Valley, *in* B. G. Hill and S. R. Bereskin, eds., Oil and gas fields of Utah. Utah Geological Association (unpaginated), 2 p.

Severy, C. L., 1943, Whiterock River bituminous sandstone deposit, Uintah County, Utah. U.S. Bureau of Mines unpublished War Minerals Report, 15 p.

Shirley, H. B., 1961, Whiterock River bituminous sandstone deposit, Uintah County, Utah. U.S. Bureau of Mines War Minerals Report, 15 p.

Sinks, D. J., 1985a, Geologic evaluation and reservoir properties of the P.R. Spring tar sand deposit, Uintah and Grand Counties, Utah. Laramie Energy Research Center report for Deparment of Enery Cooperative Agreement DE-FC21-83FE60177, 190 p.

Sinks, D. J., 1985b, Geological influences on the *in situ* processing of tar sand at the Asphalt Ridge Northwest deposit, Utah. Laramie Energy Research Center report, 81 p.

Skipper, K., 2001, Petroleum resources of Canada in the Twenty-first Century, *in* M. W. Downey, J. C. Threet, and W. A. Morgan, eds., Petroleum Provinces of the Twenty-first Century. American Association of Petroleum Geologists Memoir 74, p. 109-135.

Smouse, D., 1993, Salt Wash, *in* B. G. Hill and S. R. Bereskin, eds., Oil and gas fields of Utah. Utah Geological Association Publication 22, 2 p.

Sohio Petroleum, 1974, Proposed plan for mining and processing operations, bituminous sands deposits, Asphalt Ridge area, Uintah County, Utah: unpublished report by the Sohio Petroleum Company to the Utah Board of Oil and Gas Conservation, August 28, 1974, 14 p.

Spieker, E.M., 1930, Bituminous sandstones near Vernal, Utah: U.S. Geological Survey Bulletin 822-C, p. 77-100.

Sprinkel, D.S., 2002, Progress report geologic map of the Dutch John 30' x 60' quadrangle, Utah-Colorado-Wyoming: Utah Geological Survey Open-file Report 399, 3 plates.

Sresty, G.C., H. Dev, R.H. Snow, and J.E. Bridges, 1986, Recovery of bitumen from tar sand deposits with the radio frequency process: Society of Petroleum Engineers Reservoir Engineering, v. 1, no. 1, p. 85-94.

Stone, D.S., 1977, Tectonic history of the Uncompahgre uplift, *in* H.K, Veal, ed., Exploration frontiers of the central and southern Rockies: Denver, CO, Rocky Mountain Association of Geologists, p. 23-30.

Stone, D. S., 1993, Tectonic evolution of the Uinta Mountains - palinspastic restoration of a structural cross section along longitude 109°15: Utah Geological Survey Miscellaneous Publication 93-8, 19 p.

Stosur, J. J. G., and J. A. Slater, 1987, Recovery methods for heavy oil and tar sand, *in* R. F. Meyer, ed., Exploration for Heavy Crude Oil and Natural Bitumen. American Association of Petroleum Geologists Studies in Geology 25, p. 679-683.

Stowe, C., 1972, Oil and gas production in Utah to 1970. Utah Geological and Mineralogical Survey Bulletin 94, 179 p.

Terwilliger, P.L., 1957, Coring and testing wells, Asphalt Ridge, Utah: Unpublished Gulf Oil File Note SR-92 dated 10/21/57, unpaginated, released to Utah Geological Survey on 12/11/74.

Thomas, K. P., P. M. Harnsberger, and F. D. Guffey, 1994, An evaluation of oil produced from Asphalt Ridge (Utah) tar sand as a feedstock for the production of asphalt and turbine fuels: Research Investigations in Oil Shale, Tar Sand, Coal Research, Advanced Exploratory Process Technology, and Advanced Fuels Research Volume 1, DOE/ MC/11076-5057, Department of Energy Office of Fossil Energy, p. 61-65.

Thurber, J. L., and M. E. Welborn, 1977, How Shell attempted to unlock Utah tar sands. Petroleum Engineer International, v. 49, p. 31-42.

Tom Brown, Inc., 1974, Heavy oil prospect NW Asphalt Ridge, Uintah County, Utah. Unpublished in-house report, Utah Geological Survey open file, 28 p., 2 appendices.

Tripp, B. T., 1985, Reconnaissance study of the Black Dragon tar sand deposit T. 20-22 S, R. 12-13 E., San Rafael Swell, Emery County, Utah. Utah Geological and Mineral Survey Report of Investigation 194, 45 p.

Tsai, C. H., M. D. Deo, F. V. Hanson, and A. G. Oblad, 1993, Characterization and potential utilization of the Asphalt Ridge tar sand bitumen I: Gas chromatography-mass spectrometry and pyrolysis-mass spectrometry analysis. Fuel Science and Technology International, v. 11, p. 475-506.

Untermann, G.E., Untermann, B.R., and D.M. Kinney, 1964, Geologic map of Uintah County, Utah. Utah Geological Survey Map M-16, 1:125,000, 2 plates.

Wenrich, K. J., and J. G. Palacas, 1990, Organic matter and uranium in solution – Collapse breccia pipes of northern Arizona and San Rafael Swell, Utah. U.S. Geological Survey Circular 1069, p. 36-50.

Wood, R. E., and H. R. Ritzma, 1972, Analysis of oil extracted from oil-impregnated sandstone deposits in Utah. Utah Geological and Mineral Survey Special Studies 39: 19 p.

Xia, T. X., M. Greaves, and A. T. Turta, 2002, Injection well – producer well combination in THAI 'toe-to-heel air injection'. Society of Petroleum Engineers Paper 75137, 15 p.

Yazdani J., A., and B. B. Maini, 2005, Effect of drainage height and grain size on production rates in the Vapex process. Experimental study. Society of Petroleum Engineers Reservoir Evaluation & Engineering, v. 8, no. 3, p. 205-213.

Yeh, T-F., 1997, Catalytic upgrading of Asphalt Ridge bitumen over hydrodenitrogenation catalysis. PhD dissertation, Chemical and Fuels Engineering, University of Utah, 268 p.